博　士　論　文

論文題名:

Enantioselective Synthesis of Highly Functionalized Heterocycles
via Organocatalyzed C–C Bond Forming Reactions

（有機触媒による炭素–炭素結合形成反応を基盤とする多官能性複素環のエナンチオ選択的合成）

平成　３０　年　２　月　２　日

専 攻 名　　化学専攻

氏　　名　　岸　鉄馬

大阪大学大学院理学研究科

Preface and Acknowledgment

The studies discussed in this thesis have been carried out under the supervision of Professor Hiroaki Sasai at Osaka University from April 2013 to March 2018. These studies concern with organocatalyzed C–C bond forming reactions for the synthesis of highly functionalized heterocycles.

The author would like to express his sincerest gratitude to his supervisor, Professor Hiroaki Sasai, for his continuous guidance, encouragement, and stimulating discussions throughout this research work. All the results reported in this thesis could not have been achieved without his constant supervision. The author is also deeply indebted to his advisor, Associate Professor Shinobu Takizawa, for his constant support, suggestions, and enthusiasm. The author would also like to thank Associate Professor Takeyuki Suzuki, Assistant Professor Kazuhiro Takenaka, Assistant Professor Makoto Sako, and Assistant Professor Masaru Kondo for their helpful suggestions, directions, and encouragement.

The author would like to acknowledge the precious collaboration and assistance of Professor Giang Vo-Thanh, Dr. Martial Toffano, and Dr. Thi-Thuy-Duong Ngo at Paris-Sud University from October to December 2014 and author wishes to express his special thanks to them for their enormous contribution to his research and life in France.

The author is also grateful to have enjoyed the fruits of the great collaboration with Professor Susumi Hatakeyama (Nagasaki University), Professor Makoto Fujita (University of Tokyo), and Professor Hiromichi Fujioka (Osaka University).

The author would like to express his appreciation to Dr. Mitsutoshi Akita, Dr. Yasushi Yoshida and Dr. Fernando Arteaga-Arteaga for teaching him the fundamentals of organic chemistry and basic lab techniques.

The author deeply appreciates the help received from the technical staff of the Comprehensive Analysis Center (CAC) in Osaka University, Mr. Tsunayoshi Takehara for X-ray crystallographic analysis, Mr. Hitoshi Haneoka and Dr. Da-Yang Zhou for NMR measurements, and Mr. Tsuyoshi Matsuzaki for HRMS measurements.

The author would like to thank Secretary Ayaka Honda who took care of him in daily and miscellaneous affairs.

The author wishes to express his gratitude to the former and present members of Sasai group: Dr. Priyabrata Das, Dr. Suman Chandra Mohanta, Dr. Shuichi Hirata, Dr. Yogesh Daulat Dhage, Dr. Shuhei Takatani, Dr. Lulu Fan, Dr. Tue Minh-Nhat Nguyen, Dr. Xianjin Lin, Dr. Ismiyarto, Dr. Kazuhiko Wakita, Dr. Mohamed

Ahmed Abozeid, Dr. Masashi Shigenobu, Mr. Michitaka Suzuki, Mr. Yoshihiro Nagata, Mr. Yoshiki Takeuchi, Mr. Tomohiro Sakai, Mr. Kazuya Sawada, Mr. Abhijit Sen, Mr. Bijan Mohon Chaki, Mr. Kazuya Ichinose, Mr. Shin Yoneyama, Mr. Takahiro Doi, Mr. Takanori Aoki, Ms. Miki Kusaba, Mr. Akimasa Sugizaki, Mr. Yasuaki Niida, Mr. Yuya Nomoto, Ms. Wathsala H. D. P., Mr. Yuki Adachi, Mr. Kosuke Kataoka, Mr. Tomohiro Takiishi, Mr. Yuki Tamori, Mr. Yuzhao Jiang, Ms. Qingwen Chen, Mr. Park Hanseok, Mr. Steffen Mader, Dr. Daniel Hack, Mr. Lukas Schober, Ms. Nadine Zumbrägel, and Mr. Ryan Khalaf.

The author would like to thank the Japan Society for the Promotion of Science (JSPS) for their financial support via the research fellowship (DC2).

Finally, the author's sincere gratitude is dedicated to his family for their understanding and encouragement.

Kenta Kishi

Kenta Kishi

February 2018

Department of Chemistry
Graduate School of Science
Osaka University

List of Abbreviations

Ac	acetyl
AIBN	azobisisobutyronitrile
aq.	aqueous solution
Ar	aryl
atm	atmospheric pressure
α-ICPN	(1*R*,3*S*,5*R*,7*R*,8a*S*)-7-ethylhexahydro-1-(6-hydroxy-4-quinolinyl)-3,7-methano-1*H*-pyrrolo[2,1-c][1,4]oxazine
BINAP	2,2'-bis(diphenylphosphino)-1,1'-binaphthyl
BINOL	1,1'-bi-2-naphthol
Bn	benzyl
Boc	*tert*-butoxycarbonyl
bp	boiling point
BPPFA	*N,N*-dimethyl-1-[1',2-bis(diphenylphosphino)ferrocenyl]ethylamine
Bu or *n*-Bu	butyl or normal butyl
Bz	benzoyl
β-ICD	(9*S*)-3α,9-epoxy-10,11-dihydrocinchonan-6'-ol
cat.	catalyst
Cbz or Z	benzyloxycarbonyl
cod	1,5-cyclooctadiene
coe	cyclooctene
conv.	conversion
CPME	cyclopentylmethylether
Cy	cyclohexyl
D	deuterium
DABCO	1,4-diazabicyclo[2.2.2]octane
DBU	1,8-diazabicyclo[5.4.0]undec-7-ene
DCE	1,2-dichloroethane
$(DHQD)_2PHAL$	hydroquinidine 1,4-phthalazinediyl diether
DMAP	4-(*N*,*N*-dimethylamino)pyridine
DIBAL	diisobutylaluminium hydride
DIOP	4,5-bis(diphenylphosphinomethyl)-2,2-dimethyl-1,3-dioxalan
DIPEA	*N,N*-diisopropylethylamine
DME	1,2-dimethoxyethane
DMF	*N*,*N*-dimethylformamide
DMSO	dimethyl sulfoxide
dr	diastereomeric ratio

E	electrophile
EDCI	1-(3-dimethylaminopropyl)-3-ethylcarbodiimide hydrochloride
EDG	electron-donating group
ee	enantiomeric excess
Eq.	equation
equiv	equivalent(s)
ESI	electrospray ionization
Et	ethyl
EWG	electron-withdrawing group
FG	functional group
Glc	glucose
h	hour(s)
HOBt	1-hydroxybenzotriazole
HPLC	high performance liquid chromatography
HRMS	high resolution mass spectrometry
i-Pr	isopropyl
IR	infrared spectroscopy
KHMDS	potassium bis(trimethylsilyl)amide
L	ligand
LB	Lewis base
Me	methyl
min	minute(s)
MBH	Morita–Baylis–Hillman
MOP	diphenylphosphino-2'-methoxy-1,1'-binaphthyl
MS	mass spectrometry or molecular sieve
Ms	mesyl (methanesulfonyl)
MTBE	methyl *tert*-butyl ether
NHC	*N*-heterolcyclic carbene
NMR	nuclear magnetic resonance
NOE	nuclear Overhauser effect
NOESY	NOE correlated spectroscopy
Nu	nucleophile
ORTEP	Oak Ridge thermal ellipsoid plot
PG	protecting group
Ph	phenyl
PHANEPHOS	4,12-bis(diphenylphosphino)[2.2]paracyclophane
pin	pinacolato

PMB	*p*-methoxybenzyl
Pr or *n*-Pr	propyl or normal propyl
proton sponge	*N,N,N′,N′*-tetramethyl-1,8-naphthalenediamine
quant	quantitative
QUINAP	1-(2-diphenylphosphino-1-naphthyl)isoquinoline
R	alkyl or aryl
rac	racemic
RC	Rauhut–Currier
rt	room temperature
SDP	7,7’-bis(diphenylphosphanyl)-2,2’,3,3’-tetrahydro-1,1’-spirobi[indene]
SEGPHOS	5,5’-bis(diphenylphosphino)-4,4’-bi-1,3-benzodioxole
SITCP	dimethylene-[7,7’-(1,1’-spiroindan)]-phenylphospholane
TBS	tertiarybutyldimethylsilyl
t-Bu	tertiary butyl
TCA	trichloroethane
temp.	temperature
Tf	trifluoromethanesulfonyl
THF	tetrahydrofuran
TLC	thin layer chromatography
TMS	trimethylsilyl
Ts	*p*-toluenesulfonyl (tosyl)
X	hetero atom unless otherwise noted

Contents

Chapter 1

General Introduction 1

Chapter 2

Enantiodivergent Synthesis of 3-Amino-2-Oxindoles via Aza-MBH Reaction of Isatin-Derived Ketimines with Acrolein 22

Chapter 3

Multifunctional Catalysis: Stereoselective Construction of α-Methylidene-γ-Lactams via Amidation/Rauhut–Currier Reaction Sequence 40

Chapter 4

Phosphine-Catalyzed β,γ-Dual Umpolung Domino Reaction of Dienones with Allenoates: Enantioselective Synthesis of Tetrahydrobenzofuranones 74

Chapter 5

Phosphine-Catalyzed Dual Umpolung Domino Michael Reaction: A Novel Route to Hydroindole- and Hydrobenzofuran-2-Carboxylates 98

Conclusion 132

List of Publications 133

Chapter 1
General Introduction

1.1. Catalytic Asymmetric Synthesis

The word *"chirality"* refers to a property displayed by some molecules that cannot be overlapped with their mirror images. Such molecules are called *"chiral"*, and any two molecules that are nonoverlappable mirror images of each other are called enantiomers. The word *"chiral"* is derived from the Greek term for hand, χειρ (kheir), as our hands also display chirality and are enantiomers of each other. As a molecular property, chirality can be roughly classified into four categories: (1) central chirality, stemming from a carbon atom bearing four different functional groups; (2) axial chirality, stemming from constituent atoms being arranged chirally around a certain virtual axis; (3) planar chirality, stemming from a difference in atomic arrangement on the front and back in a molecule; and (4) helicity, stemming from a three-dimensional helical structure of the molecule (Figure 1.1).

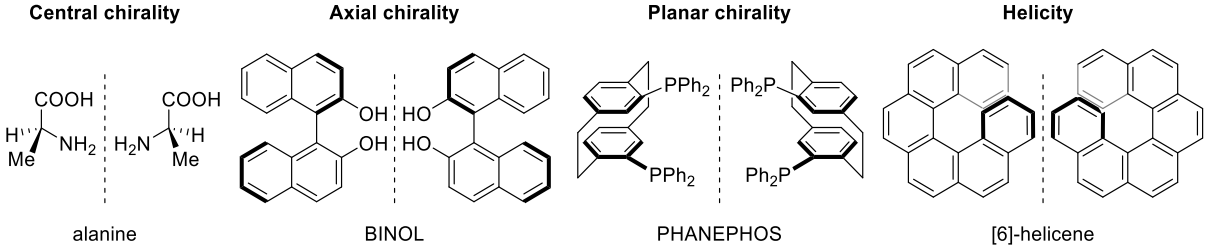

Figure 1.1. Different categories of chirality

Although two enantiomers show equal physical properties except for optical rotation, they sometimes have quite different bioactivities. For example, (*S*)-limonene and (*R*)-limonene have the smell of lemon and orange, respectively. At the basis of what is known as the most famous drug disaster in history, which occured in 1957, is the fact that the two enantiomers (*S*)-thalidomide and (*R*)-thalidomide have different biological activities; namely, the first is a teratogen and the second is a sedative. Notably, it is now known that thalidomide has a nonnegligible racemization half-life *in vivo* of ~566 min,[1] which should be taken into account when dealing with this compound. These differences are mainly derived from *L*-amino acids constituting proteins in the human body. The thalidomide case caused the Food and Drug Administration (FDA) to implement a strict enforcement of the optical purity of pharmaceuticals. Therefore, it is important to synthesize selectively one specific, desired enantiomer of chiral molecules.

Four general methodologies currently exist to obtain optically active molecules: (1) optical resolution, (2) the biological method, (3) the chiral pool method, and (4) performing a catalytic asymmetric synthesis. In optical resolution, the racemic mixture of the two enantiomers of a molecule is divided into its two enantiomeric components using chiral tools, such as chiral columns, auxiliary groups, and crystals. In this approach, therefore, the maximum theoretical yield of a desired enantiomer is 50%. Although the biological method shows excellent enantioselectivity, it often suffers from high substrate specificity and applicability is limited to some solvents and pH values. The chiral pool method utilizes naturally occurring chiral sources, such as *L*-amino acids and *D*-sugars, as a starting material. However, it requires stoichiometric amounts of

these chiral sources. On the contrary, the catalytic asymmetric synthesis is regarded as an ideal method, because it enables the production of massive amounts of optically active products from small amounts of chiral sources. In 2001, Dr. R. Noyori, Dr. W. S. Knowles, and Dr. K. B. Sharpless won the Nobel Prize in chemistry for contributing to the development of the field of catalytic asymmetric syntheses. Among these syntheses, asymmetric hydrogenation[2] and epoxidation[3] have been adapted for industrial production because of their practicality. This way, the importance of asymmetric synthesis is also socially evaluated from both academic and industrial aspects.

1.2. Organocatalysts

As mentioned in Section 1.1, the catalytic asymmetric synthesis is an ideal approach for obtaining optically active compounds. The catalysts of asymmetric syntheses are classified into three groups: (1) metal catalysts, (2) enzyme-based catalysts, and (3) the recently developed organocatalysts. Enantioselective hydrogenation and epoxidation (i.e., the reactions that were the main reason for the Nobel Prize award in chemistry in 2001) were made possible by the use of metal catalysts. Among these compounds, in general, transition metal catalysts display high reactivity and can promote unique reactions that are impossible to perform using other types of catalysts. In fact, the development of the transition metal-catalyzed metathesis reaction and that of the palladium-catalyzed cross-coupling reaction were deemed worthy of the Nobel Prize in chemistry in 2005 and 2010, respectively. The asymmetric environment of transition metal catalysts can be fine-tuned through the choice of chiral ligands, rendering a variety of enantioselective reactions possible. Nevertheless, metal catalysts have several disadvantages. When a metal catalyst is employed in a reaction, the product is contaminated by metallic residues, even after purification. This weakness in the approach can be fatal, especially during the synthesis of pharmaceuticals, because of the toxicity of some metals. Moreover, this approach depends on the use of very limited resources, such as Pd, Rh, and Ru and other rare metals. Thus, the development of species that can replace the metal catalysts is a desirable goal from the viewpoint of green, sustainable chemistry. Enzyme-based catalysts often enable achieving excellent stereoselectivity, however, their use is limited by the narrow range of suitable substrates.

Organocatalysts are expected to be a solution to the described problems associated with the use of enzymes and metal catalysts. Organocatalysts consist of carbon, hydrogen, nitrogen, oxygen, phosphorus, sulfur, and other nonmetallic elements that are universally found in organic compounds. The reaction mode and the asymmetric environment of organocatalysts can be tuned by a variety of functionalities, such as Brønsted acids or bases, Lewis acids or bases, and hydrogen donors or acceptors in hydrogen-bonding interactions. Alongside the traditional metal catalysts and enzymes, organocatalysts are expected to become "*third catalyst*" in asymmetric synthesis. In the following sections (Sections 1.2.1–1.3), organocatalysts will be discussed in detail.

1.2.1. Discovery and Breakthrough

The first example of organocatalysis dates back to 1971. In that year, Wiechert reported that (*S*)-proline catalyzes the intramolecular Robinson annulation to produce the synthetically useful Wieland–Miescher ketone with a good yield and enantioselectivity (Scheme 1.1).[4a]

Scheme 1.1. Discovery of the first organocatalysis process

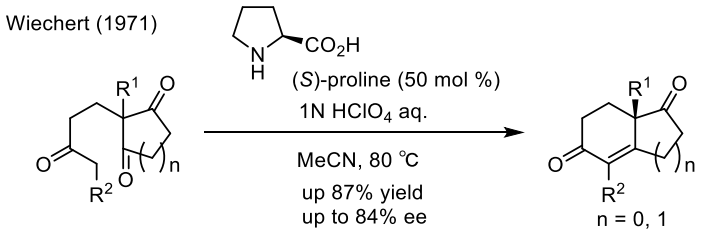

This report that a universal molecule like (*S*)-proline promotes enantioselective C–C bond formation can be regarded as a research breakthrough. However, since this study was conducted during the golden period of transition metal catalysis, it did not draw the attention it deserved, and its results were categorized as an example of a substrate-specific reaction.

In 2000, List and Barbas rediscovered the (*S*)-proline-catalyzed enantioselective intermolecular aldol reaction, and unlike what had been done in Wiechert's report, they performed it using a broad substrate scope.[4b] At the same time, MacMillan reported that a secondary amine derived from *L*-phenyl alanine promotes a Diels–Alder reaction that leads to the highly enantioselective formation of cyclohexanone derivatives (Scheme 1.2).[4c]

Scheme 1.2. Breakthrough of organocatalysis

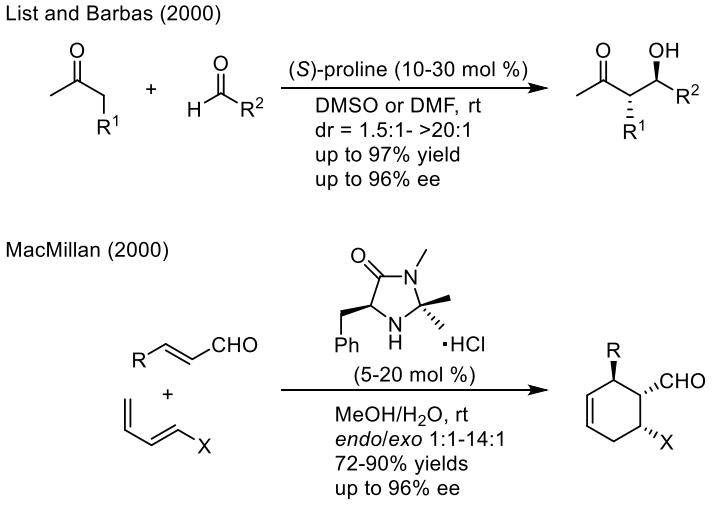

Since MacMillan defined this reaction as "*organocatalysis*," this approach to catalysis has become the focus of much active research. Therefore, the year 2000 is widely regarded as the year organocatalysis became in earnest a field of study. In fact, starting in 2000, the number of papers including the word "*organocatalyst*" in their titles has grown explosively (Figure 1.2). Representative examples of organocatalysts include proline-type catalysts (HOMO/LUMO activation),[5] ammonium-type catalysts (phase-transfer catalysts),[6] phosphoric-acid-type catalysts (Brønsted acids),[7] bifunctional-type catalysts (hydrogen bonding),[8] *N*-heterocyclic carbene-type catalysts (umpolung reaction),[9] guanidine-type catalysts (super base),[10] and tertiary phosphines and amines (Lewis bases)[11] (Figure 1.3).

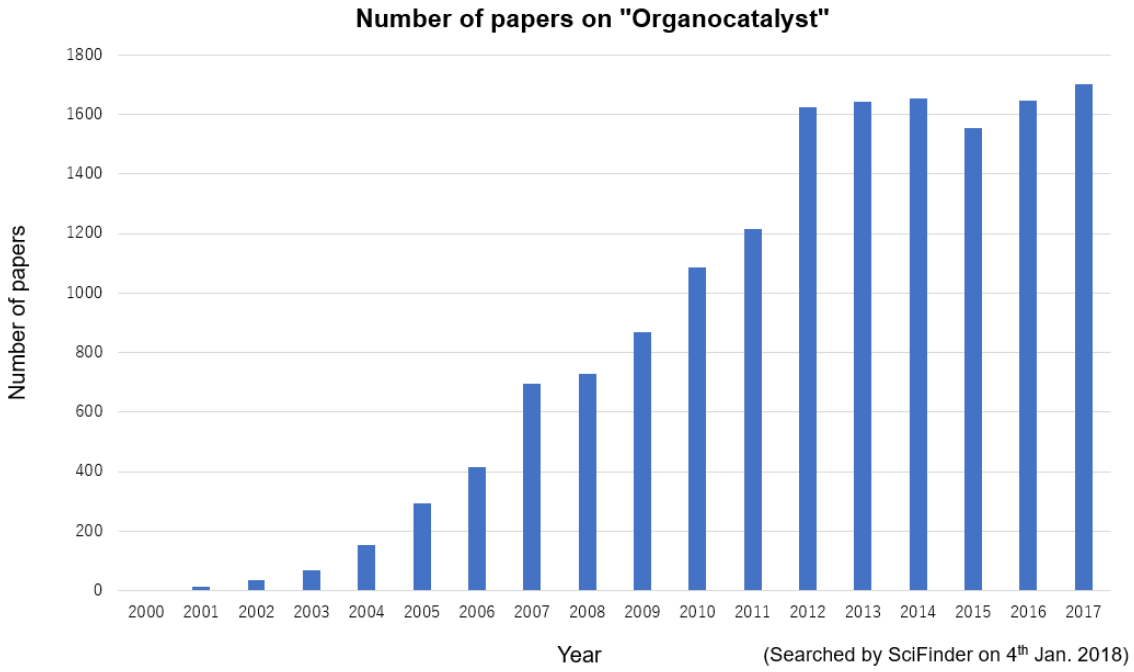

Figure 1.2. Number of papers on "Organocatalyst" from 2000

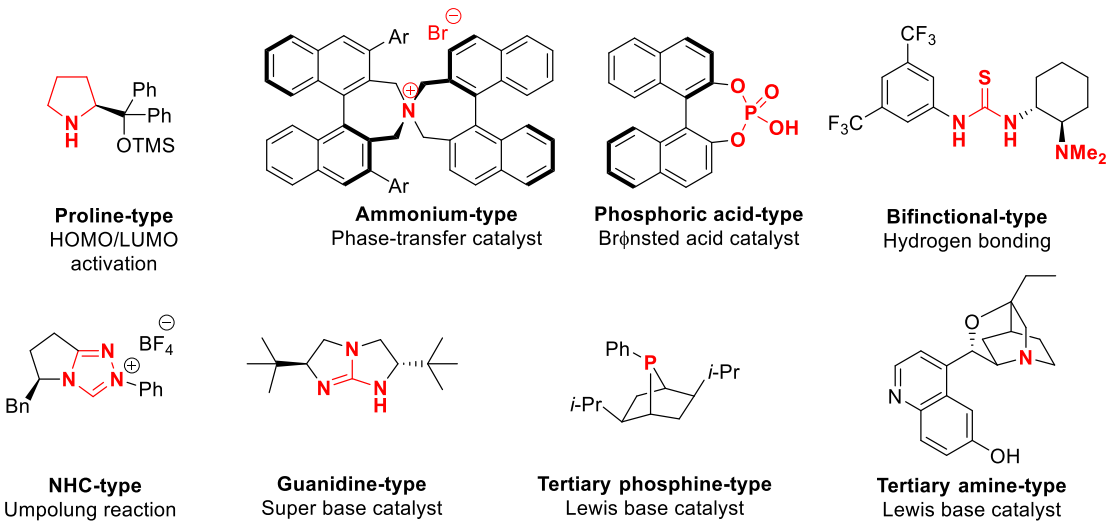

Figure 1.3. Representative organocatalysts

1.3. Lewis Base-Catalyzed C–C Bond Forming Reactions

Lewis bases, such as tertiary amines and phosphines, are known to act as organocatalysts via Michael addition to activated alkenes, like α,β-unsaturated carbonyl compounds, to generate enolate-type intermediates. These intermediates may then undergo various C–C bond forming reactions, which are summarized in Scheme 1.3.

Scheme 1.3. Overview of Lewis base-catalyzed C–C bond forming reactions

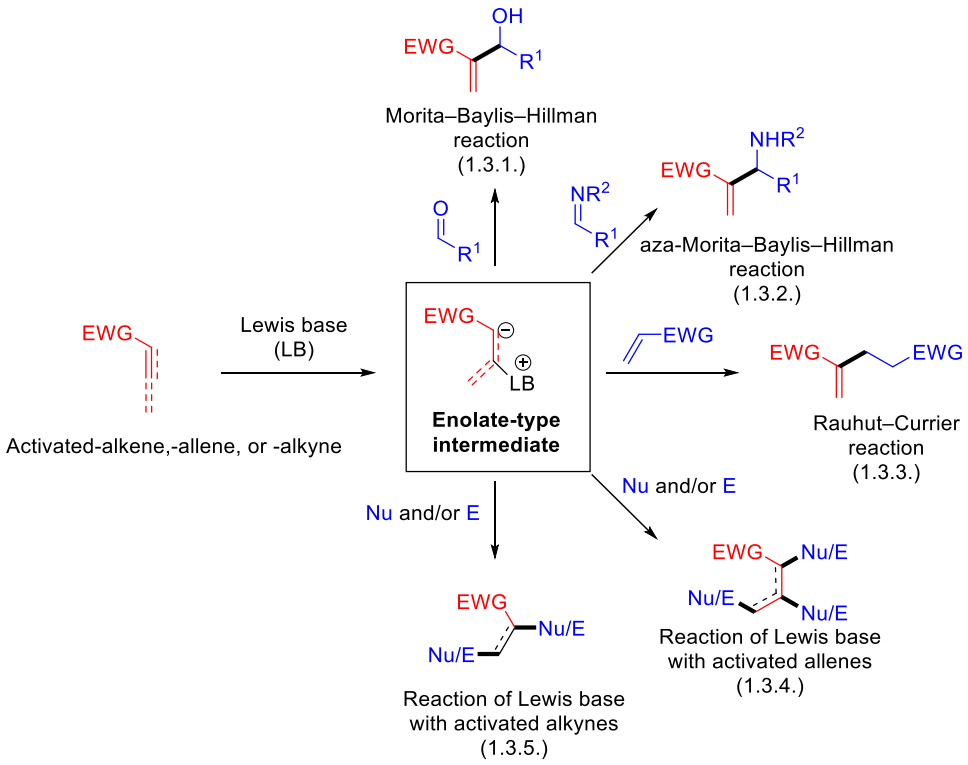

Since C–C bond formation is the most fundamental tool in organic synthesis, the fact that these bond formations are achieved in a metal-free environment is quite significant. Another great advantage of this approach is atom economy, which is 100% in many cases. In the sections that follow (Sections 1.3.1–1.3.5), representative examples of this synthetic approach are discussed.

1.3.1. Morita–Baylis–Hillman Reaction

Morita–Baylis–Hillman (MBH) reaction produces densely functionalized chiral allylic alcohols by way of the reaction of activated alkenes with aldehydes, in the presence of a Lewis base. Results from pioneering studies in this field are summarized in Scheme 1.4. In 1968, Morita reported the first example of MBH reaction using tricyclohexylphosphine as a Lewis base, despite the low conversion rate.[12b] The use of tricyclohexylphosphine as a catalyst is important in this context, as triphenylphosphine promotes the Wittig olefination via anion rearrangement as a side reaction.[12a] In 1972, Baylis and Hillman found that 1,4-

diazabicyclo[2.2.2]octane (DABCO) effectively catalyzes the same reaction reported by Morita to furnish the desired products in a high yield.[12c] The high nucleophilicity of DABCO, which results from the fact that its nitrogen center is less sterically hindered than the phosphorus of tricyclohexylphosphine, and its increased ability to act as a leaving group play a key role in the smoothness of the reaction. Despite it being reported later than the method that was first described by Morita, because of its practicality, the method introduced by Baylis and Hillman became widely utilized.

Scheme 1.4. Pioneering works of MBH reaction

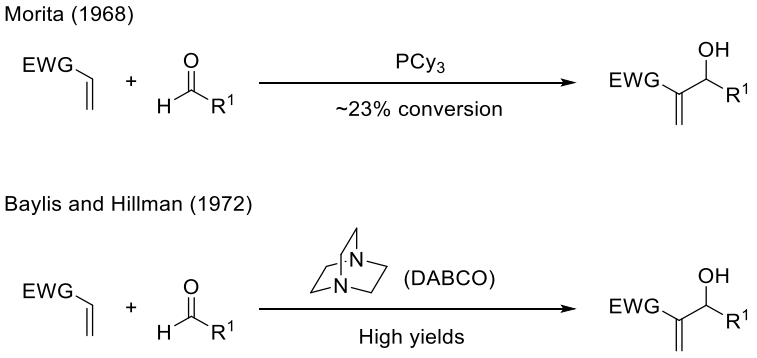

The general mechanism of the MBH reaction is depicted in Scheme 1.5. Initially, the Lewis base attacks the β-carbon of the activated alkene to form an enolate-type intermediate. Subsequently, an aldol-type C–C bond forms between this intermediate and an aldehyde. Finally, elimination of the Lewis base via proton transfer affords the desired product. Since the products of the MBH reaction are highly functionalized chiral allylic alcohols, this synthetic approach has been regarded as a fascinating methodology for the preparation of useful chiral building blocks. However, MBH reaction generally requires a long reaction time (a few days up to one month) because of the reversibility of the reaction. In general, the rate-determining step of the MBH reaction is the C–C bond formation and/or the elimination step, depending on the catalyst, substrates, and reaction conditions.[13] Therefore, accelerating the rate-determining step is one of the most important research goals to obtain useful MBH reactions.

Scheme 1.5. General reaction mechanism of MBH reaction

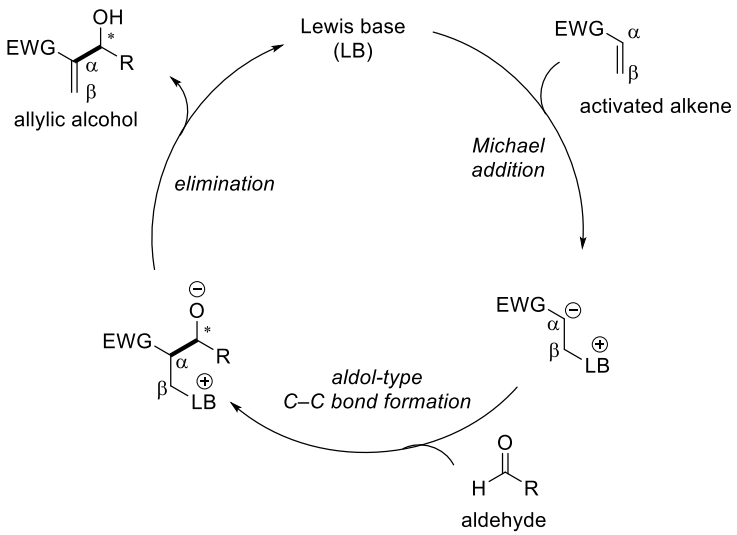

In 1988, Roos found that 3-hydroxyquinuclidine drastically accelerates the MBH reaction. After Michael addition of 3-hydroxyquinuclidine to acrylates, the intermediate gets stabilized by a hydrogen-bonding interaction involving the hydroxy group and the enolate moiety; as a result, the concentration of the active species, enolate, increases (top half of Scheme 1.6).[12d] In 1997, Ciganek investigated and ranked the reaction rates associated with the use of tertiary amines as catalysts of the MBH reaction (bottom half of Scheme 1.6).[12e] Other reported strategies to accelerate the MBH reaction include performing the reaction under a high pressure[14a] and using 1,8-diazabicyclo[5.4.0]undec-7-ene (DBU)[14b] as a catalyst.

Scheme 1.6. Reaction rate of tertiary amines in MBH reaction

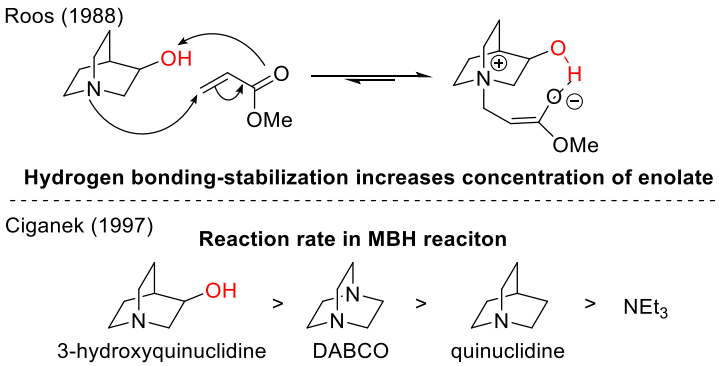

Based on these experimental results, in 1999, Hatakeyama and Iwabuchi achieved the first highly enantioselective MBH reaction catalyzed by a quinidine-derived chiral cinchona alkaloid (β-ICD) bearing a hydroxy group (Scheme 1.7).[12f] The hydroxy group of β-ICD plays a crucial role in this process by promoting

the enantioselectivity of the reaction. The same research group demonstrated the utility of optically active MBH reaction products as building blocks for the total synthesis of natural products and bioactive compounds.[12g-i]

Scheme 1.7. The first highly enantioselective MBH reaction

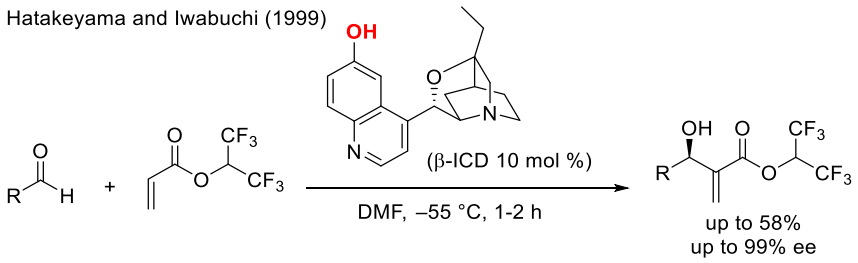

Since the 1999 report by Hatakeyama and Iwabuchi, a large number of research groups have investigated catalysts and substrates of the MBH reaction performed via cocatalysis,[15c-e] using inactive substrates like ketones and internal activated alkenes.[15f]

1.3.2. Aza-MBH Reaction

When an imine is employed as an acceptor instead of the aldehyde in an MBH reaction, the reaction is called aza-MBH reaction. The enantioselective aza-MBH reaction has been extensively studied, because it produces highly functionalized β-amino acid derivatives.[16,17] In 2002, Shi reported the first enantioselective aza-MBH reaction of aldimine catalyzed by β-ICD (Scheme 1.8).[17a]

Scheme 1.8. The first enantioselective aza-MBH reaction

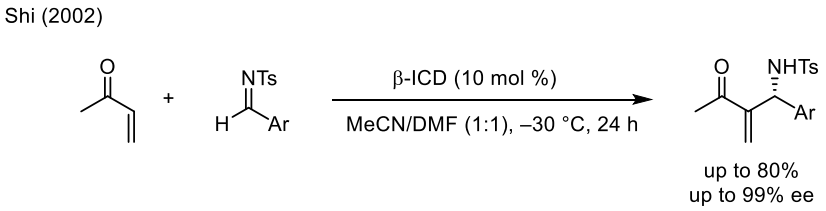

Ketimine, a ketone-derived imine, can also be used as a substrate in the aza-MBH reaction. Its use leads to the production of synthetically valuable β-amino acid derivatives bearing a chiral tetrasubstituted carbon stereogenic center. In 2013, three groups independently reported enantioselective aza-MBH reactions involving ketimines (Scheme 1.9).[18a-c]

Scheme 1.9. Early examples of enantioselective aza-MBH reaction of ketimines

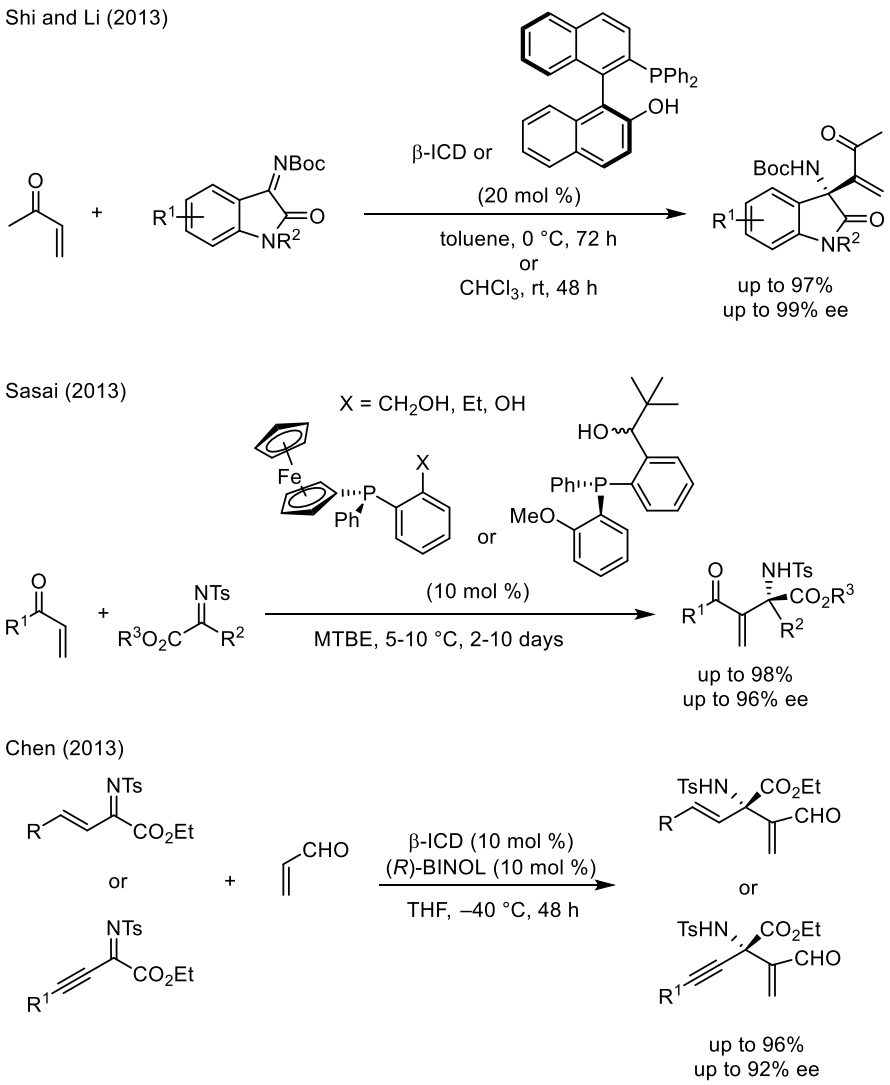

1.3.3. Rauhut–Currier Reaction

Rauhut–Currier (RC) reaction consists in a Lewis base-catalyzed C–C bond forming reaction that proceeds via the coupling of two α,β-unsaturated carbonyl compounds, wherein one acts as a latent enolate giving exo-methylidene products (Scheme 1.10). This reaction was first discovered by Rauhut and Currier in 1963.[19] The RC reaction can be considered as a vinylogous-MBH reaction, because it relies on the use of a vinyl compound as a Michael acceptor, instead of the aldehyde used in the "classic" MBH reaction.

Scheme 1.10. General reaction mechanism of Rauhut–Currier (RC) reaction

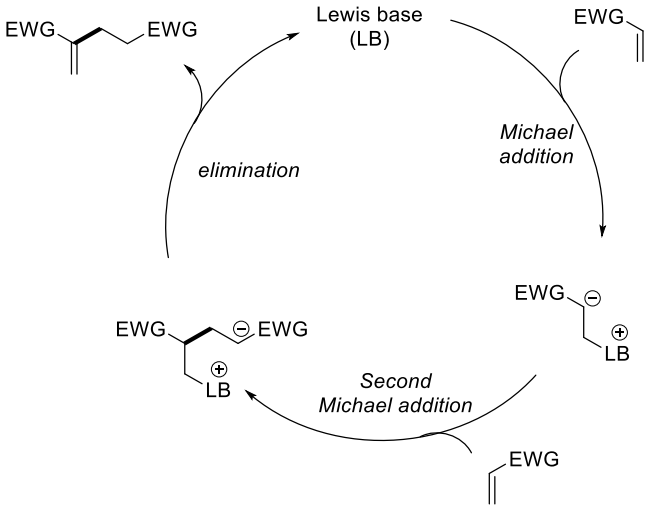

Although the implementation of the RC reaction leads to the synthesis of highly functionalized exo-methylidene compounds, activated alkenes are less reactive than aldehydes and imines in the MBH reaction. Furthermore, the use of two kinds of activated alkenes often results in the formation of a mixture of up to four isomers derived from two homocouplings and two heterocouplings (Scheme 1.11).[20a] Therefore, only a few reports have been published on the application of the RC reaction to the synthesis of useful compounds.[21a-c,23]

Scheme 1.11. Issues of RC reaction in reactivity and chemoselectivity

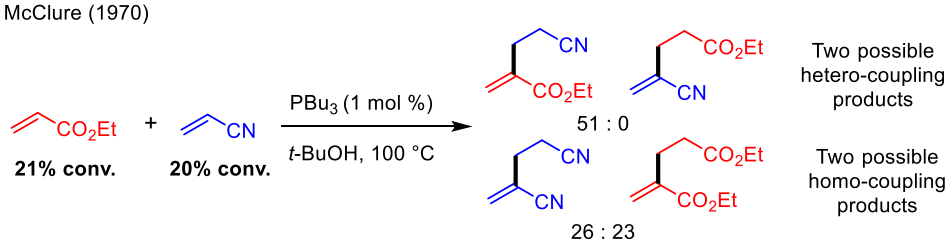

The first enantioselective RC reaction was reported by Miller in 2007. To avoid the mentioned problems associated with low reactivity and chemoselectivity, a symmetrical bis(enone) was employed as the substrate of an intramolecular RC reaction (Scheme 1.12).[21d]

Scheme 1.12. The first enantioselective RC reaction

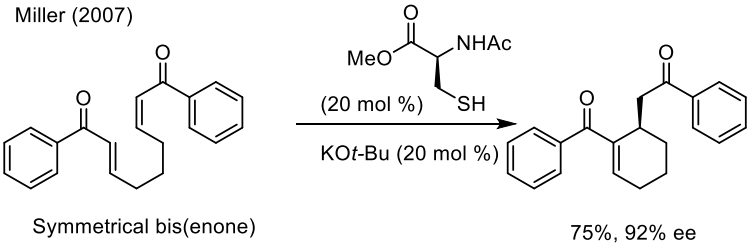

Since the publication of this study, some additional enantioselective intramolecular RC reactions have been reported, including the use of asymmetrical substrates.[21a-c,e] However, they are all intramolecular reactions, so as to avoid the reactivity and chemoselectivity issues associated with the implementation of intermolecular reactions.

In 2015, Huang and Zhang independently presented the first enantioselective intermolecular RC reaction of enones with activated internal alkenes (Scheme 1.13).[22a,b] Despite the reports being independent, the two groups used the same substrate, in a reaction course that also exemplified the difficulty of controlling the selectivity of RC reactions.

Scheme 1.13. Pioneering works on enantioselective intermolecular RC reaction

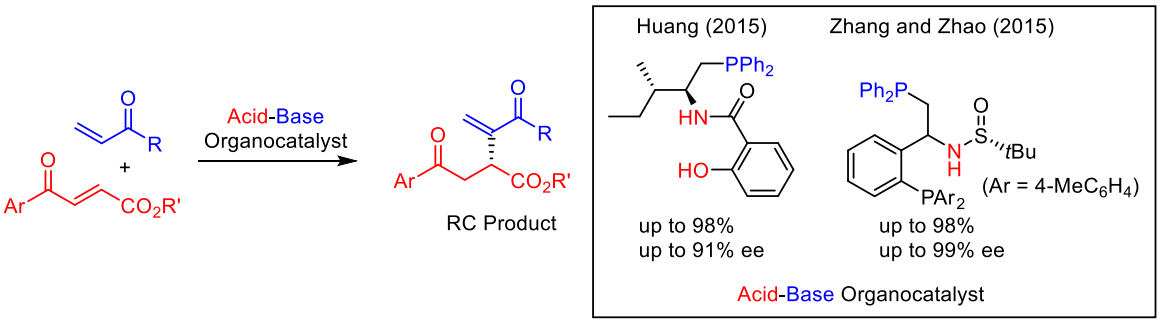

As discussed above, to date, the main focus of research conducted on the RC reaction has been the design of substrates. Consequently, only a few reports exist on the application of the enantioselective RC reaction for the synthesis of useful building blocks.[23]

1.3.4. Reactions of Lewis Bases with Activated Allenes

In MBH and RC reactions described above, nucleophilicity occurs at the α-position of enones by nucleophilic addition of Lewis base. On the other hand, the reaction between a Lewis base and an activated allene forms nucleophilicity at the γ-position, also. The resulting zwitterionic intermediate can undergo a variety of reactions with nucleophiles and/or electrophiles to afford structurally diverse products (Scheme 1.14).

Scheme 1.14. Reactions of Lewis base with allenoates

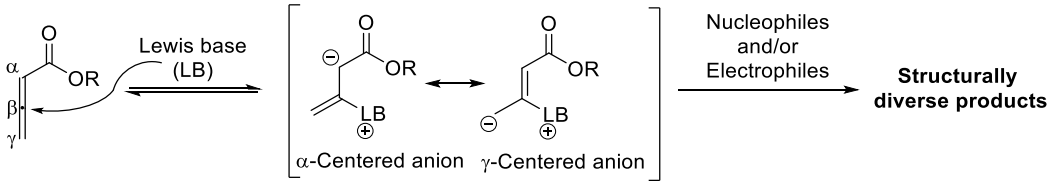

In 1995, Zhang and Lu found that, in the presence of triphenylphosphine as a Lewis base, the reaction between an allenoate and an acrylate as an electrophile produces a five-membered ring via [3+2] annulation.[24c] Although this reaction was a straightforward approach for obtaining complex molecules from simple substrates, it gives a mixture of regioisomers **2** (α-adduct) and **2′** (γ-adduct) (top half of Scheme 1.15). In 1997, Zhang reported the catalytic regio- and enantioselective reaction (bottom half of Scheme 1.15).[24d]

Scheme 1.15. [3+2] annulation between allenoate and acrylate

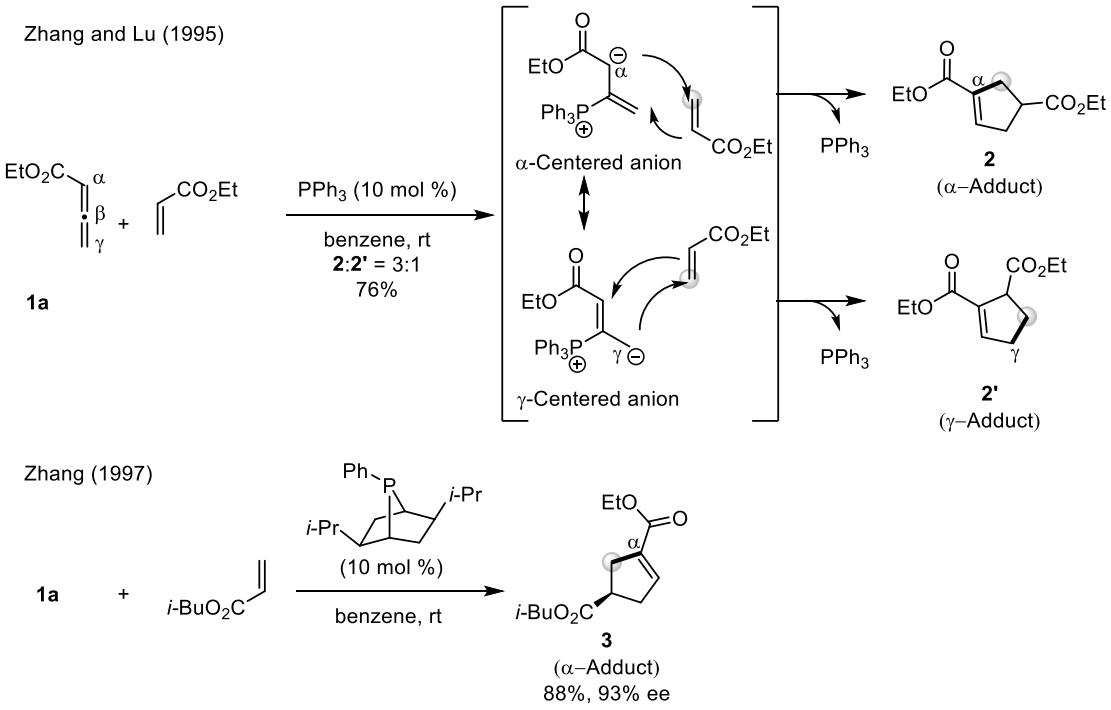

Since these reports, this type of enantioselective formal annulation using allenoates has been widely investigated for the synthesis of cyclic compounds. As representative examples, in 2006, Fu reported the synthesis of spirocycles via selective γ-addition to an allenoate, and in 2008, Jacobsen achieved the synthesis of *N*-heterocycles via selective α-addition.[24e,f]

Notably, the zwitterionic intermediate alluded to above can also react with a pronucleophile bearing acidic protons.[25] Based on the stoichiometric stepwise reaction reported by Cristau, Trost achieved in 1994 the first catalytic reaction of this type (Scheme 1.16).[25a,b] In it, an α-centered anion abstracts the proton of malonate to become activated. Subsequently, the malonate attacks the γ-position induced by the electron-withdrawing ability of the phosphonium moiety. This reaction can be regarded as an umpolung reaction, since the nucleophile (malonate) is installed at the nucleophilic γ-position of the allenoate.

Scheme 1.16. The first example of nucleophilic addition at γ-position of allenoate

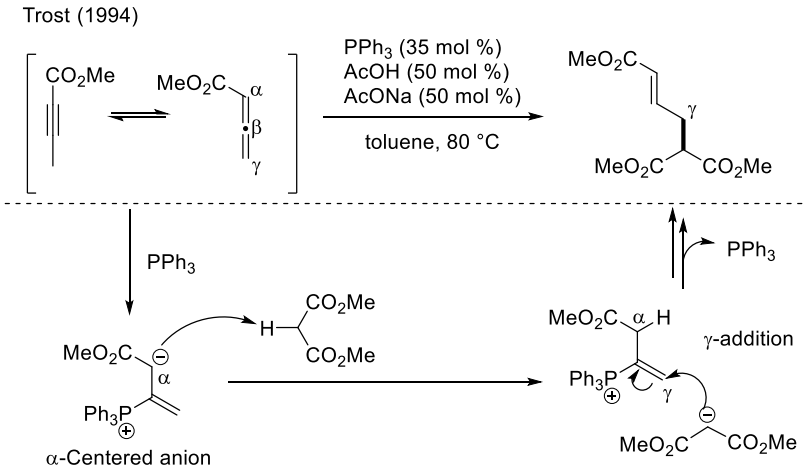

The first enantioselective reaction of this type was reported by Zhang in 1998 (Scheme 1.17).[26a] In this case, the chiral center is generated at the δ-position.

Scheme 1.17. Enantioselective nucleophilic additions at γ-position of allenoate

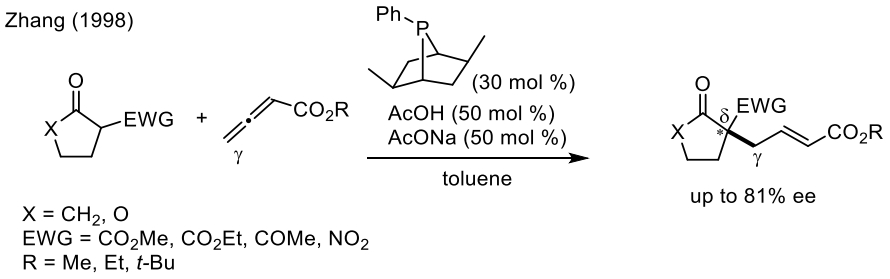

Fu and coworkers have extensively studied the enantioselective γ-addition of allenoates. They used for this reaction a number of different pronucleophiles, such as nitromethane,[26b] thiols,[26c] and alcohols[26d], which can nucleophilically attack allenoates at the substrate's γ-position, in a process catalyzed by a selection of appropriate chiral phosphines.

Despite the unique reactivity of activated allenes, few reports have been published on the use of these species for the synthesis of important structural motifs, because of the difficulty of achieving chemo-, regio-, and stereoselective control of the products.

1.3.5. Reactions of Lewis Base with Activated Alkynes

The reaction of Lewis bases with activated alkynes, like alkynals, alkynones, and alkynoates, also produces enolate-type intermediates (int. A) shown in Scheme 1.18, which undergoes a variety of C–C and C–X bond forming reactions with pronucleophiles.[27]

Scheme 1.18. Overview of the reactions of activated alkynes with Lewis base

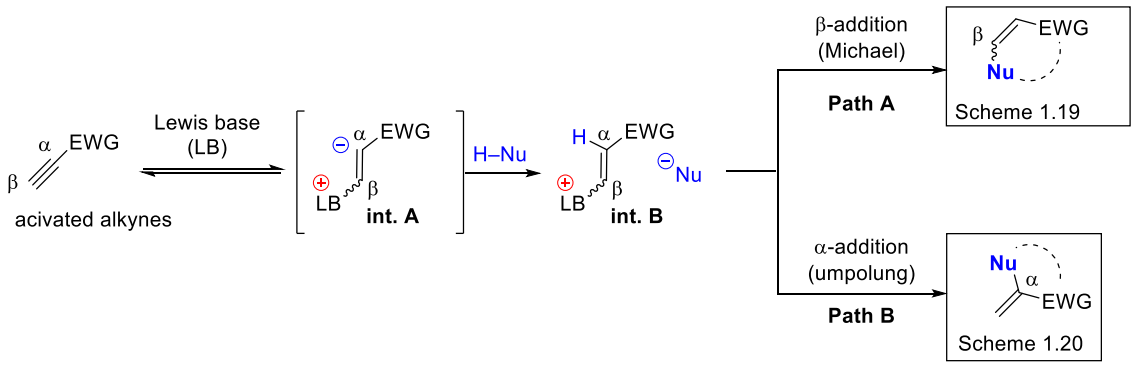

In 1993, Inanaga presented the first phosphine-catalyzed Michael addition of activated alkynes (Scheme 1.19, Path A).[28a] A variety of primary and secondary alcohols undergo the reaction within 30 min with high *E*-selectivity. Because of this high reactivity and selectivity, in 1999, Evans successfully employed this phosphine-catalyzed Michael addition of alkynoate to realize the total synthesis of (−)-kumausallene.[28d] After this result was published, a variety of substrates have become available by studies of some groups.[28b,e-g]

Scheme 1.19. The first example of phosphine-catalyzed Michael addition of activated alkynes

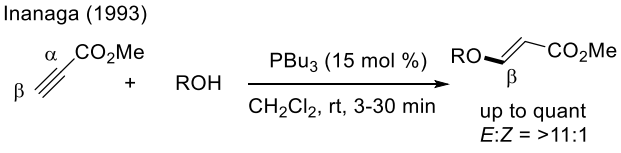

When a nitrogen-containing or, a bulky nucleophile is employed for the Lewis base-catalyzed reaction of activated alkynes, an α-nucleophilic addition occurs in some cases (Scheme 1.18, Path B).[29] This reaction can be regarded as an umpolung Michael-type reaction, which is one of the effective strategies to access natural and unnatural amino acid derivatives. In a pioneering study published in 1997, Trost presented the phosphine-catalyzed α-addition of alkynoate with sulfonamide or phthalimide affording dehydro-amino acids (Scheme 1.20).[29b]

Scheme 1.20. The first example on α-addition of activated alkyne

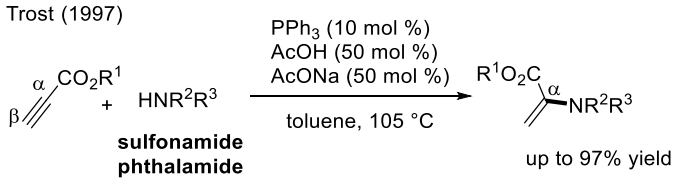

After the publication of this work, some research groups have described the α-nucleophilic addition between activated alkynes and a variety of nitrogen-,[29c-d,j] oxygen-,[29b,g,h] and sulfur-based nucleophiles.[29i] However, performing this reaction often produces regioisomers resulting from the concomitant formation of α- and β-nucleophilic adducts. Therefore, only two examples of the application of α-nucleophilic addition exist: the synthesis of thrombin inhibitors[29e] and ligands.[29f]

1.4. Purpose and Outline of This Thesis

As described in the previous sections (Sections 1.3.1–1.3.5), although Lewis base-catalyzed C–C bond formation can be a straightforward and atom-economical approach for accessing complex molecules in the absence of metal-based catalysts, these reactions have not yet fully demonstrated their potential, because of their sometimes unsatisfactory chemo-, regio-, and stereoselectivity. The goal of this thesis is to develop practical Lewis base-catalyzed reactions for the preparation of synthetically attractive chiral molecules via precise control. In this thesis, the author describes the enantioselective synthesis of pharmaceutically important and highly functionalized *N*- and *O*-heterocycles with tetrasubstituted chiral carbon centers via organocatalyzed C–C bond forming reactions: aza-MBH reaction, RC reaction, and the umpolung transformations of activated allenes and alkynes. As part of this research work, a novel organocatalyst was developed, as well as new reaction courses. This thesis consists of the four chapters described below.

Chapter 2 details the enantiodivergent synthesis of 3-amino-2-oxindoles, whose enantiomers are both desirable compounds to synthesize, via aza-MBH reaction. Both enantiomers of these species could be obtained by the selection of organocatalysts under identical reaction conditions.

Chapter 3 describes the enantioselective synthesis of α-methylidene-γ-lactams via an amidation/RC reaction sequence catalyzed by a newly developed chiral amine catalyst. This reaction is the first example of an enantioselective RC reaction involving acrylamide.

Chapter 4 details the phosphine-catalyzed enantioselective synthesis of tetrahydrobenzofuranones via an unprecedented β,γ-dual umpolung reaction involving allenoates.

Chapter 5 discusses the synthesis of the medicinally important intermediates hydroindoles and hydrobenzofurans, which bear a carbonyl group at their 2-positions, via a novel dual umpolung domino Michael reaction involving alkynoates. The hydroindole-2-carboxylates thus obtained could be delivered to an analog of a bioactive compound.

1.5. References

1. (a) Knoche, B.; Blaschke, G. *J. Chromatogr. A* **1994**, *660*, 235. (b) Nishimura, K.; Hashimoto, Y.; Iwasaki, S. *Chem. Pharm. Bull.* **1994**, *42*, 1157. (c) Wnendt, S.; Finkam, M.; Winter, W.; Ossing, J.; Rabbe, G.; Zwingenberger, K. *Chirality* **1996**, *8*, 390.
2. (a) Miyashita, A.; Yasuda, A.; Takaya, H.; Toriumi, K.; Ito, T.; Souchi, T.; Noyori, R. *J. Am. Chem. Soc.* **1980**, *102*, 7932. (b) Knowles, W. S. *Angew. Chem. Int. Ed.* **2002**, *41*, 1998. (c) Noyori, R. *Angew. Chem. Int. Ed.* **2002**, *41*, 2008.
3. Katsuki, T.; Sharpless, K. B. *J. Am. Chem. Soc.* **1980**, *102*, 5974.
4. (a) Ender, U.; Sauer, G.; Wiechert, R. *Angew. Chem. Int. Ed.* **1971**, *10*, 496. (b) List, B.; Lerner, R.

A.; Barbas, C. F., III *J. Am. Chem. Soc.* **2000**, *122*, 2395. (c) Ahrendt, K. A.; Borths, C. J.; MacMillan, D. W. C. *J. Am. Chem. Soc.* **2000**, *122*, 4243.

5. For reviews of proline-type catalyst, see: (a) Jensen, K. L.; Dickmeiss, G.; Jiang, H.; Albrecht, L.; Jørgensen, K. A. *Acc. Chem. Res.* **2012**, *45*, 248. (b) Wroblewska, A. *Synlett* **2012**, *23*, 953. Pioneering works, see: (c) Marigo, M.; Wabnitz, T. C.; Fielenbach, D.; Jørgensen, K. A. *Angew. Chem. Int. Ed.* **2005**, *44*, 794. (d) Hayashi, Y.; Gotoh, H.; Hayashi, T.; Shoji, M. *Angew. Chem. Int. Ed.* **2005**, *44*, 4212. (e) Franzen, J.; Marigo, M.; Fielenbach, D.; Wabnitz, T. C.; Kjarsgaard, A.; Jørgensen, K. A. *J. Am. Chem. Soc.* **2005**, *127*, 18296.
6. For reviews of asymmetric phase-transfer reactions, see: (a) Shirakawa, S.; Maruoka, K. *Angew. Chem. Int. Ed.* **2013**, *52*, 4312. Pioneering works, see: (b) Dolling, U. H.; Davis, P.; Edward J. J.; Grabowski, E. J. J. *J. Am. Chem. Soc.* **1984**, *106*, 446. (c) Ooi, T.; Kameda, M.; Maruoka, K. *J. Am. Chem. Soc.* **1999**, *121*, 6519.
7. For recent reviews of phosphoric acid catalyst, see: (a) Akiyama, T. *J. Synth. Org. Chem. Jpn.* **2011**, *69*, 913. (b) Terada, M. *Synthesis* **2010**, 1929. Pioneering works, see: (c) Akiyama, T.; Itoh, J.; Yokota, K.; Fuchibe, K. *Angew. Chem. Int. Ed.* **2004**, *43*, 1566. (d) Uraguchi, D.; Terada, M. *J. Am. Chem. Soc.* **2004**, *126*, 5365.
8. For reviews of bifunctional catalyst, see: (a) Takemoto, Y.; *Chem. Pharm. Bull.* **2010**, *58*, 593. (b) Zhang, Z.; Schreiner, P. R. *Chem. Soc. Rev.* **2009**, *38*, 1187. (c) Doyle, A. G.; Jacobsen, E. N. *Chem. Rev.* **2007**, 107, 5713. Pioneering works, see: (d) Vachal, P.; Jacobsen, E. N. *J. Am. Chem. Soc.* **2002**, *124*, 10012. (e) Okino, T.; Hoashi, Y.; Takemoto, Y. *J. Am. Chem. Soc.***2003**, *125*, 12672. (f) McCooey, S. H.; Connon, S. J. *Angew. Chem. Int. Ed.* **2005**, *44*, 6367.
9. For review of NHC as organocatalyst, see: (a) By Dwivedi, S.; Gupta, S.; Das, S. *Current Organocatalysis* **2014**, *1*, 13. Pioneering work, see: (b) Kerr, M. S.; Alaniz, J. R.; Rovis, T. *J. Am. Chem. Soc.* **2002**, *124*, 10298.
10. For recent reviews of chiral guanidine-catalysis, see: (a) Yuan, J.; Li, M.; Ji, N.; He, W.; Liu, Y. *Current Organic Chemistry* **2017**, *21*, 1205. (b) Wee, K. C.; Tan, C. T. *RSC Green Chemistry Series (Sustainable Catalysis, Part 2)* **2016**, *41*, 381.
11. For recent reviews of Lewis base-catalysis, see: (a) Li, H.; Lu, Y. *Asian J. Org. Chem.* **2017**, *6*, 1130. (b) Denmark, S. E.; Beutner, G. L. *Angew. Chem. Int. Ed.* **2008**, *47*, 1560.
12. (a) Oda, R.; Kawabata, T.; Tanimoto, S. *Tetrahedron Lett.* **1964**, 1653. (b) Morita, K.; Suzuki, Z.; Hirose, H. *Bull. Chem. Soc. Jpn.* **1968**, *41*, 2815. (c) Baylis, A. B.; Hillman, M. E. D. *German Patent* 2155113, **1972**. (d) Drewes, S. E.; Freese, S. D.; Emslie, N. D.; Roos, G. H. P. *Synth. Comm.* **1988**, *18*, 1565. (e) Ciganek, E. *Org. React.* **1997**, *51*, 201. (f) Iwabuchi, Y.; Nakatani, M.; Yokoyama, N.; Hatakeyama, S. *J. Am. Chem. Soc.* **1999**, *121*, 10219. (g) Iwabuchi, Y.; Furukawa, M.; Esumi, T.; Hatakeyama, S. *Chem. Commun.* **2001**, 2030. (h) Iwabuchi, Y.; Sugihara, T.; Esumi, T.; Hatakeyama, S. *Tetrahedron Lett.* **2001**, *42*, 7867. (i) Sarkar, S. M.; Wanzala, E. N.; Shibahara, S.; Takahashi, K.; Ishihara, J.; Hatakeyama, S. *Chem. Commun.* **2009**, 5907.

13. (a) Hoffmann, H. M. R.; Rabe, J. *Angew. Chem. Int. Ed.* **1983**, *22*, 795. (b) Hill, J. S.; Isaacs, N. S. *J. Phys. Org. Chem.* **1990**, *3*, 285. (c) Price, K. E.; Broadwater, S. J.; Walker, B. J.; McQuade, D. T. *J. Org. Chem.* **2005**, *70*, 3980. (d) Price, K. E.; Broadwater, S. J.; Jung, H. M.; McQuade, D. T. *Org. Lett.* **2005**, *7*, 147. (e) Aggarwal, V. K.; Fulford, S. Y.; Lloyd-Jones, G. C. *Angew. Chem. Int. Ed.* **2005**, *44*, 1706. (f) Robiette, R.; Aggarwal, V. K.; Harvey, J. N. *J. Am. Chem. Soc.* **2007**, *129*, 15513. (g) Lindner, C.; Liu, Y.; Karaghiosoff, K.; Maryasin, B.; Zipse, H. *Chem. Eur. J.* **2013**, *19*, 6429. (h) Verma, P.; Verma, P.; Sunoj, R. B. *Org. Biomol. Chem.* **2014**, *12*, 2176. (i) Plata, R. E.; Singleton, D. A. *J. Am. Chem. Soc.* **2015**, *137*, 3811. (j) Galaverna, R.; Camilo, N. S.; Godoi, M. N.; Coelho, F.; Eberlin, M. N. *J. Org. Chem.* **2016**, *81*, 1089.
14. (a) Hill, J. S.; N. S. Isaacs, N. S. *Tetrahedron Lett.* **1986**, *27*, 5007. (b) Aggarwal, V. K.; Mereu, A. *Chem. Commun.* **1999**, 2311.
15. For recent reviews of MBH reaction, see: (a) Pellissier, H. *Tetrahedron* **2017**, *73* 2831. (b) Basavaiah, D.; Reddy, G. C. *ARKIVOC* **2016**, *ii*, 172. (c) Wei, Y.; Shi, M. *Chem. Rev.* **2013**, *113*, 6659. Representative examples, see: (c) Yamada, Y. M. A.; Ikegami, S. *Tetrahedron Lett.* **2000**, *41*, 2165. (d) McDougal, N. T.; Schaus, S. E. *J. Am. Chem. Soc.* **2003**, *125*, 12094. (e) Sohtome, Y.; Tanatani, A.; Hashimoto, Y.; Nagasawa, K. *Tetrahedron Lett.* **2004**, *45*, 5589. (f) Liu, Y.-L.; Wang, B.-L.; Cao, J.-J.; Chen, L.; Zhang, Y.-X.; Wang, C.; Zhou, J. *J. Am. Chem. Soc.* **2010**, *132*, 15176.
16. For review of aza-MBH reaction, see: Sasai, H.; Takizawa, S. *Comprehensive Chirality* **2012**, *6*, 234.
17. (a) Shi, M.; Xu, Y.-M. *Angew. Chem. Int. Ed*. **2002**, *41*, 4507. (b) Matsui, K.; Takizawa, S.; Sasai, H. *J. Am. Chem. Soc.* **2005**, *127*, 3680.
18. (a) Hu, F.-L.; Wei, Y.; Shi, M.; Pindic, S.; Li, G. *Org. Biomol. Chem.* **2013**, *11*, 1921. (b) Takizawa, S.; Rémond, E.; Arteaga, F. A.; Yoshida, Y.; Sridharan, V.; Bayardon, J.; Jugé S.; Sasai, H. *Chem. Commun.* **2013**, *49*, 8392. (c) Yao, Y.; Li, J.-L.; Zhou, Q.-Q.; Dong, L.; Chen, Y.-C. *Chem. Eur. J.* **2013**, *19*, 9447.
19. Rauhut, M. M.; Currier, H. *Patent* 3074999, **1963**.
20. McClure, J. D. *J. Org. Chem*. **1970**, *35*, 3045.
21. For reviews of Rauhut–Currier reaction, see: (a) Aroyan, C. E.; Dermenci, A.; Miller, S. J. *Tetrahedron* **2009**, *65*, 4069. (b) Xie, P.; Huang, Y. *Eur. J. Org. Chem.* **2013**, 6213. (c) Bharadwaj, K. C. *RSC Adv*. **2015**, *5*, 75923. Selected examples, see: (d) Aroyan, C. E.; Miller, S. J. *J. Am. Chem. Soc*. **2007**, *129*, 256. (e) Marques-Lopez, E.; Herrera, R. P.; Marks, T.; Jacobs, W. C.; Konning, D.; de Figueiredo, R. M.; Christmann, M. *Org. Lett*. **2009**, *11*, 4116.
22. (a) Dong, X.; Liang, L.; Li, E.; Huang, Y. *Angew. Chem. Int. Ed.* **2015**, *54*, 1621. (b) Zhou, W.; Su, X.; Tao, M.; Zhu, C.; Zhao, Q.; Zhang, J. *Angew. Chem. Int. Ed.* **2015**, *54*, 14853.
23. (a) Takizawa, S.; Nguyen, T. M.-N.; Grossmann, A.; Enders, D.; Sasai H. *Angew. Chem. Int. Ed.* **2012**, *51*, 5423. (b) Takizawa, S.; Nguyen, T. M.-N.; Grossmann, A.; Suzuki, M.; Enders, D.; Sasai H. *Tetrahedron* **2013**, *69*, 1202. (c) Jeon, S.; Han, S. *J. Am. Chem. Soc.* **2017**, *139*, 6302.

24. For recent reviews of reactions of Lewis base with allenes, see: (a) Wang, Z.; Xub, X.; Kwon, O. *Chem. Soc. Rev.* **2014**, *43*, 2927. (b) Zhao Q.-Y.; Lian, Z.; Wei, Y.; Shi, M. *Chem. Commun.* **2012**, *48*, 1724. Selected examples, see: (c) Zhang, C.; Lu, X. *J. Org. Chem.* **1995**, *60*, 2906. (d) Zhu, G.; Chen, Z.; Jiang, Q.; Xiao, D.; Cao, P.; Zhang, X. *J. Am. Chem. Soc.* **1997**, *119*, 3836. (e) Wilson, J. E.; Fu, G. C. *Angew. Chem. Int. Ed.* **2006**, *45*, 1426. (f) Fang, Y.-Q.; Jacobsen, E. N.; *J. Am. Chem. Soc.* **2008**, *130*, 5660.

25. (a) Cristau, H.-J.; Viala, J.; Christol, H. *Tetrahedron Lett*. **1982**, *23*, 1569. (b) Trost, B. M.; Li, C.-J. *J. Am. Chem. Soc.* **1994**, *116*, 3167.

26. (a) Chen, Z.; Zhu, G.; Jiang, Q.; Xiao, D.; Cao, P.; Zhang, X. *J. Org. Chem.* **1998**, *63*, 5631. (b) Smith, S. W.; Fu, G. C. *J. Am. Chem. Soc.* **2009**, *131*, 14231. (c) Sun, J.; Fu, G. C. *J. Am. Chem. Soc.* **2010**, *132*, 4568. (d) Ziegler, D. T.; Fu, G. C. *J. Am. Chem. Soc.* **2016**, *138*, 12069.

27. Review, see: Fraile, A.; Parra, A.; Tortosa, M.; Alemán, J. *Tetrahedron*, **2014**, *70*, 9145.

28. (a) Inanaga, J.; Baba, Y.; Hanamoto, T. *Chem. Lett.* **1993**, 241. (b) Kuroda, H.; Tomita, I.; Endo, T. *Synth. Commun.* **1996**, *26*, 1539. (c) Yavari, I.; Hekmat-Shoar, R.; Zonouzi, A. *Tetrahedron Lett.* **1998**, *39*, 2391. (d) Evans, P. A.; Murthy, V. S.; Roseman, J. D.; Rheingold, A. L. *Angew. Chem. Int. Ed.* **1999**, *38*, 3175. (e) Liu, B.; Davis, R.; Joshi, B.; Reynolds, D. W. *J. Org. Chem.* **2002**, *67*, 4595. (f) Pedduri, Y.; Williamson, J. S. *Tetrahedron Lett.* **2008**, *49*, 6009. (g) Tejedor, D.; Méndez, S. J. Á.; Soria, J. M. L.; Martín, V. S.; Tellado, F. G. *Eur. J. Org. Chem.* **2014**, 198.

29. (a) Wilson, I. F.; Tebby, J. C. *J. Chem. Soc. Perkin Trans. 1* **1972**, 2830. (b) Trost, B. M.; Dake, G. R. *J. Am. Chem. Soc.* **1997**, *119*, 7595. (c) Yavari, I.; Norouzi-Arasi, H. *Phosphorus, Sulfur Silicon Relat. Elem.* **2002**, *177*, 87. (d) Lu, C.; Lu, X. *Org. Lett.* **2002**, *4*, 4677. (e) Boatman, P. D.; Urban, J.; Nguyen, M.; Qabar, M.; Kahn, M. *Bioorg. Med. Chem. Lett.* **2003**, *13*, 1445. (f) Meunier, S.; Siaugue, J.-M.; Sawicki, M.; Calbour, F.; Dézard, S.; Taran, F.; Mioskowski, C. *J. Comb. Chem.* **2003**, *5*, 201. (g) Silva, F.; Sawicki, M.; Gouverneur, V. *Org. Lett.* **2006**, *8*, 5417; (h) Gabillet, S.; Lecerclé, D.; Loreau, O.; Dézard, S.; Gomis, J.-M.; Taran, F. *Synthesis* **2007**, 515. (i) Gabillet, S.; Lecerclé, D.; Loreau, O.; Carboni, M.; Dézard, S.; Gomis, J.-M.; Taran, F. *Org. Lett.* **2007**, *9*, 3925. (j) Carboni, M.; Gomis, J.-M.; Loreau, O.; Taran, F. *Synthesis* **2008**, 417.

Chapter 2
Enantiodivergent Synthesis of 3-Amino-2-Oxindoles via Aza-MBH Reaction of Isatin-Derived Ketimines with Acrolein

Abstract: A highly enantioselective aza-Morita−Baylis−Hillman (aza-MBH) reaction of isatin-derived ketimines with acrolein was developed, which is based on the use of β-isocupreidine (β-ICD) or α-isocupreine (α-ICPN) as chiral acid–base organocatalysts. The present protocol readily furnished (*S*)- or (*R*)-3-amino-2-oxindoles containing a chiral tetrasubstituted carbon stereogenic center in up to 98% ee.

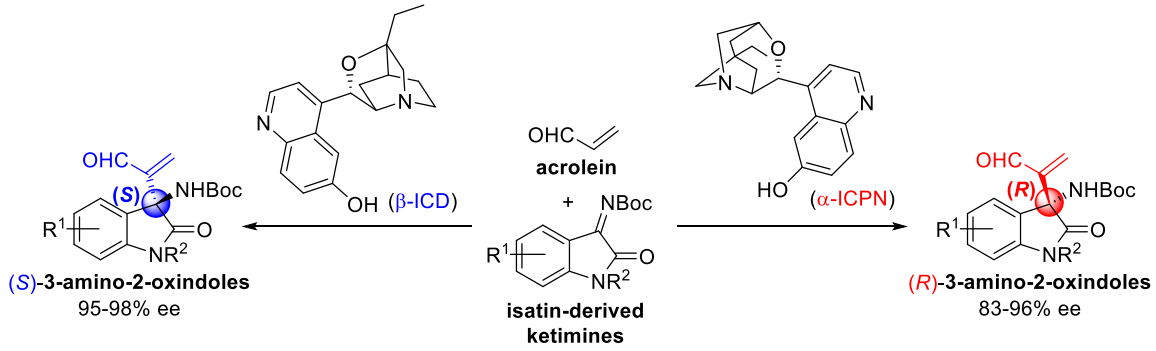

2.1. Introduction

Chiral 3-amino-2-oxindoles are important structural motifs that are found in various biologically active compounds, such as AG-041R, a gastrin/cholecystokinin-B receptor antagonist, and nelivaptan (SSR-149,415), an orally active, nonpeptidic vasopressin receptor antagonist. Some spiro-type 3-amino-2-oxindoles are also known to display a biological activity. In fact, some of these compounds are antitumor and antibacterial agents (Figure 2.1).[1] Since these compounds have (*S*)- or (*R*)-configuration, the enantiodivergent construction of their skeleton is an important synthetic goal to achieve.

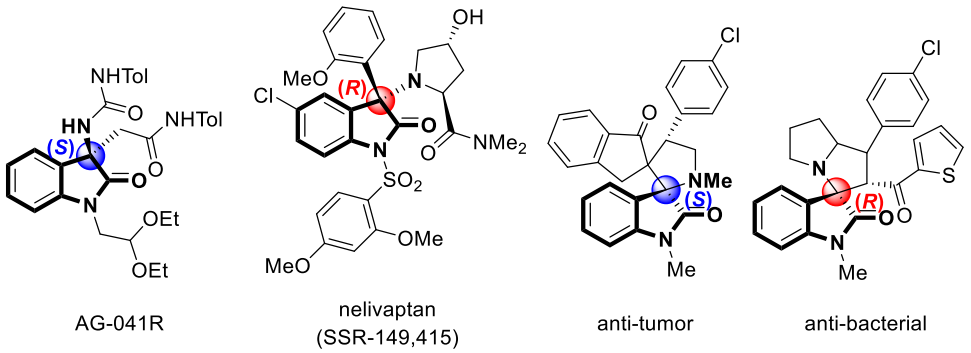

Figure 2.1. The elected bioactive compounds bearing 3-amino-2-oxindole skeleton

To date, considerable efforts have been devoted to the development of efficient strategies to synthesize chiral 3-amino-2-oxindoles.[2] As general approaches to this synthesis, the nucleophilic addition to isatin-derived imines (Scheme 2.1, Eq. 1) and aldol-type reactions of oxindoles with electrophilic nitrogen sources, such as nitroso compounds and azodicarboxylates, are known.

Scheme 2.1. General approaches for 3-amino-2-oxindoles

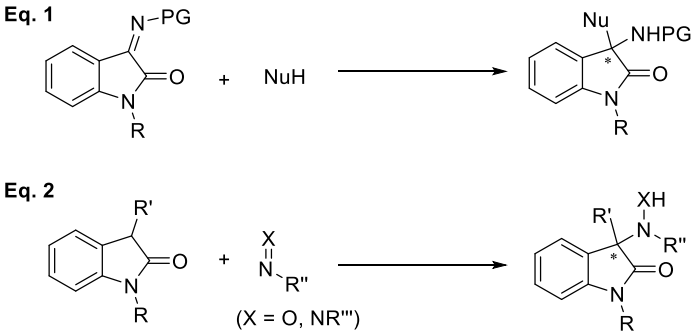

As part of the pioneering work that led to the enantioselective synthesis of 3-amino-2-oxindole, in 2008, List found that a chiral phosphoric acid catalyst promotes the formation of an aminal between an amide and isatin, despite limited to 3,3-diamino-2-oxindole.[2d] Additionally, in 2009, Chen reported the first enantioselective α-amination of 2-oxindoles with azocarboxylates catalyzed by (DHQD)2PHAL, a commercially available *bis*-cinchona alkaloid (Scheme 2.2).[2e] After these studies were published, various approaches to the synthesis of chiral 3-amino-2-oxindoles were investigated.[2]

Scheme 2.2. Pioneering work of enantioselective synthesis of 3-amino-2-oxindole

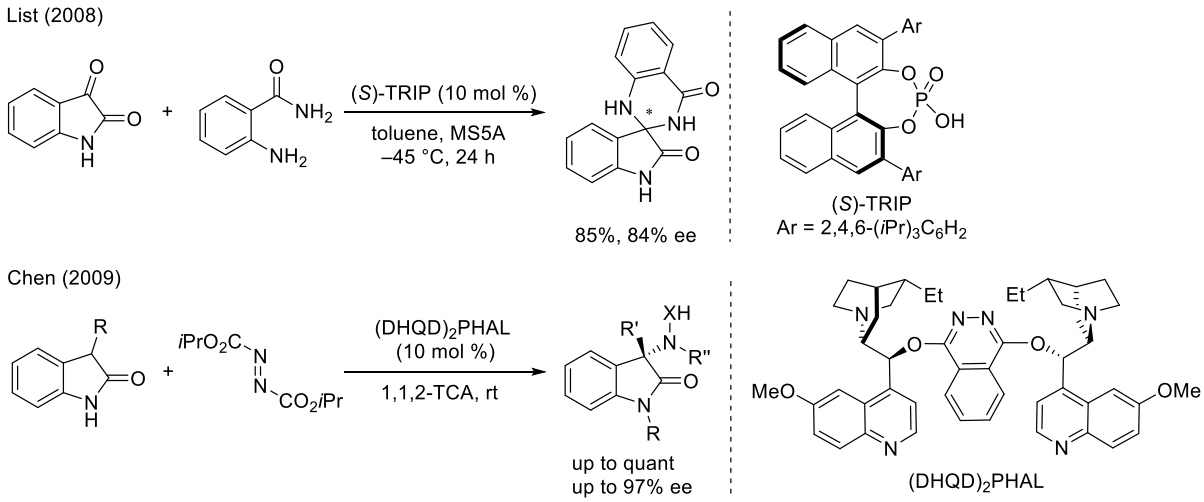

As described in Chapter 1, the Morita–Baylis–Hillman (MBH) reaction is an atom-economical, organocatalyzed C–C bond-forming reaction. The enantioselective aza-MBH reaction[3] of isatin-derived ketimines produces highly functionalized 3-amino-2-oxindoles that include a chiral tetrasubstituted carbon stereogenic center.[4-7]

Scheme 2.3. Enantioselective aza-MBH reaction of isatin-derived ketimines

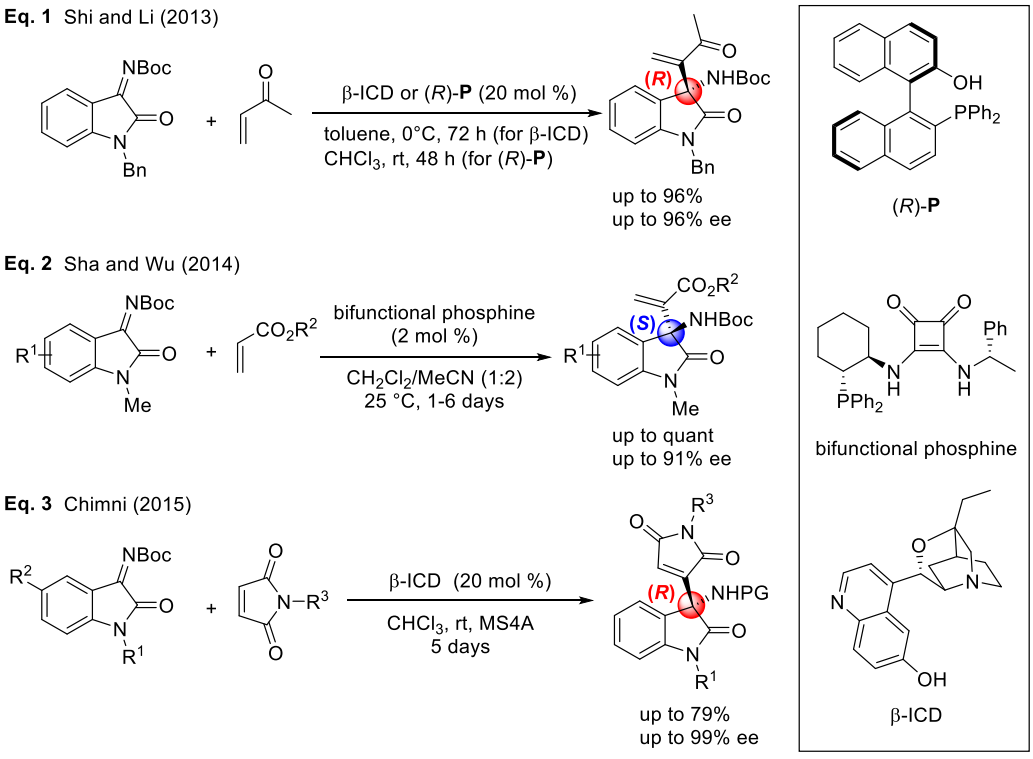

In 2013, Shi and Li reported the aza-MBH reaction of *N-tert*-butoxycarbonyl- (Boc-) protected ketimines with methyl vinyl ketone carried out using chiral acid–base organocatalysts. Although different reaction conditions are necessary when using the two catalysts reported as follows, the study authors found that both the cinchona-alkaloid catalyst and the phosphine catalyst effectively promote the enantioselective aza-MBH reaction to produce the (*R*)-enantiomer of 3-amino-2-oxindole (Scheme 2.3, Eq. 1).[4] Sha and Wu also discovered that a chiral phosphine-squaramide promoted the aza-MBH reaction of acrylates with 1-Me-protected isatin-derived ketimines (Scheme 2.3, Eq. 2).[5] In 2015, Chimni found that maleimides were appropriate nucleophilic partners for the aza-MBH process (Scheme 2.3, Eq. 3).[6] In all cases, the moiety of the catalyst with the character of a Brønsted acid plays a key role in controlling the enantioselectivity of the reaction. However, only one enantiomer is obtained through these approaches, although both enantiomers of 3-amino-2-oxindole are important structural motifs, as illustrated in Figure 2.1. Herein, the author reports an enantiodiscriminating aza-MBH process involving the reaction of isatin-derived ketimine (**1**) with acrolein (**2**) that relies on β-isocupreidine (β-ICD)[8a-c] or α-isocupreine (α-ICPN)[8d] as natural alkaloid-derived chiral acid–base organocatalysts (Scheme 2.4). The implementation of the present protocol selectively led to the synthesis of (*S*)- or (*R*)-adduct **3** in up to 98% ee. Notably, regardless of whether β-ICD or α-ICPN was used as a catalyst, the reaction proceeded under identical conditions.

Scheme 2.4. **This work**: An enantiodiscriminating aza-MBH reaction of isatine-derived ketimine **1** with acrolein (**2**)

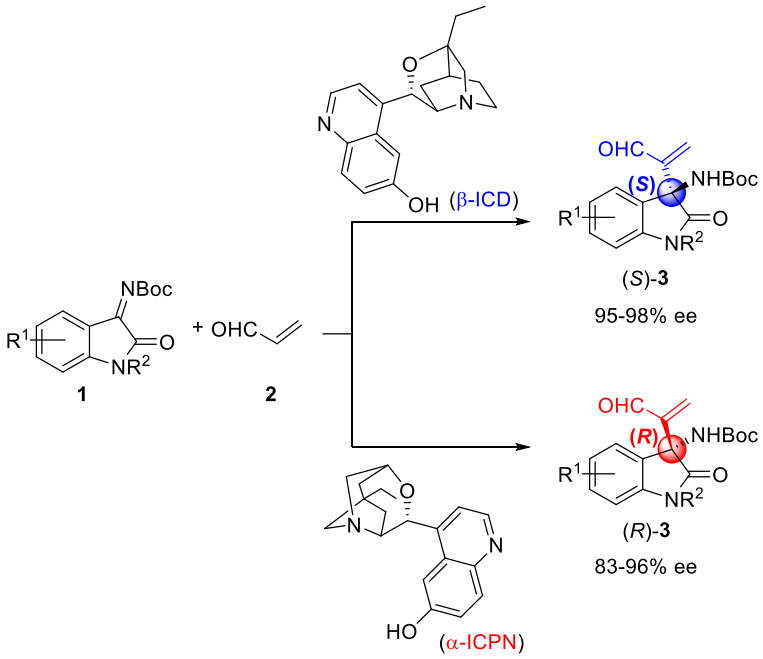

2.2. Results and Discussion

2.2.1. Optimization of Reaction Conditions

During the initial solvent screening (–15 °C, 20 mol % β-ICD), the author found that the reaction proceeded better in toluene or cyclopentyl methyl ether (CPME) than in other solvents such as CH_2Cl_2 and THF (Table 2.1. entries 1−4). Next the author investigated the effect of the reaction temperature. Decreasing the reaction temperature to –40 °C gave **3a** in an acceptable yield (46%) with 94% ee (entry 8).

Table 2.1. Optimization of reaction conditions[a]

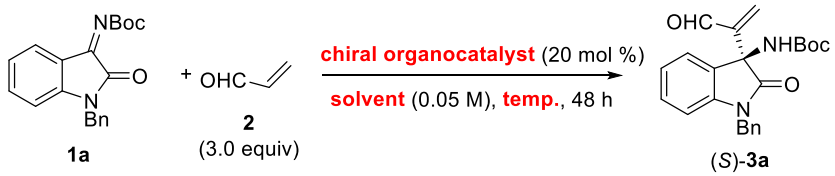

entry	solvent	chiral organocatalyst	temp. (°C)	yield (%)[b]	ee (%)[c]
1	toluene	β-ICD	–15	54	89
2	CH_2Cl_2	β-ICD	–15	51	64
3	THF	β-ICD	–15	62	80
4	CPME	β-ICD	–15	58	87
5	toluene	β-ICD	10[d]	27	93
6	toluene	β-ICD	–10	65	88
7	toluene	β-ICD	–20	53	90
8	toluene	β-ICD	–40	46	94
9	toluene	β-ICD	–60	19	97
10	toluene/CPME = 1/1	β-ICD	–40	60	94
11	toluene/CPME = 1/1	**4**	–40	trace	-
12	toluene/CPME = 1/1	**5**	–40	16	90
13	toluene/CPME = 1/1	**6**	–40	35	80
14[e]	toluene/CPME = 1/1	β-ICD	–40	81	97

[a] **1a** (0.060 mmol) in the stated solvent (0.05 M for **1a**), chiral organocatalyst (0.012 mmol) and **2** (0.18 mmol) were stirred for 48 h.
[b] ^{1}H-NMR yield of product **3a** using 1,3,5-trimethoxybenzene as an internal standard.
[c] Determined by HPLC (Daicel Chiralpak IE).
[d] Over reaction of **3a** with **2** was observed.
[e] **1a** (0.060 mmol) in the stated solvent (0.05 M for **1a**), chiral organocatalyst (0.0090 mmol) and **2** (0.12 mmol) were stirred in the presence of MS3A (20 mg) for 96 h. Yield is of isolated **3a**.

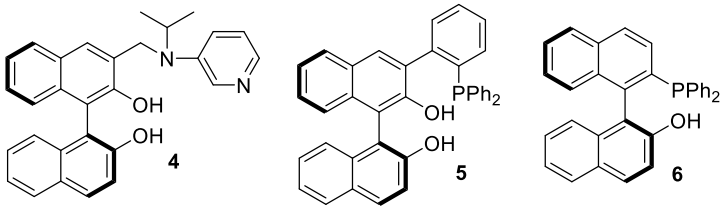

When the reaction was performed at 10 °C or –60 °C, **3a** was obtained in low yields because of either over reaction of **3a** with **2** (involving the polymerization of **2**)[9] (entry 5) or low conversion (entry 9), respectively. Finally, the author discovered that the use of mixed-solvent system toluene/CPME (1/1) for the aza-MBH

reaction of **1a** with **2** at –40 °C gave **3a** in 60% yield with 94% ee (entry 10). Chiral acid-base organocatalysts **4**−**6**, which are known to mediate enantioselective aza-MBH processes,[10] were virtually ineffective at improving the chemical yields and ee values for **3a** (entries 11−13). The optimal result (**3a**: 81% yield, 97% ee) was obtained when the reaction of **1a** and **2** (2.0 equiv) was performed with β-ICD (15 mol %) in toluene/CPME (1/1; 0.05 M with respect to **1**) at –40 °C for 96 hours in the presence of 3Å molecular sieves (MS3A) as an additive (entry 14). MS3A probably suppressed the hydrolysis of ketimine **1a** to increase yield.

2.2.2. Substrate Scope

With optimized condition in hand, substrate scope of enantioselective aza-MBH reaction of isatin-derived ketimine **1** with acrolein (**2**) was examined (Table 2.2). *N*-Substituted ketimines **1b**–**1d** (R^1 = allyl, Ph, prenyl) were transformed to **3b**–**3d** in 48–70% yields with excellent enantioselectivities (95–98% ee) (entries 3–5). Ketimines **1e**–**1j** bearing an electron-withdrawing or electron-donating substituent on the aromatic ring also afforded the corresponding aza-MBH adducts **3e**–**3j** in 68–83% yields with excellent enantioselectivities (95–98% ee) (entries 6–11).

Table 2.2. Substrate scope in the enantiodiscriminating aza-MBH reaction catalyzed by β-ICD or α-ICPN[a]

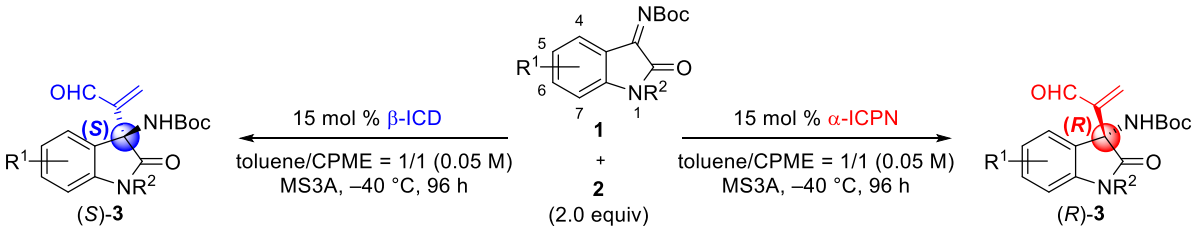

entry	β-ICD or α-ICPN	**1**	**3** yield (%)[b]	ee (%)[c]
1	β-ICD	**1a**, R^1 = H, R^2 = Bn	**3a** 81	97 (***S***)
2[d]	β-ICD	**1a**	**3a** 76	97 (***S***)
3	β-ICD	**1b**, R^1 = H, R^2 = allyl	**3b** 70	96 (***S***)
4	β-ICD	**1c**, R^1 = H, R^2 = Ph	**3c** 52	98 (***S***)
5	β-ICD	**1d**, R^1 = H, R^2 = prenyl	**3d** 48	95 (***S***)
6	β-ICD	**1e**, R^1 = 5-Cl, R^2 = Bn	**3e** 68	98 (***S***)
7	β-ICD	**1f**, R^1 = 6-Cl, R^2 = Bn	**3f** 83	98 (***S***)
8	β-ICD	**1g**, R^1 = 7-Cl, R^2 = Bn	**3g** 81	97 (***S***)
9	β-ICD	**1h**, R^1 = 5-Br, R^2 = Bn	**3h** 73	96 (***S***)
10	β-ICD	**1i**, R^1 = 5-F, R^2 = Bn	**3i** 78	98 (***S***)
11[e]	β-ICD	**1j**, R^1 = 5-Me, R^2 = Bn	**3j** 77	95 (***S***)
12	α-ICPN	**1a**, R^1 = H, R^2 = Bn	**3a** 78	95 (***R***)
13	α-ICPN	**1b**, R^1 = H, R^2 = allyl	**3b** 59	90 (***R***)
14	α-ICPN	**1c**, R^1 = H, R^2 = Ph	**3c** 37	87 (***R***)
15	α-ICPN	**1d**, R^1 = H, R^2 = prenyl	**3d** 44	89 (***R***)
16	α-ICPN	**1e**, R^1 = 5-Cl, R^2 = Bn	**3e** 74	87 (***R***)
17	α-ICPN	**1g**, R^1 = 7-Cl, R^2 = Bn	**3g** 44	94 (***R***)
18	α-ICPN	**1h**, R^1 = 5-Br, R^2 = Bn	**3h** 79	88 (***R***)
19[f]	α-ICPN	**1j**, R^1 = 5-Me, R^2 = Bn	**3j** 58	96 (***R***)
20	α-ICPN	**1k**, R^1 = H, R^2 = Me	**3k** 45	83 (***R***)
21	β-ICD or α-ICPN	**1m**, R^1 = 4-Cl, R^2 = Bn	**3m** trace	-
22	β-ICD or α-ICPN	**1n**, R^1 = R^2 = H	**3n** trace	-

[a]**1** (0.060 mmol) in the stated solvent (0.05 M for **1**), β-ICD or α-ICPN (0.0090 mmol) and **2** (0.12 mmol) were stirred for 96 h.
[b]Isolated yield.
[c]Determined by HPLC (Daicel Chiralpak IE). Configuration of the major isomer is shown in parentheses.
[d]0.64 mmol scale of **1a.**
[e]β-ICD (25 mol %) was used at –20 °C.
[f]α-ICPN (25 mol %) was used.

Although the β-ICD-mediated aza-MBH process exhibited high asymmetric induction, the present system is difficult to apply to the synthesis of (*R*)-**3** because the required enantiomer of β-ICD is not readily available. One solution to this problem was the use of α-ICPN, derived from quinine, as an effective enantiocomplementary catalyst of β-ICD, which gave the corresponding aza-MBH adducts (*R*)-**3** in 37−79% yields with high enantioselectivities (83−96% ee) (entries 12−20). Although the reaction of **1j** with **2** required a higher catalyst loading (25 mol %) due to the low reactivity of **1j** (entries 11 and 19), the reaction of **1m** and **1n** gave no product because of quite low reactivity of **1m** and instability of **1n** (entries 21 and 22).

2.2.3. Transformation of the Products and Determination of the Absolute Configuration

The absolute configuration of **3k** catalyzed by β-ICD was assigned as being (*S*) by comparison with the reported optical rotation and HPLC data of allylic alcohol **7a** derived from the known compound **3l** (Scheme 2.5).[5] The aza-MBH product **3a** was also able to be converted into allylic alcohol derivatives **7b** and **9** without impairing the optical purity (Scheme 2.6).

Scheme 2.5. Synthetic transformation of **3k** and determination of its absolute configuration

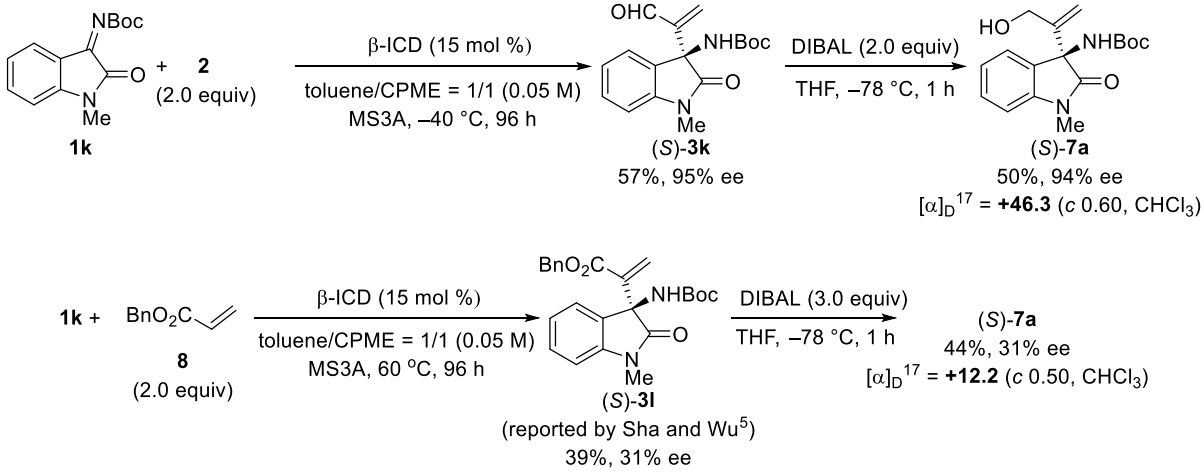

Scheme 2.6. Synthetic transformation of product **3a**

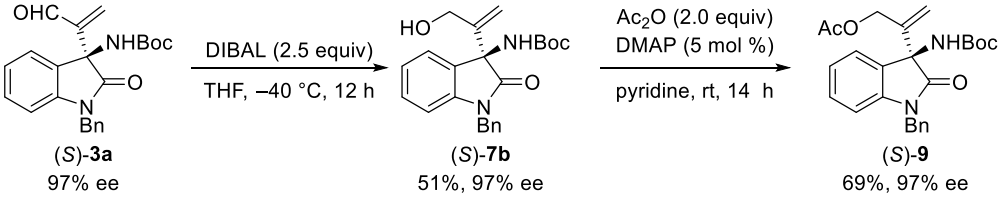

2.2.4. Consideration about Enantioselection

A proposed model for the enantioselectivity is shown in Figure 2.2. Since proton transfer is a known rate-determining step in aza-MBH reactions,[11] the proton shift mediated by the acidic unit on the catalyst could proceed smoothly via an intermediate of conformation with the least steric hindrance between the quinuclidine moiety of the catalyst and the aromatic ring of the substrate, leading to the formation of (*S*)-**3** with β-ICD or (*R*)-**3** with α-ICPN.

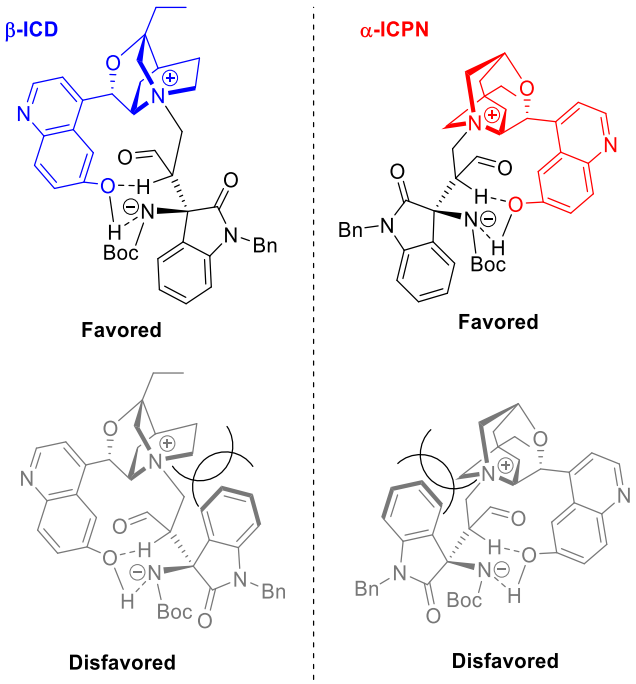

Figure 2.2. Mode of enantioselection

2.3. Conclusion

In Chapter 2, the author has described the development of a highly enantioselective organocatalyzed aza-MBH reaction of isatin-derived ketimine (**1**) with acrolein (**2**). Aza-MBH adducts **3** were obtained with excellent levels of enantioselectivity (up to 98% ee), irrespective of the electronic nature of the ketimine moiety. Moreover, both enantiomers of aza-MBH adducts **3**, which have a chiral tetrasubstituted carbon stereogenic center, were successfully obtained using either β-ICD or α-ICPN as organocatalysts.

2.4. Experimental Section

2.4.1. General

^{1}H-, ^{13}C-, and ^{19}F-NMR spectra were recorded with a JEOL JMN ECS400 FT NMR, JNM ECA600 FT NMR or Bruker AVANCE II (^{1}H-NMR 400, 600 or 700 MHz, ^{13}C-NMR 100, 150 or 176 MHz, ^{19}F-NMR 565 MHz. ^{1}H-NMR spectra are reported as follows: chemical shift in ppm relative to the chemical shift of $CHCl_3$ at 7.26 ppm, integration, multiplicities (s = singlet, d = doublet, t = triplet, q = quartet, m = multiplet),

and coupling constants (Hz). ^{13}C-NMR spectra reported in ppm relative to the central line of triplet for $CDCl_3$ at 77 ppm. CF_3CO_2H used as external standards for ^{19}F-NMR. FT-MS spectra were obtained with LTQ Orbitrap XL (Thermo Fisher Scientific). High resolution-MS spectra were obtained with JMS-T100LC (JEOL). Optical rotations were measured with JASCO P-1030 polarimeter. HPLC analyses were performed on a JASCO HPLC system (JASCO PU 980 pump and UV-975 UV/Vis detector) using a mixture of *n*-hexane/2-propanol as eluents. Column chromatography on SiO_2 was performed with Kanto Silica Gel 60 (40-100 μm).

2.4.2. Materials

Dehydrated toluene, CPME, CH_2Cl_2, THF, and other commercially available organic and inorganic compounds were purchased and used without further purification. *N-tert*-butoxycarbonyl (Boc) protected ketimines **1** were prepared following the reported procedures.[4]

2.4.3. General procedure for enantioselective organocatalyzed aza-MBH reaction of isatin-derived ketimines 1 with acrolein (2) or benzyl acrylate (8)

A test tube was filled with *N*-Boc protected ketimines **1** (0.060 mmol), β-ICD or α-ICPN (0.0090 mmol) and MS3A (20 mg) in toluene/CPME (1/1, 1.2 mL). Then, **2** or **8** (0.12 mmol) was added under –40 °C (for **2**) or 60 °C (for **8**). After 96 h, reaction mixture was filtered quickly with silica-gel, washed with ethyl acetate and dried *in vacuo*. Resulting crude product was purified by silica-gel column chromatography using *n*-hexane/EtOAc as eluent followed by GPC using chloroform as eluent to give product **3** as white solid or colorless oil.

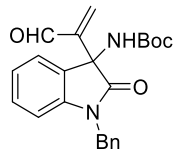

3a

3a: 81% yield (19.1 mg) with β-ICD, 78% yield (18.4 mg) with α-ICPN; white solid; ^{1}H-NMR (400 MHz, $CDCl_3$) δ 9.57 (s, 1H) 7.60-7.26 (m, 6H), 7.18 (td, 1H, *J* = 7.8, 0.8 Hz), 7.00 (td, 1H, *J* = 7.8, 0.8 Hz), 6.72 (d, 1H, *J* = 7.8 Hz), 6.44 (s, 1H), 6.23 (s, 1H), 6.05 (s, 1H), 5.15 (d, 1H, *J* = 15.6 Hz), 4.86 (d, 1H, *J* = 15.6 Hz), 1.33 (s, 9H); ^{13}C-NMR (100 MHz, $CDCl_3$) δ 192.7, 174.3, 154.0, 145.4, 142.7, 137.2, 135.6, 129.3, 129.0, 128.8, 127.6, 127.3, 124.8, 123.0, 109.4, 80.6, 63.4, 44.4, 28.1; HRMS (ESI) calcd for $C_{23}H_{24}N_2O_4Na^+$ 415.1628, found 415.1624; IR (KBr) *v* 3329, 2972, 1712, 1612, 1487, 1366, 1167, 1004, 758 cm^{-1}; $[\alpha]_D^{22}$ = –132.7 (*c* 0.40, $CHCl_3$) for (*S*)-**3a** in 97% ee; $[\alpha]_D^{17}$ = +130.1 (*c* 0.40, $CHCl_3$) for (*R*)-**3a** in 95% ee; HPLC analysis (Chiralpak IE, *n*-hexane/2-propanol = 65/35, flow rate 1.0 ml/min, λ= 225 nm) first peak: t_R = 14.2 min for (*R*), second peak: t_R = 32.8 min for (*S*).

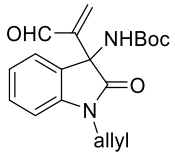

3b

3b: 70% yield (14.4 mg) with β-ICD, 59% yield (12.1 mg) with α-ICPN; colorless oil; ^{1}H-NMR (400 MHz, $CDCl_3$) δ 9.54 (s, 1H) 7.46 (d, 1H, *J* = 5.2 Hz), 7.28-7.25 (m, 1H), 7.02 (t, 1H, *J* = 5.2 Hz), 6.84 (d, 1H, *J* = 5.2 Hz), 6.46 (s, 1H), 6.23 (s, 1H), 6.00 (s, 1H), 5.92-5.87 (m, 1H), 5.33 (dd, 1H, *J* = 11.6, 0.8 Hz), 5.24 (dd, 1H, *J* = 7.2, 0.8 Hz), 4.58 (d, 1 H, *J* = 10.4 Hz), 4.27 (d, 1H, *J* = 10.4 Hz), 1.31 (s, 9H); ^{13}C-NMR (100 MHz, $CDCl_3$) δ 192.6, 173.9, 154.0, 145.5, 142.8, 137.0, 131.2, 129.2, 129.0, 124.9, 122.9, 117.7, 109.3, 80.6, 63.3, 42.8, 28.1; HRMS (ESI) calcd for $C_{19}H_{22}N_2O_4Na^+$ 365.1472, found 365.1462; IR (KBr) *v* 3332, 2976, 2931, 2882, 1699, 1612, 1521, 1363, 1283, 1169, 762 cm^{-1}; $[\alpha]_D^{22}$ = –145.0 (*c* 0.70, $CHCl_3$) for (*S*)-**3b** in 96% ee; $[\alpha]_D^{22}$ = +105 (*c* 0.41, $CHCl_3$) for (*R*)-**3b** in 90% ee; HPLC analysis (Chiralpak IE, *n*-hexane/2-propanol = 65/35, flow rate 1.0 ml/min, λ = 212 nm) first peak: t_R = 10.8 min for (*R*), second peak: t_R = 22.1 min for (*S*).

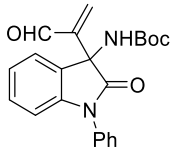

3c

3c: 52% yield (11.8 mg) with β-ICD, 37% yield (8.4 mg) with α-ICPN; white solid; ^{1}H-NMR (400 MHz, $CDCl_3$) δ 9.57 (s, 1H) 7.60-7.40 (m, 6H), 7.22 (t, 1H, *J* = 8.0 Hz), 7.05 (t, 1H, *J* = 8.0 Hz), 6.79 (d, 1H, *J* = 8.0 Hz), 6.61 (s, 1H), 6.30 (s, 1H), 6.01 (s, 1H), 1.35 (s, 9H); ^{13}C-NMR (100 MHz, $CDCl_3$) δ 192.6, 173.8, 154.1, 145.9, 144.0, 137.0, 134.2, 129.7, 129.3, 128.6, 128.3, 126.8, 125.0, 123.2, 109.6, 80.7, 63.4, 28.2; HRMS (ESI) calcd for $C_{22}H_{22}N_2O_4Na^+$ 401.1472, found 401.1465; IR (KBr) *v* 3348, 2976, 1273, 1726, 1499, 1369, 1167, 758, 702, 607 cm^{-1}; $[\alpha]_D^{22}$ = –82.2 (*c* 0.30, $CHCl_3$) for (*S*)-**3c** in 98% ee; $[\alpha]_D^{24}$ = +122.6 (*c* 0.40, $CHCl_3$) for (*R*)-**3c** in 87% ee; HPLC analysis (Chiralpak IE, *n*-hexane/2-propanol = 60/40, flow rate 1.0 ml/min, λ = 212 nm) first peak: t_R = 11.6 min for (*R*), second peak: t_R = 32.6 min for (*S*).

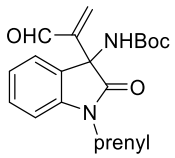

3d

3d: 48% yield (10.7 mg) with β-ICD, 44% yield (9.8 mg) with α-ICPN; white solid; ^{1}H-NMR (400 MHz, $CDCl_3$) δ 9.54 (s, 1H), 7.46 (d, 1H, *J* = 8.0 Hz), 7.27 (td, 1H, *J* = 7.8, 2.1 Hz), 7.01 (td, 1H, *J* = 7.8, 2.1 Hz), 6.82 (d, 1H, *J* = 8.0 Hz), 6.42 (s, 1H), 6.20 (s, 1H), 5.95 (s, 1H), 5.22 (m, 1H), 4.55 (dd, 1H, *J* = 7.8, 6.4 Hz), 4.27 (dd, 1H, *J* = 7.8, 6.4 Hz), 1.83 (s, 3H), 1.74 (s, 3H), 1.31 (s, 9H); ^{13}C-NMR (100 MHz, $CDCl_3$) δ 192.7, 173.7, 154.0, 145.4, 142.9, 136.85, 136.75, 129.24, 129.15, 124.9, 122.7, 118.2, 109.0, 80.5, 63.4, 38.6, 28.1, 25.6, 18.2; HRMS (ESI) calcd for $C_{21}H_{26}N_2O_4Na^+$ 393.1785, found 393.1778; IR (KBr) *v* 3359, 2970, 2921,

2340, 1711, 1610, 1489, 1366, 751, 598 cm^{-1}; $[\alpha]_D^{22}$ = –59.0 (*c* 0.40, $CHCl_3$) for (*S*)-**3d** in 95% ee; $[\alpha]_D^{26}$ = +107.6 (*c* 0.50, $CHCl_3$) for (*R*)-**3d** in 89% ee; HPLC analysis (Chiralpak IE, *n*-hexane/2-propanol = 60/40, flow rate 1.0 ml/min, λ = 212 nm) first peak: t_R = 10.6 min for (*R*), second peak: t_R = 22.9 min for (*S*).

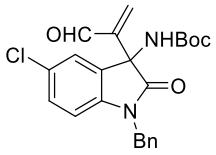

3e

3e: 68% yield (17.4 mg) with β-ICD, 74% yield (19.0 mg) with α-ICPN; white solid; ^{1}H-NMR (400 MHz, $CDCl_3$) δ 9.55 (s, 1H), 7.44 (d, 1H, *J* = 2.4 Hz), 7.38-7.27 (m, 5H), 7.14 (dd, 1H, *J* = 8.0, 2.4 Hz), 6.62 (d, 1H, *J* = 8.4 Hz), 6.49 (s, 1H), 6.27 (s, 1H), 6.01 (s, 1H), 5.09 (d, 1H, *J* = 16.0 Hz), 4.89 (d, 1H, *J* = 16.0 Hz), 1.36 (s, 9H); ^{13}C-NMR (100 MHz, $CDCl_3$) δ 192.5, 173.9, 153.9, 145.0, 141.4, 137.7, 135.1, 130.5, 129.2, 128.8, 128.3, 127.8, 127.2, 125.2, 110.4, 81.0, 63.2, 44.5, 28.1; HRMS (ESI) calcd for $C_{23}H_{23}ClN_2O_4Na^+$ 449.1239, found 449.1231; IR (KBr) *v* 2964, 2926, 2860, 2357, 2329, 1708, 1484, 1363, 1254, 1167, 752 cm^{-1}; $[\alpha]_D^{25}$ = –147.0 (*c* 0.40, $CHCl_3$) for (*S*)-**3e** in 98% ee; $[\alpha]_D^{17}$ = +114.4 (*c* 0.30, $CHCl_3$) for (*R*)-**3e** in 87% ee; HPLC analysis (Chiralpak IE, *n*-hexane/2-propanol = 65/35, flow rate 1.0 ml/min, λ = 208 nm) first peak: t_R = 8.0 min for (*R*), second peak: t_R = 13.0 min for (*S*).

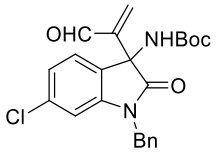

3f

3f: 83% yield (21.3 mg) with β-ICD; white solid; ^{1}H-NMR (400 MHz, $CDCl_3$) δ 9.54 (s, 1H), 7.39-7.26 (m, 6H), 6.97 (dd, 1H, *J* = 7.8, 1.6 Hz), 6.71 (d, 1H, *J* = 1.6 Hz), 6.47 (s, 1H), 6.26 (s, 1H), 5.98 (s, 1H), 5.09 (d, 1H, *J* = 15.6 Hz), 4.85 (d, 1H, *J* = 15.6 Hz), 1.35 (s, 9H); ^{13}C-NMR (100 MHz, $CDCl_3$) δ 192.6, 174.3, 154.0, 145.2, 144.0, 137.6, 135.04, 135.00, 128.9, 127.8, 127.3, 127.2, 125.9, 122.9, 110.0, 80.9, 62.9, 44.5, 28.1; HRMS (ESI) calcd for $C_{23}H_{23}ClN_2O_4Na^+$ 449.1239, found 449.1228; IR (KBr) *v* 3288, 2973, 1707, 1608, 1488, 1371, 1278, 1171, 876 cm^{-1}; $[\alpha]_D^{20}$ = –121.0 (*c* 1.1, $CHCl_3$) for (*S*)-**3f** in 98% ee; HPLC analysis (Chiralpak IE, *n*-hexane/2-propanol = 65/35, flow rate 1.0 ml/min, λ = 263 nm) first peak: t_R = 8.4 min for (*R*), second peak: t_R = 15.5 min for (*S*).

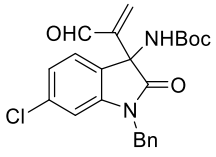

3g

3g: 81% yield (20.7 mg) with β-ICD; 44% yield (11.3 mg) with α-ICPN; white solid; ^{1}H NMR (400 MHz, $CDCl_3$) δ 9.54 (s, 1H), 7.39-7.29 (m, 5H), 7.26-7.23 (m, 1H), 7.18 (dd, 1H, *J* = 8.0, 0.8 Hz), 6.97-6.95 (m,

1H), 6.35 (s, 1H), 6.21 (s, 1H), 6.12 (s, 1H), 5.47 (d, 1H, *J* = 16.4 Hz), 5.36 (d, 1H, *J* = 16.4 Hz), 1.35 (s, 9H); ^{13}C-NMR (100 MHz, $CDCl_3$) δ 192.6, 174.9, 153.9, 145.0, 138.9, 137.9, 137.5, 132.0, 131.9, 128.5, 127.1, 126.6, 123.8, 123.2, 115.6, 80.9, 63.0, 45.5, 28.1; HRMS (ESI) calcd for $C_{23}H_{23}ClN_2O_4Na^+$ 449.1239, found 449.1229 IR (KBr) *v* 3342, 2976, 1721, 1496, 1455, 1366, 1162, 734 cm^{-1}; $[\alpha]_D^{23}$ = –88.2 (*c* 1.0, $CHCl_3$) for (*S*)-**3g** in 97% ee, $[\alpha]_D^{22}$ = +113.9 (*c* 0.40, $CHCl_3$) for (*R*)-**3g** in 94% ee; HPLC analysis (Chiralpak IE, *n*-hexane/2-propanol = 65/35, flow rate 1.0 ml/min, λ = 216 nm) first peak: t_R = 8.7 min for (*R*), second peak: t_R = 17.6 min for (*S*).

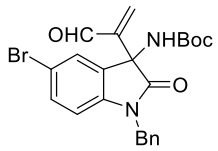

3h

3h: 73% yield (20.6 mg) with β-ICD, 79% yield (22.3 mg) with α-ICPN; white solid; ^{1}H-NMR (400 MHz, $CDCl_3$) δ 9.55 (s, 1H), 7.57 (d, 1H, *J* = 2.0 Hz), 7.37-7.28 (m, 6H), 6.57 (d, 1H, *J* = 8.0 Hz), 6.49 (s, 1H), 6.27 (s, 1H), 6.01 (s, 1H), 5.08 (d, 1H, *J* = 15.8 Hz), 4.89 (d, 1H, *J* = 15.8 Hz), 1.36 (s, 9H); ^{13}C-NMR (100 MHz, $CDCl_3$) δ 192.5, 173.8, 153.9, 145.0, 141.8, 137.7, 135.1, 132.1, 130.8, 128.8, 127.9, 127.8, 127.2, 115.7, 110.9, 81.0, 63.2, 44.4, 28.1; HRMS (ESI) calcd for $C_{23}H_{23}BrN_2O_4Na^+$ 493.0733, found 493.0721; IR (KBr) *v* 3342, 2979, 2926, 1721, 1606, 1367, 1254, 1162, 737 cm^{-1}; $[\alpha]_D^{22}$ = –114.1 (*c* 1.0, $CHCl_3$) for (*S*)-**3h** in 96% ee; $[\alpha]_D^{22}$ = +148.3 (*c* 1.5, $CHCl_3$) for (*R*)-**3h** in 88% ee; HPLC analysis (Chiralpak IE, *n*-hexane/2-propanol = 65/35, flow rate 1.0 ml/min, λ = 216 nm) first peak: t_R = 8.5 min for (*R*), second peak: t_R = 13.6 min for (*S*).

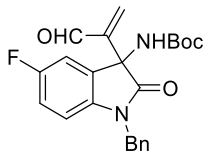

3i

3i: 78% yield (19.2 mg) with β-ICD; white solid; ^{1}H-NMR (400 MHz, $CDCl_3$) δ 9.56 (s, 1H), 7.37-7.32 (m, 4H), 7.29-7.24 (m, 2H), 6.87 (td, 1H, *J* = 6.0, 2.0 Hz), 6.62 (dd, 1H, *J* = 5.6, 2.8 Hz), 6.50 (s, 1H), 6.28 (s, 1H), 6.00 (s, 1H), 5.11 (d, 1H, *J* = 10.4 Hz), 4.87 (d, 1H, *J* = 10.4 Hz), 1.36 (s, 9H); ^{13}C-NMR (100 MHz, $CDCl_3$) δ 192.5, 174.1, 159.2 (d, $^1J_{CF}$ = 159.9 Hz), 153.9, 145.0, 138.7, 137.8, 135.2, 130.4 (d, $^3J_{CF}$ = 5.3 Hz), 128.8, 127.7, 127.2, 115.5 (d, $^2J_{CF}$ = 16.0 Hz), 113.1 (d, $^2J_{CF}$ = 16.0 Hz), 110.0 (d, $^3J_{CF}$ = 5.3 Hz), 80.9, 63.4, 44.5, 28.1; ^{19}F NMR (565 MHz, $CDCl_3$): δ –119.5; HRMS (ESI) calcd for $C_{23}H_{23}FN_2O_4Na^+$ 433.1534, found 433.1527; IR (KBr) *v* 3299, 2980, 1732, 1709, 1525, 1490, 1367, 1264, 1164 cm^{-1}; $[\alpha]_D^{23}$ = –99.4 (*c* 0.90, $CHCl_3$) for (*S*)-**3i** in 98% ee; HPLC analysis (Chiralpak IE, *n*-hexane/2-propanol = 65/35, flow rate 1.0 ml/min, λ = 216 nm) first peak: t_R = 8.6 min for (*R*), second peak: t_R = 14.6 min for (*S*).

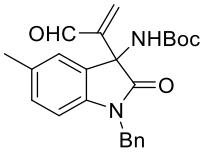

3j

3j: 77% yield (18.8 mg) with β-ICD, 58% yield (14.1 mg) with α-ICPN; White solid; ^{1}H-NMR (400 MHz, $CDCl_3$) δ 9.57 (s, 1H), 7.38-7.24 (m, 6H), 6.98 (d, 1H, *J* = 8.0 Hz), 6.60 (d, 1H, *J* = 8.0 Hz), 6.42 (s, 1H), 6.21 (s, 1H), 6.06 (s, 1H), 5.11 (d, 1H, *J* = 15.6 Hz), 4.86 (d, 1H, *J* = 15.6 Hz), 2.26 (s, 3H), 1.34 (s, 9H); ^{13}C-NMR (100 MHz, $CDCl_3$) δ 192.9, 174.2, 154.0, 145.5, 140.2, 137.2, 135.7, 132.6, 129.6, 129.0, 128.7, 127.5, 127.2, 125.5, 109.2, 80.6, 63.5, 44.3, 28.1, 21.1; HRMS (ESI) calcd for $C_{24}H_{26}N_2O_4Na^+$ 429.1785, found 429.1776; IR (KBr) *v* 3419, 2976, 2926, 1715, 1497, 1367, 1164, 997, 805 cm^{-1}; $[\alpha]_D^{22}$ = –157.0 (*c* 0.30, $CHCl_3$) for (*S*)-**3j** in 95% ee; $[\alpha]_D^{24}$ = +122.1 (*c* 0.25, $CHCl_3$) for (*R*)-**3j** in 96% ee; HPLC analysis (Chiralpak IE, *n*-hexane/2-propanol = 65/35, flow rate 1.0 ml/min, λ = 262 nm) first peak: t_R = 13.0 min for (*R*), second peak: t_R = 28.3 min for (*S*).

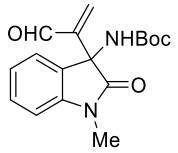

3k

3k: 57% yield (10.8 mg) with β-ICD, 45% yield (8.5 mg) with α-ICPN; White solid; ^{1}H-NMR (400 MHz, $CDCl_3$) δ 9.54 (s, 1H) 7.45 (dd, 1H, *J* = 7.2, 0.8 Hz), 7.31 (td, 1H, *J* = 7.2, 0.8 Hz), 7.03 (td, 1H, *J* = 7.2, 0.8 Hz), 6.86 (d, 1H, *J* = 7.2 Hz), 6.43 (s, 1H), 6.21 (s, 1H), 5.98 (s, 1H), 3.30 (s, 3H), 1.30 (s, 9H); ^{13}C-NMR (100 MHz, $CDCl_3$) δ 192.7, 174.2, 154.0, 145.4, 143.5, 137.0, 129.4, 129.1, 124.7, 123.0, 108.4, 80.6, 63.4, 28.1, 26.7; HRMS (ESI) calcd for $C_{17}H_{20}N_2O_4Na^+$ 339.1315, found 339.1306; IR (KBr) *v* 3304, 2976, 1712, 1613, 1483, 1371, 1252, 1166, 756 cm^{-1}; $[\alpha]_D^{23}$ = –108.0 (*c* 0.50, $CHCl_3$) for (*S*)-**3k** in 95% ee; $[\alpha]_D^{19}$ = +129.2 (*c* 0.60, $CHCl_3$) for (*R*)-**3k** in 83% ee; HPLC analysis (Chiralpak IE, *n*-hexane/2-propanol = 65/35, flow rate 1.0 ml/min, λ = 216 nm) first peak: t_R = 13.3 min for (*R*), second peak: t_R = 24.7 min for (*S*).

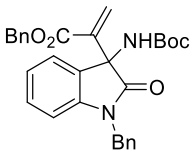

3l

3l: Analytical data were well matched with reported value.[5] 39% yield (9.9 mg), 31% ee; yellow solid; ^{1}H-NMR (400 MHz, $CDCl_3$) δ 7.43 (d, 1H, *J* = 7.2 Hz), 7.37-7.26 (m, 4H), 7.24-7.20 (m, 2H), 7.01 (td, 1H, *J* = 7.6, 0.8 Hz), 6.76 (d, 1H, *J* = 7.6 Hz), 6.37 (s, 1H), 6.03 (s, 1H), 5.91 (s, 1H), 5.09 (s, 2H), 3.15 (s, 3H), 1.30 (s, 9H); $[\alpha]_D^{24}$ = –30.4 (*c* 0.68, CH_2Cl_2) for (*S*)-**3l** in 31% ee (lit.[5] $[\alpha]_D^{25}$ = –76.3 (*c* 0.68, CH_2Cl_2) for (*S*)-**3l** in 87% ee); HPLC analysis (Chiralpak OD-H, *n*-hexane/2-propanol = 9/1, flow rate 1.0 ml/min, λ = 236 nm) first peak: t_R = 10.7 min for (*R*), second peak: t_R = 13.9 min for (*S*).

2.4.4. Preparation of 7 from 3

To stirred **3k** (0.050 mmol) in THF (0.50 mL) was added DIBAL in THF (0.10 mmol, 0.10 mL) under –78 °C. After 1 h, aq. HCl (1.0 M, 0.50 mL) was added and extracted with EtOAc. After dried *in vacuo*, resulting crude product was purified by silica-gel column chromatography using *n*-hexane/EtOAc as eluent to provide product **7a**. The procedures for preparation **7a**−**7b** from **3a**, **3l** are similar to that of preparation **7a** from **3k**, using DIBAL (0.10−0.13 mmol).

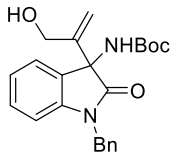

7a

7a: 50% yield (8.0 mg) from **3k**; 44% yield (7.0 mg) from **3l**; white solid; ^{1}H-NMR (400 MHz, $CDCl_3$) δ 7.40-7.26 (m, 2H), 7.10 (t, 1H, *J* = 7.6 Hz), 6.84 (d, 1H, *J* = 7.6 Hz), 6.30 (s, 1H), 5.26 (s, 1H), 4.94 (s, 1H), 4.60-4.45 (m, 1H), 4.33-4.21 (m, 1H), 3.21 (s, 3H), 2.80-2.70 (m, 1H), 1.25 (s, 9H); ^{13}C-NMR (100 MHz, $CDCl_3$) δ 176.0, 153.9, 143.7, 143.5, 130.1, 129.0, 124.1, 122.9, 118.8, 108.3, 80.3, 65.7, 63.8, 28.0, 26.6; HRMS (ESI) calcd for $C_{17}H_{22}N_2O_4Na^+$ 341.1472, found 341.1466; IR (KBr) *v* 3354, 2970, 2931, 2357, 1709, 1611, 1497, 1365, 1256, 1170, 1014, 795, 752 cm^{-1}. $[\alpha]_D^{17}$ = +46.3 (*c* 0.60, $CHCl_3$) for (*S*)-**7a** in 94% ee ($[\alpha]_D^{17}$ = +12.2 (*c* 0.50, $CHCl_3$) for (*S*)-**7a** in 31% ee); HPLC analysis (Chiralpak IE, *n*-hexane/2-propanol = 60/40, flow rate 1.0 ml/min, λ = 240 nm) first peak: t_R = 8.2 min for (*R*), second peak: t_R = 9.4 min for (*S*).

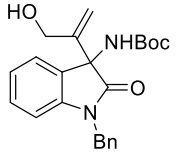

7b

7b: 51% yield (10.1 mg); white solid; ^{1}H-NMR (400 MHz, $CDCl_3$) δ 7.40-7.15 (m, 4H), 7.06 (t, 1H, *J* = 7.6 Hz), 6.70 (d, 1H, *J* = 7.6 Hz), 6.49 (brs, 1H), 5.30 (s, 1H), 5.14 (brd, 1H, *J* = 10.8 Hz), 4.95 (s, 1H), 4.71 (br, 1H), 4.58 (dd, 1H, *J* = 12.8, 4.8 Hz), 4.32 (dd, 1H, *J* = 12.8, 2.8 Hz), 2.91 (s, 1H), 1.29 (s, 9H); ^{13}C-NMR (100 MHz, $CDCl_3$) δ 176.1, 154.0, 143.9, 142.6, 135.7, 128.9, 128.7, 127.5, 127.1, 124.0, 122.9, 118.8, 109.3, 80.4, 65.8, 63.8, 44.0, 28.1; HRMS (ESI) calcd for $C_{23}H_{26}N_2O_4Na^+$ 417.1785, found 417.1774; IR (KBr) *v* 3458, 3337, 2970, 2361, 1699, 1500, 1364, 1173, 1003, 749 cm^{-1}. $[\alpha]_D^{24}$ = +27.5 (*c* 1.0, $CHCl_3$) for (*S*)-**7b** in 97% ee; HPLC analysis (IE, *n*-hexane/2-propanol = 70/30, flow rate 1.0 ml/min, λ = 214 nm) first peak: t_R = 9.8 min for (*R*), second peak: t_R = 11.5 min for (*S*).

2.4.5. Preparation of 9

A mixture of **7b** (0.038 mmol), DMAP (1.92 μmol) and Ac_2O (0.077 mmol) in pyridine (0.19 mL) was stirred

at rt for 14 h. The reaction mixture was directly purified by silica-gel column chromatography using *n*-hexane/EtOAc as eluent to provide product **9** as colorless oil.

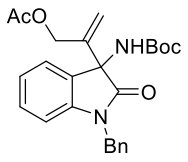

9

9: 69% yield (11.4 mg); colorless oil; ^{1}H-NMR (400 MHz, $CDCl_3$) δ 7.32-7.25 (m, 6H), 7.19 (td, 1H, J = 7.8 Hz, 1.1 Hz), 7.05 (td, 1H, J = 7.8 Hz, 1.1 Hz), 6.69 (d, 1H, J = 7.8 Hz), 6.09 (bs, 1H), 5.39 (s, 1H), 5.19 (s, 1H), 5.13-5.10 (m, 1H), 4.93 (d, 1H, J = 13.5 Hz), 4.72-4.69 (m, 2H), 2.05 (s, 3H), 1.30 (s, 9H); ^{13}C-NMR (100 MHz, $CDCl_3$) δ 175.0, 170.8, 154.0, 142.8, 140.4, 135.7, 129.1, 128.7. 127.5, 127.1, 124.2, 122.8, 109.4, 80.6, 65.3, 63.3, 44.1, 28.2, 21.0; HRMS (ESI) calcd for $C_{25}H_{28}N_2O_5Na^+$ 459.1896, found 459.1884; IR (KBr) v 3346, 2977, 2351, 1722, 1614, 1489, 1369, 1242, 1172, 999, 757, 698 cm^{-1}. $[\alpha]_D^{25}$ = +14.3 (c 0.60, $CHCl_3$) in 97% ee; HPLC analysis (Chiralpak IE, *n*-hexane/2-propanol = 70/30, flow rate 1.0 ml/min, λ = 210 nm) first peak: t_R = 14.5 min for (*R*), second peak: t_R = 23.5 min for (*S*).

2.5. References

1. (a) Ochi, M.; Kawasaki, K.; Kataoka, H.; Uchio, Y.; Nishi, H. *Biochem. Biophys. Res. Commun.* **2001**, *283*, 1118. (b) Claudine, S.-L. G.; Sylvain, D.; Gabrielle, B.; Maurice, M.; Jacques, S.; Rolf, G.; Guy, G.; Gilles, G. *Stress* **2003**, *6*, 199. (c) Bernard, K.; Bogliolo, S.; Ehrenfeld, J. *Br. J. Pharmacol.* **2005**, *144*, 1037. (d) Periyasami, G.; Raghunathan, R.; Surendiran, G.; Mathivanan, N. *Bioorg. Med. Chem. Lett.* **2008**, *18*, 2342. (e) Kumar, R. R.; Perumal, S.; Senthilkumar, P.; Yogeeswari, P.; Sriram, D. *J. Med. Chem.* **2008**, *51*, 5731. (f) Girgis, A. S. *Eur. J. Med. Chem.* **2009**, *44*, 91. (g) Ali, M. A.; Ismail, R.; Choon, T. S.; Yoon, Y. K.; Wei, A. C.; Pandian, S.; Kumar, R. S.; Osman H.; Manogaran, E. *Bioorg. Med. Chem. Lett.* **2010**, *20*, 7064. (h) Vintonyak, V. V.; Warburg, K.; Kruse, H.; Grimme, S.; Hübel, K.; Rauh, D.; Waldmann, H. *Angew. Chem. Int. Ed.* **2010**, *49*, 5902. (i) Rottmann, M.; McNamara, C.; Yeung, B. K. S..; Lee, M. C. S.; Zou, B.; Russell, B.; Seitz, P.; Plouffe, D. M.; Dharia, N. V.; Tan, J.; Cohen, S. B.; Spencer, K. R.; González-Páez, G. E.; Lakshminarayana, S. B.; Goh, A.; Suwanarusk, R.; Jegla, T.; Schmitt, E. K.; Beck, H.-P.; Brun, R.; Nosten, F.; Renia, L.; Dartois, V.; Keller, T. H.; Fidock, D. A.; Winzeler E. A.; Diagana, T. T. *Science* **2010**, *329*, 1175. (j) Crosignani, S; Jorand-Lebrun, C; Page, P.; Campbell, G.; Colovray, V.; Missotten, M.; Humbert, Y.; Cleva, C.; Arrighi, J.-F.; Gaudet, M.; Johnson, Z.; Ferro, P.; Chollet, A. *ACS Med. Chem. Lett.* **2011**, *2*, 644.

2. Recent reviews, see: (a) Zhou, F.; Liu, Y.-L.; Zhou, J. *Adv. Synth. Catal.* **2010**, *352*, 1381. (b) Chauhan, P.; Chimni, S. S. *Tetrahedron: Asymmetry* **2013**, *24*, 343. (c) Zhou, F.; Liao, F.-M.; Yu, J.-S.; Zhou, J. *Synthesis* **2014**, *46*, 2983. Selected examples, see: (d) Cheng, X.; Vellalath, S.; Goddard,

R.; List, B. *J. Am. Chem. Soc.* **2008**, *130*, 15786. (e) Cheng, L.; Liu, L.; Wang, D.; Chen, Y-J. *Org. Lett.* **2009**, *11*, 3874. (f) Liu, Y.-L.; Wang, B.-L.; Cao, J.-J.; Chen, L.; Zhang, Y.-X.; Wang, C.; Zhou, J. *J. Am. Chem. Soc.* **2010**, *132*, 15176. (g) Liu, Y.-L.; Zhou, F.; Cao, J.-J.; Ji, C.-B.; Ding, M.; Zhou, J. *Org. Biomol. Chem.* **2010**, *8*, 3847. (h) Yan, W.; Wang, D.; Feng, J.; Li, P.; Zhao, D.; Wang, R. *Org. Lett.* **2012**, *14*, 2512. (i) Liu, Y.-L.; Zhou, J. *Chem. Commun.* **2013**, *49*, 4421. (j) Rao, V. U. B.; Jadhav, A. P.; Garad, D.; Singh, R. P. *Org. Lett.* **2014**, *16*, 648. (k) Li, T.-Z.; Wang, X.-B.; Sha F.; Wu, X.-Y. *J. Org. Chem.* **2014**, *79*, 4332. (l) Arai, T.; Matsumura, E.; Masu, H. *Org. Lett.* **2014**, *16*, 2768. (m) Kumar, A.; Sharma, V.; Kaur, J.; Kumar, V.; Mahajan, S.; Kumar, N.; Chimni, S. S. *Tetrahedron* **2014**, *70*, 7044. (n) Montesinos-Magraner, M.; Vila, C.; Cantón, R.; Blay, G.; Fernández, I.; Muñoz, M. C.; Pedro, J. R. *Angew. Chem. Int. Ed.* **2015**, *54*, 6320.

3. For recent reviews on asymmetric MBH reaction, see: (a) Wei, Y.; Shi, M. *Acc. Chem. Res.* **2010**, *43*, 1005. (b) Basavaiah, D.; Reddy, B. S.; Badsara, S. S. *Chem. Rev.* **2010**, *110*, 5447. (c) Mansilla, J.; Saá, J. M. *Molecules* **2010**, *15*, 709; (d) Basavaiah, D.; Veeraraghavaiah, G. *Chem. Soc. Rev.* **2012**, *41*, 68. (c) Wang, S.-X.; Han, X.; Zhong, F.; Wang, Y.; Lu, Y. *Synlett* **2011**, 2766. (e) Wei, Y.; Shi, M. *Chem. Rev.* **2013**, *113*, 6659.
4. Hu, F.-L.; Wei, Y.; Shi, M.; Pindi, S. Li, G. *Org. Biomol. Chem.* **2013**, *11*, 1921.
5. Zhao, X.; Li, T.-Z.; Qian, J.-Y.; Sha, F.; Wu, X.-Y. *Org. Biomol. Chem.* **2014**, *12*, 8072.
6. Kumar, A.; Sharma, V.; Kaur, J.; Kumar, N.; Chimni, S. S. *Org. Biomol. Chem*. **2015**, *13*, 5629.
7. For enantioselective aza-MBH reaction of ketimines, see: (a)Yao, Y; Li, J.-L.; Zhou, Q.-Q.; Dong, L.; Chen, Y.-C. *Chem. Eur. J.* **2013**, *19*, 9447. (b) Takizawa, S.; Rémond, E.; Arteaga, F. A.; Yoshida, Y.; Sridharan, V.; Bayardon, J. Jugé, S. Sasai, H. *Chem. Commun.* **2013**, *49*, 8392.
8. (a) Iwabuchi, Y.; Nakatani, M.; Yokoyama, N.; Hatakeyama, S. *J. Am. Chem. Soc.* **1999**, *121*, 10219. (b) Shi, M.; Xu, Y.-M. *Angew. Chem. Int. Ed.* **2002**, *41*, 4507. (c) Kawahara, S.; Nakano, A.; Esumi, T.; Iwabuchi, Y.; Hatakeyama, S. *Org. Lett.* **2003**, *5*, 3103. (d) Nakamoto, Y.; Urabe, F.; Takahashi, K.; Ishihara, J.; Hatakeyama, S. *Chem. Eur. J.* **2013**, *19*, 12653.
9. Takizawa, S.; Inoue, N.; Sasai, H. *Tetrahedron Lett.* **2011**, *52*, 377.
10. (a) Shi, M.; Chen, L.-H. *Chem. Commun.* **2003**, 1310. (b) Matsui, K.; Takizawa, S.; Sasai, H. *J. Am. Chem. Soc.* **2005**, *127*, 3680. (c) Matsui, K.; Takizawa, S.; Sasai, H. *Synlett* **2006**, 761.
11. For recent mechanistic studies, see: (a) Lindner, C.; Liu, Y.; Karaghiosoff, K.; Maryasin, B.; Zipse, H. *Chem. Eur. J.* **2013**, *19*, 6429. (b) Verma, P.; Verma, P.; Sunoj, R. B. *Org. Biomol. Chem.* **2014**, *12*, 2176. (c) Plata, R. E.; Singleton, D. A. *J. Am. Chem. Soc.* **2015**, *137*, 3811.

Chapter 3

Multifunctional Catalysis: Stereoselective Construction of α-Methylidene-γ-Lactams via Amidation/Rahut-Currier Reaction Sequence

Abstract: Mixing acryloyl chloride, dienone, and *N*,*N*-diisopropylethylamine (DIPEA) with a newly developed chiral amine organocatalyst, which could simultaneously act as a Brønsted and Lewis base, led to a one-pot amidation/Rauhut–Currier sequence, affording α-methylidene-γ-lactams. The chiral amine catalyst could be recovered and reused by acid/base extraction without any loss of catalytic activity in the stepwise protocol.

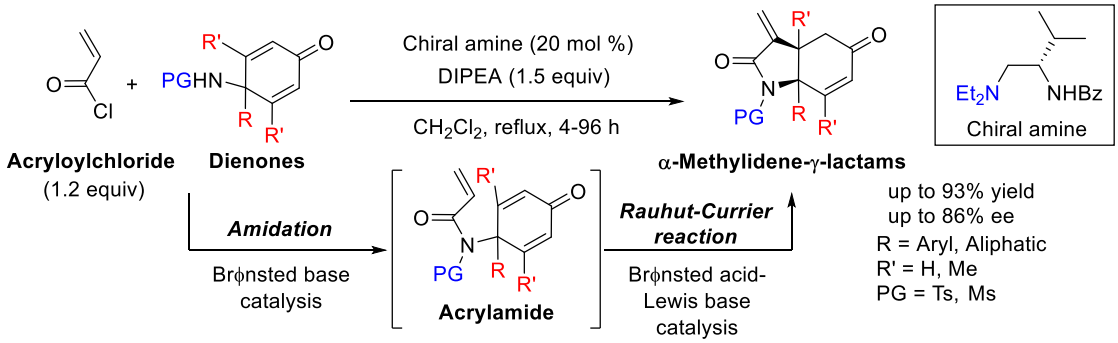

3.1. Introduction

The α-alkylidene-γ-lactam skeleton is commonly found in a vast number of natural and related compounds exhibiting a range of biological activities (Figure 3.1).[1] The antitussive pukeleimide E was isolated from the cyanobacterium *Lyngbya majuscula*, which grows on seagrass and causes human skin irritation.[1b] The analgesics anatin and isoanatin were discovered in the leaves of *Cynometra*, a genus of plants used as a folk medicine remedy in Africa.[1g] Perfumery materials and herbicides also have an α-alkylidene-γ-lactam skeleton.

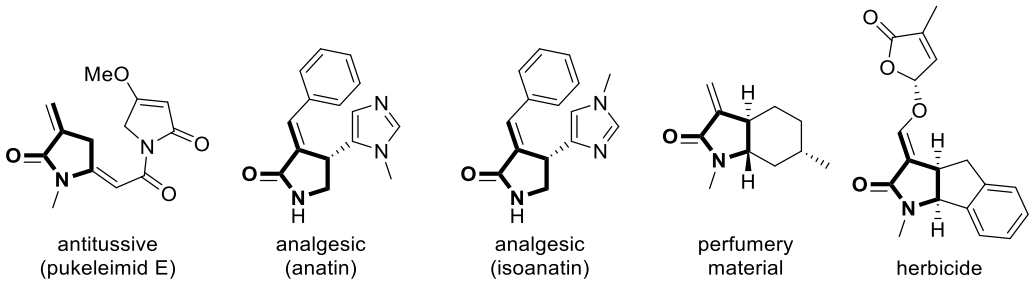

Figure 3.1. Bioactive compounds possessing an α-alkylidene-γ-lactam skeleton

Since lactams display a number of desirable pharmaceutical properties that are similar in nature to those of their lactone analogs, with lower toxic side effects,[1c,g,h,j] attractive synthetic approaches for the production of α-alkylidene-γ-lactams have been developed by numerous researchers (Scheme 3.1).[1c,l,2]

Scheme 3.1. Overview of the synthetic approaches for α-alkylidene-γ-lactams

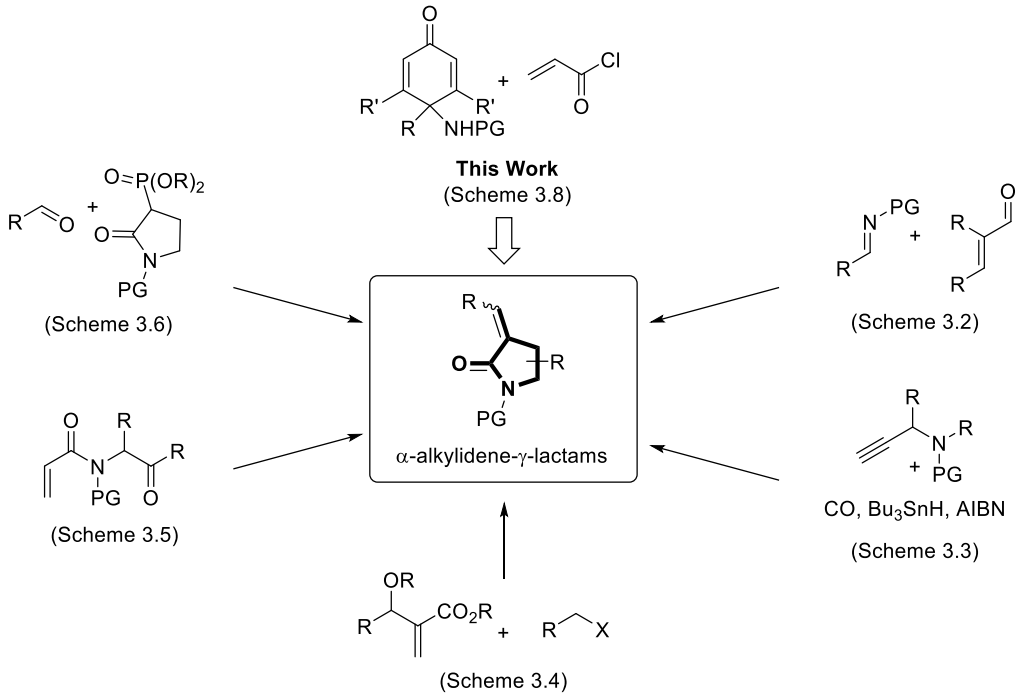

In 1985, Villiéras reported for the first time the synthesis of α-methylidene-γ-lactams with *in situ*-generated allylic organometallic reagents via the Mannich process. In 1992, the same research group employed for the reaction an enantiomerically pure imine to produce an optically active product (Scheme 3.2).[1c,d]

Scheme 3.2. The first report on the synthesis of α-alkylidene-γ-lactams.

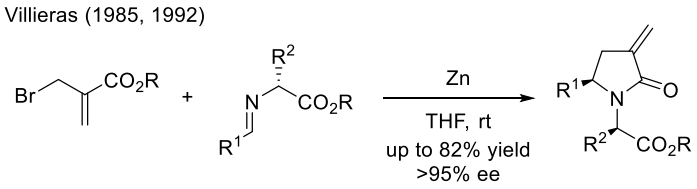

In 2003, Ryu and Komatsu evaluated the potential of hydrostannation and carbonylation of the azaenynes for the synthesis of α-alkylidene-γ-lactams via radical chemistry. Notably, this strategy proved successful not just for the synthesis of γ-lactams but also for that of various lactams having 4–9-membered rings (Scheme 3.3).[2b]

Scheme 3.3. Ryu and Komatsu's approach using radical source

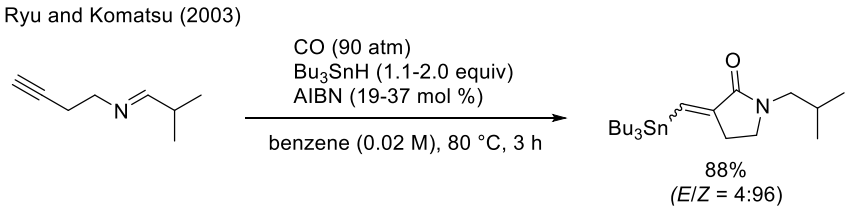

In 2004, Basavaiah demonstrated that MBH adducts can become a useful building block for the synthesis of α-alkylidene-γ-lactams (Scheme 3.4).[2f]

Scheme 3.4. Employment of MBH adducts reported by Basavaiah

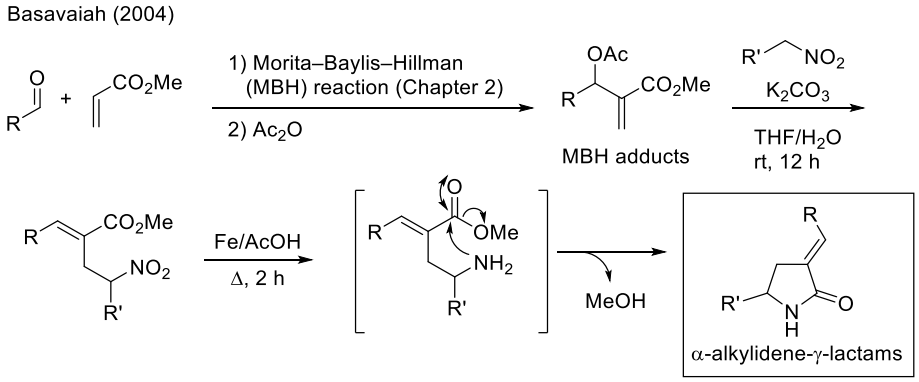

In studies published in 2004 and 2005, Corey employed the intramolecular MBH reaction to obtain α-alkylidene-γ-lactams that were used for the total synthesis of salinosporamide A and antiprotealide, respectively (Scheme 3.5).[2d,e] This evidence confirms the usefulness of α-alkylidene-γ-lactams as synthetic building blocks.

Scheme 3.5. Corey's work: Intramolecular MBH reaction

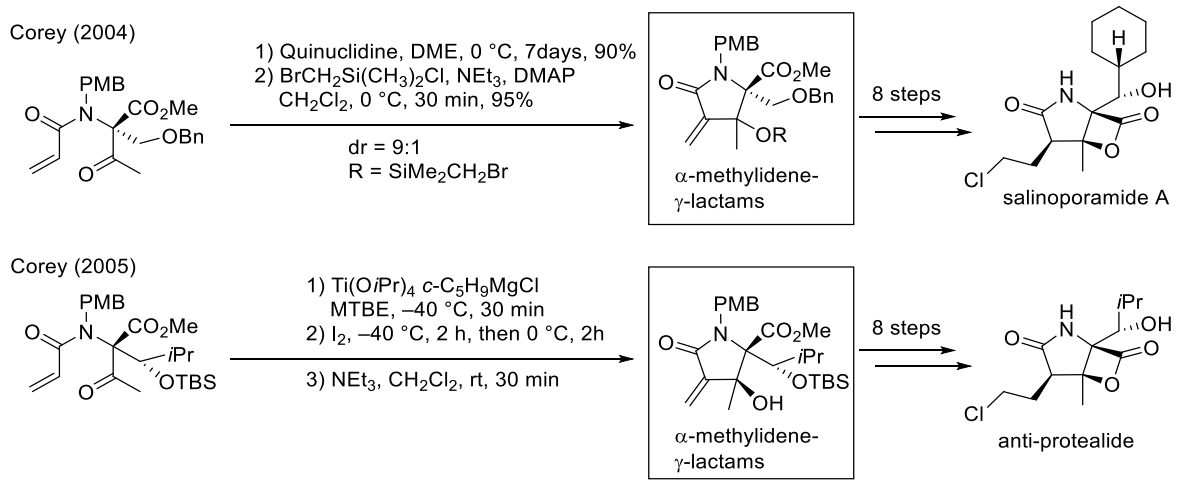

Another interesting approach to the synthesis of α-alkylidene-γ-lactams is to utilize the Horner–Wadsworth–Emmons reaction of α-(dialkoxyphosphoryl)lactams, as reported by Janecki in 2004.[2c] Although this method requires multistep reactions and gives an *N*-hydroxymethylated by-product, it enables synthesizing α-alkylidene-γ-lactams with relatively simple structures (Scheme 3.6). In 2010, the same research group expanded this method to the synthesis of β-aryl-γ-ethyl-α-methilidene-γ-lactams.[1k]

Scheme 3.6. Janecki's approach using Horner-Wadsworth-Emmons reaction

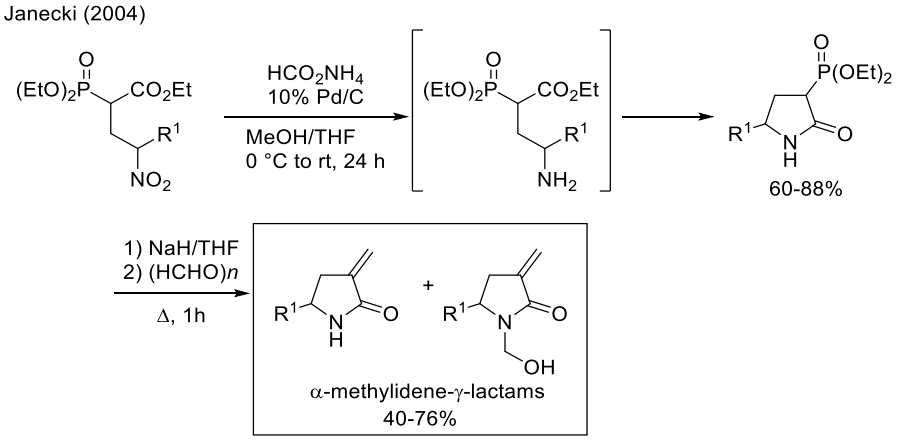

The enantioselective synthesis of α-alkylidene-γ-lactams was reported by Lu in 2006 for the first time.[3a] Despite the narrow substrate scope of this approach, the products obtained through it can be transformed into a natural product, (−)-isocynometrine (Scheme 3.7). After the publication of this study, some research groups reported the enantioselective synthesis of additional α-alkylidene-γ-lactams.[3b-e]

Scheme 3.7. Enantioselective synthesis of α-alkylidene-γ-lactams and their application

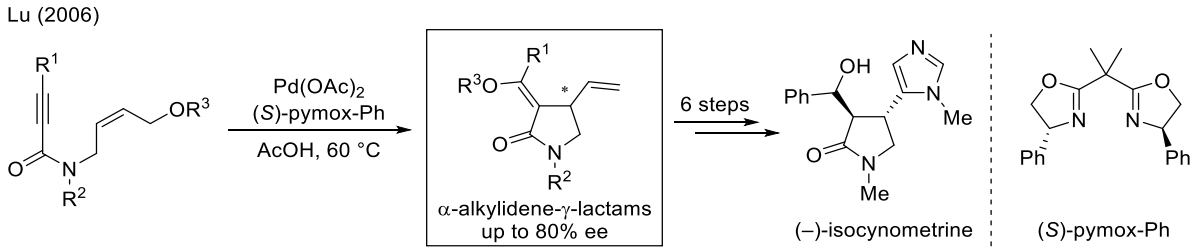

Despite the importance of α-alkylidene-γ-lactams discussed above, their syntheses often require complex building blocks and suffer from side reactions resulting from the high reactivity of the exo-alkylidene group. Therefore, the development of a facile synthetic approach to obtain α-alkylidene-γ-lactams involving asymmetric processes remains quite challenging for organic chemists.

As described in Chapter 1, Rauhut–Currier (RC) reaction is one of the Lewis base-catalyzed C–C bond forming reactions via the coupling of two different α,β-unsaturated carbonyl compounds wherein one acts as a latent enolate giving exo-methylidene products.[4] The author envisioned that the amidation of cyclohexadienone **2** with acryloyl chloride (**1**), followed by the Lewis base-catalyzed C–C bond formation of intermediary **3** would lead to the formation of α-methylidene-γ-lactam **4** in high yields and high enantioselectivities (Scheme 3.8).

Scheme 3.8. **This work**: A novel synthetic approach for α-methylidene-γ-lactams

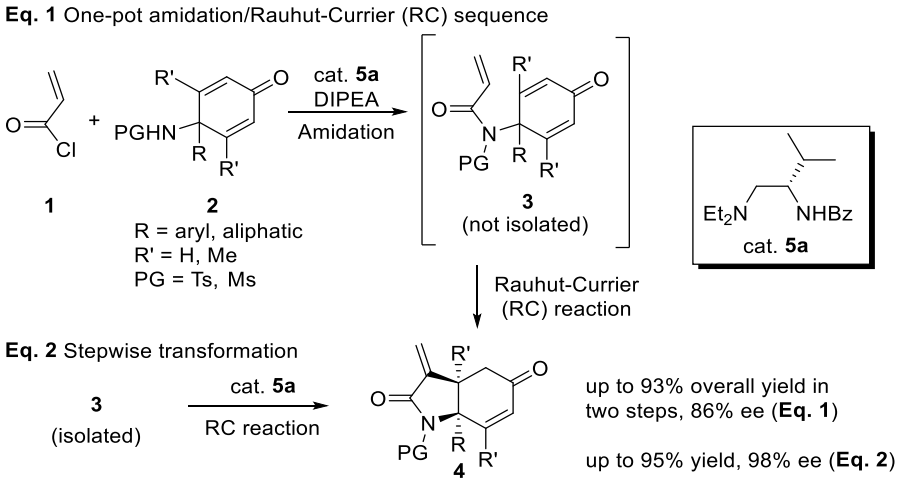

Herein, a combination of substrates **1**, **2**, and *N*,*N*-diisopropylethylamine (DIPEA) with novel chiral organocatalyst **5a** was found to promote a one-pot amidation/RC sequence, yielding highly functionalized α-alkylidene-γ-lactams **4** with a chiral tetrasubstituted carbon stereogenic center (Eq. 1). Moreover, a stepwise protocol could improve the enantioselectivities of products **4** with up to 98% ee (Eq. 2).

3.2. Results and Discussion

3.2.1. Unexpected RC Reaction in the Substrate Synthesis

For the synthesis of the model starting material **3a**, cyclohexadienone **2a**[5] was reacted with commercially available acryloyl chloride (**1**) in the presence of NEt_3 (Scheme 3.9). Surprisingly, formation of the desired product **3a** was not observed. Instead, the RC product **4a** was obtained in a 65% yield. Probably, the *in situ*-generated **3a** underwent an RC reaction catalyzed by residual NEt_3 acting as a Lewis base catalyst.

Scheme 3.9. Unexpected RC reaction in the substrate synthesis

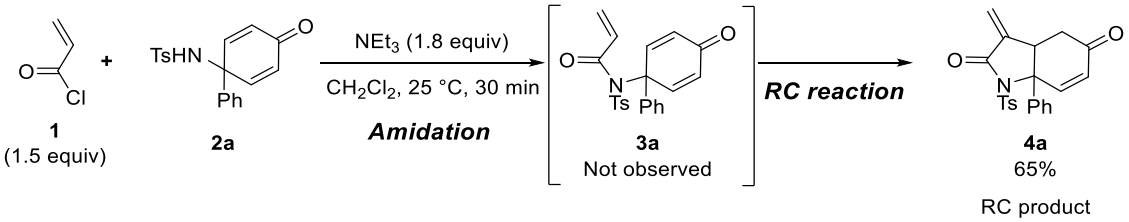

In general, RC reaction is catalyzed by strong Lewis bases, such as tertiary phosphines and thiolates.[4] Since this result indicates that the reaction of **3a** was catalyzed by a weak Lewis base like NEt_3, the author envisioned the occurrence of a sequential amidation/enantioselective RC reaction, in the presence of a chiral amine catalyst.

3.2.2. Optimization of the Reaction Conditions for Amidation/RC Sequence

Initially, the author selected acryloyl chloride (**1**) and cyclohexadienone **2a** as prototypical substrates to determine the optimal sequential reaction conditions. Among screening of the chiral organocatalysts (discussed later), the novel catalyst **5a** (Scheme 3.8), prepared from (*S*)-valine, exhibited a high catalytic activity (Table 3.1). When 150 mol % of catalyst **5a** was used at 25 °C in dichloromethane, α-methylidene-γ-lactam **4a** was obtained as a single diastereomer in 85% yield with 84% ee, whereas no corresponding RC precursor **3a** was detected (entry 1). Since **5a**-HCl salt had formed *in situ* as an inactive catalyst, various achiral bases that can trap the generated hydrogen chloride were studied to regenerate active catalyst **5a**. As results, the addition of *N,N,N′,N′*-tetramethyl-1,8-naphthalenediamine (proton sponge) or *N,N*-diisopropylethylamine (DIPEA) was found to restore the catalytic activity of **5a**: In the presence of 20 mol % of **5a** with proton sponge or DIPEA (1.5 equiv), product **4a** was obtained in 51% yield with 64% ee (for proton sponge) and 82% yield with 76% ee (for DIPEA), respectively (entries 2 and 8). In contrast, tetramethylguanidine and 1,8-diazabicyclo[5.4.0]undec-7-ene (DBU) did not show any improvements for the reaction (entries 6 and 7), respectively. Other solvents such as $CHCl_3$, toluene, and THF were not effective for the reaction, because of the low solubility of substrate **2a** (entries 3–5).

Table 3.1. Screening of bases and solvents

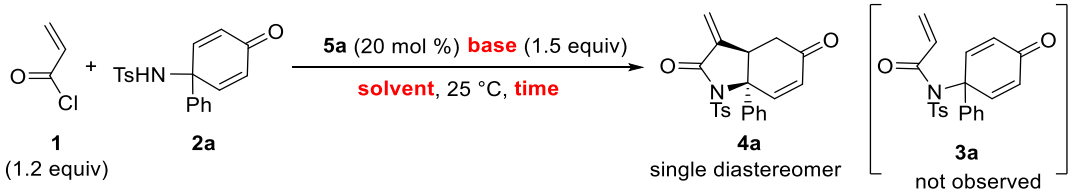

1 (1.2 equiv) **2a** **4a** single diastereomer **3a** not observed

entry	base	solvent	time (h)	NMR yield (%)[a]	ee (%)[b]
1[c]	-	CH_2Cl_2	17	84	85
2	proton sponge	CH_2Cl_2	72	51	64
3	proton sponge	$CHCl_3$	72	44	63
4	proton sponge	toluene	72	0	-
5	proton sponge	THF	72	0	-
6	tetramethylguanidine	CH_2Cl_2	48	5>	-
7	DBU	CH_2Cl_2	12	25	0
8	DIPEA	CH_2Cl_2	12	82	76

[a] 1,3,5-Trimethoxybenzene was used as an internal standard.
[b] Determined by HPLC (Daicel Chiralpak IC).
[c] 150 mol % of **5a** was used.

Next, the reaction temperature was screened using DIPEA in CH_2Cl_2 (Table 3.2). Compared with the 25°C case, the reaction rate and yield decreased at −20°C despite the increased ee value (entry 2). On the other hand, at reflux temperature, the reaction proceeded smoothly giving product **4a** in a 92% isolated yield with 80% ee (entry 3). With a lower loading of catalyst **5a** (10 mol %), the yield and enantioselectivity dropped (entry 4). Since in the absence of **5a** DIPEA did not promote the reaction (entry 5), the role of DIPEA is likely to be to restore the activity of the chiral catalyst. These outcomes indicate that **5a** works as a Brønsted- and Lewis base catalyst for the amidation and RC processes. Thus, the optimized conditions for this reaction were determined to be those detailed in entry 3 in Table 3.2.

Table 3.2. Screening of the reaction temperature

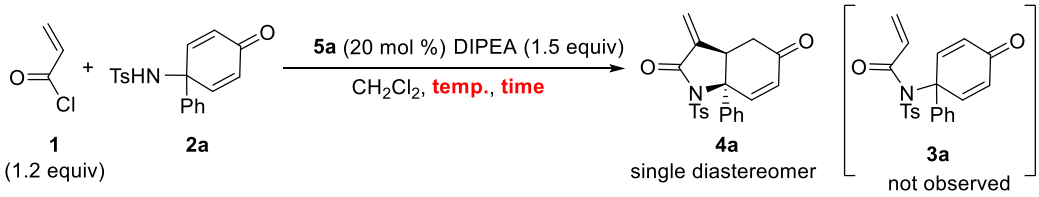

entry	temp. (°C)	time (h)	NMR yield (%)[a]	ee (%)[b]
1	25	12	82	76
2	–20	60	72	81
3	reflux	8	95 (92)[c]	80
4[d]	reflux	24	85	78
5[e]	25	24	0	-

[a] 1,3,5-Trimethoxybenzene was used as an internal standard.
[b] Determined by HPLC (Daicel Chiralpak IC).
[c] Isolated yield.
[d] 10 mol % of **5a** was used.
[e] In the absence of **5a**

3.2.3. Substrate Scope of Amidation/RC sequence

With the optimized condition in hand, the scope and limitations of the amidation/RC sequence were evaluated (Scheme 3.10). High enantiocontrol of products **4b-i** (63–86% ee) was achieved when using cyclohexadienones **2** with various substituents [R^1 = 4-tol (**2b**), 2-tol (**2c**), 4-*t*-Bu-C_6H_4 (**2d**), 4-Br-C_6H_4 (**2e**), 3-Cl-C_6H_4 (**2f**), Me (**2g**), Et (**2h**), or vinyl (**2i**); R^2 = Ts; R^3 = H]. The chiral amine **5a** also promoted the reaction of **2j-k** with methanesulfonyl amide (R^1 = Ph or Me, R^2 = Ms, R^3 = H) to give **4j-k** in good yields but with slightly decreased enantioselectivity. The construction of structural motifs bearing two contiguous stereogenic quaternary carbon centers is considered as especially challenging in organic synthesis.[6] When **2l** (R^1 = R^3 = Me, R^2 = Ts) was used in this enantioselective sequence, the corresponding lactam **4l** was obtained in 84% ee.

Scheme 3.10. Substrate scope of the amidation/RC sequence

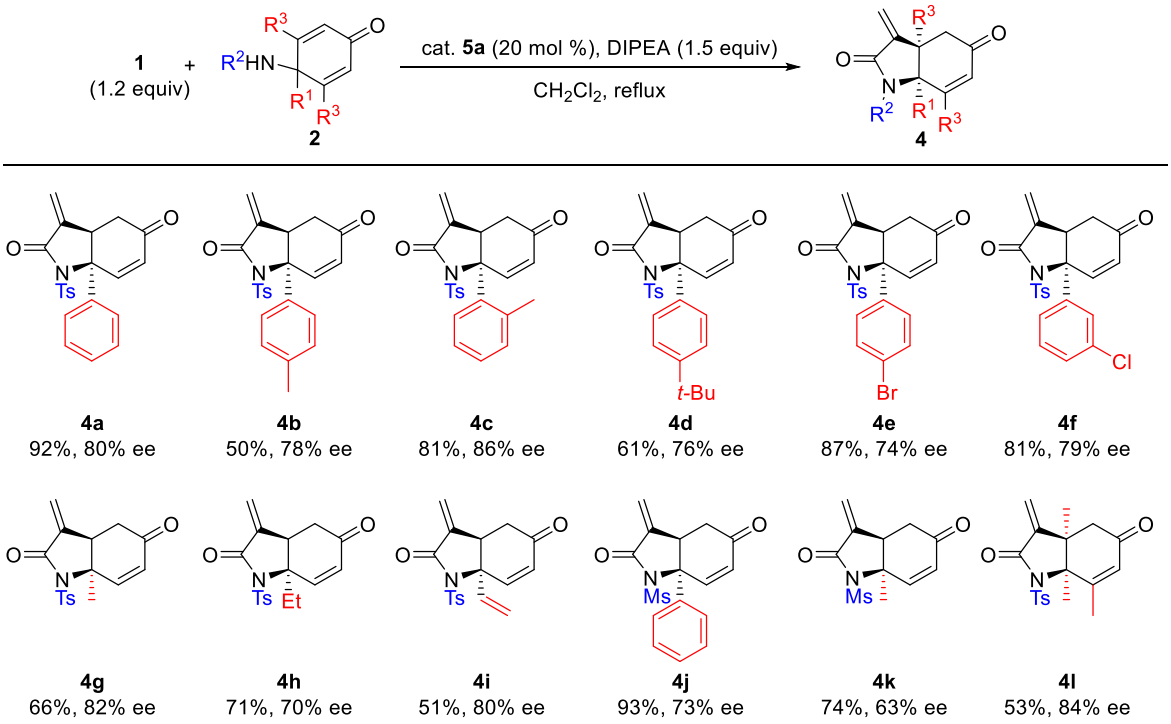

3.2.4. Isolation of Intermediate 3

In this reaction course, the author concluded that **5a** works as a Brønsted- and Lewis base catalyst for the amidation and RC processes, whereas DIPEA itself does not promote the reaction, and it effects the restoration of the activity of the chiral catalyst instead (Table 3.2, entry 5). To clarify the reaction mechanism, the isolation of the acrylamide intermediate **3** was attempted using a variety of non-nucleophilic bases that are inactive in the RC reaction (Table 3.3). Although the use of some strong bases resulted in the formation of a complex mixture or in no reaction (entries 2 and 3), the use of inorganic bases such as K_2CO_3, Cs_2CO_3,

and powdered NaOH enabled the isolation of intermediate **3a**, albeit in low yield, because of this compound's instability in silica-gel columns (entries 4–6). Finally, powdered NaOH afforded the best results: **3a** was obtained in a 32% isolated yield. Using this methodology, other **3**-type acrylamides were also isolated in 4–65% yields.

Table 3.3. Screening of non-nucleophilic bases for the isolation of intermediate **3a**

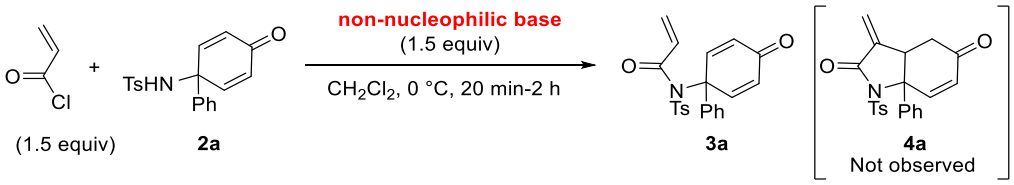

entry	non-nucleophilic base	isolated yield of **3a** (%)
1	-	No reaction
2	NaH	Complex mixture
3	tetramethylguanidine	No reaction
4	K_2CO_3	5
5	Cs_2CO_3	10
6	powdered NaOH	32

3.2.5. Optimization of the Reaction Conditions for the Stepwise RC Reaction

To investigate the reactivity of the reaction intermediate **3**, the isolated compound **3g** (R^1 = Me) was made to react with a variety of amine catalysts (Table 3.4). As expected, DIPEA itself did not promote the RC reaction (entry 1), whereas other achiral amines like DABCO, DMAP , and NEt_3 showed good reactivity (entries 2–4). Notably, the use of the chiral amine **5a** caused the reaction leading to the formation of **4g** to proceed with higher enantioselectivity (94% ee, entry 5) than the sequential process (82% ee; see Scheme 3.10). The use of other chiral amine catalysts—**5b**[7] (PG = Boc), **5c**[8] (PG = H), and **5d**[9] (*t*-Bu instead of *i*-Pr)—did not lead to any improvements in either reactivity or enantioselectivity (entries 6–8). In particular, the data obtained after the use of catalyst **5c** (39% ee) suggested the importance of the Brønsted acidity and/or steric environment around the NH group of the catalyst **5**. The use of β-ICD,[10] pyridine-type catalyst **6**,[11] and proline-type catalyst **7**[12] having a Brønsted acidic unit also resulted in inferior outcomes (entries 9–11). Finally, the catalyst **5a**, which worked well in the sequential reaction, was determined to be the optimal catalyst (entry 5).

Table 3.4. Screening of chiral amine catalysts

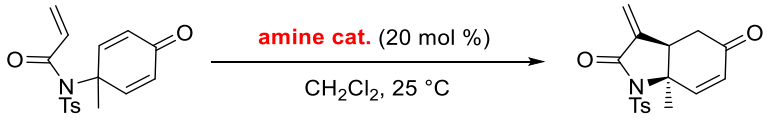

3g **4g**

entry	amine cat.	time (h)	NMR yield (%)[a]	ee (%)
1	DIPEA	96	0	-
2	DABCO	0.1	82	-
3	DMAP	0.1	80	-
4	NEt_3	0.5	85	-
5	**5a**	48	97 (95)[b]	94
6	**5b**	48	87	67
7	**5c**	48	95	39
8	**5d**	48	93	90
9	β-ICD	96	87	70
10	**9**	1.5	97	7
11	**10**	96	40	15

[a] 1,3,5-Trimethoxybenzene was used as an internal standard.
[b] Isolated yield.

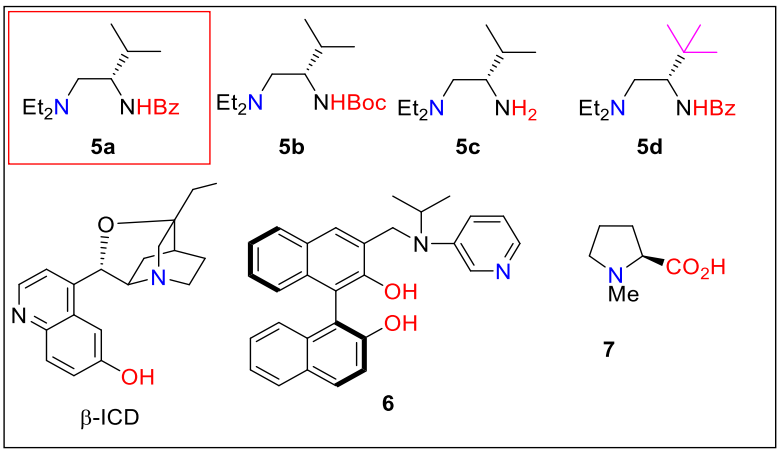

Table 3.5. The effect of the reaction temperature

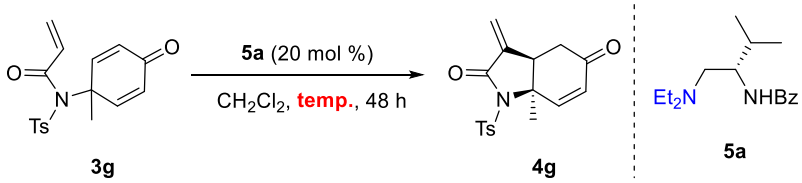

3g **4g** **5a**

entry	temp. (°C)	NMR yield (%)[a]	ee (%)
1	40	95	93
2	25	97 (95)[b]	94
3	0	92	92
4	–20	92	90

[a] 1,3,5-Trimethoxybenzene was used as an internal standard.
[b] Isolated yield.

Next, the reaction temperature was screened using the chiral amine catalyst **5a** (Table 3.5). Changes in the reaction temperature did not substantially affect either the yield or the enantioselectivity of the stepwise RC reaction; thus, the conditions detailed in entry 2 (at 25°C) were concluded to be optimal.

3.2.6. Substrate Scope for Stepwise RC Reaction

With the optimized condition in hand, the author also studied the stepwise transformation as shown in Scheme 3.11. In a comparison of outcomes between the one-pot amidation/RC sequence (Scheme 3.10) and the stepwise transformation, the latter one displayed higher enantioselectivities in all cases, however, RC precursors **3c-e** (R^1 = 2-tol, 4-*t*Bu-C_6H_4 or 4-Br- C_6H_4; R^2 = Ts, R^3 = H) and **3j** (R^1 = Ph, R^2 = Ms, R^3 = H) could not be isolated due to their instability. Therefore, the one-pot method can be useful as an alternative synthetic procedure for highly functionalized α-methylidene-γ-lactams **4**. Finally, the amine catalyst **5a** was found to be the best candidate for this reaction since chiral phosphine catalysts **5e-f**,[13] that are known to mediate asymmetric RC and MBH processes, led to low yields of product **4g** due to immediate polymerization of **3g** under optimized conditions (Eq. 3 in Scheme 3.11).

Scheme 3.11. Substrate scope for stepwise RC reaction of intermediate **3**

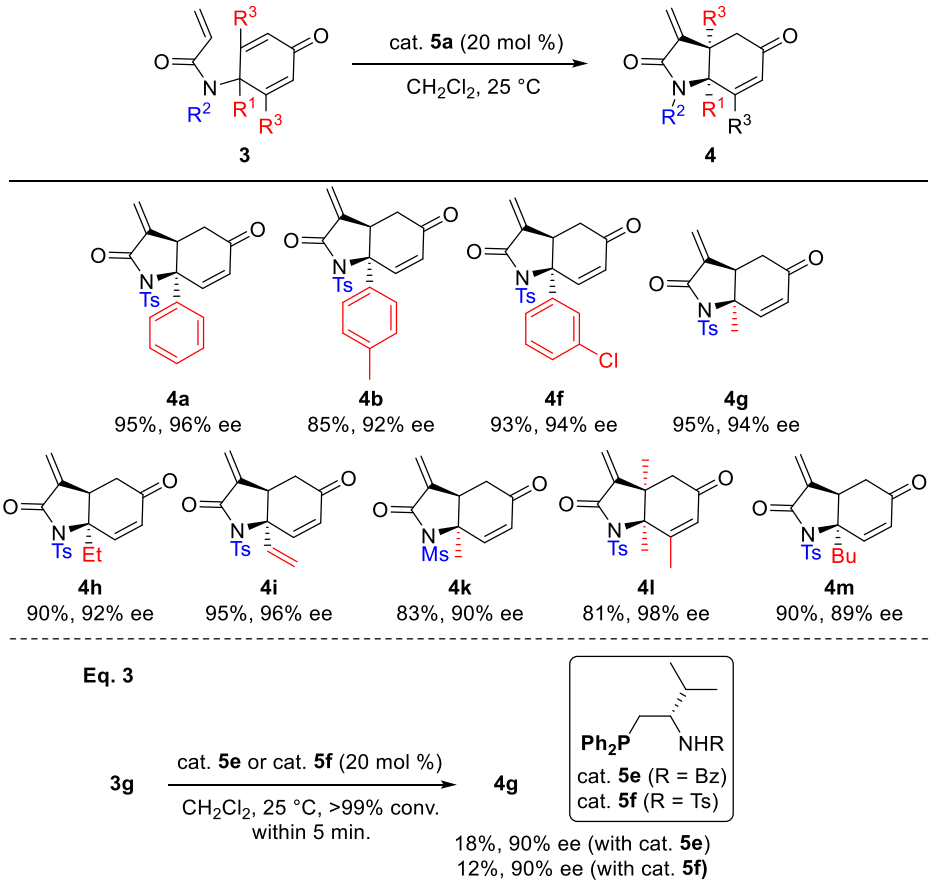

3.2.7. Reuse of the Catalyst and Determination of the Absolute Configuration of the RC product

Encouraged by the success with the stepwise reaction, the author examined the recovery and reuse of the catalyst **5a** (Table 3.6).[14] After completion of the RC reaction of **3g**, the product **4g** and organocatalyst **5a** were separated by simple acid/base extraction. Recovered catalyst **5a** was directly used for the next run without further purification. Catalyst **5a** maintained its activity even after being reused at least five times, affording the product **4g** in 95% yield with 94% ee.

Table 3.6. Reuse of the catalyst **5a** in the stereoselective RC reaction of **3g**

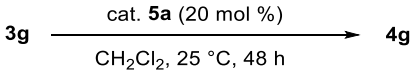

Cycle	1st	2nd	3rd	4th	5th
Results	95% 94% ee	95% 94% ee	95% 94% ee	95% 94% ee	95% 94% ee

Furthermore, optically pure **4g** could be readily isolated by single recrystallization of the enantioenriched product from CH_2Cl_2 and *n*-hexane. The absolute configuration of product **4g** obtained using catalyst (*S*)-**5a** was unequivocally determined by single crystal X-ray analysis to be (*R,R*) on the basis of the Flack parameter (Figure 3.2).

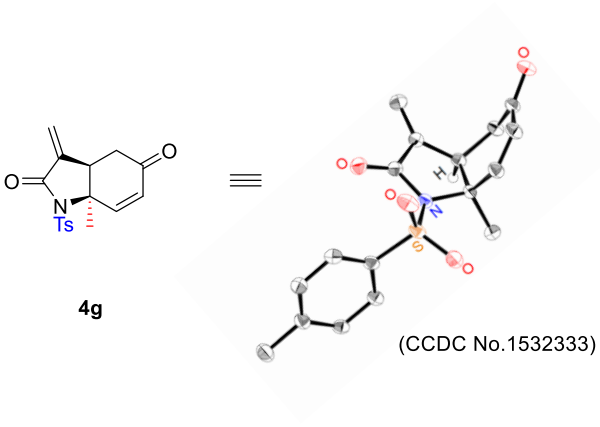

Figure 3.2. X-ray structure of **4g** (Most of hydrogen atoms are omitted for clarity).

3.2.8. The Reaction Mechanism for the Sequential Reaction

A plausible reaction mechanism for the sequential reaction consisting of an amidation step and RC cycle is depicted in Scheme 3.12. In the amidation step, catalyst **5a**, acting as a Brønsted base, abstracts a proton on the nitrogen atom of **2** and immediately reacts with **1**, resulting in the formation of RC precursor **3** along with the protonated form of **5a**. DIPEA could efficiently restore the Brønsted base catalyst activity of **5a** from protonated **5a** *in situ*, without any inhibition of the amidation and RC reactions (Table 3.4. entry 1). In the RC cycle, the Michael addition of **5a** to the acrylamide unit of **3** generates the ammonium intermediate A

(**Int. A**) stabilized byBrønsted acid moiety of catalyst **5a**,[4,13] which reacts with one of the olefins on the dienone part of the molecule. In order to avoid steric interactions between the *i*-Pr-substituent of the chiral catalyst **5a** and the NTs and R substituent on the substrate, the reaction using (*S*)-**5a** may afford the (*R,R*)-configuration in **Int. B**. The second Michael process forms intermediate B (**Int. B**). Proton-transfer from the α-position of a carbonyl group of the lactam to the enolate anion part in **Int. B** *via* the Brønsted acid moiety[4,13] results in formation of chiral α-methylidene-γ-lactams **4** together with regeneration of the organocatalyst through the retro-Michael reaction of the Lewis base unit in catalyst **5a**. The reaction of **3g** in the presence of D_2O (excess) gave the partially α-deuterated product **4g** [D content (%) α: 50, α': 0], thus indicating that the intramolecular Michael reaction of **Int. A** involves non-reversibility under optimized conditions (Eq. 4 in Scheme 3.12).

Scheme 3.12. Plausible reaction mechanism

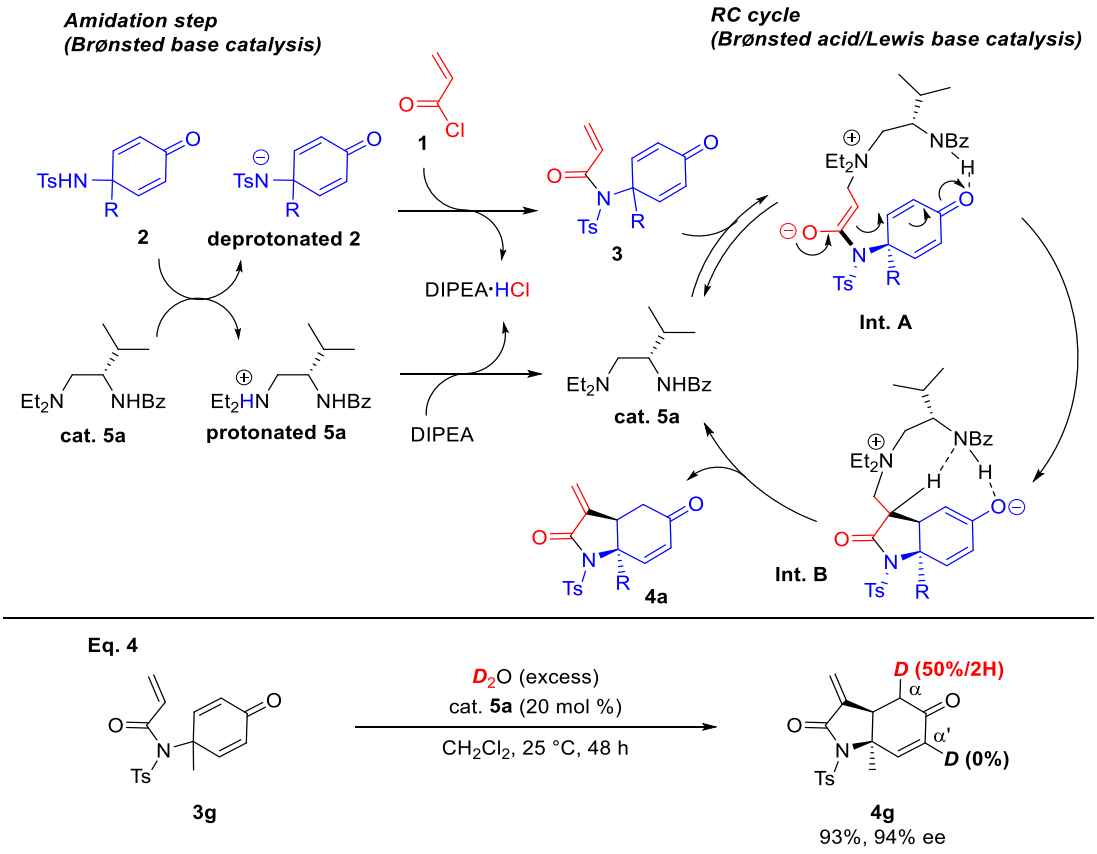

3.2.9. Synthetic Transformation of α-Methylidene-γ-Lactam

As mentioned in the introduction of this chapter, α-methylidene-γ-lactams are not important just as a basic structure present in many bioactive compounds; they are also useful synthetic building blocks because of their reactive exo-methylidene moiety. In the presence of triphenylphosphine (PPh_3), α-methylidene-γ-lactam **4g** and ethyl allenoate underwent [3+2] annulation[15] to form the tricyclic spiro-compound **8**, which comprises three contiguous chiral carbon centers in a single diastereomer (Scheme 3.13).

Scheme 3.13. Construction of three-contiguous chiral carbon centers

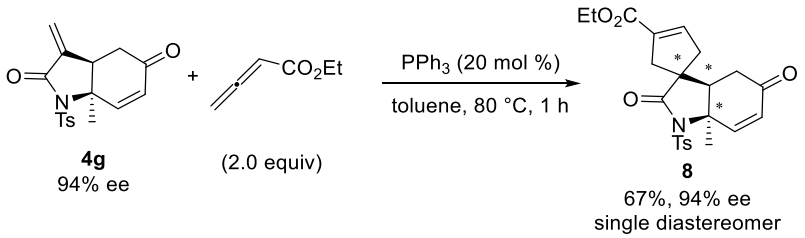

3.3. Conclusion

In summary, the author has developed a facile method for the construction of the α-methylidene-γ-lactam skeleton *via* an amidation/RC reaction sequence. The newly developed multifunctional catalyst **5a** works as a Brønsted base catalyst in the amidation step and a Lewis base-Brønsted acid catalyst in the RC cycle. Current chiral organocatalyst **5a** could be recovered easily by acid/base extraction and reused without any loss of catalytic activity. This study is the first example of enantioselective RC reaction using acrylamide.[16]

3.4. Experimental Section

3.4.1. General

^{1}H- and ^{13}C-NMR spectra were recorded with a JEOL JMN ECS400 FT NMR, JNM ECA600 FT NMR or Bruker AVANCE II (^{1}H-NMR 400, 600 or 700 MHz, ^{13}C-NMR 100, 150 or 176 MHz. ^{1}H-NMR spectra are reported as follows: chemical shift in ppm relative to the chemical shift of $CHCl_3$ at 7.26 ppm, integration, multiplicities (s = singlet, d = doublet, t = triplet, q = quartet, m = multiplet), and coupling constants (Hz). ^{13}C-NMR spectra reported in ppm relative to the central line of triplet for $CDCl_3$ at 77 ppm. CF_3CO_2H used as external standards for ^{19}F-NMR. FT-MS spectra were obtained with LTQ Orbitrap XL (Thermo Fisher Scientific). High resolution-MS spectra were obtained with JMS-T100LC (JEOL). Optical rotations were measured with JASCO P-1030 polarimeter. HPLC analyses were performed on a JASCO HPLC system (JASCO PU 980 pump and UV-975 UV/Vis detector) using a mixture of *n*-hexane/2-propanol as eluents. Column chromatography on SiO_2 was performed with Kanto Silica Gel 60 (40-100 μm).

3.4.2. Materials

Dehydrated THF, CH_2Cl_2, $CHCl_3$, toluene, and other commercially available organic and inorganic compounds were purchased and used without further purification. Known imines **11** were synthesized according to reported procedures.[5a] Known cyclohexadienones **2** were synthesized according to reported procedures.[5b]

3.4.3. Procedure for the Preparation of 10l.

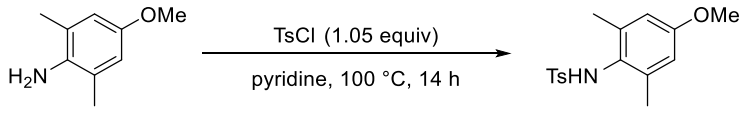

9l **10l** Quant

A solution of **9l** (8.67 mmol) and TsCl (9.10 mmol) in pyridine (29 mL) was heated to 100 °C. After 14 h, the solution was cooled to room temperature and concentrated. The resulting crude mixture was dissolved with EtOAc (40 mL) and washed with 10% aq. HCl (30 mL). The separated organic layer was dried over Na_2SO_4, dried *in vacuo,* giving pure product **10l** as white solid quantitatively.

10l: Quant; white solid; ^{1}H-NMR (400 MHz, $CDCl_3$) δ 7.60 (d, *J* = 8.2 Hz, 2H), 7.25 (d, *J* = 8.2 Hz, 2H), 6.54 (s, 2H), 5.80 (s, 1H), 3.76 (s, 3H), 2.42 (s, 3H), 1.99 (s, 6H); ^{13}C-NMR (100 MHz, $CDCl_3$) δ 158.4, 143.5, 139.3, 137.7, 129.6, 127.2, 125.3, 113.7, 55.2, 21.6, 19.0; HRMS (ESI) calcd for $C_{16}H_{19}NO_3SNa$ m/z = 328.0978, found m/z = 328.0977 [$(M+Na)^+$]; IR (KBr): ν 3283, 2361, 1517, 1327, 543 cm^{-1}.

3.4.4. Procedure for the Preparation of 2l

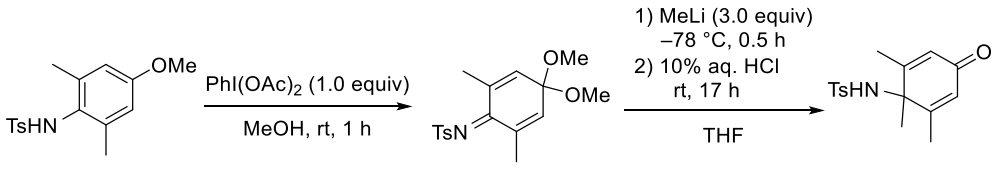

10l **11l** Not isolated **2l** 17% from **10l**

To a solution of **10l** (3.08 mmol) in MeOH (15 mL) was added $PhI(OAc)_2$ (3.08 mmol) at 0 °C and stirred at room temperature. After 1 h, saturated aq. $NaHCO_3$ was added to the reaction solution to quench. EtOAc (50 mL) was added to the reaction mixture and washed with brine (30 mL). The organic layer was separated and dried over Na_2SO_4. Evaporation of the solvent followed by evaporation gave **11l** as crude product. This crude product was dissolved in THF (10 mL) and reacted with MeLi (1.13M ether solution, 8.2 mL) at –78 °C. After 0.5 h, 10% aq. HCl (10 mL) was added to the reaction mixture, and then it warmed to room temperature and stirred for 17 h. The reaction mixture was dissolved with EtOAc (30 mL) and the organic phase was washed with saturated aq. $NaHCO_3$. The separated organic layer was dried over Na_2SO_4,

evaporated, dried *in vacuo* affording crude product which was purified by silica-gel column chromatography. Pure **2l** was obtained as yellow solid in 17% overall yield from **10l**.

2l: 17% yield; yellow solid; ^{1}H-NMR (400 MHz, $CDCl_3$) δ 7.63 (d, *J* = 8.4 Hz, 2H), 7.26 (d, *J* = 8.4 Hz, 2H), 6.04 (s, 2H), 5.09 (s, 1H), 2.43 (s, 3H), 1.79 (s, 6H), 1.40 (s, 3H); ^{13}C-NMR (100 MHz, $CDCl_3$) δ 185.0, 159.3, 144.0, 137.0, 129.4, 128.3, 127.7, 59.2, 26.3, 21.6, 18.6; HRMS (ESI) calcd for $C_{16}H_{19}NO_3SNa$ m/z = 328.0978 , found m/z = 328.0980 [$(M+Na)^+$]; IR (KBr): ν 3087, 2867, 1670, 1607, 1455, 1330, 988, 633 cm^{-1}.

3.4.5. General Procedure for the Preparation of Unknown Cyclohexadienones 2.

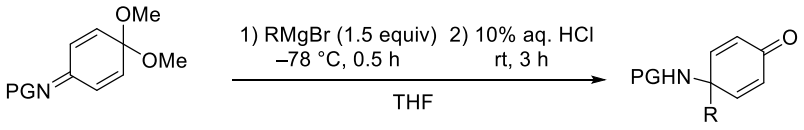

11 **2**

To a solution of **11** (5.0 mmol) in THF (10 mL) was added a solution of the corresponding Grignard reagents (7.5 mmol) in THF (7.5 mL) at –78 °C. After 0.5 h, the reaction mixture was acidified by aq. HCl, then, heated to room temperature. After 3 h, the organic layer was extracted with EtOAc and dried *in vacuo*. The resulting crude product was purified by silica-gel column chromatography, followed by recrystallization to provide dienones **2** as a solid.

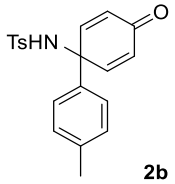

2b

2b: 63% yield; White solid; ^{1}H-NMR (400 MHz, $CDCl_3$) δ 7.66 (d, *J* = 8.2 Hz, 2H), 7.31 (d, *J* = 8.2 Hz, 2H), 7.26 (d, *J* = 8.2 Hz, 2H), 7.16 (d, *J* = 8.2 Hz, 2H), 6.75 (d, *J* = 10.1 Hz, 2H), 6.05 (d, *J* = 10.1 Hz, 2H), 5.27 (s, 1H), 2.43 (s, 3H), 2.33 (s, 3H); ^{13}C-NMR (100 MHz, $CDCl_3$) δ 185.0, 148.9, 144.2, 139.3, 137.4, 134.7, 130.1, 129.6, 127.8, 127.7, 125.6, 59.6, 21.6, 21.0; HRMS (ESI) calcd for $C_{20}H_{19}NO_3SNa$ m/z = 376.0978; found m/z = 376.0969 [$(M+Na)^+$]; IR (KBr): ν 3092, 2893, 1661, 1616, 1338, 1163, 962 cm^{-1}.

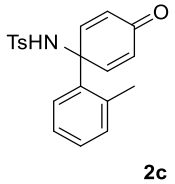

2c

2c: 73% yield; white solid; ^{1}H-NMR (400 MHz, $CDCl_3$) δ 7.62 (dt, *J* = 8.5, 1.8 Hz, 2H), 7.31 (dd, *J* = 8.0, 1.1 Hz, 1H), 7.19-7.27 (m, 4H), 7.11-7.15 (t, *J* = 8.0 Hz, 1H), 6.98 (dt, *J* = 11.0, 2.5 Hz, 2H), 6.07 (dt, *J* = 11.0, 2.5 Hz, 2H), 5.10 (s, 1H), 2.61 (s, 3H), 2.42 (s, 3H); ^{13}C-NMR (100 MHz, $CDCl_3$) δ 184.7, 147.2, 144.3,

137.5, 137.2, 135.7, 134.0, 129.7, 129.5, 128.3, 127.9, 126.9, 126.7, 60.4, 22.0, 21.7; HRMS (ESI) calcd for $C_{20}H_{19}NO_3SNa$ m/z = 376.0978; found m/z = 376.0980 [$(M+Na)^+$]; IR (KBr): ν 3115, 2875, 1662, 1616, 1334, 753 cm^{-1}.

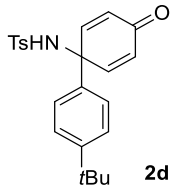

2d

2d: 51% yield; white solid; ^{1}H-NMR (400 MHz, $CDCl_3$) δ 7.65 (d, *J* = 8.2 Hz, 2H), 7.34 (s, 4H), 7.25 (d, *J* = 8.2 Hz, 3H), 6.78 (d, *J* = 10.1 Hz, 2H), 6.05 (d, *J* = 10.1 Hz, 2H), 5.44 (s, 1H), 2.42 (s, 3H), 1.28 (s, 9H); ^{13}C-NMR (100 MHz, $CDCl_3$) δ 184.9, 152.5, 148.9, 144.2, 137.4, 134.5, 129.6, 127.8, 127.7, 126.4, 125.5, 59.5, 34.6, 31.1, 21.6 HRMS (ESI) calcd for $C_{23}H_{25}NO_3SNa$ m/z = 418.1447; found m/z = 418.1440 [$(M+Na)^+$]; IR (KBr): ν 3095, 2953, 1664, 1618, 1340, 722 cm^{-1}.

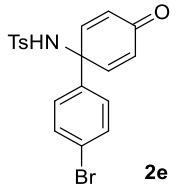

2e

2e: 45% yield; white solid; ^{1}H-NMR (400 MHz, $CDCl_3$) δ 7.63 (d, *J* = 8.2 Hz, 2H), 7.43 (d, *J* = 8.7 Hz, 2H), 7.24-7.30 (m, 4H), 6.76 (d, *J* = 10.5 Hz, 2H), 6.05 (d, *J* = 10.5 Hz, 2H), 5.82 (s, 1H), 2.43 (s, 3H); ^{13}C-NMR (100 MHz, $CDCl_3$) δ 184.6, 147.9, 144.4, 137.1, 136.8, 132.4, 129.7, 128.0, 127.8, 127.6, 123.3, 59.4, 21.6; HRMS (ESI) calcd for $C_{19}H_{16}BrNO_3SNa$ m/z = 439.9926; found m/z = 439.9921 [$(M+Na)^+$]; IR (KBr): ν 3107, 2899, 1662, 1617, 1335, 712 cm^{-1}.

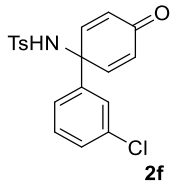

2f

2f: 40% yield; white solid; ^{1}H-NMR (400 MHz, $CDCl_3$) δ 7.64 (d, *J* = 8.2 Hz, 2H), 7.40 (d, *J* = 1.8 Hz, 1H), 7.25-7.34 (m, 5H), 6.77 (d, *J* = 10.1 Hz, 2H), 6.09 (d, *J* = 10.1 Hz, 2H), 5.41 (s, 1H), 2.43 (s, 3H); ^{13}C-NMR (100 MHz, $CDCl_3$) δ 184.5, 147.7, 144.5, 139.7, 137.2, 135.4, 130.6, 129.7, 129.4, 128.3, 127.8, 126.2, 124.0, 59.4, 21.6; HRMS (ESI) calcd for $C_{19}H_{16}ClNO_3SNa$ m/z = 396.0432; found m/z = 396.0432 [$(M+Na)^+$]; IR (KBr): ν 3094, 2881, 1656, 1619, 1336, 1155, 857 cm^{-1}.

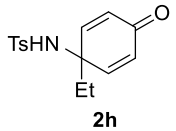

2h

2h: 43% yield; white solid; ^{1}H-NMR (400 MHz, $CDCl_3$) δ 7.66 (d, *J* = 8.2 Hz, 2H), 7.26 (d, *J* = 8.2 Hz, 2H),

6.53 (d, *J* = 10.1 Hz, 2H), 6.09 (d, *J* = 10.1 Hz, 1H), 5.25 (s, 1H) , 2.42 (s, 3H), 1.76 (q, *J* = 7.6 Hz, 2H), 0.79 (t, *J* = 7.6 Hz, 3H); ^{13}C-NMR (100 MHz, $CDCl_3$) δ 185.0, 149.2, 144.2, 137.4, 129.6, 127.8, 58.1, 33.4, 21.6, 7.5; HRMS (ESI) calcd for $C_{15}H_{17}NO_3SNa$ m/z = 314.0821; found m/z = 314.0811 [$(M+Na)^+$]; IR (KBr): ν 3133, 2971, 2775, 1661, 1615, 1320, 1181, 869 cm^{-1}.

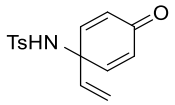

2i

2i: 13% yield; white solid; ^{1}H-NMR (600 MHz, $CDCl_3$) δ 7.69 (d, *J* = 8.4 Hz, 2H), 7.27 (d, *J* = 8.4 Hz, 2H), 6.65 (d, *J* = 10.8 Hz, 2H), 6.06 (d, *J* = 10.8 Hz, 2H), 5.89 (s, 1H), 5.62 (dd, *J* = 17.2, 10.3 Hz, 1H), 5.38 (d, *J* = 17.2 Hz, 1H), 5.24 (d, *J* = 10.3 Hz, 1H), 2.42 (s, 3H); ^{13}C-NMR (100 MHz, $CDCl_3$) δ 184.9, 147.8, 144.3, 137.2, 135.1, 129.6, 128.2, 127.7, 117.7, 58.4, 21.5 HRMS (ESI) calcd for $C_{15}H_{15}NO_3SNa$ m/z = 312.0665; found m/z = 312.0659 [$(M+Na)^+$]; IR (KBr): ν 3088, 2878, 1661, 1616, 1334, 1160, 998, 555 cm^{-1}.

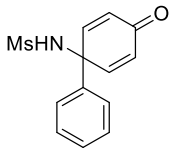

2j

2j: 31% yield; white solid; ^{1}H-NMR (400 MHz, $CDCl_3$) δ 7.47-7.52 (m, 2H), 7.33-7.41 (m, 3H), 7.08-7.12 (m, 2H), 6.32-6.36 (m, 2H), 5.75 (s, 1H), 3.02 (s, 3H); ^{13}C-NMR (100 MHz, $CDCl_3$) δ 184.8, 148.9, 137.5, 129.4, 129.2, 128.2, 125.8, 59.8, 43.0; HRMS (ESI) calcd for $C_{13}H_{13}NO_3SNa$ m/z = 286.0508; found m/z = 286.0510 [$(M+Na)^+$]; IR (KBr): ν 3153, 2881, 1661, 1613, 1336, 1161, 980, 756 cm^{-1}.

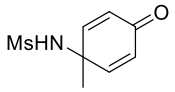

2k

2k: 57% yield; white solid; ^{1}H-NMR (400 MHz, $CDCl_3$) δ 6.96 (d, *J* = 10.4 Hz, 2H), 6.29 (d, *J* = 10.4 Hz, 2H), 5.30 (s, 1H), 3.00 (s, 3H), 1.56 (s, 3H); ^{13}C-NMR (100 MHz, $CDCl_3$) δ 184.5, 150.5, 128.6, 54.6, 43.0, 27.4; HRMS (ESI) calcd for $C_8H_{11}NO_3SNa$ m/z = 224.0352; found m/z = 224.0348 [$(M+Na)^+$]; IR (KBr): ν 3293, 2986, 1712, 1671, 1631, 1139, 594 cm^{-1}.

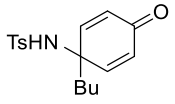

2k

2m: 12% yield; white solid; ^{1}H-NMR (400 MHz, $CDCl_3$) δ 7.67 (d, *J* = 8.2 Hz, 2H), 7.25 (d, *J* = 8.2 Hz, 2H), 6.56 (d, *J* = 10.1 Hz, 2H), 6.05 (d, *J* = 10.1 Hz, 2H), 5.68 (s, 1H), 2.41 (s, 3H), 1.70-1.66 (m, 2H), 1.24-1.10 (m, 4H), 0.80 (t, *J* = 7.3 Hz, 3H); ^{13}C-NMR (100 MHz, $CDCl_3$) δ 185.2, 149.7, 144.1, 137.4, 129.6, 129.2,

127.7, 57.6, 40.1, 25.1, 22.4, 21.6, 13.7; HRMS (ESI) calcd for $C_{17}H_{21}NO_3SNa$ m/z = 342.1134; found m/z = 342.1128 [$(M+Na)^+$]; IR (KBr): ν 3117, 2934, 1659, 1614, 1343, 1161, 873 cm^{-1}.

3.4.6. General Procedure for the Preparation of Acrylamide 3.

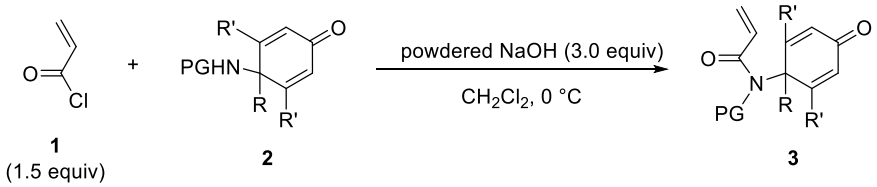

A round bottom flask was charged with a dichloromethane solution of dienone **2** (10 mL, 1.0 mmol) and powdered NaOH (3.0 mmol). Then, acrolylchloride (1.5 mmol) was added to the reaction solution at 0 °C. The reaction mixture was stirred vigorously at 0 °C for 1 h The reaction was then quenched with water, extracted with dichloromethane, and dried over Na_2SO_4. The combined organic solvent was removed *in vacuo* and the obtained crude product was quickly purified by silica-gel column chromatography using *n*-hexane/EtOAc as an eluent to give the desired product (product **3** is not so stable in silica-gel).

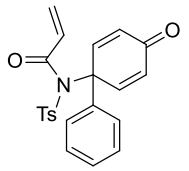

3a

3a: 32% yield; white solid; ^{1}H-NMR (400 MHz, $CDCl_3$) δ 7.61-7.64 (m, 2H), 7.24-7.33 (m, 9H), 6.94 (dd, *J* = 16.9, 10.1 Hz, 1H), 6.21 (dd, *J* = 16.9, 1.1 Hz, 1H), 6.04 (d, *J* = 10.4 Hz, 2H), 5.78 (dd, *J* = 10.1, 1.1 Hz, 1H), 2.44 (s, 3H); ^{13}C-NMR (100 MHz, $CDCl_3$) δ 184.7, 169.4, 147.9, 145.7, 138.9, 134.7, 133.2, 130.9, 129.8, 129.4, 128.6, 128.5, 127.6, 125.0, 65.6, 21.7; HRMS (ESI) calcd for $C_{22}H_{19}NO_4SNa$ m/z = 416.0927; found m/z = 416.0927 [$(M+Na)^+$]; IR (KBr): ν 3030, 2368, 1702, 1670, 1397, 1349, 1191, 1176, 989, 751, 661 cm^{-1}.

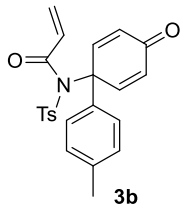

3b

3b: 12% yield; pale yellow oil; ^{1}H-NMR (400 MHz $CDCl_3$) δ 7.62 (d, *J* = 8.2 Hz, 2H), 7.31-7.26 (m, 4H), 7.17 (d, *J* = 8.2 Hz, 2H), 7.07 (d, *J* = 8.2 Hz, 2H), 6.92 (dd, *J* = 17.4, 10.1 Hz, 1H), 6.23 (dd, *J* = 17.4, 0.9 Hz, 1H), 6.02 (d, *J* = 10.1 Hz, 2H), 5.78 (dd, *J* = 10.1, 0.9 Hz, 1H), 2.44 (s, 3H), 2.28 (s, 3H); ^{13}C-NMR (100 MHz, $CDCl_3$) δ 184.8, 169.5, 148.1, 145.6, 138.6, 136.4, 135.5, 133.3, 130.8, 130.1, 129.7, 128.5, 127.4,

124.9, 65.4, 21.7, 21.0; HRMS (ESI) calcd for $C_{23}H_{21}NO_4SNa$ m/z = 430.1083; found m/z = 430.1082 [$(M+Na)^+$]; IR (KBr): ν 3033, 2921, 1703, 1666, 1496, 1355, 1177, 984 cm^{-1}.

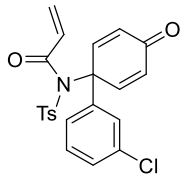

3f

3f: 4% yield; pale yellow oil; ^{1}H-NMR (400 MHz $CDCl_3$) δ 7.61 (d, *J* = 8.2 Hz, 2H), 7.18-7.31 (m, 8H), 6.96 (dd, *J* = 16.9, 10.1 Hz, 1H), 6.24 (dd, *J* = 16.9, 1.1 Hz, 1H), 6.06 (d, *J* = 10.5 Hz, 2H), 5.83 (dd, *J* = 10.1, 1.1 Hz, 1H), 2.45 (s, 3H) ^{13}C-NMR (100 MHz, $CDCl_3$) δ 184.4, 169.3, 147.2, 145.9, 140.7, 136.2, 135.3, 133.0, 131.3, 130.5, 129.9, 128.8, 128.4, 128.1, 125.3, 123.1, 65.1, 21.7; HRMS (ESI) calcd for $C_{22}H_{18}ClNO_4SNa$ m/z = 450.0537; found m/z = 450.0536 [$(M+Na)^+$]; IR (KBr): ν 3035, 2925, 1705, 1660, 1354, 1179, 980 cm^{-1}.

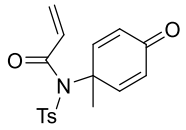

3g

3g: 65% yield; white solid; ^{1}H-NMR (400 MHz, $CDCl_3$) δ 7.61 (d, *J* = 8.2 Hz, 2H), 7.25-7.27 (m, 2H), 7.07-7.11 (m, 2H), 6.75 (dd, *J* = 16.9, 10.1 Hz, 1H), 6.45 (dd, *J* = 16.9, 1.4 Hz, 1H), 5.92-6.00 (m, 3H), 2.41 (s, 3H), 1.54 (s, 3H); ^{13}C-NMR (150 MHz, $CDCl_3$) δ 184.2, 170.1, 150.2, 145.2, 136.4, 133.7, 131.5, 129.6, 128.1, 127.2, 60.1, 26.7, 21.5; HRMS (ESI) calcd for $C_{17}H_{17}NO_4SNa$, m/z = 354.0770; found m/z = 354.0774 [$(M+Na)^+$]; IR (KBr): ν 3044, 1672, 1345, 1182, 973, 866, 666, 592 cm^{-1}.

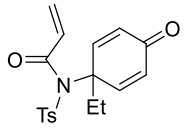

3h

3h: 43% yield; white solid; ^{1}H-NMR (400 MHz, $CDCl_3$) δ 7.58 (d, *J* = 8.2 Hz, 2H), 7.24 (d, *J* = 8.2 Hz, 2H), 7.06 (d, *J* = 10.1 Hz, 2H), 6.81 (dd, *J* = 16.9, 10.1 Hz, 1H), 6.49 (dd, *J* = 16.9, 0.9 Hz, 1H), 6.01 (d, *J* = 10.1 Hz, 2H), 5.96 (dd, *J* = 10.1, 0.9 Hz, 1H), 2.41 (s, 3H), 1.93 (q, *J* = 7.3 Hz, 2H), 0.74 (t, *J* = 7.3 Hz, 3H,); ^{13}C-NMR (100 MHz, $CDCl_3$) δ 184.6, 170.8, 148.6, 145.4, 136.5, 134.5, 131.5, 129.6, 128.8, 128.5, 64.1, 31.0, 21.6, 8.2; HRMS (ESI) calcd for $C_{18}H_{19}NO_4SNa$ m/z = 368.0927; found m/z = 368.0912 [$(M+Na)^+$]; IR (KBr): ν 3042, 1677, 1340, 1180, 865, 656, 590 cm^{-1}.

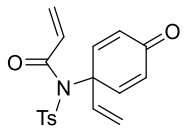

3i

3i: 53% yield; white solid; ^{1}H-NMR (600 MHz $CDCl_3$) δ 7.62 (d, *J* = 8.4 Hz, 2H), 7.27 (d, *J* = 8.4 Hz, 2H), 7.06 (d, *J* = 10.0 Hz, 2H), 6.84 (dd, *J* = 16.9, 10.1 Hz, 1H), 6.42 (dd, *J* = 16.9, 1.4 Hz, 1H), 6.05 (d, *J* = 10.0 Hz, 2H), 5.89 (dd, *J* = 10.1, 1.4 Hz, 1H), 5.69 (dd, *J* = 17.2, 10.3 Hz, 1H), 5.21 (d, *J* = 17.2 Hz, 1H), 5.12 (d, *J* = 10.3 Hz, 1H), 2.43 (s, 3H); ^{13}C-NMR (100 MHz, $CDCl_3$) δ 184.7, 169.3, 147.0, 145.5, 136.5, 134.9, 133.3, 131.3, 129.8, 128.3, 128.0, 117.1, 64.2, 21.7; HRMS (ESI) calcd for $C_{18}H_{17}NO_4SNa$ m/z = 366.0770; found m/z = 366.0766 [$(M+Na)^+$]; IR (KBr): ν 3063, 2252, 1699, 1670, 1631, 1400, 1177, 663 cm^{-1}

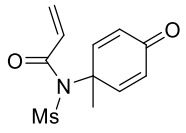

3k

3k: 12% yield; white solid; ^{1}H-NMR (400 MHz $CDCl_3$) δ 7.19 (d, *J* = 10.1 Hz, 2H), 6.44-6.46 (m, 2H), 6.26 (d, *J* = 10.1 Hz, 2H), 5.90 (dd, *J* = 8.2, 3.2 Hz, 1H), 3.26 (s, 3H), 1.79 (s, 3H); ^{13}C-NMR (100 MHz, $CDCl_3$) δ 184.1, 169.3, 150.3, 132.5, 131.9, 128.1, 60.7, 44.5, 26.8; HRMS (ESI) calcd for $C_{11}H_{13}NO_4SNa$ m/z = 278.0457; found m/z = 278.0453 [$(M+Na)^+$]; IR (KBr): ν 3025, 2937, 1702, 1667, 1626, 1350, 1180, 862 cm^{-1}.

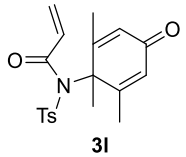

3l

3l: 45% yield; white solid; ^{1}H-NMR (400 MHz $CDCl_3$ at 60 °C) δ 7.87 (br, 2H), 7.36 (d, *J* = 8.2 Hz, 2H), 6.79 (dd, *J* = 16.3, 10.3 Hz, 1H), 6.36 (d, *J* = 16.3 Hz, 1H), 6.04 (s, 2H), 5.76 (d, *J* = 10.3 Hz, 1H), 2.45 (s, 3H), 1.92 (s, 6H), 1.82 (s, 3H); ^{13}C-NMR (100 MHz, $CDCl_3$) δ 184.5, 162.1, 145.2, 137.4, 131.4, 129.8, 128.4, 126.9, 77.3, 77.0, 76.7, 27.5, 21.2, 19.7 (Some peaks are broad out or overlapped); HRMS (ESI) calcd for $C_{19}H_{21}NO_4SNa$ m/z = 382.1083; found m/z = 382.1086 [$(M+Na)^+$]; IR (KBr): ν 3092, 2991, 1666, 1623, 1353, 1190, 964, 819 cm^{-1}.

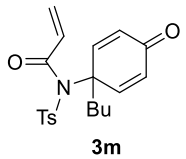

3m

3m: 33% yield; white solid; ^{1}H-NMR (400 MHz, $CDCl_3$) δ 7.55-7.58 (m, 2H), 7.23 (d, *J* = 8.2 Hz, 2H), 7.08

(dt, *J* = 11.0, 2.5 Hz, 2H), 6.81 (dd, *J* = 16.9, 11.0 Hz, 1H), 6.48 (dd, *J* = 16.9, 2.5 Hz, 1H), 5.94-6.01 (m, 3H), 2.41 (s, 3H), 1.83-1.87 (m, 2H), 1.06-1.20 (m, 4H), 0.78 (t, *J* = 7.1 Hz, 3H); ^{13}C-NMR (100 MHz, $CDCl_3$) δ 184.7, 170.8, 149.0, 145.4, 136.5, 134.6, 131.4, 129.6, 128.6, 128.5, 63.6, 37.7, 25.7, 22.4, 21.6, 13.7; HRMS (ESI) calcd for $C_{20}H_{23}NO_4SNa$ m/z = 396.1240; found m/z = 396.1239 [$(M+Na)^+$]; IR (KBr): ν 3253, 3122, 2958, 1662, 1616, 1512, 1338, 1159, 814 cm^{-1}.

3.4.7. General Procedure for the Preparation of α-Methylidene-γ-Lactam 4.

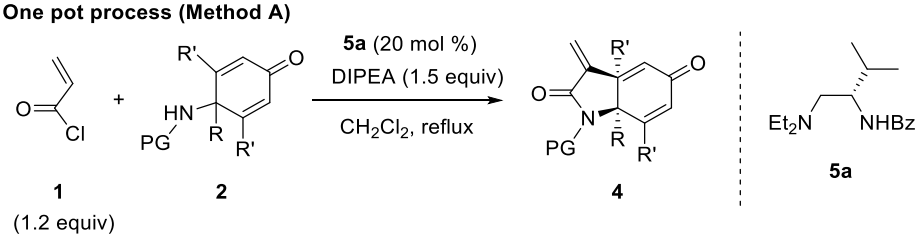

Acryloyl chloride **1** (0.12 mmol) was added to a mixture of dienone **2** (0.10 mmol), DIPEA (0.15 mmol) and catalyst **5a** (0.020 mmol, 20 mol%) in dichloromethane (0.50 mL) under reflux conditions. After the full conversion of **2** as determined by TLC, crude reaction mixture was directly purified by silica-gel column chromatography using *n*-hexane/EtOAc as an eluent to provide the corresponding product **4** as a white solid or colorless oil.

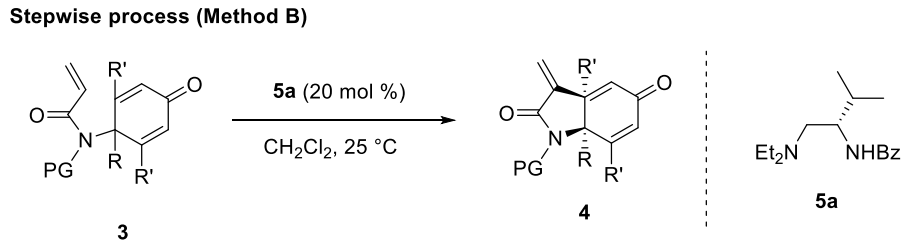

The chiral amine catalyst **5a** (0.020 mmol, 20 mol%) was added to a dichloromethane solution of acrylamide **3** (0.10 mmol, 0.50 mL) at 25 °C. After the full conversion of **3** on TLC, the reaction mixture was directly purified by silica-gel column chromatography using *n*-hexane/EtOAc as eluents to provide the corresponding product **4** as a white solid or colorless oil.

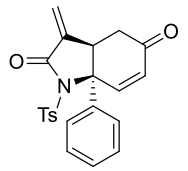

4a

4a: 92% yield for **Method A**, 95% yield for **Method B**; white solid; ^{1}H-NMR (400 MHz, $CDCl_3$) δ 7.85 (d, *J* = 8.6 Hz, 2H), 7.51 (dd, *J* = 10.4, 1.6 Hz, 1H), 7.48-7.37 (m, 5H), 7.33 (d, *J* = 8.6 Hz, 2H), 6.33 (d, *J* = 10.4 Hz, 1H), 6.24 (d, *J* = 3.7 Hz, 1H), 5.44 (d, *J* = 2.7 Hz, 1H), 3.45-3.37 (m, 1H), 2.74-2.54 (m, 2H), 2.45 (s, 3H); ^{13}C-NMR (100 MHz, $CDCl_3$) δ 194.6, 165.8, 145.7, 144.6, 139.4, 138.3, 135.4, 130.3, 129.3, 129.2, 128.9, 128.8, 125.8, 120.7, 69.9, 48.7, 35.0, 21.7; HRMS (ESI) calcd for $C_{22}H_{19}NO_4SNa$ m/z = 416.0927; found m/z = 416.0921 [$(M+Na)^+$]; IR (KBr): ν 3056, 2925, 2300, 1720, 1691, 1366, 1240, 1172, 1062, 909, 700 cm^{-1}; $[\alpha]_D^{24}$ = –39 (*c* 0.71, $CHCl_3$) for 96% ee; Enantiomeric excess: 80% for **Method A**, 96% for **Method B**, determined by HPLC (Daicel Chiralpak IC, *n*-hexane/EtOH = 2/1; flow rate 1.0 ml/min; 25°C; 225 nm) first peak (Minor): t_R = 9.5 min, second peak (Major): t_R = 14.1 min.

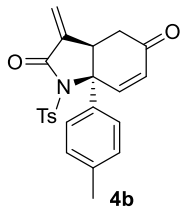

4b

4b: 50% yield for **Method A**, 85% yield for **Method B**; white solid; ^{1}H-NMR (400 MHz, $CDCl_3$) δ 7.86 (d, *J* = 8.7 Hz, 2H), 7.50 (dd, *J* = 10.5, 1.8 Hz, 1H), 7.24-7.34 (m, 6H), 6.31 (d, *J* = 10.5 Hz, 1H), 6.22 (d, *J* = 3.2 Hz, 1H), 5.43 (d, *J* = 3.2 Hz, 1H), 3.38-3.40 (m, 1H), 2.56-2.70 (m, 2H), 2.45 (s, 3H), 2.41 (s, 3H); ^{13}C-NMR (100 MHz, $CDCl_3$) δ 194.6, 165.8, 145.6, 144.8, 138.8, 138.5, 136.5, 135.6, 130.1, 129.6, 129.3, 129.2, 125.7, 120.5, 77.3, 77.0, 76.7, 69.9, 48.8, 35.1, 21.7, 21.2; HRMS (ESI) calcd for $C_{23}H_{21}NO_4SNa$ m/z = 430.1083; found m/z = 430.1084 [$(M+Na)^+$]; IR (KBr): ν 2925, 2852, 1725, 1691, 1359, 660, 544 cm^{-1}; $[\alpha]_D^{24}$ = –42 (*c* 0.85, $CHCl_3$) for 92% ee; Enantiomeric excess: 78% for **Method A,** 92% for **Method B**, determined by HPLC (Daicel Chiralpak AD-H, *n*-hexane/EtOH = 2/1; flow rate 1.0 ml/min; 25°C; 220 nm) first peak (Minor): t_R = 18.8 min, second peak (Major): t_R = 32.8 min.

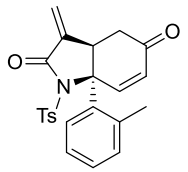

4c

4c: 81% yield for **Method A**; white solid; ^{1}H-NMR (400 MHz, $CDCl_3$) δ 7.84 (d, *J* = 8.2 Hz, 2H), 7.61 (dd,

J = 10.5, 1.8 Hz, 1H), 7.28-7.38 (m, 6H), 6.29 (d, *J* = 3.2 Hz, 1H), 6.24 (d, *J* = 10.5 Hz, 1H), 5.49 (d, *J* = 3.2 Hz, 1H), 3.75 (m, 1H), 2.58-2.73 (m, 2H), 2.43 (s, 3H), 2.25 (s, 3H); ^{13}C-NMR (100 MHz, $CDCl_3$) δ 194.7, 165.4, 146.0, 145.7, 138.3, 136.2, 135.4, 135.2, 133.8, 129.4, 129.2, 129.1, 128.8, 128.0, 126.3, 121.5, 70.3, 44.2, 35.6, 21.7, 21.1; HRMS (ESI) calcd for $C_{23}H_{21}NO_4SNa$ m/z = 430.1083; found m/z = 430.1083 [$(M+Na)^+$]; IR (KBr): ν 1725, 1693, 1341, 1155, 575 cm^{-1}; $[\alpha]_D^{24}$ = –35 (*c* 1.0, $CHCl_3$) for 86% ee; Enantiomeric excess: 86%, determined by HPLC (Daicel Chiralpak AD-H, *n*-hexane/EtOH = 2/1; flow rate 1.0 ml/min; 25°C; 221 nm) first peak (Minor): t_R = 12.6 min, second peak (Major): t_R = 22.3 min.

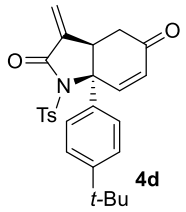

4d

4d: 61% yield for **Method A**; white solid; ^{1}H-NMR (400 MHz, $CDCl_3$) δ 7.82 (d, *J* = 8.2 Hz, 2H), 7.52 (dd, *J* = 10.5, 1.8 Hz, 1H), 7.43 (d, *J* = 8.7 Hz, 2H), 7.29-7.32 (m, 4H), 6.31 (d, *J* = 10.5 Hz, 1H), 6.22 (d, *J* = 3.2 Hz, 1H), 5.42 (d, *J* = 3.2 Hz, 1H), 3.42 (t, *J* = 1.6 Hz, 1H), 2.56-2.70 (m, 2H), 2.45 (s, 3H), 1.36 (s, 9H); ^{13}C-NMR (100 MHz, $CDCl_3$) δ 194.7, 165.8, 151.8, 145.5, 144.9, 138.6, 136.3, 135.7, 130.1, 129.3, 129.1, 125.8, 125.5, 120.4, 69.8, 48.7, 35.2, 34.7, 31.3, 21.7; HRMS (ESI) calcd for $C_{26}H_{27}NO_4SNa$ m/z = 472.1553; found m/z = 472.1551 [$(M+Na)^+$]; IR (KBr): ν 1732, 1693, 1359, 1150, 580 cm^{-1}; $[\alpha]_D^{27}$ = –46 (*c* 4.1, $CHCl_3$) for 76% ee; Enantiomeric excess: 76%, determined by HPLC (Daicel Chiralpak IC, *n*-hexane/EtOH = 2/1; flow rate 1.0 ml/min; 25°C; 225 nm) first peak (Minor): t_R = 6.9 min, second peak (Major): t_R = 14.8 min.

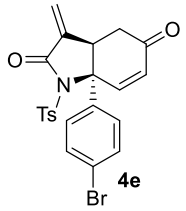

4e

4e: 87% yield for **Method A**; white solid; ^{1}H-NMR (400 MHz, $CDCl_3$) δ 7.86 (d, *J* = 8.2 Hz, 2H), 7.58 (d, *J* = 8.2 Hz, 2H), 7.46 (dd, *J* = 8.2, 1.8 Hz, 1H), 7.32 (dd, *J* = 19.0, 8.2 Hz, 4H), 6.32-6.34 (m, 1H), 6.24 (d, J = 3.2 Hz, 1H), 5.45 (d, J = 3.2 Hz, 1H), 3.34-3.36 (m, 1H), 2.55-2.72 (m, 2H), 2.46 (s, 3H); ^{13}C-NMR (100 MHz, $CDCl_3$) δ 194.1, 165.6, 145.9, 143.8, 138.8, 138.0, 135.3, 132.2, 130.6, 129.5, 129.2, 127.5, 123.0, 121.0, 69.4, 48.6, 34.9, 21.8; HRMS (ESI) calcd for $C_{22}H_{18}BrNO_4SNa$ m/z = 494.0032; found m/z = 494.0021 [$(M+Na)^+$]; IR (KBr): ν 1732, 1693, 1359, 1150, 580 cm^{-1}; $[\alpha]_D^{27}$ = –70 (*c* 4.1, $CHCl_3$) for 74% ee; Enantiomeric excess: 74%, determined by HPLC (Daicel Chiralpak IC, *n*-hexane/EtOH = 2/1; flow rate 1.0 ml/min; 25°C; 225 nm) first peak (Minor): t_R = 6.9 min, second peak (Major): t_R = 12.2 min.

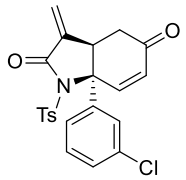

4f

4f: 81% yield for **Method A**, 93% yield for **Method B**; white solid; ^{1}H-NMR (400 MHz, $CDCl_3$) δ 7.86 (dd, *J* = 8.5, 2.1 Hz, 2H), 7.31-7.48 (m, 7H), 6.34 (dd, *J* = 10.5, 0.9 Hz, 1H), 6.26 (d, *J* = 3.0 Hz, 1H), 5.46 (d, *J* = 3.0 Hz, 1H), 3.36-3.38 (m, 1H), 2.57-2.74 (m, 2H), 2.46 (s, 3H); ^{13}C-NMR (100 MHz, $CDCl_3$) δ 194.0, 165.5, 145.9, 143.8, 141.6, 138.0, 135.3, 135.1, 130.6, 130.3, 129.5, 129.1, 126.1, 124.1, 120.9, 69.4, 48.6, 34.9, 21.7; HRMS (ESI) calcd for $C_{22}H_{18}ClNO_4SNa$ m/z = 450.0537; found m/z = 450.0537 [$(M+Na)^+$]; IR (KBr): ν 2364, 1725, 1699, 1358, 1150, 782 cm^{-1}; $[\alpha]_D^{24}$ = –33 (*c* 1.0, $CHCl_3$) for 94% ee; Enantiomeric excess: 79% for **Method A**, 94% for **Method B**, determined by HPLC (Daicel Chiralpak AD-H, *n*-hexane/EtOH = 2/1; flow rate 1.0 ml/min; 25°C; 220 nm) first peak (Minor): t_R = 14.4 min, second peak (Major): t_R = 40.1 min.

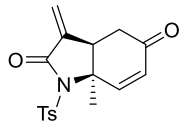

4g

4g: 66% yield for **Method A**, 95% yield for **Method B**; white solid; ^{1}H-NMR (400 MHz, $CDCl_3$) δ 7.98 (d, 2H, *J* = 8.4 Hz), 7.35 (d, *J* = 8.4 Hz, 2H), 7.24 (dd, *J* = 10.6, 1.4 Hz, 1H), 6.17 (d, *J* = 2.8 Hz, 1H), 6.02 (d, *J* = 10.6 Hz, 1H), 5.45 (d, *J* = 2.8 Hz, 1H), 3.14-3.21 (m, 1H), 2.70-2.81 (m, 2H), 2.44 (s, 3H), 1.98 (s, 3H); ^{13}C-NMR (100 MHz, $CDCl_3$) δ 194.3, 165.3, 146.8, 145.5, 138.4, 135.9, 129.6, 128.6, 128.1, 120.8, 64.7, 45.2, 36.2, 25.1, 21.7; HRMS (ESI) calcd for $C_{17}H_{17}NO_4SNa$ m/z = 354.0770; found m/z = 354.0775 [$(M+Na)^+$]; IR (KBr): ν 2967, 1722, 1684, 1350, 1167, 805, 661, 583 cm^{-1}; $[\alpha]_D^{25}$ = –58 (*c* 1.1, $CHCl_3$) for 94% ee; Enantiomeric excess: 82% for **Method A**, 94% for **Method B**, determined by HPLC (Daicel Chiralpak AD-H, *n*-hexane/EtOH = 2/1; flow rate 1.0 ml/min; 25°C; 215 nm) first peak (Major): t_R = 18.1 min, second peak (Minor): t_R = 28.1 min.

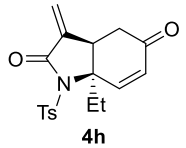

4h

4h: 71% yield for **Method A**, 90% yield for **Method B**; White solid; ^{1}H-NMR (400 MHz, $CDCl_3$) δ 7.96 (d, *J* = 8.2 Hz, 2H), 7.33 (d, *J* = 8.2 Hz, 2H), 7.27 (d, *J* = 10.5 Hz, 1H), 6.16 (d, *J* = 2.4 Hz, 1H), 6.12 (d, *J* = 10.5 Hz, 1H), 5.47 (d, *J* = 2.4 Hz, 1H), 3.30-3.39 (m, 1H), 2.55-2.70 (m, 2H), 2.37-2.48 (m, 4H), 2.11-2.22 (m, 1H), 1.09 (t, *J* = 7.6 Hz, 3H); ^{13}C-NMR (100 MHz, $CDCl_3$) δ 194.9, 165.7, 146.5, 145.5, 139.0, 135.6,

129.5, 129.3, 128.9, 120.9, 68.2, 40.5, 37.9, 30.3, 21.7, 8.8; HRMS (ESI) calcd for $C_{18}H_{19}NO_4SNa$ m/z = 368.0927; found m/z = 368.0926 [$(M+Na)^+$]; IR (KBr): ν 2972, 2359, 1725, 1688, 1353, 1155, 665 cm^{-1}; $[\alpha]_D^{23}$ = –48 (*c* 2.5, $CHCl_3$) for 92% ee; Enantiomeric excess: 70% for **Method A**, 92% for **Method B**, determined by HPLC (Daicel Chiralpak AD-H, *n*-hexane/EtOH = 2/1; flow rate 1.0 ml/min; 25°C; 221 nm) first peak (Major): t_R = 14.6 min, second peak (Minor): t_R = 18.4 min.

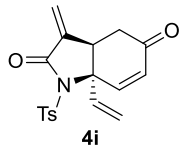

4i

4i: 51% yield for **Method A**, 95% yield for **Method B**; white solid; ^{1}H-NMR (400 MHz, $CDCl_3$) δ 8.00 (d, *J* = 8.2 Hz, 2H), 7.36 (d, *J* = 8.2 Hz, 2H), 7.13 (dd, *J* = 10.7, 1.7 Hz, 1H), 6.17-6.24 (m, 3H), 5.50 (d, *J* = 10.7 Hz, 1H), 5.44 (d, *J* = 2.7 Hz, 1H), 5.35 (d, *J* = 17.2 Hz, 1H), 3.18 (m, 1H), 2.75 (m, 2H), 2.45 (s, 3H); ^{13}C-NMR (100 MHz, $CDCl_3$) δ 194.4, 165.1, 145.6, 143.6, 138.0, 136.8, 135.8, 130.4, 129.7, 128.8, 120.9, 117.3, 68.3, 44.1, 34.5, 21.7; HRMS (ESI) calcd for $C_{18}H_{17}NO_4SNa$ m/z = 366.0770; found m/z = 366.0760 [$(M+Na)^+$]; IR (KBr): ν 3003, 2357, 1735, 1690, 1515, 1362, 1173, 666 cm^{-1}; $[\alpha]_D^{22}$ = –71 (*c* 0.38, $CHCl_3$) for 96% ee; Enantiomeric excess: 80% for **Method A**, 96% for **Method B**, determined by HPLC (Daicel Chiralpak IA, *n*-hexane/2-propanol = 9/1; flow rate 1.0 ml/min; 25°C; 225 nm) first peak (Major): t_R = 29.4 min, second peak (Minor): t_R = 33.7 min.

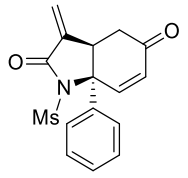

4j

4j: 93% yield for **Method A**; white solid; ^{1}H-NMR (400 MHz, $CDCl_3$) δ 7.38-7.47 (m, 5H), 7.26 (d, *J* = 10.4 Hz, 1H), 6.31-6.37 (m, 2H), 5.56 (d, *J* = 2.7 Hz, 1H), 3.47 (q, *J* = 2.7 Hz, 1H), 3.36 (s, 3H), 2.63-2.78 (m, 2H); ^{13}C-NMR (100 MHz, $CDCl_3$) δ 194.3, 166.8, 143.5, 139.4, 138.1, 130.6, 129.2, 128.8, 125.1, 121.5, 69.7, 48.6, 43.1, 34.7; HRMS (ESI) calcd for $C_{16}H_{15}NO_4SNa$ m/z = 340.0614; found m/z = 340.0616 [$(M+Na)^+$]; IR (KBr): ν 2354, 1731, 1672, 1353, 1145, 750 cm^{-1}; $[\alpha]_D^{24}$ = –90 (*c* 1.1, $CHCl_3$) for 73% ee; Enantiomeric excess: 73%, determined by HPLC (Daicel Chiralpak AD-H, *n*-hexane/EtOH = 2/1; flow rate 1.0 ml/min; 25°C; 216 nm) first peak (Minor): t_R = 13.6 min, second peak (Major): t_R = 20.8 min.

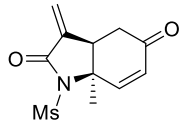

4k

4k :74% yield for **Method A**, 83% yield for **Method B**; white solid; ^{1}H-NMR (400 MHz, $CDCl_3$) δ 7.04 (dd, *J* = 10.5, 1.6 Hz, 1H), 6.32 (d, *J* = 3.2 Hz, 1H), 6.01 (d, *J* = 10.5 Hz, 1H), 5.57 (d, *J* = 3.2 Hz, 1H), 3.39 (s, 3H), 3.26 (qd, *J* = 3.2, 1.6 Hz, 1H), 2.83 (d, *J* = 5.0 Hz, 2H), 1.93 (s, 3H); ^{13}C-NMR (100 MHz, $CDCl_3$) δ 194.1, 166.6, 145.9, 138.1, 128.4, 121.7, 64.9, 45.1, 43.1, 36.1, 25.2; HRMS (ESI) calcd for $C_{11}H_{13}NO_4SNa$ m/z = 278.0463; found m/z = 278.0449 [$(M+Na)^+$]; IR (KBr): ν 3013, 2926, 2357, 1722, 1684, 1357, 1231, 1164, 971 cm^{-1}; $[\alpha]_D^{22}$ = –130 (*c* 0.21, $CHCl_3$) for 90% ee; Enantiomeric excess: 63% for **Method A**, 90% for **Method B**, determined by HPLC (Daicel Chiralpak AD-H, *n*-hexane/EtOH = 2/1; flow rate 1.0 ml/min; 25°C; 215 nm) first peak (Major): t_R = 17.9 min, second peak (Minor): t_R = 46.5 min.

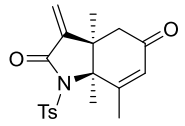

4l

4l: 53% yield for **Method A**, 81% yield for **Method B**; white solid; ^{1}H-NMR (400 MHz, $CDCl_3$) δ 7.98 (d, *J* = 8.2 Hz, 2H), 7.35 (d, *J* = 8.2 Hz, 2H), 6.01 (s, 1H), 5.84 (s, 1H), 5.29 (s, 1H), 2.62 (m, 2H), 2.44 (s, 3H), 2.31 (d, *J* = 1.4 Hz, 3H), 1.88 (s, 3H), 0.95 (s, 3H); ^{13}C-NMR (100 MHz, $CDCl_3$) δ 194.4, 160.1, 145.4, 144.0, 135.5, 129.5, 128.7, 127.3, 118.4, 73.2, 48.5, 41.7, 24.8, 21.7, 21.3, 17.6; HRMS (ESI) calcd for $C_{19}H_{21}NO_4SNa$ m/z = 382.1083; found m/z = 382.1080 [$(M+Na)^+$]; IR (KBr): ν 3743, 3650, 2971, 2366, 1741, 1677, 1356, 1173, 1089, 816, 663 cm^{-1}; $[\alpha]_D^{26}$ = –87 (*c* 0.31, $CHCl_3$) for 98% ee; Enantiomeric excess: 84% for **Method A**, 98% for **Method B**, determined by HPLC (Daicel Chiralpak AD-H, *n*-hexane/EtOH = 2/1; flow rate 1.0 ml/min; 25°C; 216 nm) first peak (Major): t_R = 10.1 min, second peak (Minor): t_R = 11.9 min.

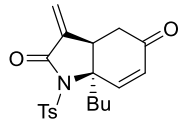

4m

4m: 90% yield for **Method B**; colorless oil; ^{1}H-NMR (400 MHz, $CDCl_3$) δ 7.96 (d, *J* = 8.0 Hz, 2H), 7.34 (d, *J* = 8.0 Hz, 2H), 7.29 (d, *J* = 0.9 Hz, 1H), 6.16 (d, *J* = 2.3 Hz, 1H), 6.10 (d, *J* = 10.5 Hz, 1H), 5.46 (d, *J* = 2.3 Hz, 1H), 3..40-3.33 (m, 1H), 2.72-2.55 (m, 2H), 2.44 (s, 3H), 2.41-2.29 (m, 1H), 2.21-2.02 (m, 1H), 1.49-1.22 (m, 4H), 0.95 (t, *J* = 7.1 Hz, 3H); ^{13}C-NMR (100 MHz, $CDCl_3$) δ 194.9, 165.7, 146.7, 145.5, 139.1, 135.6, 129.5, 129.1, 128.9, 120.9, 67.8, 41.1, 38.0, 37.3, 26.4, 22.8, 21.7, 13.9; HRMS (ESI) calcd for $C_{20}H_{23}NO_4SNa$ m/z = 396.1240; found m/z = 396.1236 [$(M+Na)^+$]; IR (KBr): ν 2922, 2853, 2361, 1729,

1697, 1355, 1086, 802, 590 cm^{-1}; $[\alpha]_D^{25}$ = –39 (*c* 0.36, $CHCl_3$) for 89% ee; Enantiomeric excess: 89%, determined by HPLC (Daicel Chiralpak ID, *n*-hexane/EtOH = 2/1; flow rate 1.0 ml/min; 25°C; 215 nm) first peak (Minor): t_R = 11.5 min, second peak (Major): t_R = 14.3 min.

3.4.8. Synthesis of chiral amine catalyst 5a

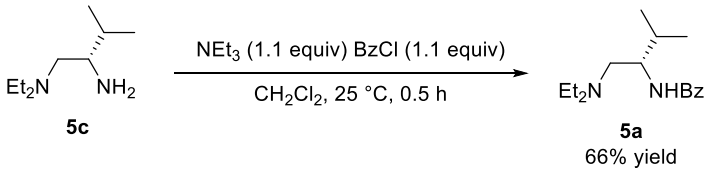

A solution of **5c** (0.32 mmol) and triethylamine (0.35 mmol) in dichloromethane (1.6 mL) was treated with benzoylchloride (0.35 mmol) at 0 °C. The reaction mixture was warmed to room temperature and stirred for 0.5 h. The reaction was quenched with saturated aq. $NaHCO_3$ (3.0 mL) followed by extraction with EtOAc (3.0 mL). The separated organic layer was dried over Na_2SO_4 and reduced *in vacuo*. The obtained residue was purified by silica-gel column chromatography using *n*-hexane/EtOAc/NEt_3 (10/10/1) mixed eluent, giving **5a** in 66% yield as a white solid.

^{1}H-NMR (400 MHz, $CDCl_3$) δ 7.76-7.78 (m, 2H), 7.40-7.50 (m, 3H), 6.42 (d, *J* = 6.0 Hz, 1H), 4.03 (qd, *J* = 7.3, 5.0 Hz, 1H), 2.45-2.62 (m, 6H), 2.15-2.23 (m, 1H), 0.95-1.00 (m, 12H); ^{13}C-NMR (100 MHz, $CDCl_3$) δ 167.6, 135.3, 131.1, 128.5, 126.8, 53.0, 52.3, 47.0, 29.8, 18.6, 17.9, 11.8; HRMS (ESI) calcd for $C_{16}H_{26}NO_4SNa$ m/z = 285.1937; found m/z = 285.1938 [$(M+Na)^+$]; IR (KBr): ν 3313, 2964, 1634, 1546, 1187, 696 cm^{-1}; $[\alpha]_D^{26}$ = +18 (*c* 1.0, $CHCl_3$) for >99% ee.

3.4.9. Procedure for the Reuse of Catalyst 5a in the Stepwise RC Reaction of 3g

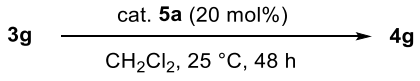

Cycle	1st	2nd	3rd	4th	5th
Results	95% 94% ee	95% 94% ee	95% 94% ee	95% 94% ee	95% 94% ee

After the full conversion of **3g** with **Method B**, diethyl ether (1.5 mL) and saturated aq. NH_4Cl (2.0 mL) was added to the reaction mixture. Evaporation of the separated organic layer gave product **4g**. The aqueous layer was basified with saturated aq. $NaHCO_3$ followed by extraction using $CHCl_3$/MeOH (4:1) mixed solvent (2.0 mL×2). Evaporation of the organic layer gave catalyst **5a**, which can be used for the next reaction without further purification.

3.4.10. Procedure for the [3+2] Annulation

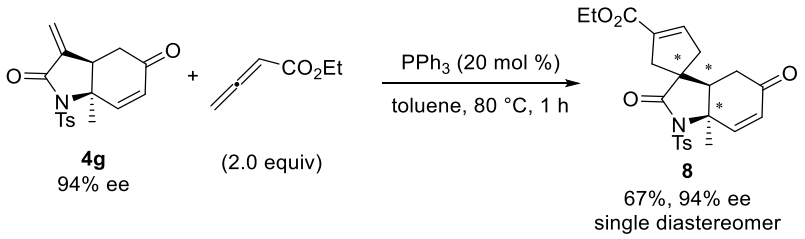

To a solution of **4g** (0.10 mmol) and ethyl allenoate (0.20 mmol) in toluene (10 mL) was added PPh_3 (0.020 mmol) at 80 °C and stirred for 1 h. The solution was cooled to room temperature and purified by silica-gel column chromatography using *n*-hexane/EtOAc mixed solvent as eluent giving pure product **8** as a colorless oil.

^{1}H-NMR (400 MHz, $CDCl_3$) δ 7.94 (d, *J* = 8.0 Hz, 2H), 7.49 (dd, *J* = 10.5, 2.0 Hz, 1H), 7.34 (d, *J* = 8.0 Hz, 2H), 6.62 (t, *J* = 2.0 Hz, 1H), 6.14 (d, *J* = 10.5 Hz, 1H), 4.08-4.15 (m, 2H), 2.94-2.99 (m, 1H), 2.77 (dd, *J* = 18.5, 7.6 Hz, 1H), 2.52-2.60 (m, 2H), 2.36-2.49 (m, 6H), 1.95 (s, 3H), 1.23 (t, *J* = 7.1 Hz, 3H); ^{13}C-NMR (100 MHz, $CDCl_3$) δ 194.14, 176.25, 163.45, 148.11, 145.49, 140.20, 135.68, 133.97, 129.62, 128.61, 63.66, 60.51, 52.47, 48.91, 42.23, 37.52, 33.32, 27.02, 21.70, 14.16 (One peak overlapped); HRMS (ESI) calcd for $C_{23}H_{25}NO_6SNa$ m/z = 466.1295; found m/z = 466.1295 [$(M+Na)^+$]; Enantiomeric excess: 94%, determined by HPLC (Daicel Chiralpak ID, *n*-hexane/EtOH = 2/1; flow rate 1.0 ml/min; 25°C; 236 nm) first peak: t_R = 30.0 min, second peak: t_R = 54.0 min.

3.4.11. X-ray Crystal Data of 4g

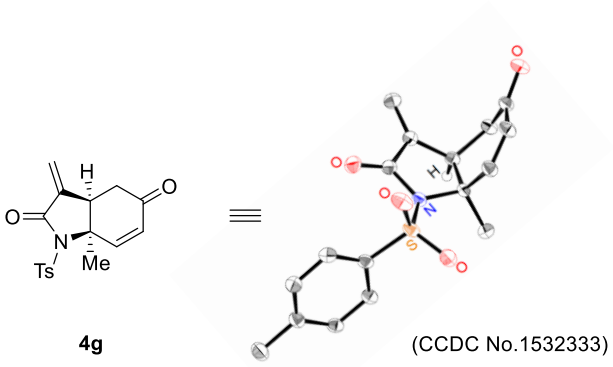

Empirical Formula	$C_{17}H_{17}NO_4S$
Formula Weight	331.39
Crystal Color, Habit	colorless, block
Crystal Dimensions	0.267 X 0.108 X 0.094 mm
Crystal System	orthorhombic
Lattice Type	Primitive
Lattice Parameters	a = 9.591(2) Å
	b = 12.641(3) Å
	c = 13.035(3) Å
	V = 1580.3(5) $Å^3$
Space Group	$P2_12_12_1$ (#19)
Z value	4
D_{calc}	1.393 g/cm^3
F_{000}	696.00
m(MoKa)	2.245 cm^{-1}
Residuals: R_1 (I>2.00s(I))	0.0388
Residuals: R (All reflections)	0.0404
Residuals: wR_2 (All reflections)	0.1174
Goodness of Fit Indicator	1.002
Flack Parameter (Friedel pairs = 1547)	-0.00(7)

3.5. References

1. (a) Kornet, M. J. *J. Pharm. Sci.* **1979**, *68*, 350. (b) Cardellina, J. H.; Moore, R. E. *Tetrahedron Lett.* **1979**, *22*, 2007. (c) Belaud, C.; Roussakis, C.; Letourneux, Y.; Alami, N. E.; Villiéras, J. *Synth. Commun.* **1985**, *15*, 1233. (d) Dembélé, Y. A.; Belaud, C.; Hitchcock, P.; Villiéras, J. *Tetrahedron: Asymmetry* **1992**, *3*, 351. (e) Omura, S.; Fujimoto, T.; Otoguro, K.; Matsuzaki, K.; Moriguchi, R.; Tanaka, H.; Sasaki, Y. *J. Antibiot*. **1991**, *44*, 113. (f) Omura, S.; Matsuzaki, K.; Fujimoto, T.; Kosuge, K.; Furuya, T.; Fujita, S. Nakagawa, A. *J. Antibiot.* **1991**, *44*, 117. (g) Natio, T.; Honda, M.; Miyata, O.; Ninomiya, I. *Chem. Pharm. Bull.* **1993**, *41*, 217. (h) Janecki, T.; Błaszczyk, E.; Studzian, K.; Janecka, A.; Krajewska, U.; Rózalski, M. *J. Med. Chem.* **2005**, *48*, 3516. (i) Albrecht, A.; Koszuk, J.; Modranka, J.; Rózalski, M.; Krajewska, U.; Janecka, A.; Studzian, A.; Janecki, T. *Bioorg. Med. Chem.* **2008**, *16*, 4872. (j) Krawczyk, H.; Albrecht, Ł.; Wojciechowski, J.; Wolf, W. M.; Krajewska, U.; Rózalski, M. *Tetrahedron*, **2008**, *64*, 6307. (k) Albrecht, A.; Albrecht, Ł.; Rózalski, M.; Krajewska, U.; Janecka, A.; Studzian, K.; Janecki, T.; *New J. Chem.* **2010**, *34*, 750. (l) Atbrecht, L.; Albrecht, A.; Janecki, T. *In Natural Lactones and Lactams: Synthesis, Occurrence and Biological Activity; T. Janecki, Ed.; Wiley-VCH* 2014, 147.
2. (a) Watanabe, S.; Fujita, T.; Sakamoto, M.; Natori, I. *Yukagaku* **1988**, *37*, 370. (b) Ryu, I.; Miyazato, H.; Kuriyama, H.; Matsu, K.; Tojino, M.; Fukuyama, T.; Minakata, S.; Komatsu, M. *J. Am. Chem. Soc.* **2003**, *125*, 5632. (c) Błaszczyk, E.; Krawczyk, H.; Janecki, T. *Synlett* **2004**, 2685. (d) Reddy, L. R.; Saravanan, P.; Corey, E. J. *J. Am. Chem. Soc.* **2004**, *126*, 6230. (e) Reddy, L. R.; Fournier, J. F.; Reddy, B. V. S.; Corey, E. J. *J. Am. Chem. Soc.* **2005**, *127*, 8974. (f) Basavaiah, D.; Rao, J. S.; *Tetrahedron Lett.* **2004**, *45*, 1621. (g) Albrecht, A.; Albrecht, Ł.; Janecki, T. *Eur. J. Org. Chem.* **2011**, 2747. (h) Pan, F.; Chen, J.-M.; Qin, T.-Y.; Zhang, S. X.-A.; Liao, W.-W. *Eur. J. Org. Chem.* **2012**, 5324. (i) Xu, J.; Chen, J.; Yang, Q.; Ding, L.; Liu, X.; Xu, D.; Zhao, B. *Adv. Synth. Catal.* **2014**, *356*, 3219. (j) Maso, M. J. D.; Nepomuceno, G. M.; Peter, M. A. St.; Gitre, H. H.; Martin, K. S.; Shaw, J. T. *Org. Lett.* **2016**, *18*, 1740.
3. (a) Xu, W.; Kong, A.; Lu, X. *J. Org. Chem.* **2006**, *71*, 3854. (b) Companyó, X.; Geant, P.-Y.; Mazzanti, A.; Moyano, A.; Rios, R. *Tetrahedron* **2014**, *70*, 75. (c) Holstein, P. M.; Dailler, D.; Vantourout, J.; Shaya, J.; Millet, A.; Baudoin, O. *Angew. Chem. Int. Ed.* **2016**, *55*, 2805. (d) Li, X.; Su, J.; Liu, Z.; Zhu, Y.; Dong, Z.; Qiu, S.; Wang, J.; Lin, L.; Shen, Z.; Yan, W.; Wang, K.; Wang, R. *Org. Lett.* **2016**, *18*, 956; (e) Long, J.; Ding, Y.-H.; Wang, P.-P.; Zhang, Q.; Chen, Y. *Tetrahedron Lett.* **2016**, *57*, 874.
4. For reviews of Rauhut–Currier reaction, see: (a) Aroyan, C. E.; Dermenci, A.; Miller, S. J. *Tetrahedron* **2009**, *65*, 4069. (b) Xie, P.; Huang, Y. *Eur. J. Org. Chem.* **2013**, 6213. (c) Bharadwaj, K. C. *RSC Adv*. **2015**, *5*, 75923.
5. (a) Banfield, S. C.; Kerr, M. A. *Can. J. Chem.* **2004**, *82,* 131. (b) Tello-Aburto, R.; Kalstabakken, K. A.; Harned, A. M. *Org. Biomol. Chem.* **2013**, *11*, 5596.
6. (a) Peterson, E. A.; Overman, L. E. *Proc. Natl. Acad. Sci. USA*, **2004**, *101*, 11943. (b) Büschleb, M.;

Dorich, S.; Hanessian, S.; Tao, D.; Schenthal, K. B.; Overman, L. E. *Angew. Chem. Int. Ed*. **2016**, *55*, 4156.

7. Richmond, M. L.; Seto, C. T. *J. Org. Chem.* **2003**, *68*, 7505.
8. Hu, S.; Zhang, L.; Li, J.; Luo, S.; Cheng, J.-P. *Eur. J. Org. Chem.* **2011**, 3347.
9. Wang, D.; Xu, C.; Zhang, L.; Luo, S. *Org. Lett.* **2015**, *17*, 576.
10. Nakano, A.; Kawahara, S.; Akamatsu, S.; Morokuma, K.; Nakatani, M.; Iwabuchi, Y.; Takahashi, K.; Ishihara, J.; Hatakeyama, S. *Tetrahedron* **2006**, *62*, 381.
11. Matsui, K.; Takizawa, S.; Sasai, H. *J. Am. Chem. Soc*. **2005**, *127*, 3680.
12. Aurelio, L.; Box, J. S.; Brownlee, R. T. C.; Hughes, A. B.; Sleebs, M. M.; *J. Org. Chem*. **2003**, *68*, 2652.
13. (a) Gong, J.-J.; Li, T.-Z.; Pana, K.; Wu, X.-Y. *Chem. Commun.* **2011**, *47*, 1491. (b) Takizawa, S.; Nguyen, T. M.-N.; Grossmann, A.; Enders, D.; Sasai, H. *Angew. Chem. Int. Ed.* **2012**, *51*, 5423. (c) Jin, Z.; Yang, R.; Du, Y.; Tiwari, B.; Ganguly, R.; Chi, Y. R. *Org. Lett.* **2012**, *14*, 3226. (d) Takizawa, S.; Nguyen, T. M.-N.; Grossmann, A.; Suzuki, M.; Enders, D.; Sasai H. *Tetrahedron* **2013**, *69*, 1202. (e) Albrecht, A.; Skrzyńska, A.; Przydacz, A.; Albrecht, Ł. *Synlett* **2015**, *26*, 2679.
14. For recent reviews on recovery and reuse of chiral organocatalysts, see: (a) Itsuno, S.; Hassan, M. M. *RSC Adv.* **2014**, *4*, 52023. (b) Nájera, C.; Yus, M. *Tetrahedron Lett.* **2015**, *56*, 2623.
15. (a) Zhang, C.; Lu, X. *J. Org. Chem.* **1995**, *60*, 2906. (b) Zhu, G.; Chen, Z.; Jiang, Q.; Xiao, D.; Cao, P.; Zhang, X. *J. Am. Chem. Soc.* **1997**, *119*, 3836. (c) Wilson, J. E.; Fu, G. C. *Angew. Chem. Int. Ed.* **2006**, *45*, 1426. (d) Fang, Y.-Q.; Jacobsen, E. N.; *J. Am. Chem. Soc.* **2008**, *130*, 5660.
16. After publication of this work in 2017, following examples on enantioselective RC reaction of acrylamide occurred. (a) Zhang, Z.-X.; Gan, K.-J.; Liu, X.-X.; Deng, Y.-H.; Wang, F.-X.; K.-Y.; Zhang, J.; Fan, C.-A. *Org. Lett.* **2017**, *19*, 3207. (b) Jin, H.; Zhang, Q.; Li, E.; Jia, P.; Li, N.; Huang, Y. *Org. Biomol. Chem.* **2017**, *15*, 7097.

Chapter 4

Phosphine-Catalyzed β,γ-Dual Umpolung Domino Reaction of Dienones with Allenoates: Enantioselective Synthesis of Tetrahydrobenzofuranones

Abstract: An enantio-, diastereo-, regio-, and chemoselective phosphine-catalyzed β,γ-umpolung domino reaction of allenoates with dienones has been developed for the first time. The designed sequence involving oxy-Michael and Rauhut–Currier reactions produced highly functionalized tetrahydrobenzofuranones bearing a chiral tetrasubstituted stereogenic center in up to 96% ee.

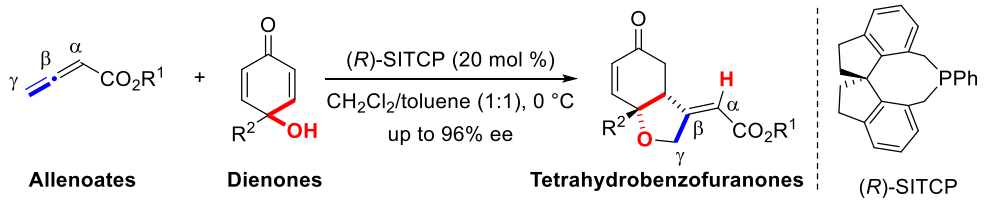

4.1. Introduction

Chiral tetraydrobenzofuranones are common to a vast number of natural products, such as loukacinol A, sorbicillactone A, (+)-cryptocaryone, and millingtonine A and they exhibit various biological activities (e.g., anticancer, anti-HIV, and glucose transport inhibitor; Figure 4.1).[1]

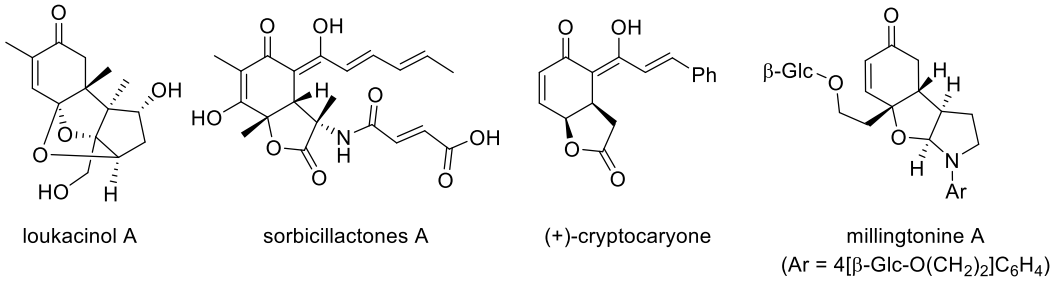

Figure 4.1. Examples of tetrahydrobenzofuranones isolated from natural sources.

Due to importance of this structure, to date, the enantioselective synthesis of tetrahydrobenzofuranone has been studied by a lot of research groups.[2] The most common approach is the enantioselective desymmetrization of cyclohexadienone which is readily available via oxidation of phenols,[3] which was summarized in Scheme 4.1.

Scheme 4.1. Overview of the synthetic approaches for tetrahydrobenzofuranone

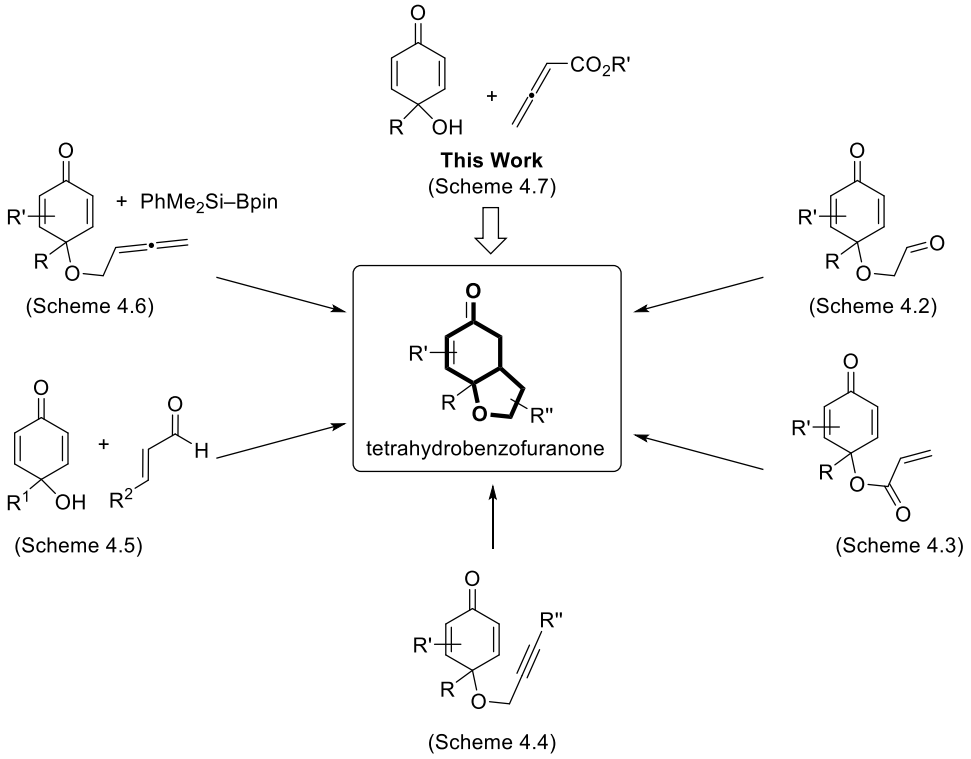

In 2006, Rovis reported an early example of the enantioselective synthesis of tetrahydrobenzofuranone via Stetter reaction catalyzed by *N*-heterocyclic carbene (Scheme 4.2).[2a,b] Although in this case the substrate had to be maintained in highly diluted conditions to suppress the intermolecular reaction, sterically congested substrates are also available.

Scheme 4.2. An early example of enantioselective synthesis of tetrahydrobenzofuranone

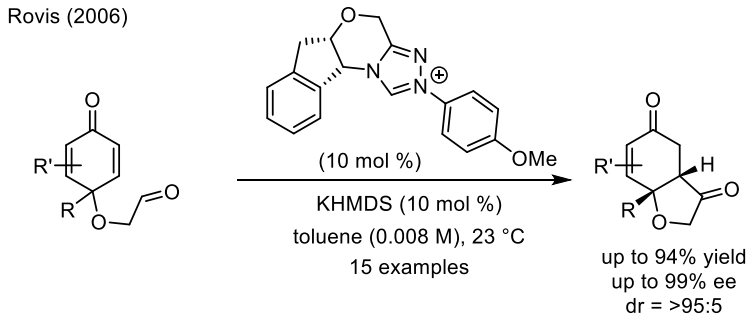

In 2012, the author's group described that enantioselective Rauhut–Currier (RC) reaction (see Chapter 2) for the synthesis of α-methylidene-γ-lactones, which can be regarded as a tetrahydrobenzofuranone (Scheme 4.3).[2c,d] Exo-methylidene moiety of this product can be used for further functionalizations.

Scheme 4.3. Enantioselective RC reaction for the synthesis of tetrahydrobenzofuranone

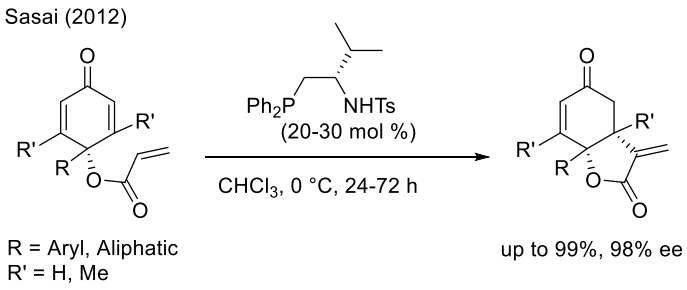

Cyclohexadienones having propargyloxy group are often employed for the synthesis of chiral tetrahydrobenzofuranones. In 2013, Lautens and Lin independently presented Rh-catalyzed domino reaction of propargyloxy cyclohexadienones with arylbronic acids. (Scheme 4.4).[2e,f] In the same year, Lin showed Cu-catalyst could also promote this enantioselective reaction.[2g]

Scheme 4.4. Enantioselective synthesis of tetrahydrobenzofuranone using propargyloxy cyclohexadienone

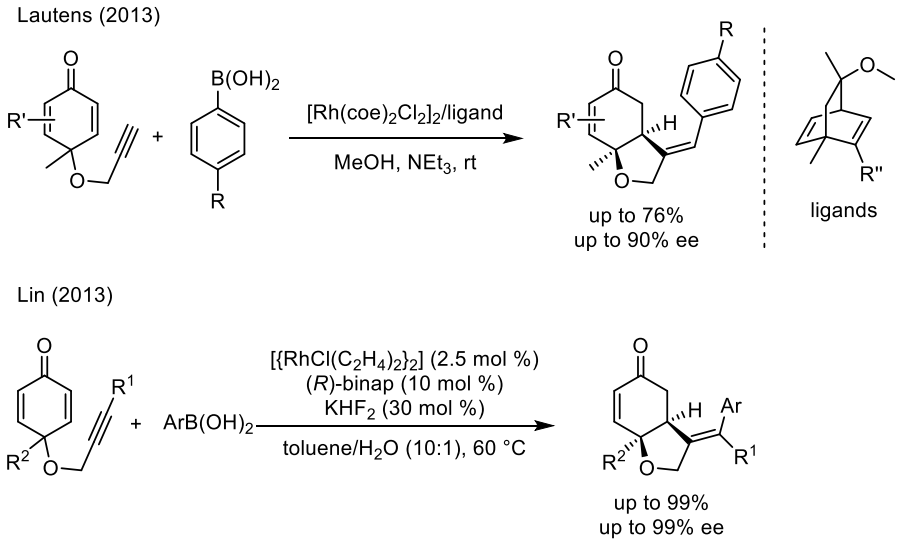

Also in 2013, Johnson presented that a proline-type organocatalyst promoted the enantioselective desymmetrization of cyclohexadienone with a Michael acceptor via sequential conjugate additions (Scheme 4.5)[2h]. In this reaction, they employed relatively simple cyclohexadienones bearing a free hydroxy group and cinnamaldehydes as a substrate, although the addition of an acid was necessary for the reaction to proceed.

Scheme 4.5. Sequential conjugate additions of simple building blocks

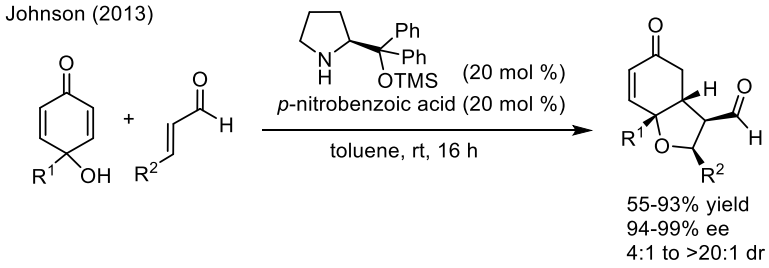

In 2015, Tian and Lin found that Cu-catalyzed silylative cyclization of allenyl cyclohexadienone (Scheme 4.6).[2i] This reaction can be used for the synthesis of *O*-heterocycles as well as *N*-heterocycles and carbocycles. Each of them was delivered to further functionalized products.

Scheme 4.6. Enantioselective silylative cyclization of allenyl cyclohexadienone

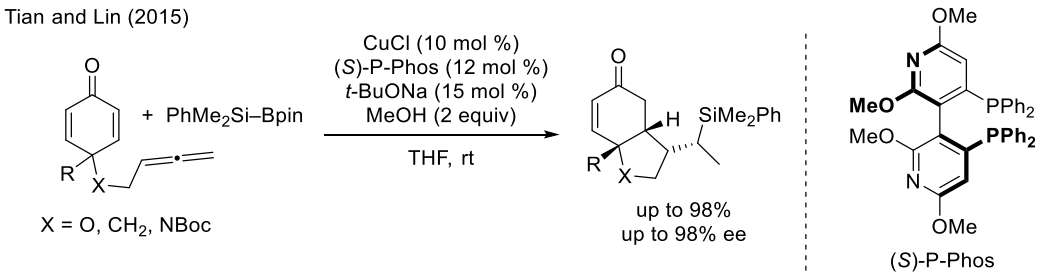

As illustrated above, the enantioselective desymmetrization of cyclohexadienones containing hydroxy- or alcoxy groups is an effective strategy for the synthesis of optically active chiral tetrahydrobenzofuranones. However, many of them require multi step reactions for the synthesis of cyclohexadienones as a substrate. Toward the more simple and practical method, the author envisioned the following strategy: the reaction of simple cyclohexadienones **2** with commercially available allenoates **1**. The reaction mechanism based on the author's working hypothesis is shown in Scheme 4.7.

Scheme 4.7. **This work**: β,γ-Dual umpolung domino reaction for the synthesis of tetrahydrobenzofuranone

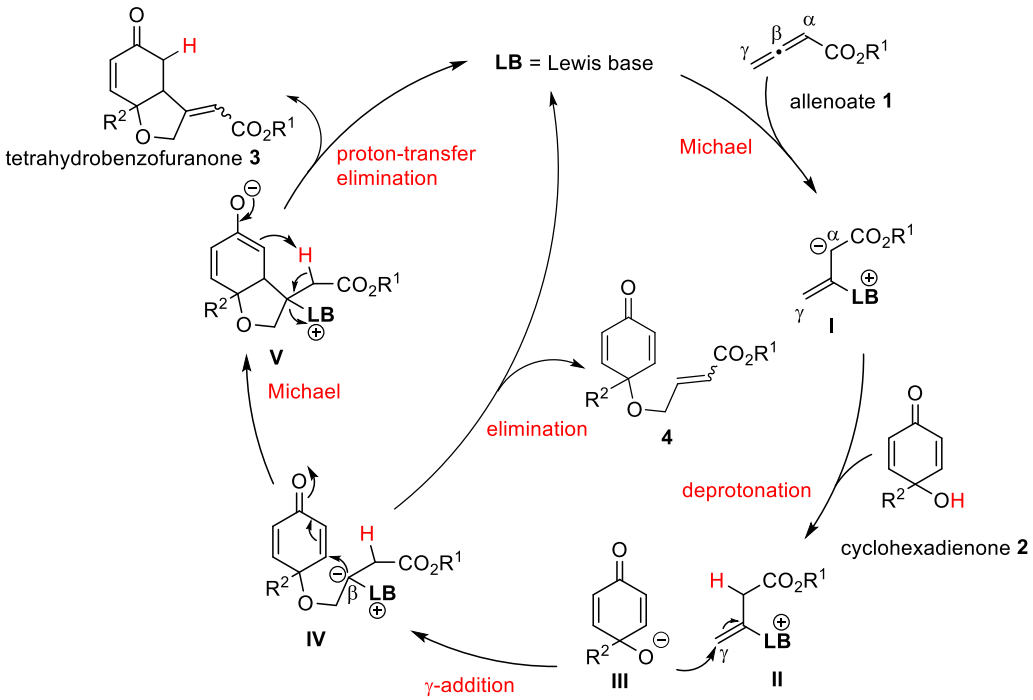

Initially, addition of a Lewis base (LB) to allenoate **1** generates the zwitterionic intermediate **I**, which could work as a Brønsted base for cyclohexadienone **2**, thus leading to the formation of the key intermediate **II** and alkoxide **III**. The γ-addition (see Chapter 1 Section 3 Paragraph 4)[4] of **III** to **II** would give the intermediate **IV**, and form an allylic ether **4** after elimination of the catalyst.[5] Alternatively, the tether ylide **IV** could react intramolecularly with a dienone through a β-addition process, thus resulting in the formation of **V** and leading to the chiral tetrahydrobenzofuranone **3** by proton transfer and the elimination of the catalyst. The present novel domino process would be a straightforward and atom-economical way to prepare a chiral tetrahydrobenzofuranone skeleton.

4.2. Results and Discussion

4.2.1. Optimization of the Reaction Conditions

As the first step in the development of β,γ-dual umpolung domino reaction, achiral LB catalysts were evaluated using **1a** and **2a** as prototypical substrates in dichloromethane at 25 °C (Table 4.1. entries 1 and 2). Fortunately, PPh_3 was found to promote the desired reaction efficiently and product **3a** was obtained as an *E*:*Z* mixture (1:1) in 72% yield (entry 1), albeit with self-condensation of **1a**, and the formation of allylic ether **4a** (R^1 = Et, R^2 = Ph) as shown in Scheme 4.7, which is difficult to purify from the crude mixture. In contrast, an amine catalyst such as DMAP, DBU, or DABCO (entry 2) rarely catalyzed the annulation reaction affording only trace amount of **3a**. Next, various chiral phosphine catalysts were tested (entries 3–12). The initial experiments revealed that axially chiral bulky triaryl phosphines, BINAP, QUINAP, and MOP are inactive in this transformation (entry 3). Bifunctional chiral organocatalysts **5** (Shi's catalyst)[6] and **6**,[7] some of which are known to mediate the enantioselective Morita–Baylis–Hillman and Rauhut–Currier (RC) processes, gave the product but in low yields with low or no selectivities (entries 4–7). The other phosphine catalysts such as (*S*,*R*)-BPPFA, (*R*,*R*)-DIOP, and **7** (Kwon's catalyst)[8] also exhibited low or no catalytic activities (entries 8–10). During this screening process, the C_2-symmetrical chiral organocatalysts **8**[9] and (*R*)-SITCP,[10] possessing a highly nucleophilic monoaryl phosphine unit, gave promising outcomes (entries 11 and 12). In particular, the reaction of **1a** and **2a** with (*R*)-SITCP for 0.5 h afforded **3a** in 57% yield with 84% ee.

Table 4.1. Screening of the Lewis base (LB) catalysts

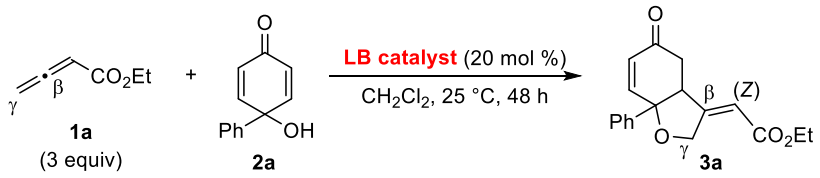

entry	LB catalyst	*E* : *Z* ratio	yield (%)	ee (%)
1	PPh_3	1:1	72	-
2	DMAP, DBU or DABCO	-	trace	-
3	(*R*)-BINAP, (*R*)-QUINAP or (*S*)-MOP	-	trace	-
4	**5**	1:5	9	15
5	**6a**	1:4	15	31
6	**6b**	1:2	30	25
7	**6c**	1:2	25	0
8	(*S*,*R*)-BPPFA	1:6	8	5
9	(*R*,*R*)-DIOP	1:3	13	5
10	**7a** or **7b**	-	no reaction	-
11	**8**	1:6	40	34
12[a]	(*R*)-SITCP	1:10	57	84

[a] For 0.5 h

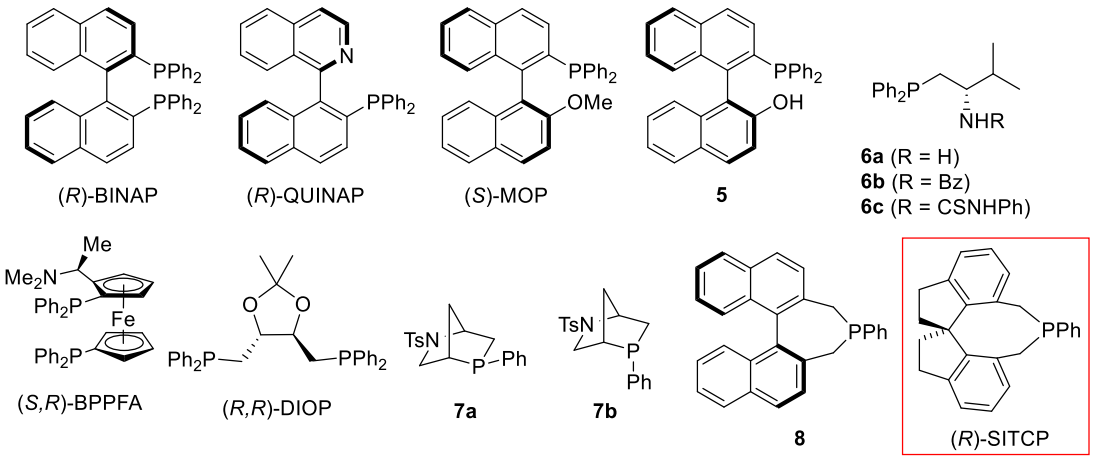

Next, the effect of the solvent on the β,γ-dual umpolung domino reaction was examined using (*R*)-SITCP at 25°C (Table 4.2). The use of CPME did not lead to any improvements in yield and selectivity (entry 2). The reaction did not proceed in DMF (entry 3). Toluene suppressed a side reaction to increase the yield, despite a decrease in diastereoselectivity (entry 4). Under the assumption that improvements would be observed in both yield and stereoselectivity, the reaction was carried out in CH_2Cl_2/toluene (1:1) as a mixed solvent. As expected, product **3a** was obtained in a good yield with good enantioselectivity and *Z*-selectivity (entry 5). Replacing CH_2Cl_2 with $CHCl_3$ (entry 6) or toluene with benzene (entry 7) did not lead to improved overall results.

Table 4.2. The effect of the solvents

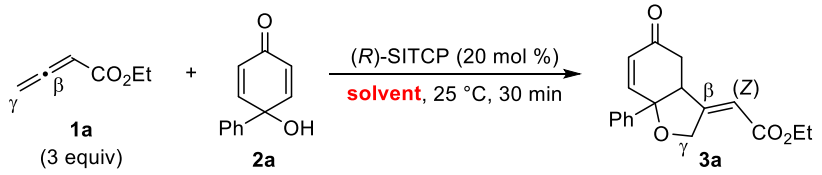

entry	solvent	*E* : *Z* ratio	yield (%)	ee (%)
1	CH_2Cl_2	1:10	57	84
2	CPME	1:2	37	59
3	DMF	-	no reaction	-
4	toluene	1:6	77	84
5	CH_2Cl_2/toluene (1:1)	1:10	73	84
6	$CHCl_3$/toluene (1:1)	1:9	81	80
7	CH_2Cl_2/benzene (1:1)	1:8	71	84

Aiming to further improve the yield and selectivity of the reaction, the effects of the reaction temperature and of varying the number of equiv. of **1a** were investigated (Table 4.3). With respect to the 25°C case, at 0°C, the enantioselectivity and diastereoselectivity of the reaction increased, despite a decrease in yield (entry 2). To suppress the side reaction resulting from the excess amount of allenoate **1a** utilized, the relative amount of **1a** was decreased to 1.5 equiv., which led to a higher yield of **3a**, whereas the stereoselectivity of the reaction remained identical (entry 3). In the presence of 1.2 equiv. of **1a**, intact cyclohexadienone **2a** was left in solution even after 48 hours, and the desired product was obtained in a lower yield than in the 1.5 equiv. case (entry 4). Performing the reaction at a lower temperature (entry 5) or in the presence of MS4A (entry 6) did not improve the results. Finally, the conditions in entry 3 (1.5 equiv. of **1a** at 0°C) were concluded to be optimal.

Table 4.3. The effect of the reaction temperature and equiv of **1a**

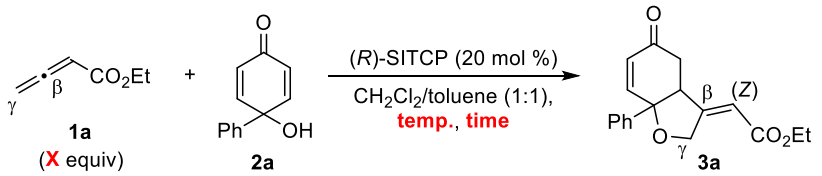

entry	X	temp. (°C)	time (h)	*E* : *Z* ratio	yield (%)	ee (%)
1	3.0	25	0.5	1:10	73	84
2	3.0	0	48	1:>20	68	93
3	1.5	0	48	1:>20	79 (78)[a]	93
4	1.2	0	48	1:>20	71	93
5	1.5	–20	48	1:>20	68	93
6[b]	1.5	0	48	1:>20	77	93

[a] Isolated yield
[b] MS4A was added

4.2.2. Substrate Scope

The results of the substrate scope of current reaction were summarized in Scheme 4.8.

Scheme 4.8. Substrate scope of β,γ-dual umpolung domino reaction[a]

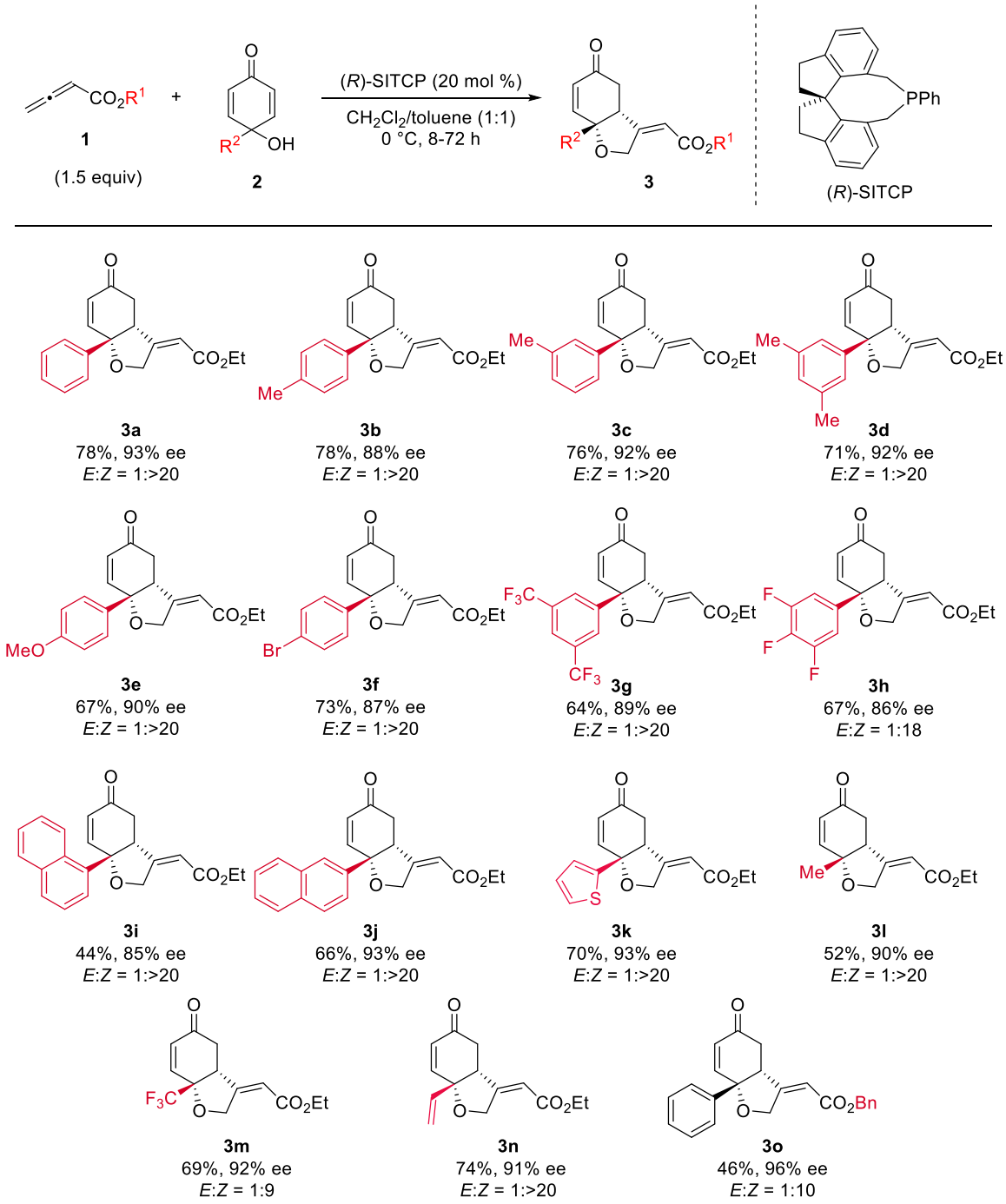

[a] Yields are of isolated **3.** Ee of **3** was determined by HPLC on a chiral stationary phase. Reaction conditions: **1** (1.5 equiv), **2** and (*R*)-SITCP (20 mol %) in CH_2Cl_2/toluene (1:1, 0.1 M) at 0 °C for 48 h (**3a-f**, and **3i-n**), for 8 h (**3g**), for 24 h (**3h**) and for 72 h (**3o**).

Under the optimal conditions, highly *Z*-selective tetrahydrobenzofuranones **3** were obtained in good yields (44–78%) with high enantioselectivities (85–96% ee) irrespective of the electronic nature of substituent R^2 in **2** involving aryl and vinyl groups. The alkyl substituent R^2 such as methyl and trifluoromethyl in **2l** and **2m** led to cyclic products **3l** and **3m** with 90% ee and 92% ee, respectively. The reaction of benzyl allenoate (**1b**: R^1 = Bn) with **2a** resulted in the formation of corresponding **3o** in 96% ee. On the other hand, sterically congested substrate **2p** and **2q** didn't give product **3** with formation of allylic ether **4** (Scheme 4.9).

Scheme 4.9. Reaction of **1a** with **2p** or **2q**

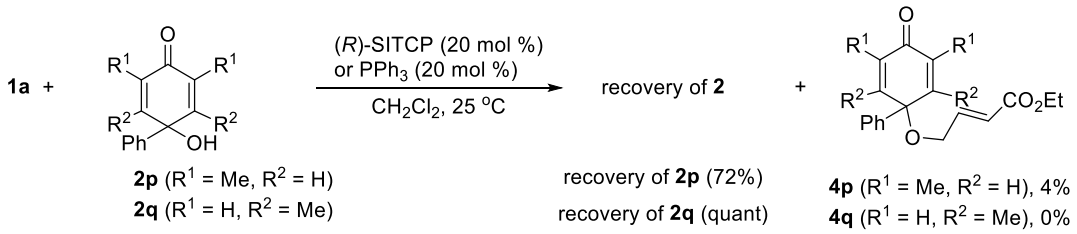

The absolute and regio configurations of cyclized product **3k** was determined by the crystalline sponge method[11] as the (*R,R*)-form, and *Z*-configuration for olefin moiety (Figure 4.2).

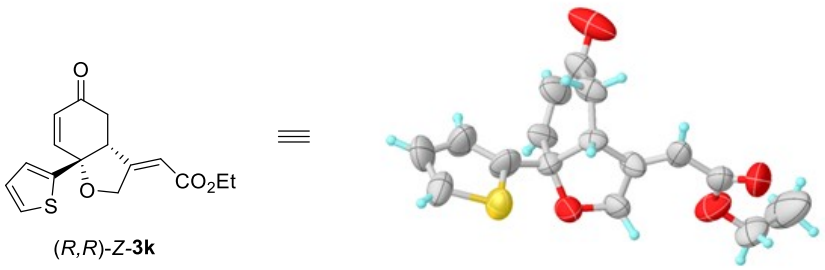

Figure 4.2. X-ray structure of tetrahydrobenzofuranone **3k** (ortep drawing with thermal ellipsoids at 30% probability level)

4.2.3. Mechanistic Studies

To clarify the reaction mechanism of the developed β,γ-dual umpolung domino reaction, some experiments were performed (Scheme 4.10). When methyl-capped **2o** or allylic ether **4a** was used in the reaction, no conversion of **2o** and **4a** was observed (Eq. 1 and 2). The free hydroxy group in **2** would be pivotal for initiating the γ-addition, and allylic ether **4** is not a reaction intermediate to give **3**. The reaction of **1a** and **2a** in the presence of $\boldsymbol{D}_2O$ (3 equiv) gave partially deuterated product **3a** [***D*** content (%) α: 60, γ: 17, δ: 50] (Eq. 3) indicating that anionic species were formed at α-, γ-, and δ-positions on the reaction sequence. These

results are in agreement with a mechanism of β,γ-dual umpolung domino Michael reaction proposed as a working hypothesis in Scheme 4.7.

Scheme 4.10. Experiments on mechanistic studies

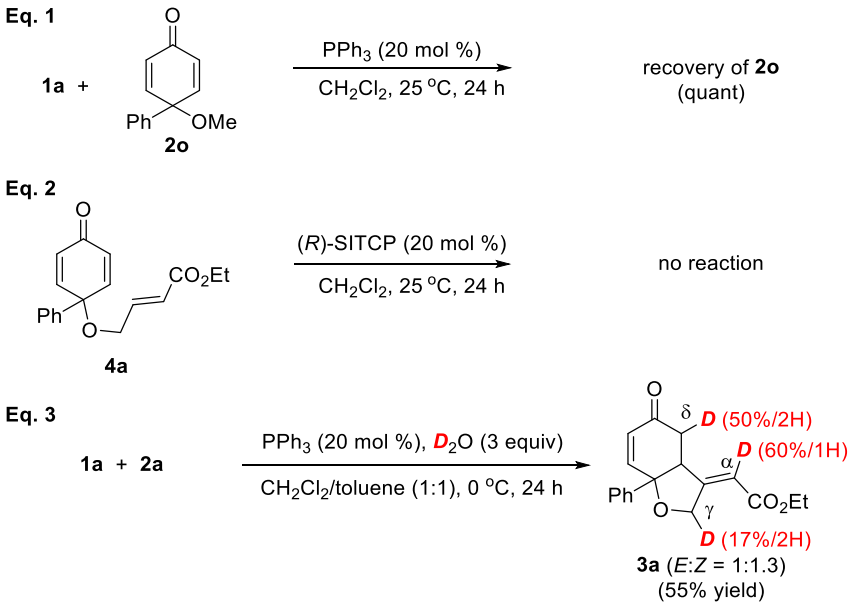

Based on these experimental results, a reaction mechanism was proposed (Scheme 4.11). The reaction is initiated by the nucleophilic attack of the phosphine catalyst (*R*)-SITCP to the β-position of allenoate **1**, affording the resonance-stabilized betaine **I** with anionic character at the carbon atom in the α- and γ-positions. Subsequent protonation of the α-position from the hydroxy group on dienone **2** establishes the electrophilic nature of the intermediate **II**, enabling a nucleophilic γ-addition of **III** to the vinyl phosphonium **II**. Thereby, ylide **IV** is formed that can then undergo an enantioselective intramolecular Michael addition to one of the enone moieties. To avoid steric interactions between the R^2 substituent of dienone **2** and the indane aromatic part in the catalyst, the reaction using (*R*)-SITCP would favor the generation of the (*R,R*)-configuration product. Finally, tetrahydrobenzofuranone **3** would be provided in the fragmentation of **V** with a stabilizing $P^{+}\cdots O^{\delta-}$ interaction[12] between a less hindered monoarylphosphine group in (*R*)-SITCP and carbonyl group in CO_2R^1 that leads to the *Z*-form with concurrent regeneration of the catalyst. Since an intermolecular oxy-Michael reaction involves reversibility of alcohol addition under basic conditions,[13] these results suggest that the intramolecular Michael reaction from **IV** to **V** could be the rate controlling step for the present domino reaction.

Scheme 4.11. Proposed reaction mechanism

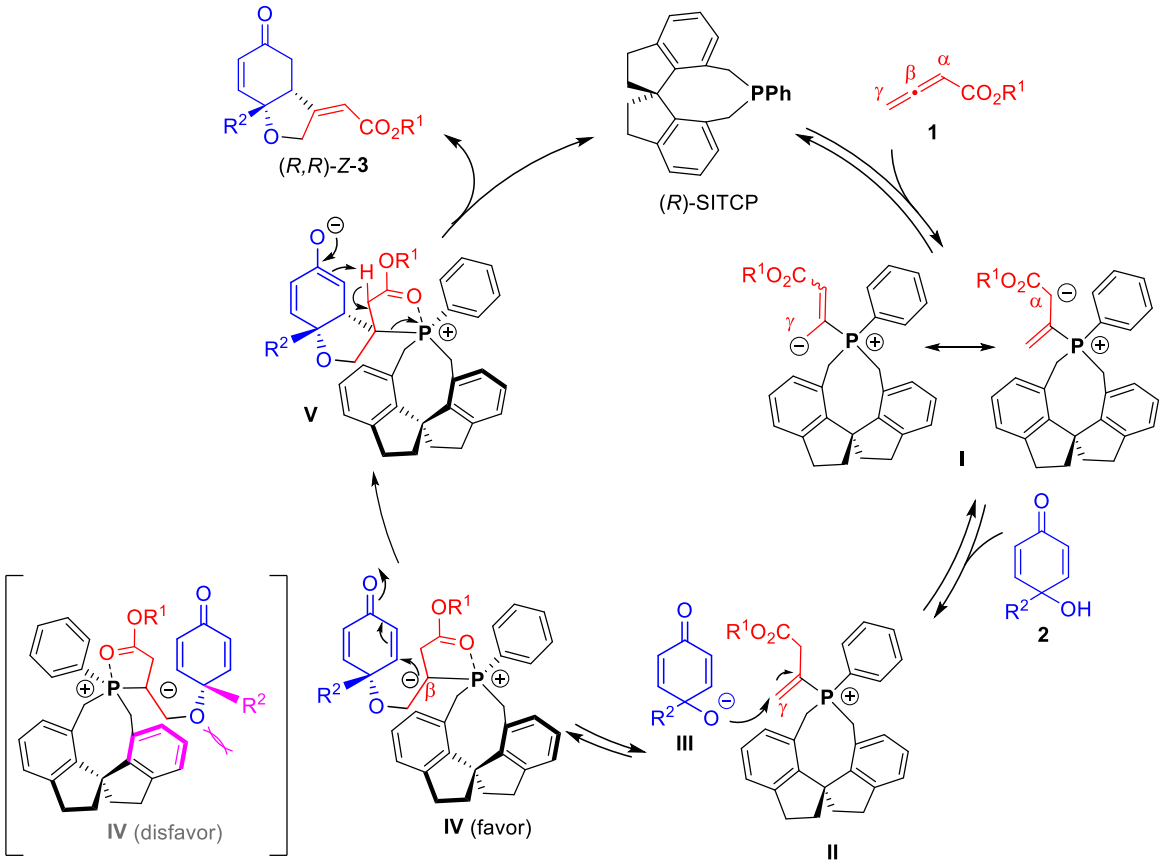

4.3. Conclusion

In summary, the author has developed a highly stereoselective phosphine-catalyzed oxy-Michael/RC sequence. The present transformation is the first example of an enantio-, diastereo-, regio- and chemoselective domino reaction initiated by the nucleophilic attack to the γ-position of allenoates.[14] Current methodology represents a straightforward- and atom economical enantioselective syntheses of highly functionalized chiral tetrahydrobenzofuranones.

4.4. Experimental Section

4.4.1. General

^{1}H-, ^{13}C-, and ^{19}F-NMR spectra were recorded with a JEOL JMN ECS400 FT NMR, JNM ECA600 FT NMR or Bruker AVANCE II (^{1}H-NMR 400, 600 or 700 MHz, ^{13}C-NMR 100, 150 or 176 MHz, ^{19}F-NMR 565 MHz. ^{1}H-NMR spectra are reported as follows: chemical shift in ppm relative to the chemical shift of $CHCl_3$ at 7.26 ppm, integration, multiplicities (s = singlet, d = doublet, t = triplet, q = quartet, m = multiplet), and coupling constants (Hz). ^{13}C-NMR spectra reported in ppm relative to the central line of triplet for $CDCl_3$ at 77 ppm. CF_3CO_2H used as external standards for ^{19}F-NMR. FT-MS spectra were obtained with LTQ Orbitrap XL (Thermo Fisher Scientific). High resolution-MS spectra were obtained with JMS-T100LC

(JEOL). Optical rotations were measured with JASCO P-1030 polarimeter. HPLC analyses were performed on a JASCO HPLC system (JASCO PU 980 pump and UV-975 UV/Vis detector) using a mixture of *n*-hexane/2-propanol as eluents. Column chromatography on SiO_2 was performed with Kanto Silica Gel 60 (40-100 μm).

4.4.2. Materials

MeOH was dried by MS3A. Dehydrated CH_2Cl_2, $CHCl_3$, toluene, benzene, DMF, CPME and other commercially available organic and inorganic compounds were purchased and used without further purification. Known cyclohexadienones **2a-b, 2e-n** and **2p-q** were synthesized according to following literatures.[3e,7c,d,15-19]

4.4.3. General Procedure for the Preparation of Unknown Cyclohexadienone 1

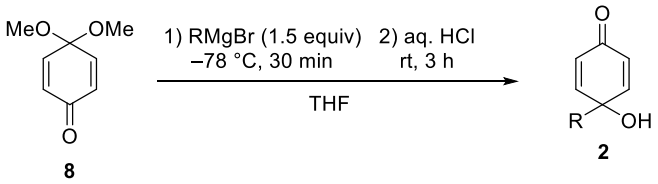

To a solution of **8** (5.0 mmol) in THF (10 mL) was added Grignard reagents (7.5 mmol) in THF (7.5 mL) at –78 °C. After 30 min, the reaction mixture was acidified by aq. HCl, then, reaction temperature was increased to room temperature. After 3 h, organic layer was extracted with EtOAc and dried *in vacuo*. The resulting crude product was purified by silica-gel column chromatography followed by recrystallization to provide dienones **2** as a white solid.

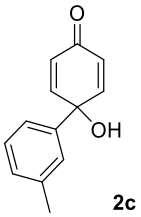

2c: 61% yield; white solid; ^{1}H-NMR (400 MHz, $CDCl_3$) δ 7.30-7.27 (m, 3H), 7.18-7.12 (m, 1H), 6.89 (d, 2H, *J* = 10.0 Hz), 6.23 (d, 2H, *J* = 10.0 Hz), 2.36 (s, 3H), 2.33 (s, 1H); ^{13}C-NMR (100 MHz, $CDCl_3$) δ 186.0, 151.2, 138.7, 138.5, 129.1, 128.3, 126.7, 125.8, 122.3, 70.9, 21.5; HRMS (ESI) calcd for $C_{13}H_{12}O_2Na^+$ 223.0730, found 223.0725; IR (KBr): ν 3359, 2361, 1614, 1397, 1140, 960, 698,430 cm^{-1}.

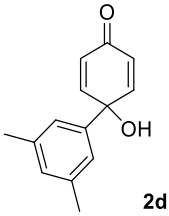

2d

2d: 65% yield; white solid; ^{1}H-NMR (400 MHz, $CDCl_3$) δ 7.08 (s, 2H), 6.97 (s, 1H), 6.89 (d, 2H, *J* = 10.0 Hz), 6.22 (d, 2H, *J* = 10.0 Hz), 2.38 (s, 1H), 2.32 (s, 6H); ^{13}C-NMR (100 MHz, $CDCl_3$) δ 186.1, 151.2, 138.7, 138.5, 130.0, 126.6, 122.9, 70.9, 21.4; HRMS (ESI) calcd for $C_{14}H_{14}O_2Na^+$ 237.0886, found 237.0879; IR (KBr): ν 3269, 1661, 1616, 1457, 1393, 1271, 1174, 867, 699, 668 cm^{-1}.

4.4.4. General Procedure for the Preparation of Tetrahydrobenzofuranone 3

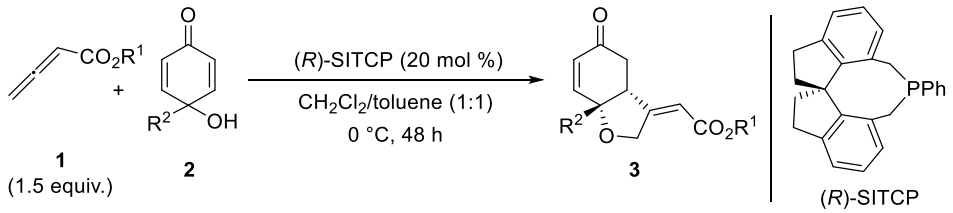

Under an atmosphere of nitrogen, allenoate **1** (0.15 mmol) was added to a solution of hydroxy dienone **2** (0.10 mmol) and (*R*)-SITCP (20 mol %) in CH_2Cl_2/toluene (1:1, 1.0 mL) at 0 °C for 8–72 h. The crude reaction mixture was purified by preparative TLC (*n*-hexanes/EtOAc 7:3) to give the desired product **3** as a colorless oil.

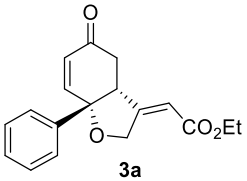

3a

3a: 78% yield; colorless oil; ^{1}H-NMR (400 MHz, $CDCl_3$) δ 7.55-7.50 (m, 2H), 7.45-7.34 (m, 3H), 6.68 (dd, 1H, *J* = 10.0, 2.0 Hz), 6.23 (d, 1H, *J* = 10.0 Hz), 5.73 (q, 1H, *J* = 2.4 Hz), 5.22 (dd, 1H, *J* = 18.0, 2.4 Hz), 4.80 (dt, 1H, *J* = 18.0, 2.4 Hz), 4.16 (q, 2H, *J* = 7.2 Hz), 3.20 (br, 1H), 2.82-2.71 (m, 2H), 1.28 (t, 3H, *J* = 7.2 Hz); ^{13}C-NMR (100 MHz, $CDCl_3$) δ 195.8, 165.7, 162.8, 148.8, 139.0, 131.5, 128.9, 128.7, 125.4, 112.3, 83.0, 71.0, 60.4, 50.9, 36.2, 14.2; HRMS (ESI) calcd for $C_{18}H_{18}O_4Na^+$ 321.1097, found 321.1099; IR (KBr): ν 2979, 1710, 1448, 1373, 1203, 1130, 1039, 855, 733, 700 cm^{-1}. Enantiomeric excess: 93% $[\alpha]_D^{22}$ = +89.7 (*c* 0.20, $CHCl_3$); HPLC analysis (Chiralpak IA, *n*-hexane/2-propanol = 9/1, flow rate 1.0 mL/min, λ = 212 nm) first peak: t_R = 13.2 min, second peak: t_R = 16.1 min.

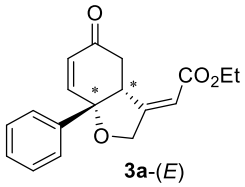

3a-(*E*)

3a-*E* (from PPh_3 catalysis): colorless oil; ^{1}H-NMR (600 MHz, $CDCl_3$) δ 7.44-7.30 (m, 5H), 6.61 (d, 1H, *J* = 10.2 Hz), 6.19 (d, 1H, *J* = 10.2 Hz), 5.76-5.73 (m, 1H), 4.70-4.56 (m, 2H), 4.18-4.12 (m, 3H), 2.87 (d, 2H, *J* = 7.1 Hz), 1.26 (t, 3H, *J* = 7.2 Hz); ^{13}C-NMR (150 MHz, $CDCl_3$) δ 197.3, 165.0, 161.0, 147.2, 141.2, 129.9, 128.9, 128.3, 125.3, 112.5, 83.6, 76.8, 60.4, 48.2, 36.9, 14.2; HRMS (ESI) calcd for $C_{18}H_{18}O_4Na^+$ 321.1097, found 321.1091; IR (KBr): ν 2979, 1710, 1448, 1373, 1203, 1130, 1040, 1016, 761, 701 cm^{-1}.

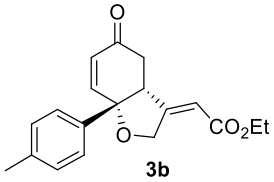

3b

3b: 78% yield; colorless oil; ^{1}H-NMR (400 MHz, $CDCl_3$) δ 7.40 (d, 2H, *J* = 8.0 Hz), 7.22 (d, 2H, *J* = 8.0 Hz), 6.66 (dd, 1H, *J* = 10.0, 2.0 Hz), 6.20 (d, 1H, *J* = 10.0 Hz), 5.72 (q, 1H, *J* = 2.8 Hz), 5.20 (dd, 1H, *J* = 17.8, 2.0 Hz), 4.78 (dt, 1H, *J* = 17.8, 2.0 Hz), 4.16 (q, 2H, *J* = 7.2 Hz), 3.18 (br, 1H), 2.80-2.69 (m, 2H), 2.37 (s, 3H), 1.28 (t, 3H, *J* = 7.2 Hz); ^{13}C-NMR (150 MHz, $CDCl_3$) δ 195.8, 165.7, 162.9, 149.0, 138.5, 136.0, 131.4, 129.5, 125.3, 112.3, 82.9, 70.9, 60.4, 50.9, 36.2, 21.1, 14.2; HRMS (ESI) calcd for $C_{19}H_{20}O_4Na^+$ 335.1254, found 335.1253; IR (KBr): ν 3053, 2981, 1704, 1377, 1216, 1134, 1038, 780, 735 cm^{-1}. Enantiomeric excess: 88% $[\alpha]_D^{20}$ = +120.3 (*c* 0.70, $CHCl_3$); HPLC analysis (Chiralpak IA, *n*-hexane/2-propanol = 9/1, flow rate 1.0 mL/min, λ = 212 nm) first peak: t_R = 24.8 min, second peak: t_R = 31.7 min.

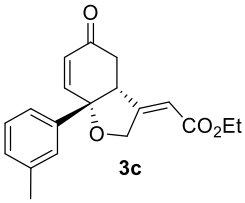

3c

3c: 76% yield; colorless oil; ^{1}H-NMR (400 MHz, $CDCl_3$) δ 7.34-7.27 (m, 3H), 7.18 (d, 1H, *J* = 6.6 Hz), 6.69 (dd, 1H, *J* = 10.8, 1.5 Hz), 6.25 (d, 1H, *J* = 10.8 Hz), 5.73 (q, 1H, *J* = 3.0 Hz), 5.22 (dd, 1H, *J* = 17.4, 3.0 Hz), 4.79 (dt, 1H, *J* = 17.4, 3.0 Hz), 4.16 (q, 2H, *J* = 7.2 Hz), 3.20 (br, 1H), 2.81-2.71 (m, 2H), 2.38 (s, 3H), 1.28 (t, 3H, *J* = 7.2 Hz); ^{13}C-NMR (150 MHz, $CDCl_3$) δ 195.9, 165.7, 162.9, 148.9, 138.9, 138.7, 131.4, 129.4, 128.7, 125.9, 122.5, 112.3, 83.0, 70.9, 60.4, 50.9, 36.2, 21.6, 14.2; HRMS (ESI) calcd for $C_{19}H_{20}O_4Na^+$ 335.1254, found 335.1244; IR (KBr): ν 2926, 2361, 1714, 1372, 1245. 1129, 1038, 415 cm^{-1}. Enantiomeric excess: 92% $[\alpha]_D^{22}$ = +94.8 (*c* 0.90, $CHCl_3$); HPLC analysis (Chiralpak IA, *n*-hexane/2-propanol = 9/1, flow rate 1.0 mL/min, λ = 212 nm) first peak: t_R = 10.0 min, second peak: t_R = 12.7 min.

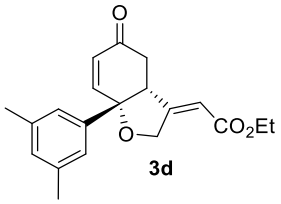

3d

3d: 71% yield; colorless oil; ^{1}H-NMR (400 MHz, $CDCl_3$) δ 7.11 (s, 2H), 7.00 (s, 1H), 6.66 (dd, 1H, *J* = 10.4, 1.6 Hz), 6.20 (d, 1H, *J* = 10.4 Hz), 5.72 (q, 1H, *J* = 2.1 Hz), 5.21 (dd, 1H, *J* = 17.4, 2.1 Hz), 4.77 (dt, 1H, *J* = 17.4, 2.1 Hz), 4.15 (q, 2H, *J* = 7.2 Hz), 3.17 (br, 1H), 2.85-2.68 (m, 2H), 2.33 (s, 6H), 1.28 (t, 3H, *J* = 7.2 Hz); ^{13}C-NMR (150 MHz, $CDCl_3$) δ 196.0, 165.7, 163.0, 149.0, 138.9, 138.6, 131.3, 130.3, 123.1, 112.2, 83.0, 70.9, 60.4, 50.8, 36.3, 21.4, 14.2; HRMS (ESI) calcd for $C_{20}H_{22}O_4Na^+$ 349.1410, found 349.1405; IR (KBr): ν 2921, 1711, 1372, 1350, 1224, 1129, 1039, 1015, 853 cm^{-1}. Enantiomeric excess: 92%; $[\alpha]_D^{23}$ = +88.8 (*c* 0.58, $CHCl_3$); HPLC analysis (Chiralpak IA, *n*-hexane/2-propanol = 9/1, flow rate 1.0 mL/min, λ = 266 nm) first peak: t_R = 7.3 min, second peak: t_R = 10.0 min.

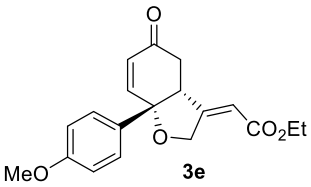

3e

3e: 67% yield; colorless oil; ^{1}H-NMR (600 MHz, $CDCl_3$) δ 7.43 (d, 2H, *J* = 8.4 Hz), 6.93 (d, 2H, *J* = 8.4 Hz), 6.67 (dd, 1H, *J* = 10.2, 1.8 Hz), 6.20 (d, 1H, *J* = 10.2 Hz), 5.72 (q, 1H, *J* = 2.1 Hz), 5.19 (dd, 1H, *J* = 17.4, 2.1 Hz), 4.77 (dt, 1H, *J* = 17.4, 2.1 Hz), 4.15 (q, 2H, *J* = 7.2 Hz), 3.82 (s, 3H), 3.17 (br, 1H), 2.79-2.70 (m, 2H), 1.27 (t, 3H, *J* = 7.2 Hz); ^{13}C-NMR (150 MHz, $CDCl_3$) δ 195.8, 165.7, 162.9, 159.8, 149.0, 131.3, 130.8, 126.7, 114.2, 112.2, 82.7, 70.9, 60.4, 55.3, 50.9, 36.1, 14.2; HRMS (ESI) calcd for $C_{19}H_{20}O_5Na^+$ 351.1203, found 351.1191; IR (KBr): ν 2921, 2361, 1714, 1687, 1511, 1373, 1250, 1203, 1037, 833 cm^{-1}. Enantiomeric excess: 90%; $[\alpha]_D^{22}$ = +105.7 (*c* 1.1, $CHCl_3$); HPLC analysis (Chiralpak IA, *n*-hexane/2-propanol = 9/1, flow rate 1.0 mL/min, λ = 212 nm) first peak: t_R = 20.2 min, second peak: t_R = 25.4 min.

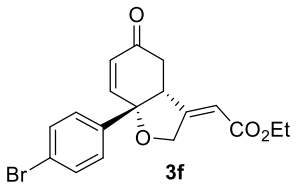

3f

3f: 73% yield; colorless oil; ^{1}H-NMR (400 MHz, $CDCl_3$) δ 7.55 (d, 2H, *J* = 8.8 Hz), 7.40 (d, 2H, *J* = 8.8 Hz), 6.63 (dd, 1H, *J* = 10.4, 2.0 Hz), 6.23 (d, 1H, *J* = 10.4 Hz), 5.72 (q, 1H, *J* = 2.0 Hz), 5.21 (dd, 1H, *J* = 17.2, 2.0 Hz), 4.78 (dt, 1H, *J* = 17.2, 2.0 Hz), 4.16 (q, 2H, *J* = 7.2 Hz), 3.15 (br, 1H), 2.80 – 2.68 (m, 2H), 1.28 (t, 3H, *J* = 7.2 Hz); ^{13}C-NMR (150 MHz, $CDCl_3$) δ 195.4, 165.6, 162.2, 148.1, 138.2, 132.0, 131.8, 127.2, 122.8, 112.6, 82.6, 71.0, 60.5, 50.9, 36.0, 14.2; HRMS (ESI) calcd for $C_{18}H_{17}BrO_4Na^+$ 399.0202, found 399.0204;

IR (KBr): ν 2963, 2353, 1682, 1373, 1133, 1041, 861, 825 cm^{-1}. Enantiomeric excess: 87% $[\alpha]_D^{18}$ = +113.9 (*c* 0.70, $CHCl_3$); HPLC analysis (Chiralpak IA, *n*-hexane/2-propanol = 9/1, flow rate 1.0 mL/min, λ = 220 nm) first peak: t_R = 15.0 min, second peak: t_R = 20.3 min.

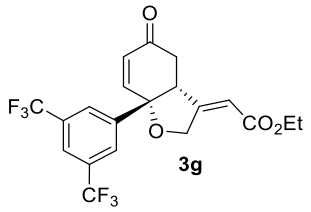

3g

3g: 64% yield; colorless oil; ^{1}H-NMR (600 MHz, $CDCl_3$) δ 7.98 (s, 2H), 7.91 (s, 1H), 6.63 (dd, 1H, *J* = 10.2, 1.8 Hz), 6.33 (d, 1H, *J* = 10.2 Hz), 5.76 (q, 1H, *J* = 2.4 Hz), 5.28 (dd, 1H, *J* = 17.4, 2.4 Hz), 4.83 (dt, 1H, *J* = 17.4, 2.4 Hz), 4.17 (q, 2H, *J* = 7.2 Hz), 3.18 (br, 1H), 2.85-2.70 (m, 2H), 1.29 (t, 3H, *J* = 7.2 Hz); ^{13}C-NMR (150 MHz, $CDCl_3$) δ 194.5, 165.5, 161.0, 146.5, 142.2, 132.8, 132.4 (q, *J* = 33.0 Hz), 125.8, 123.0 (q, *J* = 271.5 Hz), 122.8, 113.1, 82.1, 71.1, 60.6, 50.8, 35.9, 14.2; ^{19}F-NMR (565 MHz, $CDCl_3$) δ –62.7 (s); HRMS (ESI) calcd for $C_{20}H_{16}F_6O_4Na^+$ 457.0845, found 457.0839; IR (KBr): ν 2985, 1714, 1374, 1280, 1173, 1133, 899, 682 cm^{-1}. Enantiomeric excess: 89% $[\alpha]_D^{23}$ = +88.8 (*c* 1.27, $CHCl_3$); HPLC analysis (Chiralpak IA, *n*-hexane/2-propanol = 9/1, flow rate 1.0 mL/min, λ = 216 nm) first peak: t_R = 14.8 min, second peak: t_R = 16.6 min.

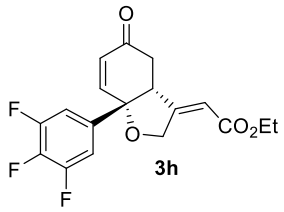

3h

3h: 67% yield; colorless oil; ^{1}H-NMR (600 MHz, $CDCl_3$) δ 7.20-7.13 (m, 2H), 6.56 (dd, 1H, *J* = 10.2, 2.4 Hz), 6.25 (d, 1H, *J* = 10.2 Hz), 5.73 (q, 1H, *J* = 2.4 Hz), 5.20 (dd, 1H, *J* = 17.4, 2.4 Hz), 4.77 (dt, 1H, *J* = 17.4, *J* = 2.4 Hz), 4.16 (q, 2H, *J* = 7.2 Hz), 3.12 (br, 1H), 2.81-2.71 (m, 2H), 1.27 (t, 3H, *J* = 7.2 Hz); ^{13}C-NMR (150 MHz, $CDCl_3$) δ 194.7, 165.5, 161.3, 151.4 (ddd, *J* = 250.0, 10.1, 4.4 Hz), 146.8, 139.6 (dt, *J* = 250.0, 16.5 Hz), 135.7 (d, *J* = 4.4 Hz), 132.4, 112.9, 110.0 (dd, *J* = 16.5, 4.4 Hz), 81.9, 71.0, 60.6, 50.8, 35.9, 14.2; ^{19}F-NMR (565 MHz, $CDCl_3$) δ –132.0 (s), –159.4 (s); HRMS (ESI) calcd for $C_{18}H_{15}F_3O_4Na^+$ 375.0815, found 375.0815; IR (KBr): ν 2922, 1714, 1531, 1439, 1354, 1241, 1151, 1128, 1048, 857, 788 cm^{-1}. Enantiomeric excess: 86% $[\alpha]_D^{20}$ = +69.6 (*c* 1.20, $CHCl_3$); HPLC analysis (Chiralpak IA, *n*-hexane/2-propanol = 9/1, flow rate 1.0 mL/min, λ = 212 nm) first peak: t_R = 22.3 min, second peak: t_R = 31.6 min.

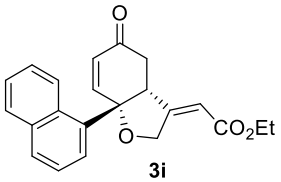

3i

3i: 44% yield; colorless oil; ^{1}H-NMR (600 MHz, $CDCl_3$) δ 8.52-8.48 (m, 1H), 7.94-7.84 (m, 2H), 7.54-7.47 (m, 3H), 7.42 (t, 1H, *J* = 7.8 Hz), 6.95 (dd, 1H, *J* = 10.2, 1.2 Hz), 6.27 (d, 1H, *J* = 10.2 Hz), 5.81 (q, 1H, *J* = 2.4 Hz), 5.40 (dd, 1H, *J* = 18.0, 2.4 Hz), 4.92 (dt, 1H, *J* = 18.0, 2.4 Hz), 4.20 (q, 2H, *J* = 7.2 Hz), 3.99 (br, 1H), 2.76-2.56 (m, 2H), 1.31 (t, 3H, *J* = 7.2 Hz); ^{13}C-NMR (150 MHz, $CDCl_3$) δ 196.1, 165.7, 162.4, 149.1, 135.1, 133.3, 130.8, 130.6, 130.5, 129.5, 126.3, 126.1, 125.9, 125.5, 124.5, 112.9, 85.3, 70.8, 60.5, 48.7, 37.1, 14.2; HRMS (ESI) calcd for $C_{22}H_{20}O_4Na^+$ 371.1254, found 371.1248; IR (KBr): ν 2978, 1705, 1453, 1377, 1205, 1131, 1039, 860, 814, 758 cm^{-1}. Enantiomeric excess: 85% $[\alpha]_D^{22}$ = –53.5 (*c* 0.78, $CHCl_3$); HPLC analysis (Chiralpak IA, *n*-hexane/2-propanol = 9/1, flow rate 1.0 mL/min, λ = 291 nm) first peak: t_R = 9.3 min, second peak: t_R = 11.1 min.

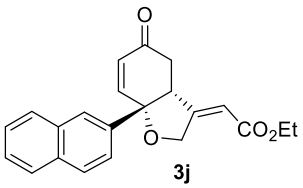

3j

3j: 66% yield; colorless oil; ^{1}H-NMR (400 MHz, $CDCl_3$) δ 7.99-7.80 (m, 4H), 7.69 (dd, 1H, *J* = 8.7, 1.8 Hz), 7.52 (td, 2H, *J* = 6.6, 3.5 Hz), 6.78 (dd, 1H, *J* = 10.1, 1.8 Hz), 6.30 (d, 1H, *J* = 10.1 Hz), 5.76 (q, 1H, *J* = 2.4 Hz), 5.29 (dd, 1H, *J* = 18.1, 2.4 Hz), 4.86 (dt, 1H, *J* = 18.1, 2.4 Hz), 4.18 (q, 2H, *J* = 7.2 Hz), 3.30 (br, 1H), 2.87-2.70 (m, 2H), 1.29 (t, 3H, *J* = 7.2 Hz); ^{13}C-NMR (100 MHz, $CDCl_3$) δ 195.8, 165.7, 162.7, 148.7, 136.4, 133.2, 132.9, 131.7, 129.0, 128.2, 127.7, 126.64, 126.61, 124.8, 122.8, 112.4, 83.1, 71.1, 60.4, 50.9, 36.2, 14.2; HRMS (ESI) calcd for $C_{22}H_{20}O_4Na^+$ 371.1254, found 371.1243; IR (KBr): ν 2925, 1709, 1666, 1372, 1246, 1130, 1039, 859, 751 cm^{-1}. Enantiomeric excess: 93% $[\alpha]_D^{21}$ = +165.0 (*c* 0.60, $CHCl_3$); HPLC analysis (Chiralpak IA, *n*-hexane/2-propanol = 9/1, flow rate 1.0 mL/min, λ = 216 nm) first peak: t_R = 18.5 min, second peak: t_R = 23.4 min.

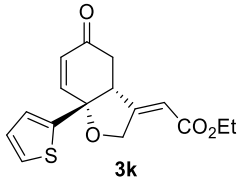

3k

3k: 70% yield; colorless oil; ^{1}H-NMR (400 MHz, $CDCl_3$) δ 7.38 (t, 1H, *J* = 3.2 Hz), 7.02 (d, 2H, *J* = 3.2 Hz), 6.73 (dd, 1H, *J* = 10.1, 1.8 Hz), 6.15 (dd, 1H, *J* = 10.1, 0.9 Hz), 5.74 (q, 1H, *J* = 2.6 Hz), 5.25-5.09 (m, 1H), 4.78 (dt, 1H, *J* = 17.6, 2.6 Hz), 4.16 (q, 2H, *J* = 7.2 Hz), 3.40-3.31 (m, 1H), 2.93-2.74 (m, 2H), 1.28 (t, 3H, *J* = 7.2 Hz); ^{13}C-NMR (100 MHz, $CDCl_3$) δ 195.3, 165.6, 161.8, 147.8, 142.9, 131.0, 127.0, 126.4, 125.0, 112.5, 81.2, 71.1, 60.5, 51.1, 36.1, 14.2; HRMS (ESI) calcd for $C_{16}H_{16}O_4SNa^+$ 327.0662, found 327.0651;

IR (KBr): ν 3381, 3101, 3031, 2980, 2904, 1715, 1693, 1381, 1250, 1183, 1129, 1030, 855, 701 cm^{-1}. Enantiomeric excess: 93% $[\alpha]_D^{22}$ = +44.7 (*c* 1.96, $CHCl_3$); HPLC analysis (Chiralpak IC, *n*-hexane/2-propanol = 8/2, flow rate 1.0 ml/min, λ = 212 nm) first peak: t_R = 21.3 min, second peak: t_R = 32.0 min.

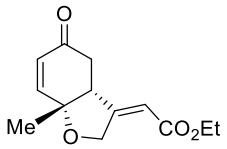

3l

3l: 52% yield; colorless oil; ^{1}H-NMR (400 MHz, $CDCl_3$) δ 6.55 (dd, 1H, *J* = 11.0, 1.8 Hz), 5.93 (d, 1H, *J* = 11.0 Hz), 5.70 (q, 1H, *J* = 2.6 Hz), 4.95 (dd, 1H, *J* = 17.6, 2.6 Hz), 4.58 (dt, 1H, *J* = 17.6, 2.6 Hz), 4.13 (q, 2H, *J* = 7.2 Hz), 3.10-2.95 (m, 1H), 2.85-2.70 (m, 2H), 1.58 (s, 3H), 1.26 (t, 3H, *J* = 7.2 Hz); ^{13}C-NMR (100 MHz, $CDCl_3$) δ 195.4, 165.7, 163.2, 151.4, 130.0, 112.4, 79.3, 70.6, 60.3, 48.5, 36.7, 22.9, 14.2; HRMS (ESI) calcd for $C_{13}H_{16}O_4Na^+$ 259.0941, found 259.0937; IR (KBr): ν 2978, 2361, 1714, 1685, 1374, 1266, 1145, 1036, 854 cm^{-1}. Enantiomeric excess: 90% $[\alpha]_D^{23}$ = –38.0 (*c* 0.50, $CHCl_3$); HPLC analysis (Chiralpak IA, *n*-hexane/2-propanol = 9/1, flow rate 1.0 mL/min, λ = 212 nm) first peak: t_R = 22.7 min, second peak: t_R = 25.0 min.

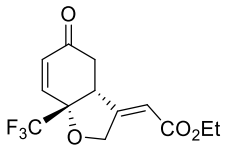

3m

3m: 69% yield; colorless oil; ^{1}H-NMR (600 MHz, $CDCl_3$) δ 6.60 (dd, 1H, *J* = 10.4, 1.5 Hz), 6.24 (d, 1H, *J* = 10.4 Hz), 5.78 (q, 1H, *J* = 2.5 Hz), 5.10 (dd, 1H, *J* = 17.4, 2.5 Hz), 4.80 (dt, 1H, *J* = 17.4, 2.5 Hz), 4.15 (q, 2H, *J* = 7.2 Hz), 3.63-3.58 (m, 1H), 2.96-2.78 (m, 2H), 1.27 (t, 3H, *J* = 7.2 Hz); ^{13}C-NMR (176 MHz, $CDCl_3$) δ 193.9, 165.2, 159.1, 140.0, 134.6, 124.0 (q, *J* = 283.0 Hz), 113.6, 79.9 (q, *J* = 31.5 Hz), 71.6, 60.7, 42.9, 36.6, 14.2; ^{19}F-NMR (565 MHz, $CDCl_3$) δ –78.0 (s); HRMS (ESI) calcd for $C_{13}H_{13}F_3O_4Na^+$ 313.0658, found 313.0652; IR (KBr): ν 2981, 2926, 2348, 1714, 1375, 1330, 1258, 1233, 1182, 1131, 1097, 1074, 1026, 859, 788 cm^{-1}; Enantiomeric excess: 92% $[\alpha]_D^{20}$ = –43.2 (*c* 0.95, $CHCl_3$); HPLC analysis (Chiralpak IF, *n*-hexane/2-propanol = 9/1, flow rate = 1.0 mL/min, λ = 210 nm) first peak: t_R = 21.1 min, second peak: t_R = 29.1 min.

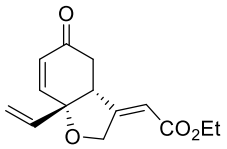

3n

3n: 74% yield; colorless oil; ^{1}H-NMR (400 MHz, $CDCl_3$) δ 6.52 (dd, 1H, *J* = 10.3, 1.6 Hz), 6.16-6.00 (m, 2H), 5.72 (q, 1H, *J* = 2.4 Hz), 5.48-5.28 (m, 2H), 5.02 (dd, 1H, *J* = 17.4, 2.4 Hz), 4.66 (dt, 1H, *J* = 17.4, 2.4

Hz), 4.14 (q, 2H, *J* = 7.1 Hz), 3.11 (brs, 1H), 2.86-2.67 (m, 2H), 1.27 (t, 3H, *J* = 7.1 Hz); ^{13}C-NMR (100 MHz, $CDCl_3$) δ 195.6, 165.6, 162.3, 148.2, 136.6, 131.6, 118.1, 112.5, 91.9, 70.8, 60.4, 48.0, 35.9, 14.2; HRMS (ESI) calcd $C_{14}H_{16}O_4Na^+$ 271.0941, found 271.0936; IR (KBr): ν = 2980, 2902, 1703, 1682, 1661, 1417, 1376, 1352, 1254, 1222, 1195, 1151, 1129, 1056, 1038, 1014, 991, 940, 867, 818, 795 cm^{-1}. Enantiomeric excess: 91% $[\alpha]_D^{20}$ = +13.7 (*c* 1.53, $CHCl_3$); HPLC analysis (Chiralpak IF, *n*-hexane/2-propanol = 9/1, flow rate = 1.0 mL/min, λ = 210 nm) first peak: t_R = 33.9 min; second peak: t_R = 43.8 min.

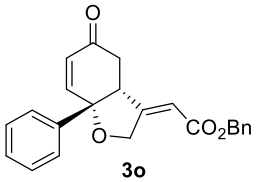

3o

3o: 46% yield; colorless oil; ^{1}H-NMR (400 MHz, $CDCl_3$) δ 7.55-7.48 (m, 2H), 7.45-7.28 (m, 8H), 6.67 (dd, 1H, *J* = 10.1, 1.8 Hz), 6.23 (d, 1H, *J* = 10.1 Hz), 5.83-5.75 (m, 1H), 5.23 (dd, 1H, *J* = 17.7, 2.6 Hz), 5.15 (m, 2H), 4.81 (dt, 1H, *J* = 17.7, 2.6 Hz), 3.24-3.18 (m, 1H), 2.86-2.68 (m, 2H); ^{13}C-NMR (100 MHz, $CDCl_3$) δ 195.6, 165.4, 163.6, 148.7, 139.0, 135.7, 131.6, 128.9, 128.7, 128.6, 128.3, 125.4, 112.0, 83.0, 77.2, 71.0, 66.4, 51.0, 36.1; HRMS (ESI) calcd for $C_{23}H_{20}O_4Na^+$ 383.1254, found 383.1248; IR (KBr): ν 3063, 3033, 2957, 2895, 1716, 1493, 1449, 1382, 1354, 1249, 1199, 743, 698 cm^{-1}. Enantiomeric excess: 96% $[\alpha]_D^{23}$ = +57.9 (*c* 0.14, $CHCl_3$); HPLC analysis (Chiralpak IF, *n*-hexane/2-propanol = 9/1, flow rate 1.0 mL/min, λ = 208 nm) first peak: t_R = 34.2 min, second peak: t_R = 51.8 min.

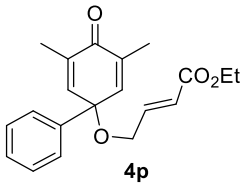

4p

4p: 4% yield; colorless oil; ^{1}H-NMR (400 MHz, $CDCl_3$) δ 7.48-7.43 (m, 2H), 7.38-7.28 (m, 3H), 7.01 (dt, 1H, *J* = 16.0, 4.0 Hz), 6.57 (s, 2H), 6.21 (dt, 1H, *J* = 16.0, 2.0 Hz), 4.26-4.19 (m, 4H), 1.95 (s, 6H), 1.31 (t, 3H, *J* = 7.4 Hz); ^{13}C-NMR (176 MHz, $CDCl_3$) δ 186.8, 166.4, 145.0, 144.5, 139.2, 136.6, 128.7, 128.1, 125.7, 121.0, 63.3, 60.5, 16.0, 14.3, 14.2; HRMS (ESI) calcd for $C_{20}H_{22}O_4Na^+$ 349.1410, found 349.1404; IR (KBr): ν 2980, 2926, 2357, 1717, 1647, 1266, 1178, 1037, 756, 696 cm^{-1}.

4.4.5. X-ray Crystal Data of (*R*,*R*)-*Z*-3k

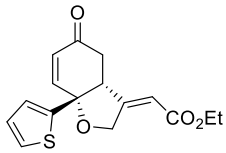

(*R*,*R*)-*Z*-**3k**

≡

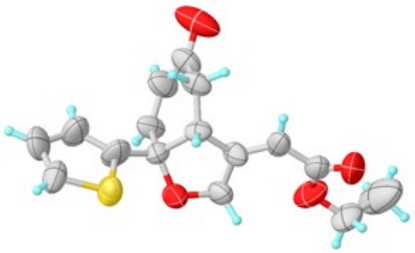

(CCDC No. 1420353)

X-ray structure of tetrahydrobenzofuranone **3k** (ortep drawing with thermal ellipsoids at 30% probability level)

Refined formula: $C_{132.98}H_{127.85}I_{12}N_{24}O_{10.52}S_{2.63}Zn_6$, formula weight ($M_r$): 4229.83, crystal system: monoclinic, space group: *C*2, $Z = 4$. 25279 unique reflections merged from recorded 89518 ones ($3.668° < \theta < 76.803°$) were used for structural analysis ($R_{int} = 0.0469$). Lattice parameters, *R*-factor on $F^2 > 2\sigma(F^2)$, weighted *R*-factor, and Goodness of Fit (*S*) are follows: $a = 35.1105(10)$ Å, $b = 14.8080(3)$ Å, $c = 31.4241(9)$ Å, $\beta = 102.544(3)°$, $V = 15947.9(7)$ Å^3, $R = 0.0625$, $wR = 0.1692$, $S = 1.016$. Calculated density is 1.762 g cm^{-3}. Linear absorption coefficient (μ) is 20.030 mm^{-1}. Residual electron density (max/min) was 1.629/–1.629 eÅ^{-3}. Friedel mate converge was 0.835. The Flack parameters determined using 8729 intensity quotients (the Parsons' method[20]) was 0.039(5). The Hooft parameter[21] was 0.045(6). Crystallographic information file (CIF) for this crystal structure was submitted to The Cambridge Crystallographic Data Centre (CCDC) under reference number 1420353.

4.5. References

1. (a) Govindachari, T. R.; Parthasarathy, P. C.; Desai, H. K.; Shanbhag, M. N. *Tetrahedron* **1973**, *29*, 3091. (b) Maddry, J. A.; Joshi, B. S.; Newton, M. G.; Pelletier, S.W.; Parthasarathy, P. C. *Tetrahedron Lett.* **1985**, *26*, 5491. (c) Hase, T.; Ohtani, K.; Kasai, R.; Yamasaki, K. *Pichansoonthon Phytochemistry* **1996**, *41*, 317. (d) Loukaci, A.; Kayser, O.; Bindseil, K.-U.; Siems, K.; Frevert, J.; Abreu, P. M. *J. Nat. Prod.* **2000**, *63*, 52. (e) Bringmann, G.; Lang, G.; Gulder, T. A. M.; Tsuruta, H.; Muhlbacher, J.; Maksimenka, K.; Steffens, S.; Schaumann, K.; Stohr, R.; Wiese, J.; Imhoff, J. F.; Perovic-Ottstadt, S.; Boreiko, O.; Muller, W. E. G. *Tetrahedron* **2005**, *61*, 7252. (f) Meragelman, T. L.; Scudiero, D. A.; Davis, R. E.; Staudt, L. M.; McCloud, T. G.; Cardellina II, J. H.; Shoemaker, R. H. *J. Nat. Prod.* **2009**, *72*, 336. (g) Hexum, J. K.; Tello-Aburto, R.; Struntz, N. B.; Harned, A. M.; Harki, D. A. *ACS Med. Chem. Lett.* **2012**, *3*, 459. (h) Wegner, J.; Ley, S. V.; Kirschning, A.; Hansen, A.-L.; Garcia, J. M.; Baxendale, I. R. *Org. Lett.* **2012**, *14*, 696. (i) Ren, Y.; Yuan, C.; Qian, Y.; Chai, H.-B.; Chen, X.; Goetz, M.; Kinghorn, A. D. *J. Nat. Prod*. **2014**, *77*, 550.
2. (a) Liu, Q.; Rovis, T. *J. Am. Chem. Soc.* **2006**, *128*, 2552. (b) Liu, Q.; Rovis, T. *Org. Process. Res. Dev.* **2007**, *11*, 598. (c) Takizawa, S.; Nguyen, T. M.-N.; Grossmann, A.; Enders, D.; Sasai H, *Angew. Chem. Int. Ed.* **2012**, *51*, 5423. (d) Takizawa, S.; Nguyen, T. M.-N.; Grossmann, A.; Suzuki, M.;

Enders, D.; Sasai H. *Tetrahedron* **2013**, *69*, 1202. (e) Keilitz, J.; Newman, S. G.; Lautens, M. *Org. Lett.* **2013**, *15*, 1148. (f) He, Z.-T.; Tian, B.; Fukui, Y.; Tong, X. Tian, P.; Lin, G.-Q. *Angew. Chem. Int. Ed.* **2013**, *52*, 5314. (g) Liu, P.; Fukui, Y.; Tian, P.; He, Z.-T.; Sun, C.-Y.; Wu, N.-Y.; Lin, G.-Q. *J. Am. Chem. Soc.* **2013**, *135*, 11700. (h) Corbett, M. T.; Johnson, J. S. *Chem. Sci.* **2013**, *4*, 2828. (i) He, Z.-T.; Tang, X.-Q.; Xie, L.-B.; Cheng, M.; Tian, P.; Lin, G.-Q. *Angew. Chem. Int. Ed.* **2015**, *54*, 14815.

3. (a) Schweizer, J.; Lattrell, R.; Hecker, E. *Experientia* **1975**, *31*, 1267. (b) McKinley, J.; Aponick, A.; Raber, J. C.; Fritz, C.; Montgomery, D.; Wigal, C. T. *J. Org. Chem.* **1997**, *62*, 4874. (c) Stern, A. J.; Swenton, J. S. *J. Org. Chem.* **1988**, *53*, 2465. (d) Sunasee, R.; Clive, D. L. J. *Chem. Commun.* **2010**, *46*, 701. (e) Yakura, T.; Omoto, M.; Yamauchi, Y.; Tian, Y.; Ozono, A. *Tetrahedron* **2010**, *66*, 5833.
4. (a) Cristau, H.-J.; Viala, J.; Christol, H. *Tetrahedron Lett*. **1982**, *23*, 1569. (b) Trost, B. M.; Li, C.-J; *J. Am. Chem. Soc*. **1994**, *116*, 3167. (c) Zhang, C.; Lu, X. *Synlett* **1995**, 645. (d) Chen, Z.; Zhu, G.; Jiang, Q.; Xiao, D.; Cao, P.; Zhang, X. *J. Org. Chem*. **1998**, *63*, 5631.
5. For selected recent examples: (a) Smith, S. W.; Fu, G. C. *J. Am. Chem. Soc.* **2009**, *131*, 14231. (b) Sun, J.; Fu, G. C. *J. Am. Chem. Soc.* **2010**, *132*, 4568. (c) Wang, T.; Yao, W.; Zhong, F.; Pang, G. H.; Lu, Y. *Angew. Chem. Int. Ed*. **2014**, *53*, 2964. (d) Fang, Y.-Q.; Tadross, P. M.; Jacobsen, E. N. *J. Am. Chem. Soc*. **2014**, *136*, 17966. (e) Ziegler, D. T.; Riesgo, L.; Ikeda, T.; Fujiwara, Y.; Fu, G. C. *Angew. Chem. Int. Ed.* **2014**, *53*, 13183. (f) Chen, J.; Cai, Y.; Zhao, G. *Adv. Synth. Catal.* **2014**, *356*, 359. (g) Wang, T.; Hoon, D. L.; Lu, Y. *Chem. Commun*. **2015**, *51*, 10186. (h) Wang, T.; Yu, Z.; Hoon, D. L.; Huang, K.-W.; Lan, Y.; Lu, Y. *Chem. Sci*. **2015**, *6*, 4912. (i) Zhou, Q.-F.; Zhang, K.; Kwon, O. *Tetrahedron Lett*. **2015**, *56*, 3273. (j) Kalek, M.; Fu, G. C. *J. Am. Chem. Soc*. **2015**, 137, 9438.
6. (a) Shi, M.; Chen, L.-H. *Chem. Commun.* **2003**, 1310. (b) Shi, M.; Chen, L.-H.; Li, C.-Q. *J. Am. Che. Soc.* **2005**, *127*, 3790.
7. (a) Wang, S.-X.; Han, X.; Zhong, F.; Wang, Y.; Lu, Y. *Synlett* **2011**, 2766. (b) Gong, J.-J.; Li, T.-Z.; Pan, K.; Wu, X.-Y. *Chem. Commun.* **2011**, *47*, 1491. (c) Dong, X.; Liang, L.; Li, E.; Huang, Y. *Angew. Chem. Int. Ed.* **2015**, *54*, 1621. (d) Scanes, R. J. H.; Grossmann, O.; Grossmann, A.; Spring, D. R. *Org. Lett.* **2015**, *17*, 2462. (e) Su, X.; Zhou, W.; Li, Y.; Zhang, J. *Angew. Chem. Int. Ed.* **2015**, *54*, 6874.
8. Henry, C. E.; Xu, Q.; Fan, Y. C.; Martin, T. J.; Belding, L.; Dudding, T.; Kwon, O. *J. Am. Chem. Soc.* **2014**, *136*, 11890.
9. (a) Gladiali, S.; Dore, A.; Fabbri, D.; Lucchi, O. D.; Manassero, M. *Tetrahedron: Asymmetry* **1994**, *5*, 511. (b) Fleury-Bregeot, N.; Jean, L.; Retailleau, P.; Marinetti, A. *Tetrahedron* **2007**, *63*, 11920. (c) Sinisi, R.; Sun, J.; Fu, G. C. *Proc. Natl. Acad. Sci.* **2010**, *107*, 20652. (d) Fujiwara, Y.; Sun, J.; Fu, G. C. *Chem Sci*. **2011**, *2*, 2196. (e) Lee, S. Y.; Fujiwara, Y.; Nishiguchi, A.; Kalek, M.; Fu, G. C.; *J. Am. Chem. Soc*. **2015**, *137*, 4587.
10. (a) Zhu, S.-F.; Yang, Y.; Wang, L.-X.; Liu, B.; Zhou, Q.-L. *Org. Lett*. **2005**, 7, 2333. (b) Chung, Y.

K.; Fu, G. C. *Angew. Chem. Int. Ed.* **2009**, *48*, 2225. (c) Wang, Q.-G.; Zhu, S.-F.; Ye, L.-W.; Zhou, C.-Y.; Sun, X.-L.; Tang, Y.; Zhou, Q.-L. *Adv. Synth. Catal.* **2010**, *352*, 1914. (d) Wang, D.; Wei, Y.; Shi, M. *Chem. Commun*. **2012**, *48*, 2764. (e) Lundgren, R. J.; Wilsily, A.; Marion, N.; Ma, C.; Chung, Y. K.; Fu, G. C. *Angew, Chem. Int. Ed*. **2013**, *52*, 2525. (f) Wang, D.; Lei, Y.; Wei, Y.; Shi, M. *Chem. Eur. J.* **2014**, *20*, 15325. (g) Kramer, S.; Fu, G. C. *J. Am. Chem. Soc.* **2015**, *137*, 3803. (h) Zhang, L.; Liu, H.; Qiao, G.; Hou, Z.; Liu, Y.; Xiao, Y.; Guo, H. *J. Am. Chem. Soc.* **2015**, *137*, 4316.

11. (a) Inokuma, Y.; Yoshioka, S.; Ariyoshi, J.; Arai, T.; Hitora, Y.; Takada, K.; Matsunaga, S.; Rissanen, K. Fujita, M. *Nature* **2013**, *495*, 461. (b) Yoshioka, S.; Inokuma, Y.; Hoshino, M.; Sato, T.; Fujita, M. *Chem. Sci.* **2015**, *6*, 3765. (c) Sairenji, S.; Kikuchi, T.; Abozeid, M. A.; Takizawa, S.; Sasai, H.; Ando, Y.; Ohmatsu, K.; Ooi, T.; Fujita, M. *Chem. Sci.* **2017**, *8*, 5132.
12. Dudding, T.; Kwon, O.; Mercier, E. *Org. Lett.* **2006**, *8*, 3643.
13. Nising, C. F.; Brase, S. *Chem. Soc. Rev.* **2012**, *41*, 988.
14. After publication of this work in 2015, a γ-addition/[3+2] cycloaddition sequence using α-substituted allenoates with PPh_3 was reported. Gu, Y.; Hu, P.; Ni, C.; Tong, X. *J. Am. Chem. Soc.* **2015**, *137*, 6400.
15. Novak, M.; Poturalski, M. J.; Johnson, W. L.; Jones, M. P.; Wang, Y.; Glover, S. A. *J. Org. Chem.* **2006**, *71*, 3788.
16. Wells, G.; Berry, J. M.; Bradshaw, T. D.; Burger, A. M.; Seaton, A.; Wang, B.; Westwell, A. D.; Stevens, M. F. G. *J. Med. Chem.* **2003**, *46*, 532.
17. Zhang, X.; Wang, F.; Qi, Z.; Yu, S.; Li, X. *Org. Lett*. **2014**, *16*, 1586.
18. Chong, H. S.; Seong, J. H.; Paik, Y.-S. *J. Korean Chem. Soc*. **1993**, *37*, 910.
19. Sorgi, K. L.; Scott, L.; Maryanoff, C. A. *Tetrahedron Lett*. **1995**, *36*, 3597.
20. Parsons, S.; Flack, H. D.; Wagner, T. Use of intensity quotients and differences in absolute structure refinement. *Acta Crystallogr. Sect. B* **2013**, *69*, 249.
21. Hooft, R. W. W., Straver, L. H., and Spek, A. L., Determination of absolute structure using Bayesian statistics on Bijvoet differences, *J. Appl. Cryst.* **2008**, *41*, 96.

Chapter 5
Phosphine-Catalyzed Dual Umpolung Domino Michael Reaction: A Novel Route to Hydroindole- and Hydrobenzofuran-2-Carboxylates

Abstract: A highly atom-economical, chemo- and stereoselective Lewis base-catalyzed dual umpolung domino Michael reaction between cyclohexadienones and alkynoates has been developed. PPh_3 as a Lewis base catalyst gave either hydroindole- or hydrobenzofuran-2-carboxylates as a single diastereomer in high yields (up to 89%). Obtained product could be transformed into an analog of PEP inhibitor.

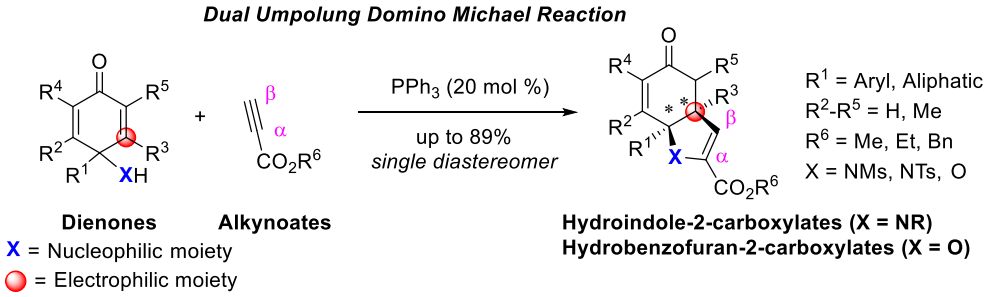

5.1. Introduction

As mentioned in Chapters 2–4, the author has achieved the facile enantioselective synthesis of highly functionalized bicyclic *N*- and *O*-heterocycles. Among bicyclic *N*- and *O*-heterocycles, hydroindoles and hydrobenzofurans that contain the carbonyl group at their 2-positions are particularly desirable to synthesize, as their basic structure is seen in many natural products and bioactive compounds (Figure 5.1).[1,2] In particular, the octahydroindole-2-carboxylic acid (Oic) is contained in approximately 1,400 natural products, according to the Dictionary of Natural Products database.[2] As representative examples of bioactive hydroindoles (X = NR), perindopril (commercially available through Kyowa Kirin)[1a] and DU-1777[1c] act as ACE inhibitors. Moreover, modified perindopril displays a PEP-inhibiting activity.[1b] Examples of bioactive hydrobenzofuran-2-carboxylates (X = O) include perenniporide C (an antifungal compound),[1e] maoecrystal V (an anticancer species),[1d] and hyperhexanone A (a crucial intermediate for CM-PPAP).[1f]

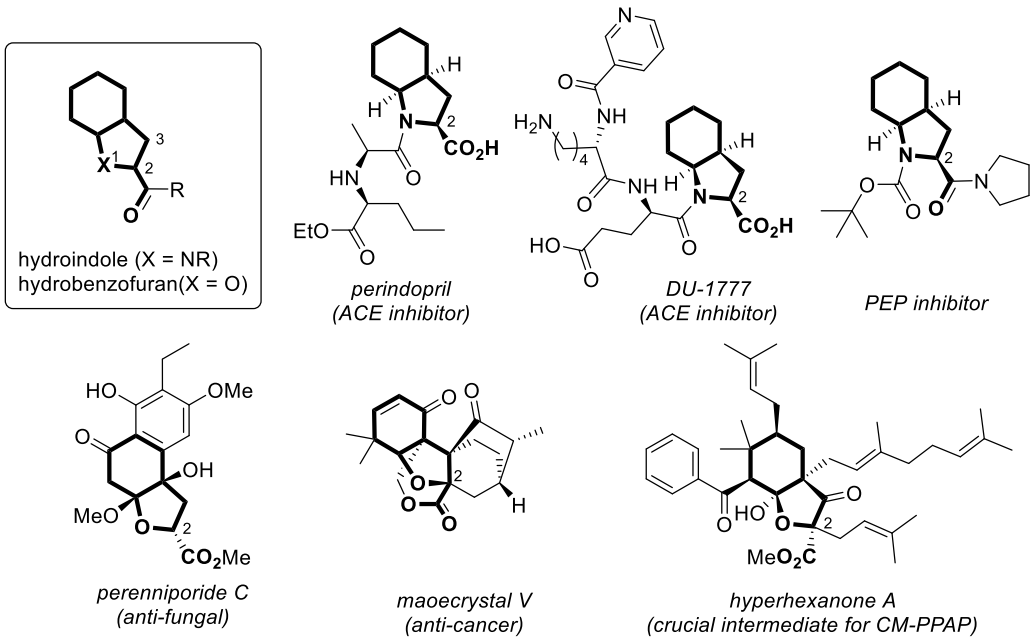

Figure 5.1. Selected examples of natural products and bioactive compounds having hydroindole or hydrobenzofuran containing carbonyl group at their 2-position.

Despite the biological importance of hydroindoles and hydrobenzofurans bearing a carbonyl group at their 2-position, developing protocols for their syntheses has been a challenging goal to achieve, because of the α-oxidized carbonyl functionality which requires umpolung reaction or α-amination/alkoxylation of carbonyl compounds using explosive peroxides or toxic nitrogen electrophiles.[3] Most of the synthetic routes for the production of these families of compounds depend on the use of indoline-2-carboxylic acid[1a,1b,4] or tyrosine[5] as building blocks (Scheme 5.1).

Scheme 5.1. Representative approaches and this work for the synthesis of hydroindoles bearing carbonyl group at their 2-position

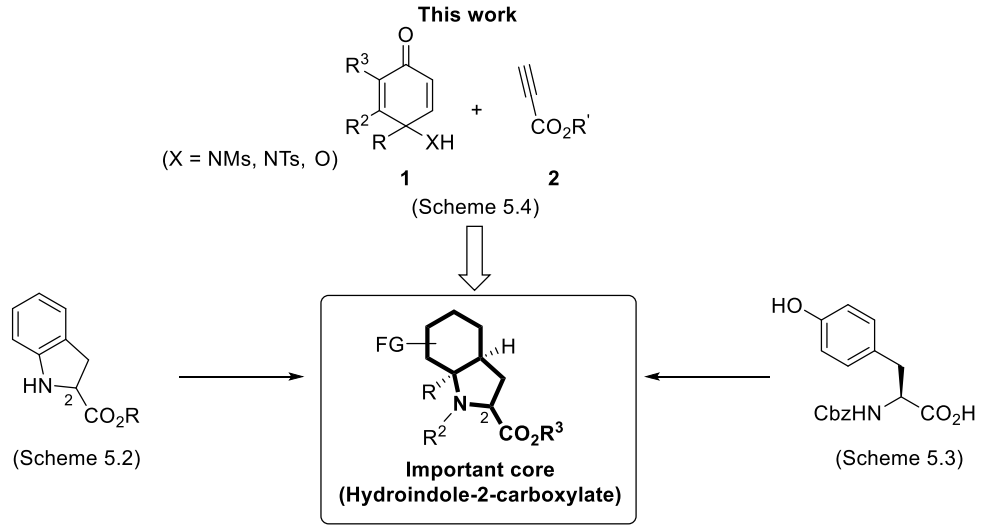

Catalytic hydrogenation of indoline-2-carboxylic acid and its derivatives is the most straightforward approach to synthesize hydroindole-2-carboxylates. In the first relevant study to be published, in 1982, Vincent reported that an optically pure indoline-2-carboxylate could be converted to the corresponding hydroindole-2-carboxylate diastereoselectively by catalytic hydrogenation (Scheme 5.2).[1a] This hydroindole-2-carboxylate was then coupled with a peptide to form perindopril. Since this report, the methodology it introduced has been utilized to synthesize a range of bioactive derivatives of hydroindole-2-carboxylic acids.[2a,4]

Scheme 5.2. Catalytic hydrogenation of indoline-2-carboxylic acid

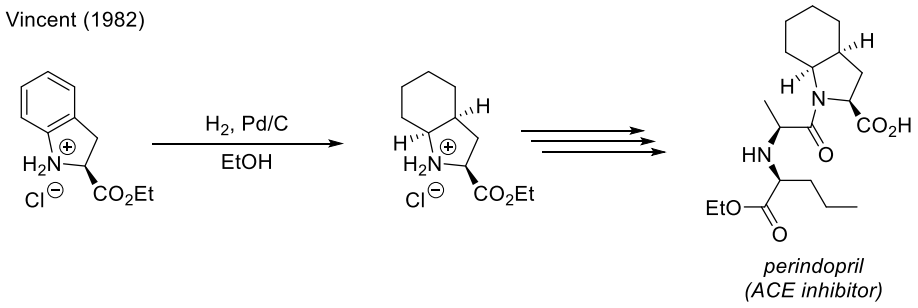

In 1992, Wipf found that the treatment of a protected tyrosine with PhI(OAc) as an oxidant undergoes oxidative cyclization to give densely functionalized hydroindole-2-carboxylate with excellent diastereoselectivity (>98:2) (Scheme 5.3).[5a] This methodology doesn't rely on any optical resolutions of the products due to the use of tyrosine as an naturally occurring chiral source.

Scheme 5.3. Oxidative cyclization of a protected tyrosine

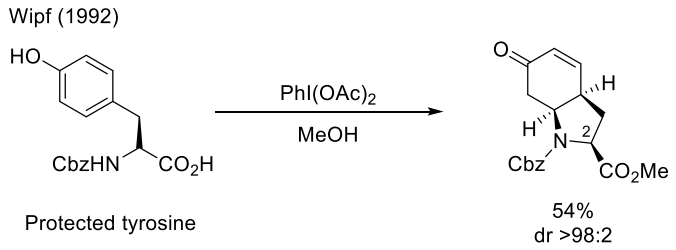

After this report, some groups including Wipf utilized this methodology for total synthesis of natural products such as (–)-stenine,[5b](+)-aeruginosin 298–A,[5e] tuberostemonine,[5f] didehydrotuberostemonine,[5f] 13-epituberostemonine,[5f] and aeruginosin KT608A,[5h]. Notably, it has also been employed in drug discovery studies.[5c,d,g] Evidence thus confirms the importance of this structural motif. Although other approaches to the synthesis of hydroindoles bearing a carbonyl group at their 2-position have been reported, including condensation of cyclic compounds and amino acids,[6] ring-closing-metathesis of proline derivatives[7], reductive cyclization of tyrosine[8], and aza-Cope rearrangement,[9] these methods require complex building blocks and multistep reactions.

As described above, indoline-2-carboxylic acid and protected tyrosines are effective substrates for the synthesis of simple and highly functionalized hydroindoles bearing a carbonyl group at their 2-position, respectively. However, as summarized in Figure 5.2, owing to the accessibility of the starting materials, when these methodologies are implemented, the substituents at the red-colored ring-condensed sites of the target compound must be hydrogen atoms (R = R′ = H), and the blue-colored heteroatom of the same compound must be an amine nitrogen (X = N). The development of a different methodology is required to diversify the functionalities, which is expected to extend the possibility of the drug discovery.

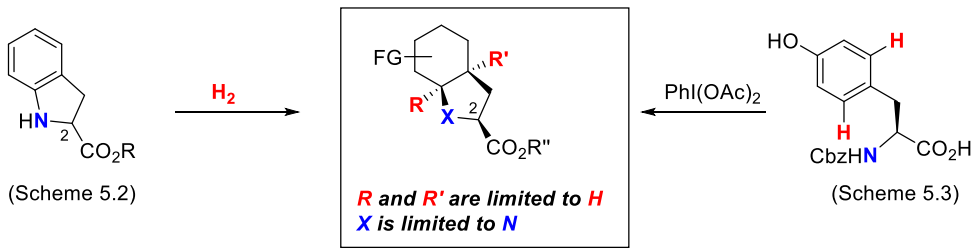

Figure 5.2. Substituent-limitation of current methodologies

To address these issues, the author envisioned the synthetic strategy detailed in Scheme 5.4. As mentioned in Chapter 1, Section 3, Paragraph 5, Lewis base-catalyzed α-addition of alkynoate is an effective method for the synthesis of amino acids (Scheme 5.4a, Path A).[10] The author assumed that the dual umpolung domino

Michael reaction of the readily accessible cyclohexadienone **1**[11,12] and alkynoate **2** could become a solution to the synthetic limitations of the approach summarized in Figure 5.2. This reaction course would lead to obtaining both hydroindole- and hydrobenzofuran-2-carboxylates **3** having an R substituent on the condensed site (Scheme 5.4a, Path B, and Scheme 5.4b). Namely, intermediate C (**Int. C**, in Scheme 5.4) generated by the α-addition of a nitrogen- or oxygen-based nucleophile undergoes a second Michael addition with an electrophile to give the desired α-oxidized heterocycles.

Scheme 5.4. **a**: Umpolung Michael reaction of alkynoate **b**: **This work**

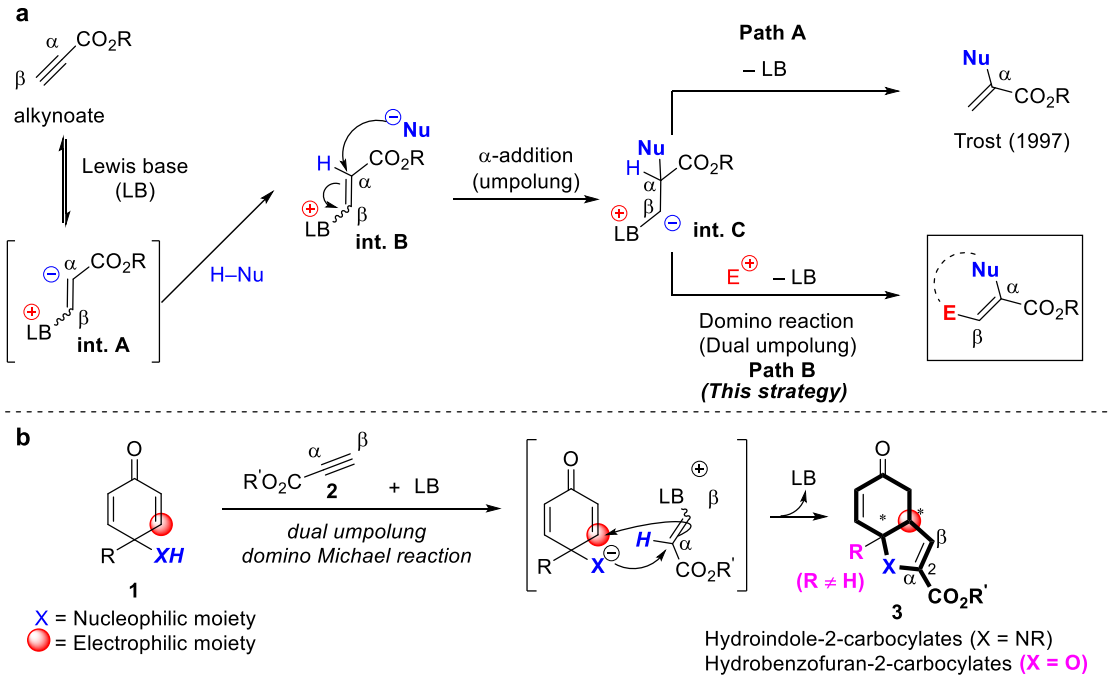

5.2. Results and Discussion

5.2.1. Optimization of the Reaction Conditions

To explore the applicability of the proposed domino process, the author first employed the known cyclohexadienone **1a**[11c] and commercially available alkynoate **2a** as prototypical substrates (Table 5.1). The use of PPh_2Me or PPh_3 was found to afford the desired umpolung product **3a** in 23% and 25% yield, respectively (entries 1 and 2). The use of an electron-rich PBu_3 resulted in the formation of the sequential adduct **4a** having a carbonyl group at the 3-position in a 4% yield, alongside many unidentified side products (entry 3).[13] The use of additional electron-deficient phosphines, such as $P(OMe)_3$ and $P(C_6F_5)_3$, led to no reaction taking place at all, because no nucleophilic addition of the phosphine catalyst to **2a** occurred (entry 4). These results supported the idea that the electron-withdrawing ability of the phosphonium group in intermediate B (**Int. B** in Scheme 5.4a) plays a key role in rendering the umpolung reaction possible. The use of amine-type Lewis base catalysts like NEt_3 and DABCO did not lead to any improvements in the yield of

the reaction[14] (entries 5 and 6), while affording the dimer of alkynoate **2a**[15], which also supports the importance of the phosphonium-based **Int. B** in the formation of **3a**.

Table 5.1. Screening of Lewis base (LB) catalysts

entry	LB catalyst	yield of **3a** (%)	yield of **4a** (%)
1	PPh_2Me	23	trace
2	PPh_3	25	0
3	PBu_3	0	4
4	$P(OMe)_3$ or $P(C_6F_5)_3$	0	0
5	NEt_3	0	20
6	DABCO	0	0

Next, the effect of the solvent was evaluated in the presence of PPh_3 at 80 °C (Table 5.2). Initially, the author found that decreasing the amount of **2a** to 1.0 equiv increased the yield with less by-products (entry 2). Although the use of toluene led to higher yield, MeCN showed less reactivity and miserable yield with formation of a trace amount of **4a** (entries 3 and 4). Halogenated solvents such as 1,2-dichloroethane (DCE)

Table 5.2. The effect of the solvent

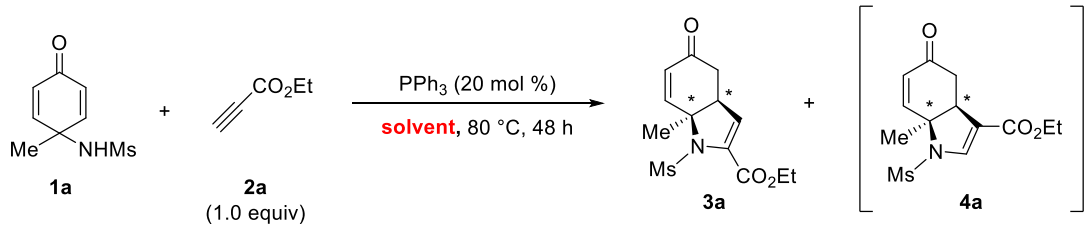

entry	solvent	yield of **3a** (%)	yield of **4a** (%)
1[a]	toluene/MeCN (4:1)	25	0
2	toluene/MeCN (4:1)	40	0
3	toluene	50	0
4	MeCN	9	trace
5	DCE	39	0
6	PhCl	47	0
7	1.4-dioxane	61	0
8	DME	53	0
9	diglyme	36	0
10	CPME	56	0

[a] : 2.0 equiv of **2a** was used

and PhCl didn't show any improvements (entries 5 and 6). Ether-type solvents showed better outcomes (entries 7–10). Among them, 1,4-dioxane gave product in 61% yield, thus, determined as optimal solvent for this reaction.

Subsequently, the influence of the reaction temperature was examined using PPh_3 in 1,4-dioxane (Table 5.3). At 50 °C, the reaction didn't proceed well to afford only a trace amount of **3a**, thus indicating that this system requires high temperature (entry 1). Although yield of **3a** was increased at higher temperature such as 90°C and 100 °C, starting material **1a** still remained unreacted (entries 3 and 4). Considering that this is due to volatilization of **2a** (bp = 119 °C), the amount of **2a** was increased to 1.5 equiv leading to the formation of **3a** in 86% isolated yield with the full conversion of **1a** (entry 5). Replacing PPh_3 with PPh_2Me, which showed a comparable result in initial screening of the catalysts, didn't improve the result. Finally, the optimal condition was determined as entry 5 in table 5.3.

Table 5.3. The influence of the reaction temperature

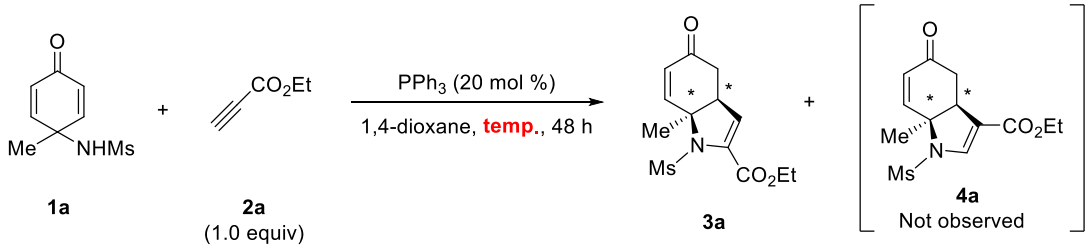

entry	temp. (C°)	conv. of **1a** (%)[a]	yield of **3a** (%)[a]
1	50	<10	trace
2	80	82	61
3	90	80	68
4	100	78	69
5[c]	100	>99	86 (86)[b]
6[d,e]	100	65	25

[a] : Determined by ^1H NMR using 1,3,5-trimethoxybenzene as an internal standard
[b] : Isolated yield
[c] : 1.5 equiv of **2a** was used
[d] : PPh_2Me was used instead of PPh_3

5.2.2. Substrate Scope

With the optimized reaction condition in hand, the author's interest shifted to the scope of the newly developed dual umpolung domino Michael reaction (Scheme 5.5). Aromatic substituents on **1** (**1b**: R^1 = Ph; **1c**: R^1 = *p*-tolyl) were compatible with the reaction, although the yields of **3b** and **3c** decreased. The Ms group could be replaced with the bulkier Ts group (**3d**–**3f**: X = NTs), while still maintaining moderate to good yields. The more electron-rich *p*-methoxybenzenesulfonyl group was also tolerated (**3g**). Methyl and benzyl esters (**2b**: R^6 = Me; **2c**: R^6 = Bn) yielded products **3h** and **3i**, respectively. Cyclohexadienone **1j**, which bears a hydroxy group[12], underwent the designed umpolung reaction to afford the corresponding

Scheme 5.5. Scope of dual umpolung domino Michael reaction

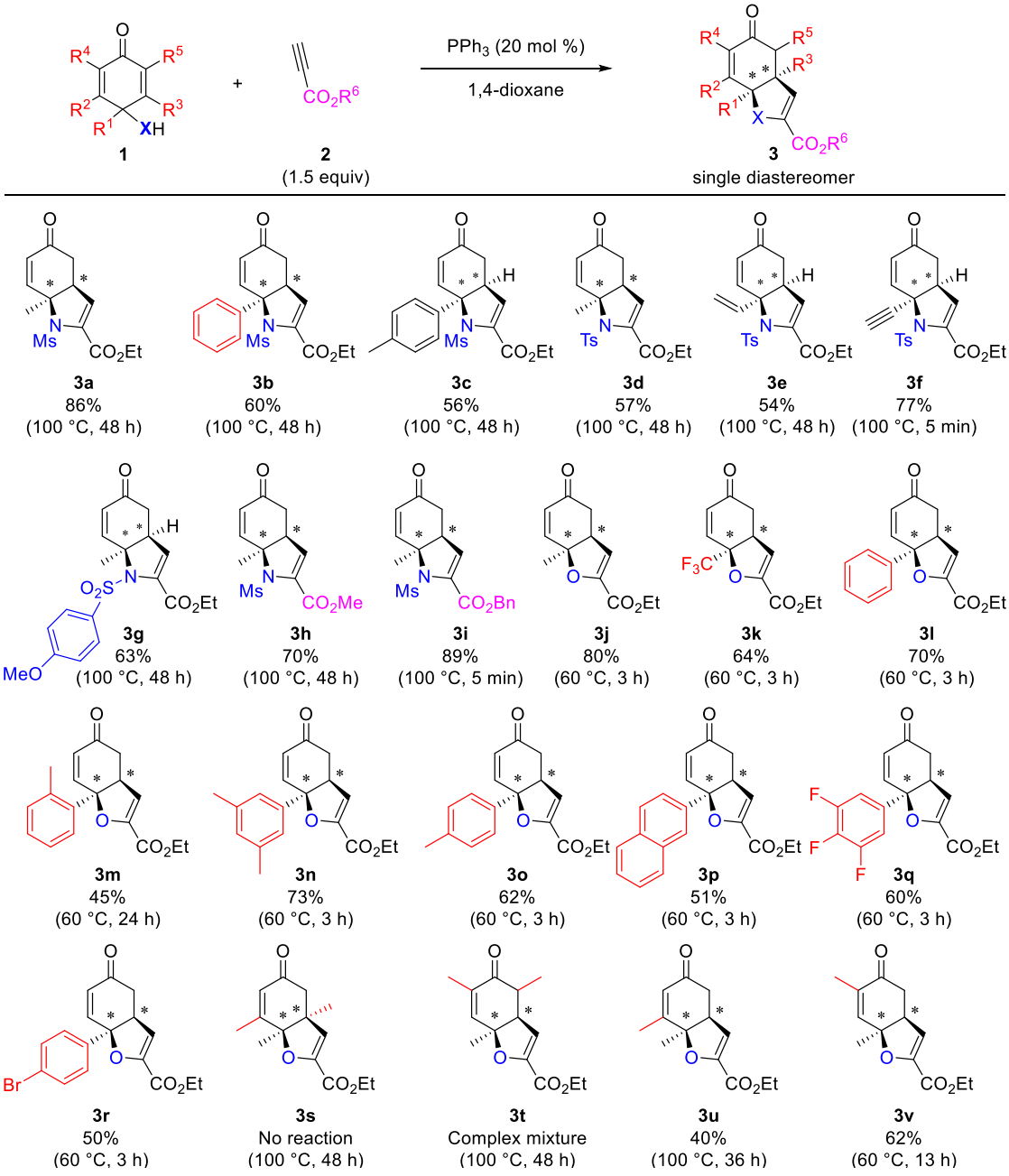

hydrobenzofuran-2-carboxylate (**3j**, X = O) in high yield even at lower temperature for the shorter reaction period (at 60 °C for 3 h) than that of cyclohexadienones possessing an amino group (X = NMs or NTs: at 100 °C for 48 h). These results indicated C–X bond formation is a rate-controlling step. The *o*-tolyl group (**1m**, R^1 = *o*-tolyl) was tolerated, and **3m** was obtained after extending the reaction time. Both electron-withdrawing and electron-donating groups at the meta and para positions of **1** (**1n**–**1r**) were tolerated (**3n**: R^1 = 3,5-Me_2-C_6H_3; **3o**: *p*-tolyl; **3p**: 2-naphthyl; **3q**: 3,4,5-$F_3C_6H_2$; **3r**: *p*-Br-C_6H_4). In all cases, a single diastereomer was obtained. Although monomethylated products (**3u**, R^2 = Me and **3v**, R^4 = Me) were regioselectively obtained with moderate yields, no reaction occurred to yield **3s** and **3t** when substrates **1s** and **1t** with α,α′-dimethyl or β,β′-dimethyl substituents on the cyclohexadienone olefins (**1s**: R^2 = R^3 = Me; **1t**: R^4 = R^5 = Me) were employed. The relative configuration and structure of the obtained product were unambiguously determined via X-ray crystallography of **3a** to be the *cis*-configuration for both chiral centers (Figure 5.3).

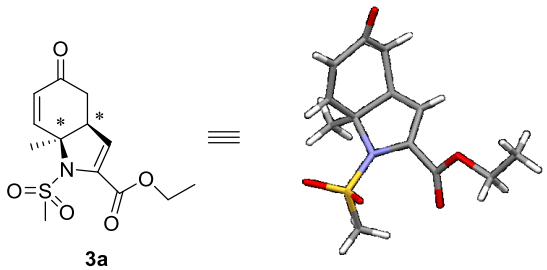

Figure 5.3. X-ray structure of **3a**

Compounds that gave unsatisfactory results as substrates of the dual umpolung domino Michael reaction are summarized in Scheme 5.6. The use of cyclohexadienones **1w** (R = Boc) and **1x** (R = Bz) gave rise to trace amounts of the desired products, in a context of low substrate conversion of **1**. These outcomes may be due to the decreased acidity of the amine moiety of the substrate **1**, resulting in low concentrations of the deprotonated active species (Eq. 1). Although the internal alkynoate **2d** has been proven to work as an agent of phosphine-catalyzed α-additions,[10b] this compound did not work well as a reagent of the current domino system, because of the steric congestion around the nucleophilic center of **1** (Eq. 2). In the present reaction context, alkynone **2e** underwent self-condensation, and the rate of conversion of **1** was low. The Brønsted basicity of the intermediate derived from the reaction of **2e** with PPh_3 may not be appropriate for the reaction. Further investigations on the catalysts and reaction conditions are necessary to realize these reactions.

Scheme 5.6. Unsuccessful Substrates

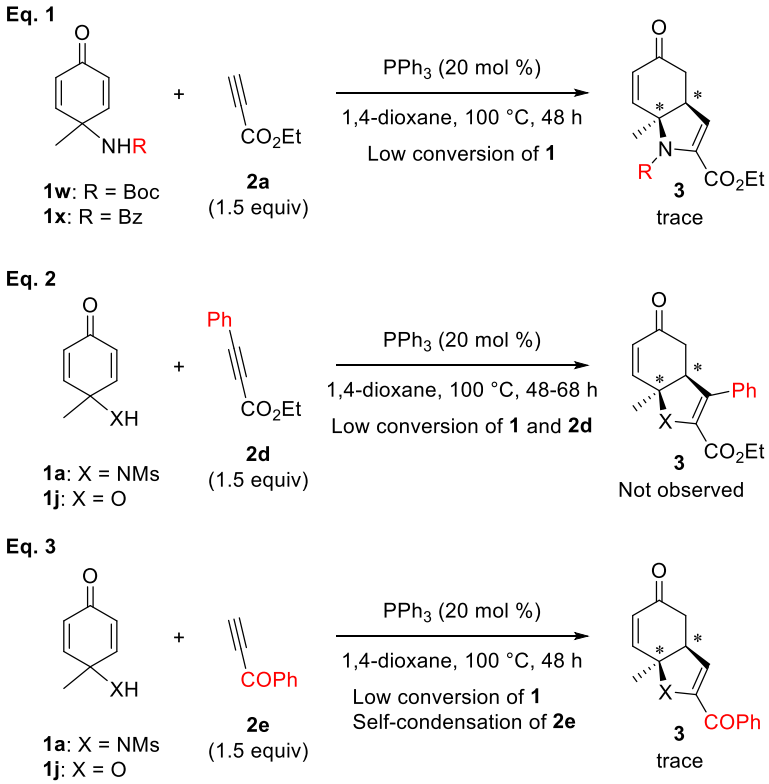

5.2.3. Preliminary Results on Enantioselective Reaction

A variety of chiral Lewis bases were investigated to explore the possibility of achieving enantioselectivity in the reaction. Although no satisfactory results could be obtained, guidelines for the catalyst design were nevertheless produced, which are summarized in Schemes 5.7–5.9. As observed while performing the optimization of the reaction conditions (Tables 5.1–5.3), the use of the monoalkyldiarylphosphine PPh_2Me and of the amines NEt_3 and DABCO did not lead to satisfactory results, whereas the triarylphosphine PPh_3 worked well in the present reaction context. Similar results were obtained when investigating chiral Lewis base catalysts: the use of monoalkyldiarylphosphines **5a**–**5c**[16,17] and amine β-ICD was associated with low product yields or no product formation. The use of (*R*)-SITCP, which mediates the domino reaction of allenoate (see Chapter 4), did not afford satisfactory results. Even employing chiral triarylphosphines like SDP, BINAP, *o*-tol-BINAP, or MOP (see their structures in Scheme 5.7) resulted in a low rate of conversion to the desired product **3a**. As for the possible reasons for the observed low conversion rates associated with the use of these chiral catalysts, shown in red are the substituents in the *ortho* positions of the aromatic ring connected to the phosphine center. The author concluded that this reaction may be quite sensitive to the steric hindrance around the phosphorous center of the catalyst and that the presence of the mentioned substituents may explain the unsatisfactory results detailed above.

Scheme 5.7. Preliminary results on screening of chiral Lewis bases for the enantioselective reaction of **1a**

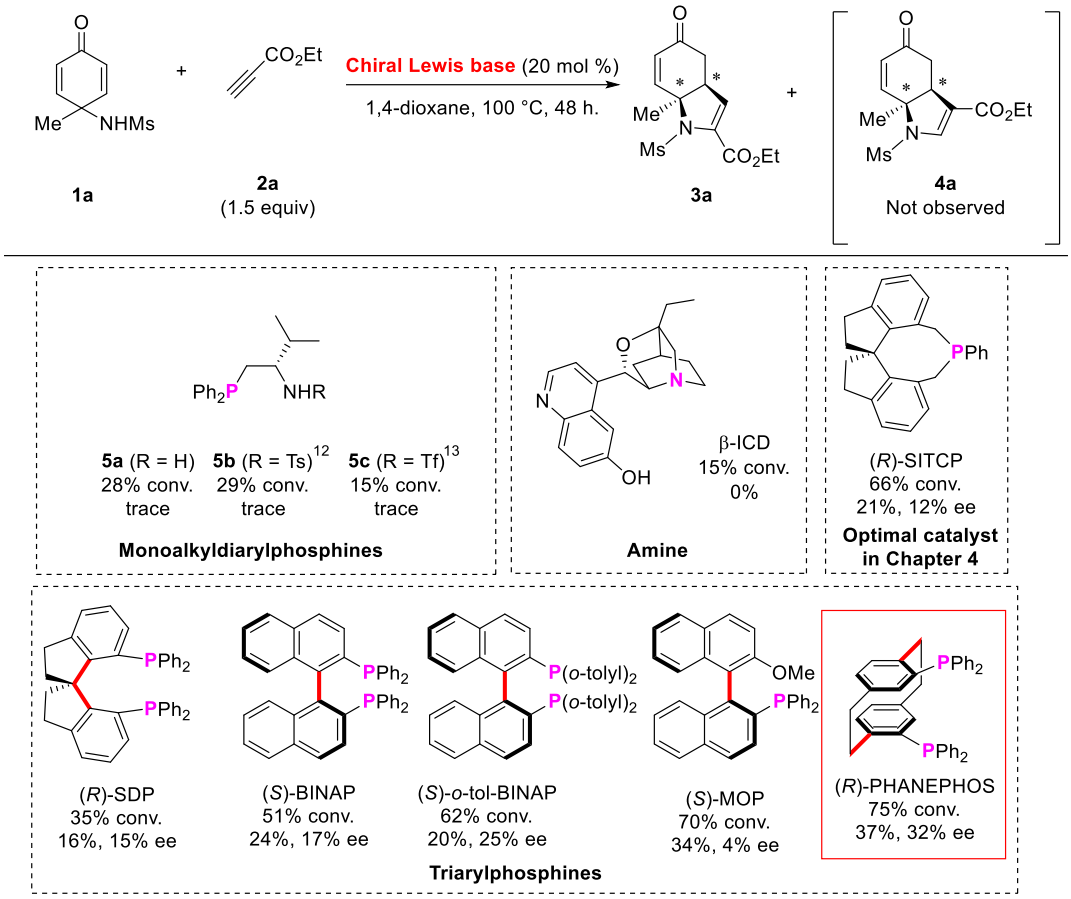

To clarify this hypothesis, when tri(*o*-tolyl)phosphine and 5-phenyl-5*H*-benzo[*b*]phosphindole, which have a methyl group in the ortho position of the aromatic ring connected to the phosphine center, were employed, the reaction hardly proceeded at all (Scheme 5.8). On the other hand, tri(*m*-tolyl)phosphine promoted a smooth reaction. Therefore, a chiral triarylphosphine catalyst that has a chiral component at the meta position of the aromatic ring connected to the phosphine center needs to be designed and prepared.

Scheme 5.8. The effect on the steric environment of triarylphosphines

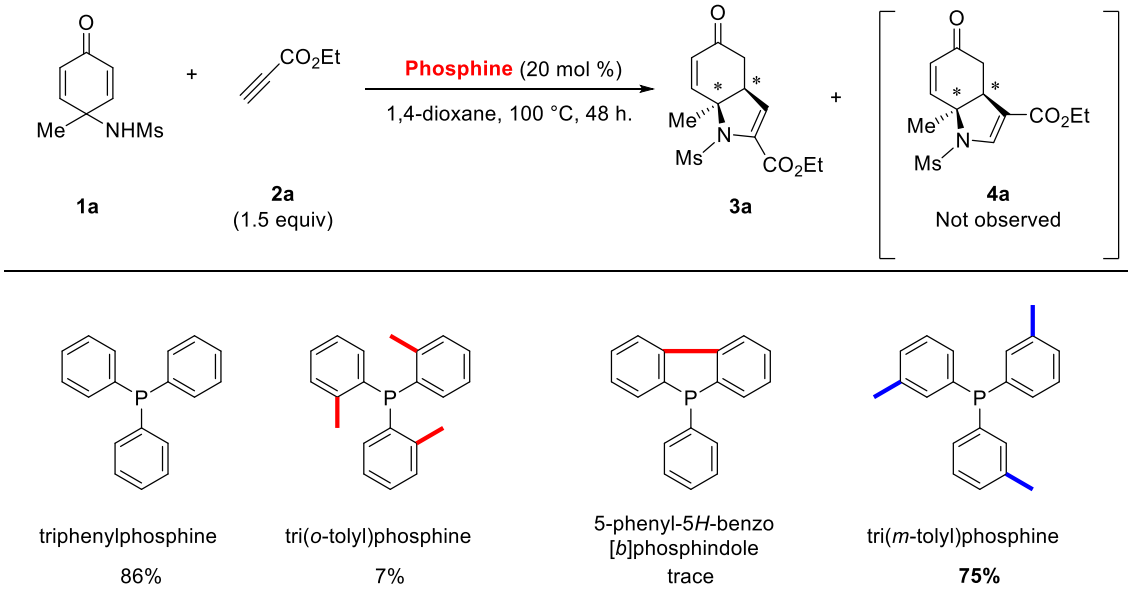

As illustrated in substrate scope (Scheme 5.5), oxygen analog has higher reactivity than that of nitrogen analog in this reaction. When **1j** was reacted with (*R*)-PHANEPHOS, the reaction proceeded smoothly even at 20 °C to form **3j** in 71% yield. However, enantioselectivity was still unsatisfactory (45% ee). Whereas, in dichloromethane at –20 °C, ee was increased to 84% despite low yield due to side reactions (Scheme 5.9).

Scheme 5.9. Enantioselective reaction of **1j** with (*R*)-PHANEPHOS

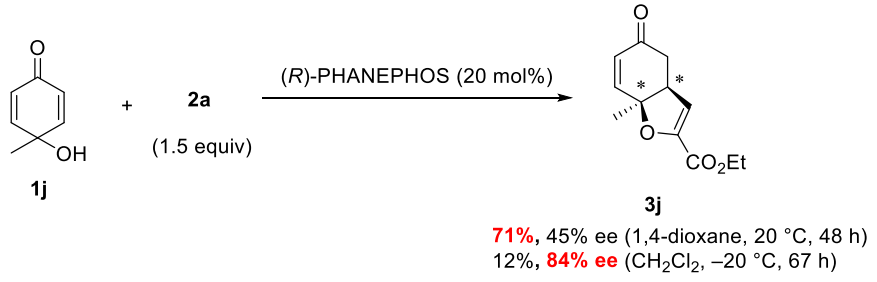

5.2.4. Mechanistic Studies

To clarify the mechanism of the dual umpolung domino Michael reaction, the experiments summarized in Scheme 5.10 were carried out. When the Me-capped substrate **1y** was treated under the optimal reaction conditions, intact **1y** was recovered quantitatively (Eq. 1). This result indicates the importance of generating nucleophiles *in situ* for initiating the α-addition to alkynoate **2a**. Performing the reaction between **1a** and **2a** in the presence of D_2O (5.0 equiv) led to the formation of the partially deuterated product **3a**, where the D content was 85% at position β and 75% at position δ (Eq. 2). This evidence indicates that, along the reaction pathway, anionic species were formed, whereby the charge was localized on the β- and δ-carbon. Moreover, a variety of nucleophilic species *in situ* would not perform a Michael addition to enone moiety of cyclohexadienone **1**, since deuterium is not incorporated at the δ′-position of **3a** (Eq. 2).

Scheme 5.10. The Results of Mechanistic studies

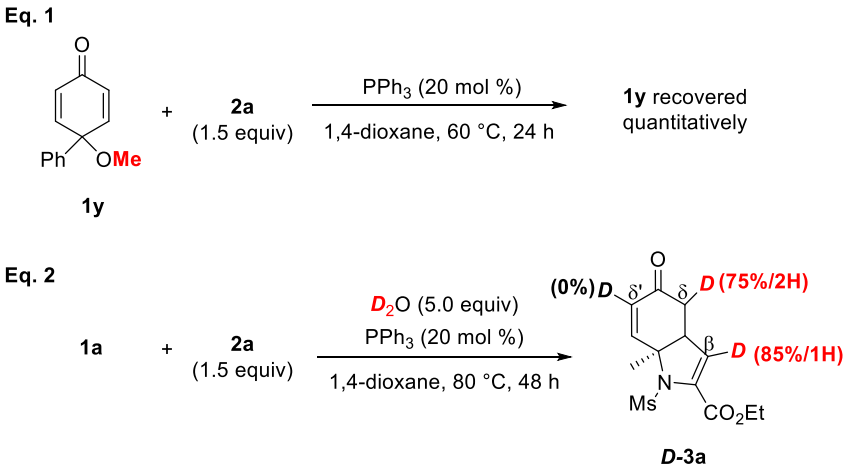

Based on these experimental results, a plausible reaction mechanism was proposed, which is depicted in Scheme 5.11. Initially, a Michael addition of PPh_3 to alkynoate **2a** takes place, which generates the phosphonium intermediate **A** (**Int. A**). **Int. A** acts then as a Brønsted base to abstract the acidic proton of **1a**. Then, the deprotonated **1a** (**Int. B**) undergoes umpolung Michael addition at the α-position induced by the electron-withdrawing ability of the phosphonium moiety of intermediate C (**Int. C**). Taking into account the reactivity of the sulfonyl amine (**1a**: X = NR, at 100°C for 48 h) and of the alcohol (**1j**: X = O, at 60°C for 3 h), this α-addition would be the rate-controlling step of the entire reaction course. In any event, a second Michael addition of the β-anion generated (**Int. D**) takes place subsequently, followed by elimination of PPh_3 via proton transfer in intermediate E (**Int. E**), leading to the formation of product **3a** and the regeneration of PPh_3.

Scheme 5.11. Proposed reaction mechanism

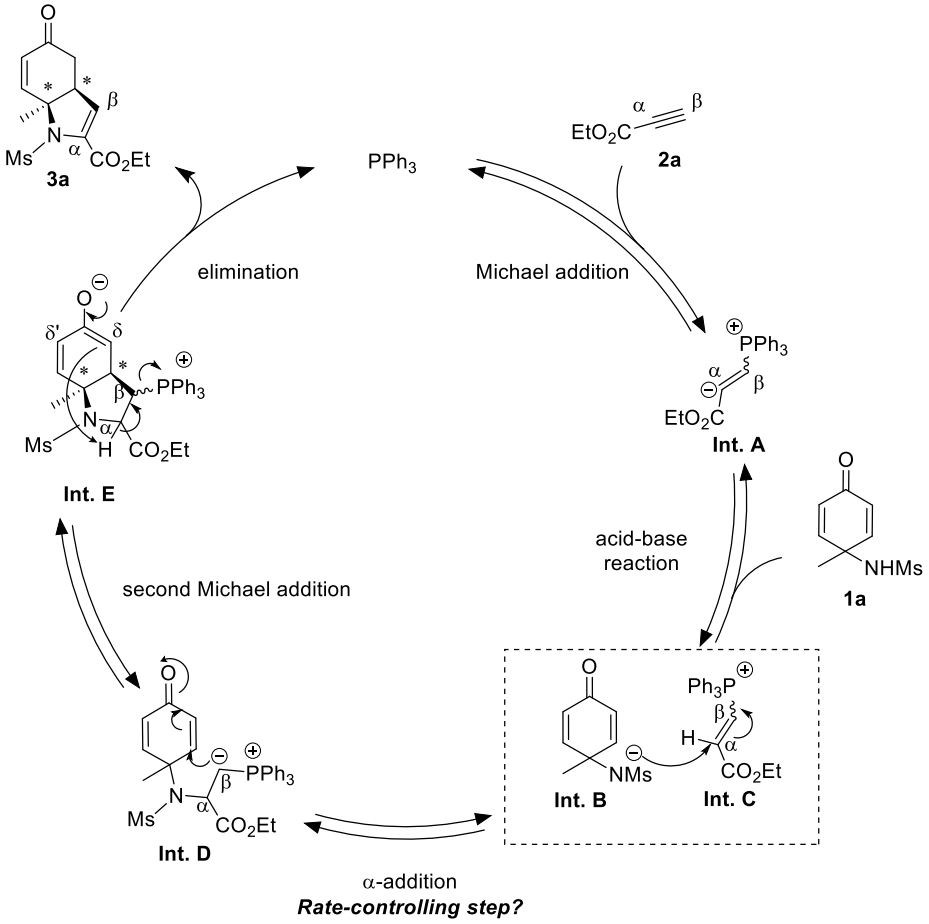

5.2.5. Synthetic Transformations and Synthesis of An Analog of PEP inhibitor

To demonstrate the utility of the obtained product, synthetic transformations of **3d** were investigated (Scheme 5.12). Luche-reduction of **3d** proceeded smoothly to give alcohol **7** in quantitative yield with good diastereoselectivity, which was determined by NOESY. Toward synthesis of PEP inhibitor analog **6**, hydrogenation of **3d** with Ir complex under H_2 atmosphere produced saturated **8** in 77% yield as a single diastereomer, which was determined by X-ray crystallography. A carbonyl group in ketone **8** could be reduced by sequential process via 1,2-reduction, elimination,[18] and catalytic hydrogenation. Reductive detosylation of obtained **9** was succeeded by using magnesium in methanol. Finally, detosylated **10** was converted to PEP inhibitor analog **6**[1b] through hydrolysis, Boc-protection, and amidation in three steps.

Scheme 5.12. Synthetic transformations and synthesis of an analog of PEP inhibitor **6**

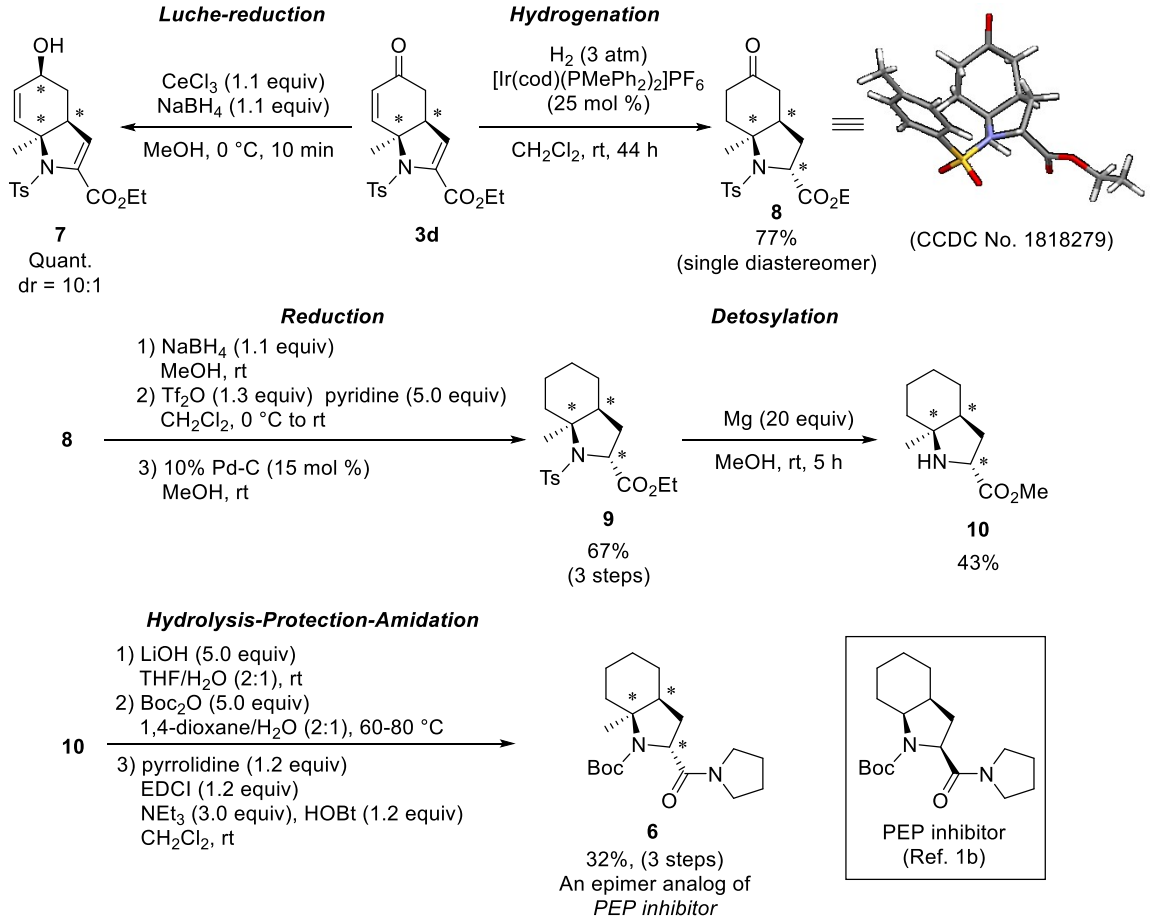

5.3. Conclusion

In summary, the author has developed a novel synthetic route for the pharmaceutically important hydroindole- and hydrobenzofuran-2-carboxylates via a newly developed phosphine-catalyzed dual umpolung domino Michael reaction. One of the obtained products could be used for a variety of synthetic transformations affording an analog of a PEP inhibitor.

5.4. Experimental Section

5.4.1. General

^{1}H-, ^{13}C-, and ^{19}F-NMR spectra were recorded with a JEOL JMN ECS400 FT NMR, JNM ECA600 FT NMR or Bruker AVANCE II (^{1}H-NMR 400, 600 or 700 MHz, ^{13}C-NMR 100, 150 or 176 MHz, ^{19}F-NMR 565 MHz. ^{1}H-NMR spectra are reported as follows: chemical shift in ppm relative to the chemical shift of $CHCl_3$ at 7.26 ppm, integration, multiplicities (s = singlet, d = doublet, t = triplet, q = quartet, m = multiplet), and coupling constants (Hz). ^{13}C-NMR spectra reported in ppm relative to the central line of triplet for $CDCl_3$ at 77 ppm. CF_3CO_2H used as external standards for ^{19}F-NMR. FT-MS spectra were obtained with LTQ Orbitrap XL (Thermo Fisher Scientific). High resolution-MS spectra were obtained with JMS-T100LC (JEOL). HPLC analyses were performed on a JASCO HPLC system (JASCO PU 980 pump and UV-975 UV/Vis detector) using a mixture of *n*-hexane/2-propanol as eluents. Column chromatography on SiO_2 was performed with Kanto Silica Gel 60 (40-100 μm).

5.4.2. Materials

1,4-dioxane was purified by atmospheric distillation from MS4A. MeOH was dried by MS3A. Dehydrated THF, CH_2Cl_2, and other commercially available organic and inorganic compounds were purchased and used without further purification. Starting materials **1a-1b**,[11c] **1d**,[11b] **1e**,[11c] **1j-l**,[12e] **1m**,[19] **1n**,[21] **1o**,[12e] **1p**,[21] **1q**,[22] **1r**,[12e] **1s**,[23] **1t**,[12e] **1u**,[23] **1v**,[19] **1w**,[24] **1x**,[25] and **1y**[26] were synthesized according to reported procedures.

5.4.3. Synthesis of Imine S2g

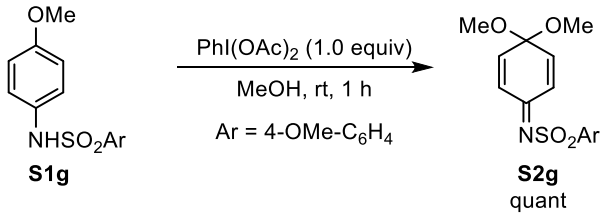

To a solution of **S1g**[27] (1.0 mmol) in MeOH (5.0 mL) was added $PhI(OAc)_2$ (1.0 mmol) at 0 °C and stirred at rt for 1 h. Reaction was quenched by sat. NaHCO aq. and extracted with EtOAc. Organic layer was washed with brine and dried over Na_2SO_4. Concentrated crude product was purified by silica-gel column chromatography using *n*-hexane/EtOAc mixed solvent as an eluent giving pure product **S2g** as a white solid. ^{1}H-NMR (400 MHz, $CDCl_3$) δ 7.91 (d, J = 9.2 Hz, 2H), 7.62 (dd, J = 10.5, 2.5 Hz, 1H), 6.99 (d, J = 9.2 Hz, 2H), 6.76 (dd, J = 10.5, 2.5 Hz, 1H), 6.70 (dd, J = 10.5, 2.5 Hz, 1H), 6.34 (dd, J = 10.5, 2.5 Hz, 1H), 3.86 (s,

3H), 3.34 (s, 6H); ^{13}C-NMR (100 MHz, $CDCl_3$) δ 163.28, 162.74, 143.20, 141.90, 132.20, 130.68, 129.47, 123.15, 114.11, 92.06, 55.61, 50.31; HRMS (ESI) calcd for $C_{15}H_{17}NO_5SNa$ m/z = 346.0720, found m/z = 346.0723[$(M+Na)^+$].

5.4.4. Synthesis of Cyclohexadienones 1

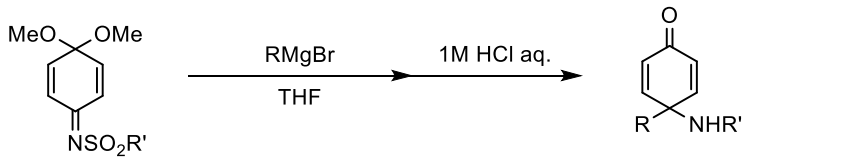

S2

1c (R = 4-tolyl, R' = Ms)
1f (R = HC≡C, R' = Ts)
1g (R = Me, R' = SO_2-4-OMe-C_6H_4)

To a solution of **S2**[11a] (1.0 mmol) in THF (2.0 mL) was added Grignard reagent (2.0 mmol in THF 4.0 mL) at –78 °C and stirred under indicated conditions (**1c**: at –78 °C for 30 min; **1f**: at rt for 28 h; **1g**: at –78 °C for 20 min). Then, 1M HCl aq. (5.0 mL) was added and stirred at rt for indicated reaction period (**1c**: for 3 h; **1h**: for 19 h; **1g**: for 3 h). Then, THF was removed under reduced pressure. Crude product was extracred with EtOAc and organic layer was dried over Na_2SO_4. Concentrated residue was purified by silica-gel column chromatography using *n*-hexane/EtOAc mixed solvent as an eluent giving pure product **1** as a white solid.

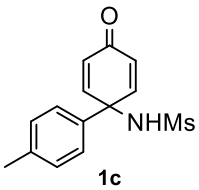

1c

1c: 40%; white solid; ^{1}H-NMR (400 MHz, $CDCl_3$) δ 7.38 (d, *J* = 8.0 Hz, 2H), 7.22 (d, *J* = 8.0 Hz, 2H), 7.10 (d, *J* = 10.1 Hz, 2H), 6.38 (d, *J* = 10.1 Hz, 2H), 5.07 (s, 1H), 3.01 (s, 3H), 2.36 (s, 3H); ^{13}C-NMR (100 MHz, $CDCl_3$) δ 184.73, 148.92, 139.44, 134.46, 130.16, 128.15, 125.70, 59.66, 43.13, 21.03; HRMS (ESI) calcd for $C_{14}H_{15}NO_3SNa$ m/z = 300.0665, found m/z = 300.0667 [$(M+Na)^+$].

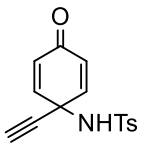

1f

1f: 55%; white solid; ^{1}H-NMR (400 MHz, $CDCl_3$) δ 7.73 (d, *J* = 8.2 Hz, 2H), 7.29 (d, *J* = 8.2 Hz, 2H), 6.75 (d, *J* = 10.1 Hz, 2H), 6.15 (d, *J* = 10.1 Hz, 2H), 5.30 (s, 1H), 2.49 (s, 1H), 2.44 (s, 3H); ^{13}C-NMR (100 MHz, $CDCl_3$) δ 183.74, 144.73, 144.52, 137.53, 129.73, 128.41, 127.88, 77.10, 75.20, 50.44, 21.70; HRMS (ESI) calcd for $C_{15}H_{13}NO_3SNa$ m/z = 310.0508, found m/z = 310.0510 [$(M+Na)^+$].

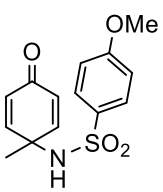

1g

1g: 73%; white solid; ^{1}H-NMR (400 MHz, $CDCl_3$) δ 7.71 (d, *J* = 9.0 Hz, 2H), 6.93 (d, *J* = 9.0 Hz, 2H), 6.66 (d, *J* = 10.1 Hz, 2H), 6.04 (d, *J* = 10.1 Hz, 2H), 5.47 (s, 1H), 3.86 (s, 3H), 1.43 (s, 3H); ^{13}C-NMR (100 MHz, $CDCl_3$)δ 184.57, 163.10, 150.74, 131.72, 129.96, 128.03, 114.17, 55.68, 54.36, 27.73; HRMS (ESI) calcd for $C_{14}H_{15}NO_4SNa$ m/z = 316.0614, found m/z = 316.0615 [$(M+Na)^+$].

5.4.5. General Procedure for the Dual Umpolung Domino Michael Reaction

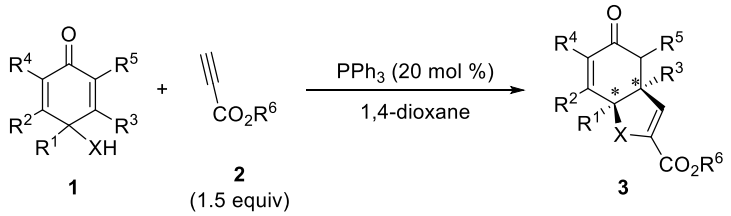

To a solution of **1** (0.10 mmol) and PPh_3 (0.020 mmol) in 1,4-dioxane (0.50 mL) was added alkynoate **2** at indicated temperature. After **1** was consumed (monitored by TLC), the solution was cooled to room temperature and quenched by short silica-gel column. After evaporation, crude product was purified by silica-gel column chromatography using *n*-hexane/EtOAc mixed solvent as an eluent giving pure product **3**.

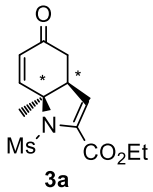

3a

3a: 86% (100 °C, 48 h); yellow solid; ^{1}H-NMR (400 MHz, $CDCl_3$) δ 7.09 (d, *J* = 10.5 Hz, 1H), 6.08 (d, *J* = 10.5 Hz, 1H), 5.76 (d, *J* = 2.1 Hz, 1H), 4.27 (q, *J* = 7.2 Hz, 2H), 3.39 (s, 3H), 3.17 (td, *J* = 6.0, 2.1 Hz, 1H), 2.57 (ddd, *J* = 26.6, 16.5, 6.0 Hz, 2H), 1.82 (s, 3H), 1.32 (t, *J* = 7.2 Hz, 3H); ^{13}C-NMR (100 MHz, $CDCl_3$) δ 195.66, 161.42, 145.82, 136.62, 129.09, 119.42, 69.73, 61.98, 48.27, 45.02, 37.50, 24.72, 13.96; HRMS (ESI) calcd for $C_{13}H_{17}NO_5SNa$ m/z = 322.0720, found m/z = 322.0718 [$(M+Na)^+$]. Enantiomeric excess: 32% determined by HPLC (Daicel Chiralpak IC, *n*-hexane/2-propanol = 7/3; flow rate 1.0 ml/min; 25°C; 215 nm) first peak (Major): t_R = 24.0 min, second peak (Minor): t_R = 26.9 min.

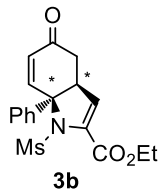

3b

3b: 60% (100 °C, 48 h); yellow oil; ^{1}H-NMR (400 MHz, $CDCl_3$) δ 7.36-7.53 (m, 6H), 6.40 (d, *J* = 10.5 Hz, 1H), 5.79 (d, *J* = 2.7 Hz, 1H), 4.31 (qd, *J* = 7.2, 2.3 Hz, 2H), 3.46 (m, 1H), 3.36 (s, 3H), 2.43-2.53 (m, 2H), 1.35 (t, *J* = 7.2 Hz, 3H); ^{13}C-NMR (100 MHz, $CDCl_3$) δ 195.74, 161.35, 143.45, 140.77, 136.94, 131.30, 128.99, 128.58, 125.73, 119.13, 75.36, 62.07, 51.73, 44.90, 36.35, 13.99; HRMS (ESI) calcd for $C_{18}H_{19}NO_5SNa$ m/z = 384.0876, found m/z = 384.0878 [$(M+Na)^+$].

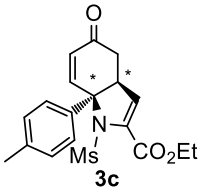

3c

3c: 56% (100 °C, 48 h); yellow solid; ^{1}H-NMR (400 MHz, $CDCl_3$) δ 7.37-7.41 (m, 3H), 7.25 (d, *J* = 8.2 Hz, 2H), 6.38 (d, *J* = 10.5 Hz, 1H), 5.77 (d, *J* = 2.3 Hz, 1H), 4.27-4.35 (m, 2H), 3.43-3.46 (m, 1H), 3.35 (s, 3H), 2.42-2.56 (m, 2H), 2.38 (s, 3H), 1.35 (t, *J* = 7.1 Hz, 3H); ^{13}C-NMR (100 MHz, $CDCl_3$) δ 195.82, 161.41, 143.68, 138.50, 137.70, 136.92, 131.19, 129.69, 125.68, 119.03, 75.29, 62.05, 51.76, 44.88, 36.34, 21.10, 14.00; HRMS (ESI) calcd for $C_{19}H_{21}NO_5SNa$ m/z = 398.1033, found m/z = 398.1033 [$(M+Na)^+$].

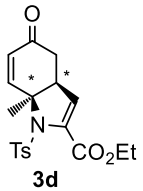

3d

3d: 57% (100 °C, 48 h); yellow solid; ^{1}H-NMR (400 MHz, $CDCl_3$) δ 7.78 (d, *J* = 8.2 Hz, 2H), 7.28 (d, *J* = 8.2 Hz, 2H), 6.90 (d, *J* = 10.5 Hz, 1H), 5.99 (d, *J* = 10.5 Hz, 1H), 5.91 (d, *J* = 3.2 Hz, 1H), 4.32 (q, *J* = 7.2 Hz, 2H), 2.89-2.93 (m, 1H), 2.41 (s, 3H), 2.32 (dd, *J* = 16.5, 6.0 Hz, 1H), 1.69 (q, *J* = 16.5 Hz, 1H), 1.62 (s, 3H), 1.35 (t, *J* = 7.2 Hz, 3H); ^{13}C-NMR (100 MHz, $CDCl_3$) δ 195.67, 162.24, 145.63, 144.36, 137.01, 136.89, 129.47, 129.21, 127.77, 123.33, 67.64, 61.99, 47.60, 37.80, 26.00, 21.59, 14.01; HRMS (ESI) calcd for $C_{19}H_{21}NO_5SNa$ m/z = 398.1033, found m/z = 398.1034 [$(M+Na)^+$].

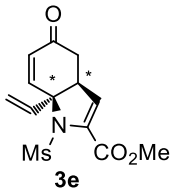

3e

3e: 54% (100 °C, 48 h); yellow solid; ^{1}H-NMR (400 MHz, $CDCl_3$) δ 7.79 (d, *J* = 8.2 Hz, 2H), 7.28 (d, *J* = 8.2 Hz, 2H), 6.79 (d, *J* = 10.3 Hz, 1H), 6.10 (d, *J* = 10.3 Hz, 1H), 5.97 (dd, *J* = 16.9, 10.5 Hz, 1H), 5.88 (d, *J* = 2.7 Hz, 1H), 5.46 (d, *J* = 16.9 Hz, 1H), 5.34 (d, *J* = 10.5 Hz, 1H), 4.31 (q, *J* = 7.2 Hz, 2H), 3.11-3.15 (m, 1H), 2.41 (s, 3H), 2.35 (dd, *J* = 16.5, 5.5 Hz, 1H), 1.85 (q, *J* = 8.1 Hz, 1H), 1.35 (t, *J* = 7.2 Hz, 3H)); ^{13}C-NMR (100 MHz, $CDCl_3$) δ 195.58, 161.87, 144.38, 142.75, 137.24, 136.86, 136.38, 130.40, 129.37, 127.94, 123.01, 117.88, 71.37, 61.96, 46.61, 37.02, 21.60, 13.98; HRMS (ESI) calcd for $C_{20}H_{21}NO_5SNa$ m/z = 410.1033, found m/z = 410.1036 [$(M+Na)^+$].

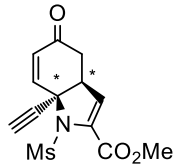

3f

3f: 77% (100 °C, 5 min); yellow solid; ^{1}H-NMR (400 MHz, $CDCl_3$) δ 7.92 (d, *J* = 7.8 Hz, 2H), 7.31 (d, *J* = 7.8 Hz, 2H), 6.76 (d, *J* = 10.3 Hz, 1H), 6.07 (d, *J* = 10.3 Hz, 1H), 5.91 (d, *J* = 1.8 Hz, 1H), 4.24-4.32 (m, 2H), 3.49 (s, 1H), 2.81 (s, 1H), 2.72 (dd, *J* = 16.9, 6.0 Hz, 1H), 2.41-2.47 (m, 4H), 1.32 (t, *J* = 7.2 Hz, 3H); ^{13}C-NMR (100 MHz, $CDCl_3$) δ 194.42, 161.17, 144.43, 142.50, 136.83, 136.69, 129.33, 129.00, 128.32, 124.10, 79.34, 77.31, 63.28, 61.99, 49.10, 36.11, 21.65, 13.96; HRMS (ESI) calcd for $C_{20}H_{19}NO_5SNa$ m/z =408.0876, found m/z = 408.0878 [$(M+Na)^+$].

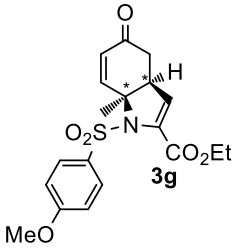

3g

3g: 63% (100 °C, 48 h); yellow solid; ^{1}H-NMR (400 MHz, $CDCl_3$) δ 7.82 (d, *J* = 9.2 Hz, 2H), 6.93 (d, *J* = 9.2 Hz, 2H), 6.89 (d, *J* = 10.3 Hz, 1H), 5.99 (d, *J* = 10.3 Hz, 1H), 5.91 (d, *J* = 2.7 Hz, 1H), 4.32 (q, *J* = 7.2 Hz, 2H), 3.84 (s, 3H), 2.88-2.93 (m, 1H), 2.32 (dd, *J* = 16.5, 6.0 Hz, 1H), 1.67 (q, *J* = 8.5 Hz, 1H), 1.60 (s, 3H), 1.35 (t, *J* = 7.2 Hz, 3H); ^{13}C-NMR (100 MHz, $CDCl_3$) δ 195.72, 163.31, 162.32, 145.69, 137.01, 131.17, 129.97, 129.15, 123.54, 113.96, 67.42, 61.96, 55.63, 47.51, 37.78, 26.10, 14.01; HRMS (ESI) calcd for $C_{19}H_{21}NO_6SNa$ m/z = 414.0982, found m/z = 414.0980 [$(M+Na)^+$].

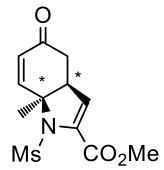

3h

3h: 70% (100 °C, 48 h); yellow solid; ^{1}H-NMR (400 MHz, $CDCl_3$) δ 7.08 (d, *J* = 10.5 Hz, 1H), 6.08 (d, *J* = 10.5 Hz, 1H), 5.79 (d, *J* = 2.7 Hz, 1H), 3.82 (s, 3H), 3.39 (s, 3H), 3.18 (td, *J* = 6.0, 2.7 Hz, 1H), 2.56 (ddd, *J* = 27.9, 16.5, 6.0 Hz, 2H), 1.81 (s, 3H); ^{13}C-NMR (100 MHz, $CDCl_3$) δ 195.52, 161.84, 145.75, 136.31, 129.10, 119.90, 69.73, 52.71, 48.30, 44.96, 37.49, 24.76; HRMS (ESI) calcd for $C_{12}H_{15}NO_5SNa$ m/z = 308.0563, found m/z = 308.0564 [$(M+Na)^+$].

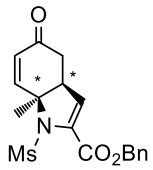

3i

3i: 89% (100 °C, 5 min); yellow solid; ^{1}H-NMR (400 MHz, $CDCl_3$) δ 7.33-7.38 (m, 5H), 7.08 (d, *J* = 10.5 Hz, 1H), 6.07 (d, *J* = 10.5 Hz, 1H), 5.80 (d, *J* = 2.7 Hz, 1H), 5.23 (dd, *J* = 25.6, 11.9 Hz, 2H), 3.35 (s, 3H), 3.16 (td, *J* = 6.0, 2.7 Hz, 1H), 2.55 (ddd, *J* = 26.1, 16.7, 6.0 Hz, 2H), 1.81 (s, 3H); ^{13}C-NMR (100 MHz, $CDCl_3$) δ 195.52, 161.13, 145.76, 136.33, 134.76, 129.10, 128.65, 128.50, 120.15, 69.77, 67.62, 48.27, 45.02, 37.40, 24.72 (One peak overlapped); HRMS (ESI) calcd for $C_{18}H_{19}NO_5SNa$ m/z = 384.0876, found m/z = 384.0877 [$(M+Na)^+$].

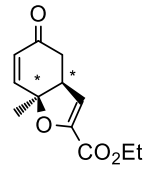

3j

3j: 80% (60 °C, 3 h); yellow solid; ^{1}H-NMR (400 MHz, $CDCl_3$) δ 6.49 (d, *J* = 10.5 Hz, 1H), 6.06 (d, *J* = 10.5 Hz, 1H), 5.84 (d, *J* = 2.3 Hz, 1H), 4.24 (q, *J* = 7.2 Hz, 2H), 3.46-3.49 (m, 1H), 2.61 (d, *J* = 5.0 Hz, 2H), 1.70 (s, 3H), 1.29 (t, *J* = 7.2 Hz, 3H); ^{13}C-NMR (100 MHz, $CDCl_3$) δ 196.39, 160.09, 146.14, 145.58, 129.31, 114.91, 84.36, 61.41, 47.38, 37.11, 24.38, 14.11; HRMS (ESI) calcd for $C_{12}H_{14}O_4Na$ m/z = 245.0784, found m/z = 245.0875 [$(M+Na)^+$]. Enantiomeric excess: 84% determined by HPLC (Daicel Chiralpak IC-3, *n*-hexane/2-propanol = 4/1; flow rate 1.0 ml/min; 25°C; 215 nm) first peak (Major): t_R = 25.4 min, second peak (Minor): t_R = 27.5 min.

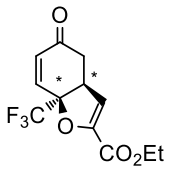

3k

3k: 64% (60 °C, 3 h); yellow solid; ^{1}H-NMR (600 MHz, $CDCl_3$) δ 6.60 (d, *J* = 10.3 Hz, 1H), 6.37 (d, *J* = 10.3 Hz, 1H), 5.91 (d, J = 2.1 Hz, 1H), 4.27 (q, *J* = 7.1 Hz, 2H), 4.03-4.05 (m, 1H), 2.66-2.77 (m, 2H), 1.31 (t, *J* = 7.1 Hz, 3H); ^{13}C-NMR (150 MHz, $CDCl_3$) δ 194.60, 158.66, 145.72, 134.97, 134.20, 123.58 (q, *J* = 280.0 Hz) 114.35, 82.90 (q, *J* = 31.6 Hz), 61.87, 41.91, 36.73, 14.07; ^{19}F-NMR (565 MHz, $CDCl_3$) δ -79.13 (s); HRMS (ESI) calcd for $C_{12}H_{11}F_3O_4Na$ m/z = 299.0502, found m/z =299.0502 [$(M+Na)^+$].

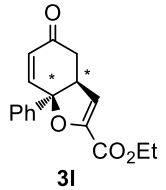

3l

3l: 70% (60 °C, 3 h); yellow oil; ^{1}H-NMR (400 MHz, $CDCl_3$) δ 7.35-7.51 (m, 5H), 6.63 (dd, *J* = 10.1, 0.9 Hz, 1H), 6.28-6.30 (dd, *J* = 10.1, 0.9 Hz, 1H), 5.93 (d, *J* = 2.3 Hz, 1H), 4.29 (q, *J* = 7.2 Hz, 2H), 3.71-3.74 (m, 1H), 2.63-2.76 (m, 2H), 1.33 (t, *J* = 7.2 Hz, 3H); ^{13}C-NMR (100 MHz, $CDCl_3$) δ 196.47, 159.78, 146.03, 143.64, 140.28, 130.18, 128.92, 128.66, 124.96, 114.87, 87.57, 61.53, 49.77, 36.69, 14.16; HRMS (ESI) calcd for $C_{17}H_{16}O_4Na$ m/z = 307.0941, found m/z = 307.0942 [$(M+Na)^+$].

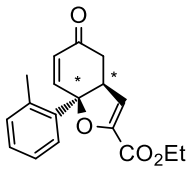

3m

3m: 45% (60 °C, 24 h); yellow oil; ^{1}H-NMR (400 MHz, $CDCl_3$) δ 7.16-7.29 (m, 4H), 6.73 (d, *J* = 11.0 Hz,1H), 6.32 (d, *J* = 11.0 Hz, 1H), 6.02 (d, *J* = 2.5 Hz, 1H), 4.24-4.32 (m, 2H), 3.86 (dd, *J* = 3.4, 2.5 Hz, 1H), 2.54-2.64 (m, 2H), 2.48 (s, 3H), 1.33 (t, *J* = 7.1 Hz, 3H); ^{13}C-NMR (100 MHz, $CDCl_3$) δ 196.89, 159.82, 145.51, 143.59, 137.14, 136.98, 133.03, 129.70, 129.02, 126.64, 125.81, 115.18, 89.06, 61.53, 48.30, 36.35, 20.80, 14.12; HRMS (ESI) calcd for $C_{18}H_{18}O_4Na$ m/z = 321.1097, found m/z = 321.1098 [$(M+Na)^+$].

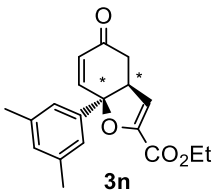

3n

3n: 73% (60 °C, 3 h); yellow oil; ^{1}H-NMR (400 MHz, $CDCl_3$) δ 7.08 (s, 2H), 7.00 (s, 1H), 6.60 (d, *J* = 11.0 Hz, 1H), 6.27 (d, *J* = 11.0 Hz, 1H), 5.92 (d, *J* = 2.7 Hz, 1H), 4.30 (q, *J* = 7.0 Hz, 2H), 3.72 (t, *J* = 2.7 Hz, 1H), 2.63-2.77 (m, 2H), 2.33 (s, 6H), 1.33 (t, *J* = 7.0 Hz, 3H); ^{13}C-NMR (100 MHz, $CDCl_3$) δ 196.62, 160.07, 146.04, 143.95, 140.19, 138.62, 130.25, 129.93, 122.61, 114.91, 87.64, 61.47, 49.68, 36.75, 21.38, 14.16; HRMS (ESI) calcd for $C_{19}H_{20}NO_4Na$ m/z = 335.1254, found m/z = 335.1252 [$(M+Na)^+$].

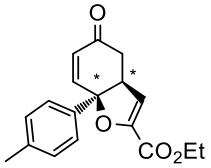

3o

3o: 62% (60 °C, 3 h); yellow oil; ^{1}H-NMR (400 MHz, $CDCl_3$) δ 7.38 (d, *J* = 8.2 Hz, 2H), 7.22 (d, *J* = 8.2 Hz, 2H), 6.62 (d, *J* = 11.0 Hz, 1H), 6.27 (d, *J* = 11.0 Hz, 1H), 5.92 (d, *J* = 2.7 Hz, 1H), 4.29 (q, *J* = 7.2 Hz, 2H), 3.69-3.73 (m, 1H), 2.63-2.75 (m, 2H), 2.37 (s, 3H), 1.33 (t, *J* = 7.2 Hz, 3H); ^{13}C-NMR (100 MHz, $CDCl_3$) δ 196.53, 159.84, 146.08, 143.90, 138.56, 137.34, 130.00, 129.56, 124.91, 114.88, 87.58, 61.49, 49.77, 36.74, 21.11, 14.15; HRMS (ESI) calcd for $C_{18}H_{18}O_4Na$ m/z = 321.1097, found m/z = 321.1092 [$(M+Na)^+$].

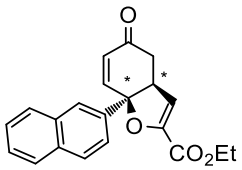

3p

3p: 51% (60 °C, 3 h); colorless oil; ^{1}H-NMR (400 MHz, $CDCl_3$) δ 7.91-7.93 (m, 2H), 7.86 (q, *J* = 3.1 Hz, 2H), 7.62 (dd, *J* = 8.7, 1.8 Hz, 1H), 7.53 (td, *J* = 6.6, 3.1 Hz, 2H), 6.74 (d, *J* = 10.1 Hz, 1H), 6.37 (d, *J* = 10.1 Hz, 1H), 5.97 (d, *J* = 2.7 Hz, 1H), 4.33 (q, *J* = 7.2 Hz, 2H), 3.80-3.83 (m, 1H), 2.67-2.81 (m, 2H), 1.36 (t, *J* = 7.2 Hz, 3H); ^{13}C-NMR (100 MHz, $CDCl_3$) δ 196.47, 159.85, 146.17, 143.61, 137.54, 133.19, 132.99, 130.43, 129.10, 128.21, 127.74, 126.73, 126.71, 124.16, 122.59, 114.95, 87.78, 61.59, 49.80, 36.78, 14.19; HRMS (ESI) calcd for $C_{21}H_{18}O_4Na$ m/z = 357.1097, found m/z = 357.1099 [$(M+Na)^+$].

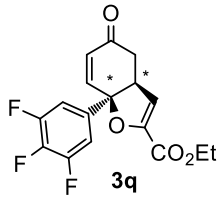

3q

3q: 60% (60 °C, 3 h); colorless oil; ^{1}H-NMR (400 MHz, $CDCl_3$) δ 7.14 (dt, *J* = 13.7, 5.7 Hz, 2H), 6.53 (d, *J* = 10.1 Hz, 1H), 6.32 (d, *J* = 10.1 Hz, 1H), 5.92 (d, *J* = 2.7 Hz, 1H), 4.30 (q, *J* = 7.0 Hz, 2H), 3.64-3.67 (m, 1H), 2.69 (d, *J* = 4.6 Hz, 2H), 1.34 (t, *J* = 7.0 Hz, 3H); ^{13}C-NMR (150 MHz, $CDCl_3$) δ 195.35, 159.34, 151.51 (dd, *J* = 254.2, 10.1 Hz) 145.97, 141.83, 139.71 (d, *J* = 254.2 Hz), 136.85, 131.12, 114.69, 109.66 (d, *J* = 17.3, 4.4 Hz), 86.23, 61.74, 49.74, 36.50, 14.11; ^{19}F-NMR (565 MHz, $CDCl_3$) δ –131.63 (s), –159.17 (s); HRMS (ESI) calcd for $C_{17}H_{13}F_3O_4Na$ m/z = 361.0658, found m/z = 361.0658 [$(M+Na)^+$].

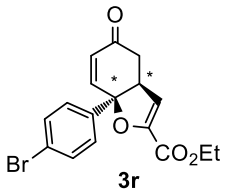

3r

3r: 50% (60 °C, 3 h); yellow oil; ^{1}H-NMR (400 MHz, $CDCl_3$) δ 7.55 (dt, *J* = 9.0, 2.1 Hz, 2H), 7.37 (dt, *J* = 9.0, 2.1 Hz, 2H), 6.58 (d, *J* = 10.5 Hz, 1H), 6.30 (d, *J* = 10.5 Hz, 1H), 5.92 (d, *J* = 2.3 Hz, 1H), 4.29 (q, *J* = 7.2 Hz, 2H), 3.66-3.69 (m, 1H), 2.63-2.73 (m, 2H), 1.33 (t, *J* = 7.2 Hz, 3H); ^{13}C-NMR (100 MHz, $CDCl_3$) δ 196.00, 159.62, 146.03, 142.96, 139.43, 132.09, 130.51, 126.73, 122.84, 114.79, 87.10, 61.61, 49.75, 36.60, 14.14; HRMS (ESI) calcd for $C_{17}H_{15}BrO_4Na$ m/z = 385.0046, found m/z = 385.0038 [$(M+Na)^+$].

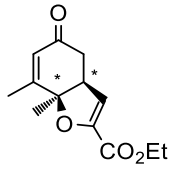

3u

3u: 40% (100 °C, 36 h); yellow oil; ^{1}H-NMR (400 MHz, $CDCl_3$) δ 5.97 (d, *J* = 1.4 Hz, 1H), 5.84 (d, *J* = 2.3 Hz, 1H), 4.18-4.28 (m, 2H), 3.47-3.50 (m, 1H), 2.54-2.64 (m, 2H), 2.03 (d, *J* = 1.4 Hz, 3H), 1.72 (s, 3H), 1.29 (t, *J* = 7.1 Hz, 3H); ^{13}C-NMR (100 MHz, $CDCl_3$) δ 195.80, 159.84, 156.78, 146.51, 128.53, 115.36, 86.60, 61.32, 48.14, 36.85, 23.18, 18.53, 14.11; HRMS (ESI) calcd for $C_{13}H_{16}O_4Na$ m/z = 259.0941, found m/z = 259.0942 [$(M+Na)^+$].

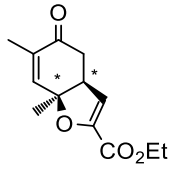

3v

3v: 62% (60 °C, 13 h); yellow oil; ^{1}H-NMR (400 MHz, $CDCl_3$) δ 6.27 (s, 1H), 5.83 (d, *J* = 2.3 Hz, 1H), 4.25 (q, *J* = 7.2 Hz, 2H), 3.41-3.44 (m, 1H), 2.55-2.66 (m, 2H), 1.79 (d, *J* = 1.4 Hz, 3H), 1.67 (s, 3H), 1.30 (t, *J* = 7.2 Hz, 3H); ^{13}C-NMR (100 MHz, $CDCl_3$) δ 197.10, 160.12, 146.15, 141.18, 136.33, 114.99, 85.12, 61.38, 47.54, 37.45, 24.77, 15.73, 14.13; HRMS (ESI) calcd for $C_{13}H_{16}O_4Na$ m/z = 259.0941, found m/z = 259.0943 [$(M+Na)^+$].

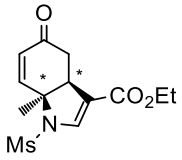

4a

4a: 20% (NEt_3 was used instead of PPh_3); yellow oil; ^{1}H-NMR (600 MHz, $CDCl_3$) δ 7.28 (s, 1H), 6.99 (d, *J* = 10.3 Hz, 1H), 6.14 (d, *J* = 10.3 Hz, 1H), 4.16-4.23 (m, 2H), 3.40 (t, *J* = 6.9 Hz, 1H), 3.11 (s, 3H), 2.75 (d, *J* = 6.9 Hz, 2H), 1.76 (s, 3H), 1.29 (t, *J* = 7.2 Hz, 3H); ^{13}C-NMR (150 MHz, $CDCl_3$) δ 196.03, 163.84, 143.81, 139.08, 129.98, 114.08, 68.37, 60.51, 48.52, 43.91, 37.80, 25.64, 14.27; HRMS (ESI) calcd for $C_{13}H_{17}NO_5SNa$ m/z = 322.0720, found m/z = 322.0720 [$(M+Na)^+$].

5.4.6. Procedure for Synthetic Transformations

5.4.6.1. Luche-Reduction of 3d

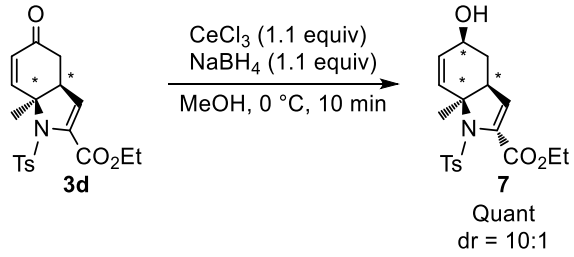

A solution of **3d** (0.050 mmol) and $CeCl_3$ (0.055 mmol) in MeOH (1.0 mL) was stirred at room temperature for 30 min. Then, $NaBH_4$ (0.055 mmol) was added at 0 °C and stirred for 10 min. Reaction was quenched by 1M HCl aq. (1.0 mL). Organic layer was extracted with EtOAc (1.0 mL, 3 times), and dried over Na_2SO_4. Reaction mixture was dried *in vacuo* and purified by silica-gel column chromatography using *n*-hexane/EtOAc as an eluent to form pure product **7** as a pale yellow oil (quantitative yield, dr = 10:1); ^{1}H-NMR (400 MHz, $CDCl_3$) δ 7.75 (d, *J* = 10.5 Hz, 2H), 7.27 (d, *J* = 10.5 Hz, 2H), 6.12 (dd, *J* = 10.3, 1.6 Hz, 1H), 5.86 (d, *J* = 3.8 Hz, 1H), 5.77 (dt, *J* = 10.3, 1.6 Hz, 1H), 4.32 (q, *J* = 7.2 Hz, 2H), 3.94 (d, *J* = 3.8 Hz, 1H), 2.40 (s, 3H), 2.34 (dt, *J* = 12.7, 3.8 Hz, 1H), 1.72-1.78 (m, 1H), 1.40 (s, 3H), 1.35 (t, *J* = 7.2 Hz, 3H), 0.85 (br s, 1H), 0.19 (td, *J* = 12.7, 10.1 Hz, 1H); ^{13}C-NMR (100 MHz, $CDCl_3$) δ 162.91, 143.84, 137.00, 136.24, 134.49, 128.89, 128.50, 127.42, 122.78, 67.37, 65.32, 61.79, 46.82, 34.71, 28.93, 21.53, 14.03; HRMS (ESI) calcd for $C_{19}H_{23}NO_5SNa$ m/z = 400.1189, found m/z = 400.1191 [$(M+Na)^+$].

5.4.6.2. Hydrogenation of 3d

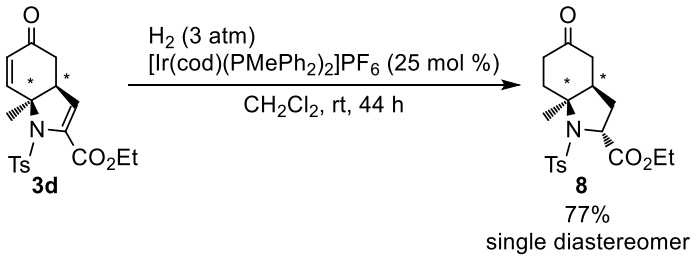

Under an atmosphere of hydrogen (3 atm), the mixture of **3d** (0.050 mmol) and Ir catalyst (0.0125 mmol) in CH_2Cl_2 (1.0 mL) was stirred at room temperature for 44 h. After reaction mixture was filtered with short silica-gel column, filtrate was dried *in vacuo*. Resulting crude reaction mixture was purified by column chromatography using *n*-hexane/EtOAc as an eluent. Semi-hydrogenated by-product could be removed by recrystallization (CH_2Cl_2 /*n*-Hexane) to form product **8** as a white solid (77%, single diastereomer).
^{1}H-NMR (600 MHz, $CDCl_3$) δ 7.75 (d, *J* = 8.2 Hz, 2H), 7.28 (d, *J* = 8.2 Hz, 2H), 4.40 (d, *J* = 8.2 Hz, 1H), 3.97-4.08 (m, 2H), 2.66-2.71 (m, 1H), 2.55 (dd, *J* = 15.8, 6.2 Hz, 1H), 2.41 (s, 3H), 2.31-2.36 (m, 1H), 2.21-2.28 (m, 3H), 1.95-2.05 (m, 2H), 1.83-1.88 (m, 1H), 1.81 (s, 3H), 1.21 (t, *J* = 7.2 Hz, 3H); ^{13}C-NMR (150 MHz, $CDCl_3$) δ 210.20, 172.13, 143.54, 138.13, 129.48, 127.50, 66.51, 61.41, 60.16, 45.29, 40.25, 36.13, 34.28, 32.55, 26.23, 21.50, 13.96; HRMS (ESI) calcd for $C_{19}H_{25}NO_5SNa$ m/z = 402.1346, found m/z = 402.1346 [$(M+Na)^+$].

5.4.6.3. Reduction of Carbonyl Group of 8

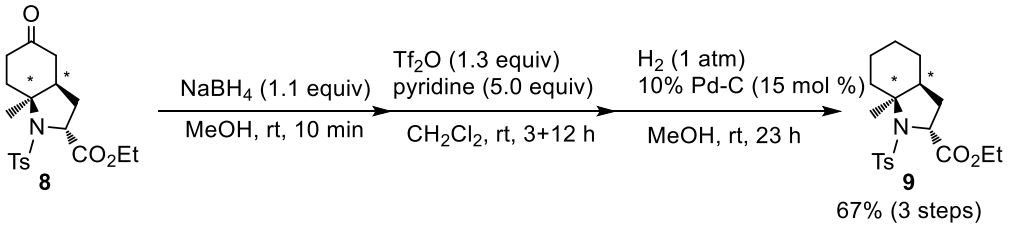

To a solution of **8** (0.58 mmol) in MeOH (12.0 mL) was added $NaBH_4$ (0.638 mmol) at 0 °C and stirred for 10 min at room temperature. Reaction was quenched by 1M HCl aq. (12.0 mL). Organic layer was extracted with EtOAc (12.0 mL, 3 times), and dried over Na_2SO_4. Crude reaction solution dried *in vacuo* was dissolved in CH_2Cl_2 (2.4 mL). Then, Tf_2O (0.62 mmol) was added to the solution at 0 °C and stirred at room temperature for 3 h. To this solution was added pyridine (2.35 mmol) at 0 °C and stirred at room temperature for 12 h. Reaction was quenched by H_2O (2.4 mL) and organic layer was washed with 1M HCl aq. (2.4 mL), saturated $NaHCO_3$ aq. (2.4 mL), brine (2.4 mL), and dried over Na_2SO_4. The concentrated residue was dissolved in MeOH (4.7 mL). Then, 10% Pd-C was added and stirred vigorously at room temperature for 23 h under hydrogen atmosphere (1 atm). Reaction mixture was filtered with celite, washed with EtOAc, and

dried *in vacuo*. Obtained crude product was purified by silica-gel column chromatography using *n*-hexane/EtOAc as an eluent to form pure product **9** as a colorless oil (67% in 3 steps);
^{1}H-NMR (400 MHz,$CDCl_3$) δ 7.76 (d, *J* = 8.2 Hz, 2H), 7.24 (d, *J* = 8.2 Hz, 2H), 4.38 (d, *J* = 8.7 Hz, 1H), 3.89-4.04 (m, 2H), 2.39 (s, 3H), 2.14-2.30 (m, 3H), 1.39-1.70 (m, 9H), 1.14-1.28 (m, 5H); ^{13}C-NMR (100 MHz, $CDCl_3$) δ 172.72, 142.91, 138.69, 129.14, 127.85, 67.68, 61.02, 59.73, 42.94, 34.45, 31.64, 24.59, 24.45, 23.00, 21.45, 20.15, 13.93; HRMS (ESI) calcd for $C_{19}H_{27}NO_4SNa$ m/z = 388.1553, found m/z = 388.1557 [$(M+Na)^+$].

5.4.6.4. Detosylation of 9

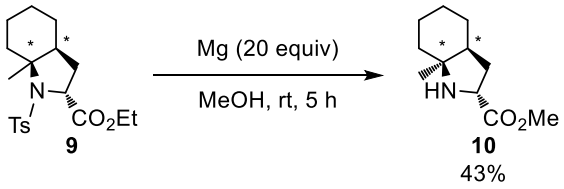

Magnesium turnings (Pre-activated by 1M HCl aq.) was added to a solution of **9** (0.55 mmol) in MeOH (5.5 mL) and stirred vigorously at room temperature for 5 h. Reaction was quenched by 1M HCl aq. (2.0 mL) and basicified with saturated $NaHCO_3$ aq. Organic layer was extracted with EtOAc (5.5 mL, 3 times), washed with brine, and dried over Na_2SO_4. After dried *in vacuo*, crude product was purified by silica-gel column chromatography using *n*-hexane/EtOAc as an eluent to afford pure product **10** as a colorless oil (43%);
^{1}H-NMR (400 MHz, $CDCl_3$) δ 3.91 (q, *J* = 5.0 Hz, 1H), 3.74 (s, 3H), 2.35 (br s, 1H), 2.14-2.22 (m, 1H), 1.95-2.02 (m, 1H), 1.71-1.75 (m, 1H), 1.47-1.57 (m, 4H), 1.28-1.42 (m, 4H), 1.21 (s, 3H); ^{13}C-NMR (100 MHz, $CDCl_3$) δ 176.42, 60.75, 56.93, 52.27, 43.82, 34.72, 34.50, 25.98, 25.48, 22.91, 21.26; HRMS (ESI) calcd for $C_{11}H_{19}NO_2Na$ m/z = 220.1308, found m/z = 220.1309 [$(M+Na)^+$].

5.4.6.5. Synthesis of An Epimer Analog of PEP Inhibitor 6

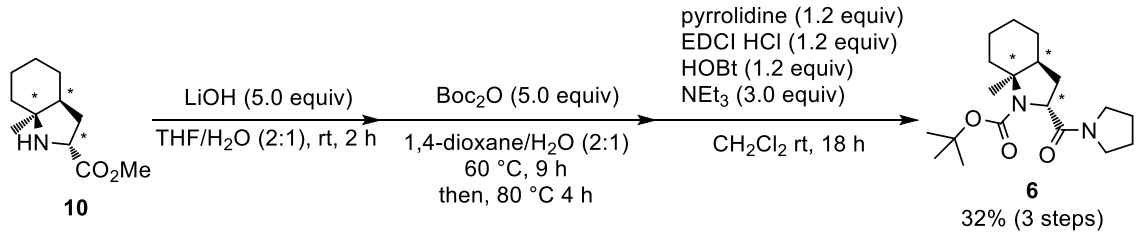

To a solution of **10** (0.086 mmol) in THF-H_2O (2:1, 0.43 mL) was added LiOH (0.43 mmol) at room temperature and stirred for 2 h. Then, THF was removed under reduced pressure followed by addition of 1,4-dioxane (0.30 mL). To this solution was added Boc_2O (0.43 mmol) and stirred at 60 °C for 9 h. Then, reactiom mixture was heated to 80 °C and stirred for 4 h. Reaction was quenched by 1M HCl aq. (0.43 mL). Organic

layer was extracted with EtOAc (0.43 mL, 3 times) and dried over Na_2SO_4. The concentrated residue was dissolved in CH_2Cl_2 (0.43 mL). To this solution was added HOBt (0.10 mmol), EDCI (0.10 mmol), pyrrolidine (0.10 mmol) and NEt_3 (0.26 mmol) and stirred at room temperature for 18 h. Reaction was quenched by 1M HCl aq. (0.43 mL). Organic layer was washed with saturated $NaHCO_3$ aq. (0.43 mL), extracted with EtOAc (0.45 mL, 3 times) and dried over Na_2SO_4. The concentrated crude product was purified by silica-gel column chromatography using *n*-hexane/EtOAc as an eluent to form pure product **6** (Exists as two rotamers) as a colorless oil (32% in 3 steps);

^{1}H-NMR (700 MHz, $CDCl_3$) δ 4.44-4.54 (m, 1H), 3.36-3.69 (m, 4H), 1.76-2.35 (m, 8H), 1.36-1.69 (m, 19H); ^{13}C-NMR (176 MHz, $CDCl_3$) δ 171.70, 171.26, 154.62, 152.87, 79.38, 78.79, 61.98, 61.16, 58.57, 58.42, 46.02, 45.97, 45.93, 42.47, 42.37, 34.21, 33.33, 30.95, 30.20, 29.70, 28.64, 28.46, 26.37, 26.28, 25.65, 24.89, 24.17, 24.05, 23.92, 23.62, 22.92, 22.54, 21.96, 21.13; HRMS (ESI) calcd for $C_{19}H_{32}N_2O_3Na$ m/z = 359.2305, found m/z = 359.2307 [$(M+Na)^+$].

5.4.7. X-ray analysis

5.4.7.1. X-ray Crystal Data of 3a

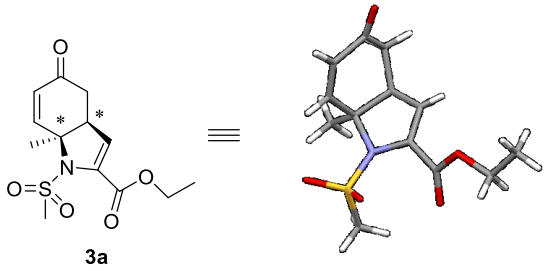

3a

(CCDC No. 1816360)

Empirical Formula	$C_{13}H_{17}NO_5S$
Formula Weight	299.34
Crystal Color, Habit	colorless, block
Crystal Dimensions	0.293 X 0.174 X 0.145 mm
Crystal System	monoclinic
Lattice Type	Primitive
Lattice Parameters	a = 5.923(4) Å b = 16.864(9) Å c = 14.255(8) Å β = 92.357(5) ° V = 1422.7(14) Å^3
Space Group	$P2_1/n$ (#14)
Z value	4
D_{calc}	1.397 g/cm^3
F_{000}	632.00
μ(MoKα)	2.456 cm^{-1}
Residuals: R1 (I>2.00σ(I))	0.0432
Residuals: R (All reflections)	0.0542
Residuals: wR2 (All reflections)	0.1183
Goodness of Fit Indicator	1.086

5.4.7.2. X-ray Crystal Data of 8

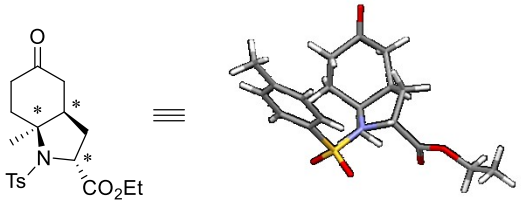

8 (CCDC No. 1818279)

Empirical Formula	$C_{19}H_{25}NO_5S$
Formula Weight	379.47
Crystal Color, Habit	colorless, block
Crystal Dimensions	0.115 X 0.049 X 0.034 mm
Crystal System	orthorhombic
Lattice Type	Primitive
No. of Reflections Used for Unit Cell Determination (2θ range)	6141 (6.3 - 55.0°)
Omega Scan Peak Width at Half-height	0.00°
Lattice Parameters	a = 16.102(5) Å b = 8.154(3) Å c = 28.140(10) Å V = 3694(2) Å^3
Space Group	Pbca (#61)
Z value	8
D_{calc}	1.364 g/cm^3
F_{000}	1616.00
μ(MoKα)	2.051 cm^{-1}
Residuals: R1 (I>2.00σ(I))	0.1564
Residuals: R (All reflections)	0.2065
Residuals: wR2 (All reflections)	0.4179
Goodness of Fit Indicator	1.183

5.5. References

1. (a) Vincent, M.; Rémond, G.; Portevin, B.; Serkiz, B.; Laubie, M. *Tetrahedron Lett.* **1982**, *23*, 1677. (b) Portevin, B.; Benoist, A.; Rémond, G.; Hervé, Y.; Vincent, M.; Lepagnol, J.; Nanteuil, G. D. *J. Med. Chem.* **1996**, *39*, 2379. (c) Nagata, S.; Takeyama, K.; Kanoo, H.; Karasawa, T. *Arzneimittel-Forschung/Drug Research* **1997**, *47*, 726. (d) Li, S. H.; Wang, J.; Niu, X. M.; Shen, Y. H.; Zhang, H. J.; Sun, H. D.; Li, M. L.; Tian, Q. E.; Lu, Y.; Cao, P.; Zheng, Q. T. *Org. Lett.* **2004**, *6*, 4327. (e) Feng, Y.; Wang, L.; Niu, S.; Li, L.; Si, Y.; Liu, X.; Che, Y. *J. Nat. Prod.* **2012**, *75*, 1339. (f) Zhu, H.; Chen, C.; Yang, J.; Li, D.; Zhang, J.; Guo, Y.; Wang, J.; Luo, Z.; Xue, Y.; Zhang, Y. *Tetrahedron* **2016**, *72*, 4655.
2. (a) Sayago, F. J.; Laborda, P.; Calaza, M. I.; Jiménez, A. I.; Cativiela, C. *Eur. J. Org. Chem.* **2011**, 2011. (b) DNP 23.2. *Taylor and Francis*, 2015.
3. For recent reviews of α-amination or α-alkoxylation, see: (a) Vilaivan, T.; Bhanthumnavin, W. *Molecules* **2010**, *15*, 917. (b) Yanagisawa, A. *Comprehensive Chirality* **2012**, *5*, 118. (c) Torre, A.; Tona, V.; Maulide, N. *Angew. Chem. Int. Ed.* **2017**, *56*, 12416.
4. (a) Vincent, M.; Baliarda, J.; Marchand, B.; Remond, G.; U.S. Pat. 4914214, **1990**. (*Chem. Abstr.* **1989**, *111*, 115749) (b) Pascard, C.; Guilhem, J.; Vincent, M.; Rémond, G.; Portevin, B.; Laubie, M. *J. Med. Chem.* **1991**, *34*, 663. (c) Vincent, M.; Marchand, B.; Rémond, G.; Jaguelin-Guinamant, S.; Damien, G.; Portevin, B.; Baumal, J.-Y.; Volland, J.-P.; Bouchet, J.-P.; Lambert, P.-H.; Serkiz, B.; Luitjen, W.; Laubie, M.; Schiavi, P. *Drug Des. Discovery* **1992**, *9*, 11. (d) Kankan, R. N.; Rao, D. R. PCT Int. Appl. WO 2005100317, **2005** (*Chem. Abstr.* **2005**, *143*, 367597). (e) Sayago, F. J.; Calaza, M. I.; Jiménez, A. I.; Cativiela, C. *Tetrahedron* **2008**, *64*, 84.
5. (a) Wipf, P.; Kim, Y. *Tetrahedron Lett.* **1992**, *33*, 5477. (b) Wipf, P.; Kim, Y.; Goldstein, D. M. *J. Am. Chem. Soc.* **1995**, *117*, 11106. (c) Henninger, T. C.; Sabat, M.; Sundberg, R. J. *Tetrahedron* **1996**, *52*, 14403. (d) Wipf, P.; Li, W.; *J. Org. Chem.* **1999**, *64*, 4576. (e) Wipf, P.; Methot, J.-L. *Org. Lett.* **2000**, *2*, 4213. (f) Wipf, P.; Spencer, S. R. *J. Am. Chem. Soc.* **2005**, *127*, 225. (g) Pierce, J. G.; Kasi, D.; Fushimi, M.; Cuzzupe, A.; Wipf, P. *J. Org. Chem.* **2008**, *73*, 7807. (h) Sydnes, M. O.; Le, P. V.; Olschimke, J.; Healy, P. C.; Garavelas, A.; Tajabadi, F. M.; Pedro, L.; Quinn, R. J.; Jenkins, I. D. *Tetrahedron* **2016**, *72*, 1225. (i) Scherer, M.; Gademann, K. *Org. Lett.* **2017**, *19*, 3915.
6. (a) Kuwano, R.; Kashiwabara, M.; Ohsumi, M.; Kusano, H. *J. Am. Chem. Soc.* **2008**, *130*, 808. (b) Dubuffet, T.; Langlois, P.; U.S. Pat. Appl. US 0167273, **2006** (*Chem. Abstr.* **2003**, *139*, 197771). (c) Haider, A.; Megevand, S.; Nicollier, B.; Pannatier, Y.; *Eur. Pat. Appl. EP 1864973*, **2006** (*Chem. Abstr.* **2007**, *148*, 55381).
7. (a) Belvisi, L.; Colombo, L.; Colombo, M.; Giacomo, M. D.; Manzoni, L.; Vodopivec, B.; Scolastico, C. *Tetrahedron* **2001**, *57*, 6463. (b) Hanessian, S.; Margarita, R.; Hall, A.; Johnstone, S.; Tremblay, M.; Parlanti, L. *J. Am. Chem. Soc.* **2002**, *124*, 13342.
8. (a) Bonjoch, J.; Catena, J.; Isábal, E.; López-Canet, M.; Valls, N. *Tetrahedron: Asymmetry* **1996**, *7*, 1899. (b) Bonjoch, J.; Catena, J.; Terricabras, D.; Fernández, J.-C.; Lopez-Canet, M.; Valls, N.

Tetrahedron: Asymmetry **1997**, *8*, 3143. (c) Valls, N.; López-Canet, M.; Vallribera, M.; Bonjoch, J. *J. Am. Chem. Soc.* **2000**, *122*, 11248.

9. Belov, D. S.; Ratmanova, N. K.; Andreev, I. A.; Kurkin, A. V. *Chem. Eur. J.* **2015**, *21*, 4141.
10. (a) Wilson, I. F.; Tebby, J. C. *J. Chem. Soc. Perkin Trans. 1* **1972**, 2830. (b) Trost, B. M.; Dake, G. R. *J. Am. Chem. Soc.* **1997**, *119*, 7595. (c) Yavari, I.; Norouzi-Arasi, H. *Phosphorus, Sulfur Silicon Relat. Elem.* **2002**, *177*, 87. (d) Lu, C.; Lu, X. *Org. Lett.* **2002**, *4*, 4677. (e) Boatman, P. D.; Urban, J.; Nguyen, M.; Qabar, M.; Kahn, M. *Bioorg. Med. Chem. Lett.* **2003**, *13*, 1445. (f) Meunier, S.; Siaugue, J.-M.; Sawicki, M.; Calbour, F.; Dézard, S.; Taran, F.; Mioskowski, C. *J. Comb. Chem.* **2003**, *5*, 201. (g) Silva, F.; Sawicki, M.; Gouverneur, V. *Org. Lett.* **2006**, *8*, 5417. (h) Gabillet, S.; Lecerclé, D.; Loreau, O.; Dézard, S.; Gomis, J.-M.; Taran, F. *Synthesis* **2007**, 515. (i) Gabillet, S.; Lecerclé, D.; Loreau, O.; Carboni, M.; Dézard, S.; Gomis, J.-M.; Taran, F. *Org. Lett.* **2007**, *9*, 3925. (j) Carboni, M.; Gomis, J.-M.; Loreau, O.; Taran, F. *Synthesis* **2008**, 417.
11. (a) Banfield, S. C.; Kerr, M. A. *Can. J. Chem.* **2004**, *82,* 131. (b) Aburto, R. T.; Kalstabakken, K. A.; Harned, A. M. *Org. Biomol. Chem.* **2013**, *11*, 5596. (c) Kishi, K.; Arteaga, F. A.; Takizawa, S.; Sasai, H. *Chem. Commun.* **2017**, *53*, 7724.
12. (a) Schweizer, J.; Lattrell, R.; Hecker, E. *Experientia* **1975**, *31*, 1267. (b) McKinley, J.; Aponick, A.; Raber, J. C.; Fritz, C.; Montgomery, D.; Wigal, C. T. *J. Org. Chem.* **1997**, *62*, 4874. (c) Stern, A. J.; Swenton, J. S. *J. Org. Chem.* **1988**, *53*, 2465. (d) Sunasee, R.; Clive, D. L. J. *Chem. Commun.* **2010**, *46*, 701. (e) Yakura, T.; Omoto, M.; Yamauchi, Y.; Tian, Y.; Ozono, A. *Tetrahedron* **2010**, *66*, 5833.
13. PBu_3-catalyzed non-umpolung Michael addition of α,β-unsaturated carbonyl compounds, see: (a) Inanaga, J.; Baba, Y.; Hanamoto, T. *Chem. Lett.* **1993**, 241. (b) Kuroda, H.; Tomita, I.; Endo, T. *Synth. Commun.* **1996**, *26*, 1539. (c) Liu, B.; Davis, R.; Joshi, B.; Reynolds, D. W. *J. Org. Chem.* **2002**, *67*, 4595. (d) Pedduri, Y.; Williamson, J. S. *Tetrahedron Lett.* **2008**, *49*, 6009.
14. In the presence of amine, alkynoate undergoes dimerization quickly as a side reaction. For details, see: Ramachandran, P. V.; Rudd, M. T.; Reddy, M. V. R. *Tetrahedron Lett.* **2005**, *46*, 2547.
15. NEt_3-catalyzed non-umpolung Michael addition of α,β-unsaturated carbonyl compounds, see: (a) Tejedor, D.; Cruz, D. G.; Expósito, A. S.; Tellado, J. J. M.; Armas, P.; Tellado, F. G. *Chem. Eur. J.* **2005**, *11*, 3502. (b) Tejedor, D.; Expósito, A. S.; Tellado, F. G. *Chem. Commun.* **2006**, 2667. (c) Tejedor, D.; Expósito, A. S.; Tellado, F. G. *Chem. Eur. J.* **2007**, *13*, 1201.
16. Krauss, I. J.; Leighton, J. L. *Org. Lett.* **2003**, *5*, 3201.
17. Okada, T.; Morimoto, T.; Achiwa, K. *Chem. Lett.* **1990**, *19*, 999.
18. Mani, N. S.; Mapes, C. M.; Wu, J.; Deng, X.; Jones, T. K. *J. Org. Chem.* **2006**, *71*, 5039.
19. Capparelli, M. P.; DeSchepper, R. E.; Swenton, J. S. *J. Org. Chem.* **1987**, *52*, 4953.
20. Takizawa, S.; Kishi, K.; Yoshida, Y.; Mader, S.; Arteaga, F. A.; Lee, S.; Hoshino, M.; Rueping, M.; Fujita, M.; Sasai, H. *Angew.Chem. Int. Ed.* **2015**, *54*,15511.
21. Wells, G.; Berry, J. M.; Bradshaw, T. D.; Burger, A. M.; Seaton, A.; Wang, B.; Westwell, A. D.;

Stevens, M. F. G. *J. Med. Chem.* **2003**, *46*, 532.

22. Takizawa, S.; Nguyen, T. M.-N.; Grossmann, A.; Enders, D.; Sasai H. *Angew. Chem. Int. Ed*. **2012**, 51, 5423.
23. McKillop, A.; McLaren, L.; Taylor, R. J. K. *J. Chem. Soc., Perkin Trans. 1* **1994**, 2047.
24. Liu, P.; Fukui, Y.; Tian, P.; He, Z.-T.; Sun, C.-Y.; Wu, N.-Y.; Lin, G.-Q. *J. Am. Chem. Soc.* **2013**, *135*, 11700.
25. Chen, C. P.; Chou, C.-T.; Swenton, J. S. *J. Am. Chem. Soc.* **1987**, *109*, 946.
26. Mitchell, A. S.; Russell, R. A. *Tetrahedron* **1997**, *53*, 4387.
27. Kato, T.; Okamoto, I.; Tanatani, A.; Hatano, T.; Uchiyama, M.; Kagechika, H.; Masu, H.; Katagiri, K.; Tominaga, M.; Yamaguchi, K.; Azumaya, I. *Org. Lett.* **2006**, *8*, 5017.

Conclusion

The research work that was described in this thesis is aimed at investigating the enantioselective synthesis of highly functionalized heterocycles based on organocatalyzed C–C bond forming reactions. Over the past 18 years, organocatalysis has rapidly become a very broad and active research field. However, interest has been mainly focused on the design of substrates and catalysts to realize unique reactions. On the other hand, the author concentrated on the utility of organocatalysts for the synthesis of highly synthetically demanding and complex heterocycles, utilizing the high functional selectivity of the organocatalysts. Through the results described in this thesis, a variety of densely functionalized *N*- and *O*-heterocycles with tetrasubstituted chiral carbon centers have become accessible from simple building blocks via a green and sustainable (domino-reaction-based, metal-free, and atom-economical) process. In Chapter 2, the processes whereby the ubiquitous prochiral heterocycle isatin derivatives were transformed into both enantiomers of 3-amino-2-oxindoles, using naturally occurring alkaloid-derived catalysts, are described. In the following chapters (Chapters 3–5), the development of a novel reusable organocatalyst (Chapter 3) and of new reactions (Chapters 4 and 5) that provide practical methodologies for the synthesis of chiral heterocycles is described. The author believes that the new findings described in this thesis will contribute to the development of synthetic approaches to obtain functionalized heterocycles, and they will broaden the scope of the applications of these heterocycles and of organocatalysis in general. Since the history of organocatalysts has just begun, the constant efforts dedicated to rendering organocatalysis a practical approach will make it the real "*third catalyst*" of asymmetric synthesis.

List of Publications

Chapter 2

"An Enantioselective Organocatalyzed aza-Morita-Baylis-Hillman Reaction of Isatin-derived Ketimines with Acrolein"

Yoshida, Y.; Sako, M.; Kishi, K.; Sasai, H.; Hatakeyama, S.; Takizawa, S.

Org. Biomol. Chem. **2015**, *13*, 9022.

Chapter 3

"Multifunctional Catalysis: Stereoselective Construction of α-Methylidene-γ-Lactams via Amidation/Rauhut–Currier Sequence"

Kishi, K.; Arteaga, F. A.; Takizawa, S.; Sasai, H.

Chem. Commun. **2017**, *53*, 7724. <Selected as an inside front cover>

Chapter 4

"Phosphine-Catalyzed β,γ-Umpolung Domino Reaction of Allenic Esters: Facile Synthesis of Tetrahydrobenzofuranones Bearing a Chiral Tetrasubstituted Carbon Stereogenic Center"

Takizawa, S.; Kishi, K.; Yoshida, Y.; Mader, S.; Arteaga, F. A.; Lee, S.; Hoshino, M.; Rueping, M.; Fujita, M.; Sasai, H.

Angew. Chem. Int. Ed. **2015**, *54*, 15511. <Highlighted in *Synfacts* **2016**, *12*, 129.>

Chapter 5

"Phosphine-Catalyzed Umpolung Domino Michael Reaction: Facile Synthesis of Hydroindole- and Hydrobenzofuran-2-Carboxylates"

Kishi, K.; Takizawa, S.; Sasai, H.

ACS Catal. **2018**, *8*, 5228.

Supplementary Publications

1. "Facile Regio- and Stereoselective Metal-Free Synthesis of All-Carbon Tetrasubstituted Alkenes Bearing a C(sp^3)−F Unit via Dehydroxyfluorination of Morita−Baylis−Hillman (MBH) Adducts"
   Takizawa, S.; Arteaga, F. A.; Kishi, K.; Hirata, S.; Sasai, H.
   Org. Lett. **2014**, *16*, 4162.

2. "Enantioselective Organocatalytic Oxidation of Ketimines"
   Takizawa, S.; Kishi, K.; Abozeid, M. A.; Murai, K.; Fujioka, H.; Sasai, H.
   Org. Biomol. Chem. **2016**, *14*, 761.

3. "Organocatalyzed [4+2] Annulation of All-Carbon Tetrasubstitued Alkenes with Allenoate: Synthesis of Highly Functionalized *2H*, and *4H*-Pyran Derivatives"
   Ngo, T.-T.-D.; Kishi, K.; Sako, M.; Shigenobu, M; Bournaud, C.; Toffano, M.; Guillot, R.; Baltaze, J.-P.; Takizawa, S.; Sasai, H.; Vo-Thanh, G.
   ChemistrySelect **2016**, *1*, 5414.

4. "Facile Synthesis of Spirooxindoles via an Enantioselective Organocatalyzed Sequential Reaction of Oxindoles with Ynone"
   Takizawa, S.; Kishi, K.; Kusaba, M.; Bai, J.; Suzuki, T.; Sasai, H.
   Heterocycles **2017**, *95*, 761.

5. "Enantio- and Diastereoselective Betti/aza-Michael Sequence: Single Operated Preparation of Chiral 1,3-Disubstituted Isoindolines"
   Takizawa, S.; Sako, M.; Abozeid, M. A.; Kishi, K.; Wathsala, H. D. P.; Hirata, S.; Murai, K.; Fujioka, H.; Sasai, H.
   Org. Lett. **2017***, 19,* 5426.

6. "Chiral Organocatalyzed Intermolecular Rauhut–Currier Reaction of Nitroalkenes with Ethyl Allenoate"
   Takizawa, S.; Sako, M.; Kishi, K.; Shigenobu, M.; Vo-Thanh, G.; Sasai, H.
   Chem. Pharm. Bull. **2017**, *65*, 997. <Selected as a cover picture>